Graham Brodie, Mohan V. Jacob, Peter Farrell

MICROWAVE AND RADIO-FREQUENCY TECHNOLOGIES IN AGRICULTURE

AN INTRODUCTION FOR AGRICULTURALISTS AND ENGINEERS

Graham Brodie, Mohan V. Jacob, Peter Farrell

Microwave and Radio-Frequency Technologies in Agriculture

An Introduction for Agriculturalists and Engineers

Graham Brodie, Mohan V. Jacob,
Peter Farrell

Microwave and Radio-Frequency Technologies in Agriculture

An Introduction for Agriculturalists and Engineers

Managing Editor: Magdalena Golachowska

DE GRUYTER
OPEN

Published by De Gruyter Open Ltd, Warsaw/Berlin
Part of Walter de Gruyter GmbH, Berlin/Munich/Boston

ISBN 978-3-11-045539-7
e- ISBN 978-3-11-045540-3

Bibliographic information published by the Deutsche Nationalbibliothek.
The Deutsche Nationalbibliothek lists this publication in the Deutsche Nationalbibliografie; detailed bibliographic data are available in the Internet at http://dnb.dnb.de.

Managing Editor: Magdalena Golachowska

www.degruyteropen.com

Cover illustration: © Graham Brodie

Contents

Section 2: **Non-destructive Characterisation Using Electromagnetic Waves**

Section 3: **Dialectric Heating**

Preface

Modern agriculture is the foundation of society and culture. Without adequate supplies of food and fibre, society has insufficient energy to do more than simply survive. Humanity's ability to produce enough food to sustain its current population is mostly due to adoption of new methods and technologies by the agricultural industries as they became available. Mechanisation transformed agricultural practices. In this modern era, new information, communication and high speed processing technologies have the potential to further transform the industry. Many of these technologies incorporate radio-frequency and microwave radiation into their systems.

This book presents an overview of some ways these parts of the electromagnetic spectrum are being used in agricultural systems. The book does not attempt to present every possible application because this field of study is progressing very rapidly. Neither does it attempt to explore every detail of the technologies. The main purposes of the book is provide a glimpse of what is possible and encourage practitioners in the engineering and agricultural industries to explore how radio-frequency and microwave systems might further enhance the agricultural industry.

Section 1: **General Introduction**

1 Introduction

A changing magnetic field will induce a changing electric field and vice-versa. These changing fields form electromagnetic waves. Electromagnetic (EM) waves differ from mechanical waves in that they do not require a medium to propagate through. This means that electromagnetic waves can travel not only through air and solid materials, but also through the vacuum of space.

During the 1860's and 1870's, James Clerk Maxwell developed a scientific theory to explain electromagnetic waves. He noticed that electrical fields and magnetic fields can couple together to form electromagnetic waves. He summarized this relationship between electricity and magnetism into what are now referred to as "Maxwell's Equations."

Electromagnetic waves are a complex phenomenon because they can propagate through vacuum without the need for a material medium, they simultaneously behave like waves and like particles (Dirac 1927, Einstein 1951), and they are intrinsically linked to the behaviour of the space-time continuum (Einstein 1916). It can be shown that magnetic fields appear through relativistic motion of electric fields, which is why electricity and magnetism are so closely linked (Chappell, *et al.* 2010). It has even been suggested that electromagnetic phenomena may be a space-time phenomenon, with gravitation being the result of space-time curvature (Einstein 1916) and electromagnetic behaviour being the result of space-time torsion (Evans 2005).

An EM wave is described in terms of its:

1. Frequency (f), which is the number of waves that pass a fixed point in an interval of time. Frequencies are usually measured as waves per second or cycles per second, which is given the unit of Hertz (Hz);
2. Wavelength (λ), which is the distance between successive crests or troughs in the wave. If frequencies are measured in Hertz, then wavelengths are measured in metres (m); and
3. Speed (c), which is measured in metres per second and is determined by the electrical and magnetic properties of the space through which the wave travels.

These three properties are related by the equation:

$$c = \lambda f \tag{1.1}$$

The speed of the electromagnetic wave is determined by:

$$c = \frac{1}{\sqrt{\mu\varepsilon}} \tag{1.2}$$

where ε is the electrical permittivity of the space in which wave exists and μ is the magnetic permeability of the space in which the wave exists.

Electromagnetic waves can be of any frequency; therefore the full range of possible frequencies is referred to as the electromagnetic spectrum. Although Maxwell's

Equations do not indicate any limits on the spectrum, the known electromagnetic spectrum extends from frequencies of around $f = 3 \times 10^3$ Hz ($\lambda = 100$ km) to $f = 3 \times 10^{26}$ Hz ($\lambda = 10^{-18}$ m). This covers everything from ultra-long radio waves to high-energy gamma rays (International Telecommunication Union 2004).

Electromagnetic waves can be harnessed to: transmit information; acquire information from a medium; or transmit energy. The first category of applications includes: terrestrial and satellite communication links; the global positioning system (GPS); mobile telephony; and so on (Commonwealth Department of Transport and Communications 1991). The second category of applications includes: radar; radio-astronomy; microwave thermography; and material permittivity measurements (Adamski and Kitlinski 2001). The third category of applications is associated with microwave heating and wireless power transmission. In these cases there is usually no signal modulation and the electromagnetic wave interacts directly with solid or liquid materials.

Radio frequency (RF) is a term that refers to a portion of the electromagnetic spectrum that can be easily generated using an alternating current (AC). If an AC current is fed into a suitable structure such as an antenna, an electromagnetic (EM) field is generated. These EM fields will usually propagate through space the same as any other form of electromagnetic radiation.

Many devices make use of RF fields. Cordless and mobile telecommunication, radio and television broadcast stations, satellite communications systems, and two-way radio services all operate in the RF spectrum. Some wireless devices operate at infra-red (IR) or visible-light frequencies, whose electromagnetic wavelengths are far shorter than those of RF fields.

The RF spectrum is divided into several ranges, or bands. With the exception of the lowest-frequency segment, each band represents an increase of frequency corresponding to an order of magnitude (power of 10). Table 1.1 depicts the eight bands in the RF spectrum, showing frequency and bandwidth ranges. The UHF, SHF and EHF bands constitute the *microwave spectrum*.

Table 1.1: Radio Frequency spectrum

Designation	Abbreviation	Frequencies	Free-space Wavelengths
Very Low Frequency	VLF	9 kHz - 30 kHz	33 km - 10 km
Low Frequency	LF	30 kHz - 300 kHz	10 km - 1 km
Medium Frequency	MF	300 kHz - 3 MHz	1 km - 100 m
High Frequency	HF	3 MHz - 30 MHz	100 m - 10 m
Very High Frequency	VHF	30 MHz - 300 MHz	10 m - 1 m
Ultra High Frequency	UHF	300 MHz - 3 GHz	1 m - 100 mm
Super High Frequency	SHF	3 GHz - 30 GHz	100 mm - 10 mm
Extremely High Frequency	EHF	30 GHz - 300 GHz	10 mm - 1 mm

Microwave frequencies occupy portions of the electromagnetic spectrum between 300 MHz to 300 GHz. Because microwaves are also used in the communication, navigation and defence industries, their use in thermal heating is restricted to a small subset of the available frequency bands. A small number of frequencies have been set aside for Industrial, Scientific and Medical (ISM) applications (Table 1.2). All these frequencies interact to some degree with moist materials. All interactions between electromagnetic waves and the media that they encounter can be described by Maxwell's equations for electro-magnetism.

Table 1.2: ISM Frequency allocations (International Telecommunication Union 2004).

Frequency	Availability
6.78 MHz ± 15 kHz	Subject to local acceptance
13.56 MHz ± 7 kHz	World wide
27.12 MHz ± 163 kHz	World wide
40.68 MHz ± 20 kHz	World wide
433.92 MHz ± 870 kHz	Region 1 only and subject to local acceptance
915.00 MHz ± 13 MHz	Region 2 only with some exceptions
2.45 GHz ± 50 MHz	World wide
5.8 GHz ± 75 MHz	World wide
24.125 GHz ± 125 MHz	World wide
61.25 GHz ± 250 MHz	Subject to local acceptance
122.5 GHz ± 500 MHz	Subject to local acceptance
245.0 GHz ± 1.0 GHz	Subject to local acceptance

The regions defined by the International Telecommunications Union (2004) are:
- **Region 1**: Europe, Africa, the Middle East west of the Persian Gulf including Iraq, Russia, and Mongolia;
- **Region 2**: The Americas, Greenland, and some of the Pacific Islands;
- **Region 3**: Most of non-Russian Asia and most of Oceania.

Some microwave and radio frequency technologies such as RFID, wireless sensor networks, microwave tempering of frozen meat, electromagnetic surveys of soil properties, GPS guidance of farm machinery, and radar terrain imaging have been "standard practice" in many agricultural industries for some time. Many new technologies are currently being explored in research institutions around the world. Knowledge of these technologies is critical for agriculturalists and engineers alike.

Although RF and microwave technologies are becoming ubiquitous in most agricultural industries, there appears to be no single text that comprehensively covers the practice and theory behind these critical technologies. This book will provide a review of microwave and radio-frequency applications that have been considered for use in agriculture, and point out the advantages of some of the key applications. The principal purpose of the book is to bring to the attention of students and practitioners in the electrical, microwave/radio-frequency and agricultural industries those applications that have been studied so that practical use may be realised.

This book is subdivided into four sections, with each section consisting of several individual chapters. The earlier chapters will provide an overview of innovations in agriculture and an introduction to electromagnetism. The second section will indicate how RF and microwave energy can be used to characterise agricultural and forestry materials. Other sections will focus on heating applications. Another section will explore how wireless systems can be used in agricultural systems. Some chapters will focus on the applications, while others will necessarily be more theoretical to provide the necessary background to the technology.

References

Adamski, W. and Kitlinski, M. 2001. On measurements applied in scientific researches of microwave heating processes. *Measurement Science Review*. 1(1): 199-203.

Chappell, J. M., Iqbal, A. and Abbott, D. 2010. A simplified approach to electromagnetism using geometric algebra.

Commonwealth Department of Transport and Communications. 1991. *Australian Radio Frequency Spectrum Allocations*. Commonwealth Department of Transport and Communications

Dirac, P. A. M. 1927. The quantum theory of the emission and absorption of radiation. *Proceedings of the Royal Society of London. Series A, Containing Papers of a Mathematical and Physical Character*. 114(767): 243-265.

Einstein, A. 1916, *Relativity: the Special and General Theory*, Methuen & Co Ltd.

Einstein, A. 1951. The Advent of the Quantum Theory. *Science*. 113(2926): 82-84.

Evans, M. W. 2005. The Spinning and Curving of Spacetime: The Electromagnetic and Gravitational Fields in the Evans Field Theory. *Foundations of Physics Letters*. 18(5): 431-454.

International Telecommunication Union. 2004. *Spectrum Management for a Converging World: Case Study on Australia*. International Telecommunication Union

2 Some Brief Examples of Technical Innovation in Agricultural Industries

Thomas Malthus (1798) studied population growth in Europe. He estimated that population was increasing exponentially and resources were only increasing linearly; therefore population was increasing faster than food production. His final conclusion was that global starvation was inevitable.

More recent systematic studies of famine and starvation around the world have revealed that, although famines have occurred ever since the development of agriculture, many of the worst famines in recent history should be attributed to poor distribution of existing food supplies, rather than the ravages of natural disaster and the consequences of population growth outstripping food production (Scrimshaw 1987). Although major innovation was beginning at the time he wrote his essay, Malthus could not foresee how technology would transform food and fibre production. The industrial revolution, green revolution and advent of precision agriculture have forestalled most of Multhus' most dire predictions.

The transformation in agricultural practices has profoundly affected society. Over the past 200 years, the number of people who are directly involved in agriculture has dramatically declined. In the 1800's, nearly 80 % of the employed population was involved in agriculture; by the 1900's those who were directly involved in agriculture had decreased to 35 % (Australian Bureau of Statistics 2000). In the year 2000, it was estimated that 4 to 5 % of the employed population of Australia were directly involved in agriculture (Australian Bureau of Statistics 2000). These employment trends are common across other developed countries. During this same period of about 200 years, the human population has grown from about 790 million in 1750 (Gelbard and Haub 1999) to an estimated 6.4 billion in 2005 (Demeny and McNicoll 2006).

Although agriculture is fundamental to feeding a growing population, the importance of modern agricultural practices to social development is not so clearly understood. Agriculture has two key economic characteristics: first, it produces goods that directly satisfy basic human needs; and second, it combines human effort with natural resources, such as land (Diao, et al. 2007) to deliver these goods. It was believed that, since natural resources were freely available, agriculture could grow independently of other economic activities (Diao, et al. 2007); however, arable land area is a fixed resource so growth is constrained by available technology (Diao, et al. 2007).

Historical evidence suggests that agriculture is the key to economic development. Gollin, et al. (2002) show that once agriculture switches from traditional to modern technology, labour is released to the industrial sector and the economy grows at higher rates. Unfortunately this means that agriculture's percentage contribution to national productivity declines due to dilution from growth in other sectors of the economy that would not be possible without an efficient agricultural sector.

Agriculture's declining share in the economy sends a confusing signal to policy makers who conclude that agriculture is relatively unimportant and the falling real prices of agricultural commodities, due to transformational improvements in the supply chain efficiency, sends the signal to investors that returns from agricultural investment are unattractive (Stringer 2001). These confusing signals also reduce the number of researchers and innovators engaging in agriculture (Anonymous 2009), which slows the rate of innovation.

This chapter will outline some historical innovations that have contributed to the transformation of agricultural practices.

2.1 Machines

It has been suggested that this modern era can be described as the machine age; however this is not strictly true (Ubbelohde 1963). Humans have been building and using machines of various types since ancient times. From around 3000 BC, several major achievements appear in the time line. These include: the development of wedges, wheels and levers; the use of animals to carry and draw loads; and the use of fire to work metals. Other achievements included the digging of irrigation canals, and open-pit mining. Monumental construction programmes such as: the Pyramids in Egypt, China and the Americas (Canadian Council of Professional Engineers 2003); and transport of massive stones (Hazell and Brodie 2005, Hazell and Fitzpatrick 2006, Hazell and Brodie 2012, Brodie and Hazell 2014) were also undertaken.

The Greeks made significant contributions to engineering in the 1000 years that straddled the centuries before and after Christ (Canadian Council of Professional Engineers 2003). They produced the screw, the ratchet, the water wheel and the aeolipile, better known as Hero's turbine (Figure 2.1).

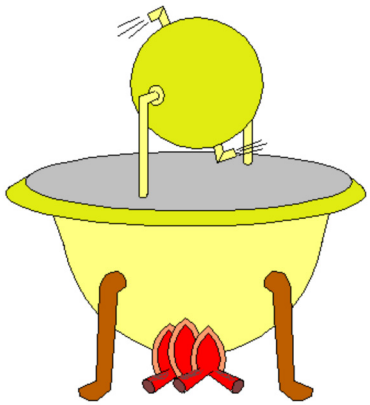

Figure 2.1: Hero's aeolipile, about AD 150.

The Persians are credited with harnessing wind power (Ubbelohde 1963). The Romans built fortifications, roads, aqueducts, water distribution systems and public buildings across the territories and cities they controlled. At the other end of the world, the Chinese have been credited with the development of the wheelbarrow, the rotary fan, the stern-post rudder and gunpowder (Canadian Council of Professional Engineers 2003). They also began making paper from vegetable fibres.

Between 1700 and 1850, the Industrial Revolution in Western Europe dominated the development of machinery (Canadian Council of Professional Engineers 2003). It was significantly influenced by the development of steam engines; machinery for the mass production of industrial goods; and the railways developed by Stephenson, Brunel and others (Canadian Council of Professional Engineers 2003). Agricultural machinery, such as seed drills, mechanical harvesters and stump-jump ploughs, and the use of engines rather than horses as a primary power source were the major legacies of this period.

2.2 Early Innovations in Agriculture

One of the earliest examples of new agricultural technology was the development of the horse drawn seed drill, which is usually attributed to Jethro Tull (1733). Whether Tull was the inventor of the seed drill is doubtful (Sayre 2010); however he did promote its wide spread adoption. What is less well known is that Tull also advocated a new theory of plant nutrition, which promoted an extensive tillage of the soil for improving fertility and maintaining weed control (Sayre 2010). This idea was controversial, because most farmers of the time applied manures and allowed natural decomposition of these manures to improve soil nutrition. Historians are divided over the value of Tull's ideas about soil nutrition. Some describe him as one of the greatest innovators in agricultural production, while others suggest that, while he was an excellent observer and experimenter, his agronomic theories were incorrect (Sayre 2010). Ultimately, the ability to quickly plant large areas of monoculture crops in relatively straight rows transformed agricultural practice. Modern cropping systems still rely on seed drills.

Eli Whitney's cotton gin (circa 1793) sped up the post processing of cotton (Peterson 1995). The invention of the cotton gin revolutionised the cotton industry in the United States. Cotton production requires the cotton seed to be removed from the raw cotton fibres. Simple seed-removing devices had been available for centuries before Whitney automated the seed separation process. One of his other important contributions was the idea of standardised interchangeable machine parts, which paved the way for mass production (Peterson 1995). Whitney's cotton gin had spiked teeth mounted on a revolving cylinder which was turned by a crank. These teeth pulled the cotton fibre through small slotted openings so that the seeds were separated from the fibre.

In 1831, Cyrus McCormick invented the mechanical reaper to help in grain harvesting (Peterson 1995). The adoption of the horse drawn reaper meant that daily harvesting capacity could be increased fivefold, compared to traditional hand methods (Peterson 1995).

The development of the stump jump plough (invented by Richard Bowyer Smith in 1876), the combine harvester and the establishment of large scale irrigation systems transformed the various colonies into significant exporters of agricultural produce (Australian Bureau of Statistics 2000).

2.3 Transportation Technologies

Transportation has played a vital role in society (Short 2010); this is especially true for agriculture. Early transport for agricultural produce was by horse and cart for short distances. For centuries, sailing ships were the fastest means of transportation over longer distances (Short 2010). In 1787, John Fitch demonstrated the first steamboat, which had twelve paddles and was propelled by a steam engine (Poddar n.d.). This allowed steam ships and river boats to become the main methods for transporting agricultural produce (Short 2010).

Of all the advancements of the Transportation Revolution, the construction of railways was the most significant (Poddar n.d.). The first railways carried goods for short distances, but inventors and engineers wanted to be able to carry goods or passengers long distance. Steam locomotion, together with the low rolling friction of iron-flanged wheels on iron rails, enabled George Stephenson (the first of the great railway engineers) to design and superintend the building of the Liverpool and Manchester Railway (1830), which began the railway age in England (Marsh 2009). Railways replaced water ways as the primary means of moving agricultural produce.

The 20th century belonged to road transportation (Short 2010). The development of internal combustion engines, pneumatic tyres, and paved roads allowed for greater trade volumes (Blondé 2010), which lead to economic and cultural development. The breakthrough for agriculture based transportation came with falling relative transformation costs, and rising agricultural prices supported by improving urban economies (Blondé 2010). Even on-farm transportation and mechanisation was transformed.

2.4 The Tractor

Before the advent of traction machines, most heavy pulling was achieved by human effort (Hazell and Brodie 2005, Hazell and Brodie 2012, Brodie and Hazell 2014) or animals (Ubbelohde 1963). Ancient Egyptian drawings illustrate ploughs being pulled by two oxen (Ubbelohde 1963). At the time of the Domesday Book Survey (1086), the

normal plough was pulled by eight oxen (Ubbelohde 1963). It was estimated that eight ox power could plough 120 acres (48.5 hectares) of land in a year (Ubbelohde 1963), which limited the amount of land that could be managed.

Experiments with steam engines can be traced back to Hero's aeolipile; however James Watt was the first to present a practical steam engine in 1769 (Goering 2008). Fawkes produced a steam tractor that could pull eight ploughs at 4.8 km/h in virgin sod (Goering 2008). Tractors with internal combustion engines first appeared in 1907 (Goering 2008). Competition between the rival technologies climaxed in a series of tractor trials in Winnipeg, Canada between 1908 and 1911, where the limitations of steam tractors became apparent (Goering 2008).

All modern tractors use internal combustion engines, with most of them using Diesel engines because of their inherent efficiency and high torque compared with petrol engines. Rudolf Diesel developed the idea for the diesel engine and obtained the German patent for it in 1892. His goal was to create an engine with high efficiency. Spark ignition engines were invented in 1876 and were not very efficient.

The transition from oxen or horses to tractors began in Australia after 1920 (Davidson 1981); however this transformation was initially slow. Based on a detailed survey of 115 farms, Perkins (Perkins 1929) demonstrated that one 24 H.P. (18.75 kW) tractor could replace 11.4 horses on an average South Australian farm; thus freeing additional cropping land that was previously used to grow feed for work animals. By 1930, only about 40 % of Australian farmers were equipped with tractors (Davidson 1981). One of the contributing factors to this relatively slow adoption rate was revealed by Perkins (1929). He demonstrated that for an average farm size of 300 acres (121.4 ha) the replacement of horses with a tractor led to a reduction in annual profit of £114. Australian grain growers had realised that mechanisation was only viable if it was applied to large scale production (Davidson 1981). It was the interaction between agricultural production and other factors in modern economies that ultimately promoted the transition to full mechanisation.

Most modern tractors are truly all purpose. They can operate a vast array of: mounted implements; trailed implements; and machines running from the power take off (PTO). They have hydraulic devices, which give the operator easy and accurate control from the driver's seat. Tractors are normally rated using two criteria: the draw bar power - a measure of how much the tractor can physically pull; and the PTO rating (Culpin 1976). Experimental PTO's were tried as early as 1878 (Goering 2008). The American Society of Agricultural Engineers adopted the first PTO standard for defining the direction of rotation, speed, size, shape, and location (Goering 2008). The inclusion of PTO's on tractors transformed agricultural practice allowing many functions to be performed on the go in the field rather than requiring a multi-pass approach.

The most recent inclusion in modern tractors is the GPS and auto steer. This has facilitated the development of high resolution farming (or precision farming).

2.5 The Green Revolution

Massive investment in agricultural research during the 20th century lead to dramatic crop yield increases in most industrialised countries. For example, it took nearly 1,000 years to increase wheat yields from 0.5 to 2 tonnes per hectare; however it took only 40 years during the 20th century to increase yields from 2 to 6 tonnes per hectare (International Food Policy Research Institute 2002). These astonishing improvements in yield can be attributed to better plant breeding, improved agronomy, the development of inorganic fertilisers, the development of chemical pesticides and herbicides, large scale irrigation schemes, and the mechanisation of farming systems (International Food Policy Research Institute 2002). Unfortunately, these advances in technology did not reach developing countries as quickly, due to various influences including lack of political will, which lead to significant famines in many places (Scrimshaw 1987).

The Green Revolution originally focused on developing high-yielding varieties for rice and wheat; however high-yielding varieties have since been developed for other major food crops, including: sorghum, millet, maize, cassava, and beans (International Food Policy Research Institute 2002). The green revolution led to substantial increases in on-farm income, which on the international scale raised rural demand for goods and services. This has given rise to new rural service industries in many countries (International Food Policy Research Institute 2002). This has profoundly affected the standard of living for many rural communities. For example, the percentage of the Indian rural population living below the poverty line fluctuated between 50 and 65 percent before the mid-1960s; however this has declined steadily to about one-third of the rural population by 1993 (International Food Policy Research Institute 2002).

The Green Revolution has also given rise to no-till agricultural practices, in which grain seed is directly planted into uncultivated soil using a planter (called a drill) that drops the seed into a very shallow furrow, which is immediately filled with soil using a press wheel. Reduced tillage reduces soil erosion, improves soil physical and chemical properties, conserves soil moisture, and saves fuel costs. No-till systems rely on extensive use of herbicides to manage weed infestations (Chauhan 2006). One of the earliest herbicides to be developed was 2,4-dichlorophenoxyacetic acid (2,4-D), which was discovered in the 1940's. It was effective at killing di-cotyledons, but not mono-cotyledons. Many other chemicals have been developed to control weeds, including chemicals such as Atrazine and Glyphosate. Chemical weed control was initially very effective; however more recently herbicide resistance (Heap 2008) and health concerns due to long term exposure (Troudi, et al. 2012) have arisen.

Genetic engineering of crops (GMC's) has the potential to double or even triple world food, feed and fibre production by the year 2050 (James and Krattiger 1996); however there has been concern about the development of GMC's (or transgenic crops) since 1971 (James and Krattiger 1996). The first field trials featured herbicide

resistance. These crops have become commercially available and widely adopted to improve production and better manage weed by allowing the use of broad spectrum herbicides, such as Glyphosate. Resistance to pests and improvement in production and nutrition have also been introduced.

More than 50 transgenic crops have been trialled worldwide. Commercialised transgenic crops include: cotton, maize, melon, canola, potato, soybean, tobacco, tomato, alfalfa, cantaloupe, carnations, flax, rice, squash, sugar-beet, and sunflower (James and Krattiger 1996). In some cases, genes have been introduced to enhance production, enhance nutrition, resist pests or introduce resistance to chemicals that are used to manage other pests.

Green revolution technologies are well suited to larger farms. In some cases, this has displaced smaller farm operators from the industry as more successful farmers acquire more land for their operations. This may have contributed to increases in urbanisation across the globe. Another consequence is that high yields are now only sustained in high input farming systems. These input expenses are only economically viable because their costs are diluted by the increased availability of saleable commodities. Attempts at better understanding and managing high inputs have prompted further innovation in the form of high resolution production systems.

2.6 High Resolution Production Systems

The objective of high resolution, precision agricultural systems is to avoid over application of inputs while maintaining optimal growing conditions for the crop (Cao, et al. 2012). High resolution agricultural systems are based on a network of sensors and actuators for real time monitoring and control of agricultural production. These are often combined with existing information technologies (Schuh, et al. 2007) such as Radio Frequency Identification (RFID), Programmable Logic Controllers (PLC), Personal Digital Assistants (PDA) and Smart Phones that can interface with these sensor networks to monitor and control some activities remotely.

These systems depend on automatic acquisition of both spatial (position-based) and temporal (time-based) data, which allows the operator, or the automated operating system, to make finer adjustments to inputs than would normally be considered in conventional farming systems.

2.7 Spatial Data

Spatial data acquisition often involves using various aerial or ground based canopy sensors. The spectral reflectance of plants is much higher in the infra-red part of the electromagnetic spectrum than in the visible part of the spectrum. Plant stresses due to water or nutrient deficiencies have a greater effect on infra-red reflectance than on

the visible light reflectance (Figure 2.2); therefore sensors that can detect infra-red light can be used to quickly identify stressed plants. For example, the GreenSeeker canopy sensor (NTech Industries, Inc., Ukiah, California, USA) is a commercially available optical sensor that captures both a red (650 ± 10 nm) and a Near Infra-red (NIR @ 770 ± 15 nm) images of the crop canopy (Cao, et al. 2012). These images can be analysed to determine the health of the crop.

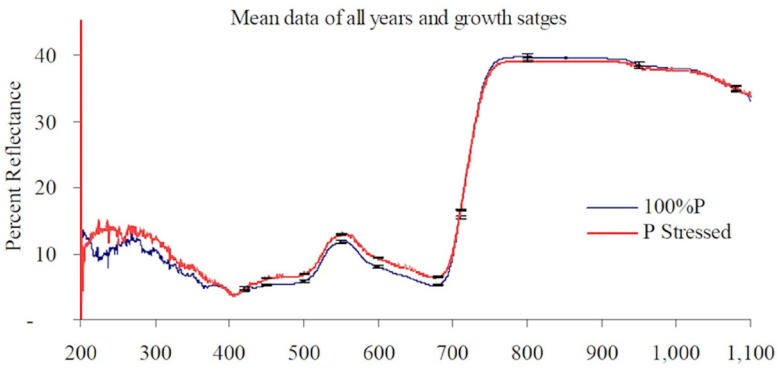

Figure 2.2: Reflectance data for wheat plants under different levels of phosphorous stress.

A common analysis option for assessing the health of plants is the Normalised Difference Vegetation Index (NDVI). NDVI values are calculated on a pixel by pixel basis using the following equation:

$$NDVI = \frac{R_{NIR} - R_R}{R_{NIR} + R_R} \tag{2.1}$$

where R_{NIR} is the crop reflectance at the NIR wavelength and R_R is the crop reflectance at the red wavelength. The resulting analysis can resemble an image; however the individual pixels within the image are calculated rather than captured as in the case of a photograph.

As an example, the NDVI for the blue sample in Figure 2.2 is approximately 0.78; however the NDVI value for the red sample in Figure 2.2 is:

$$NDVI = \frac{R_{NIR} - R_R}{R_{NIR} + R_R} = \frac{0.405 - 0.07}{0.405 + 0.07} = 0.7 \tag{2.2}$$

Figure 2.3 shows an example of an NDVI image.

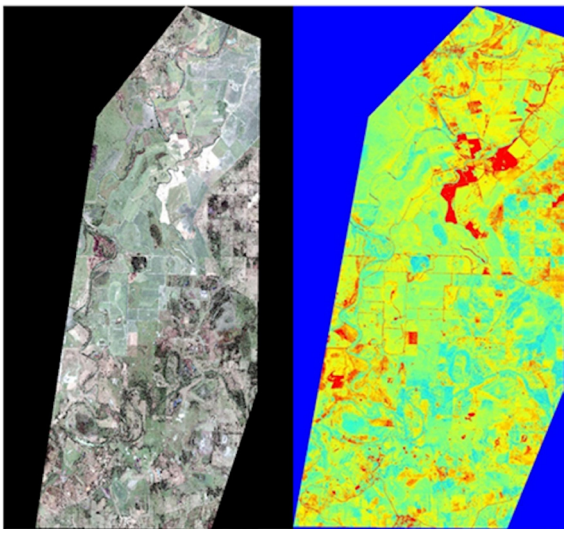

Figure 2.3: Comparison of (left) true colour image with (right) an NDVI image of extensive farmland (NDVI calculated from red and NIR bands of a satellite image)

There are several variants of the NDVI calculation. These provide better separation of healthy from unhealthy plants. For example, the Enhanced Vegetation Index (EVI) uses either two or three bands of an image (NIR, red and blue) to calculate the index:

$$EVI = G\frac{R_{NIR} - R_R}{R_{NIR} + C_1R_R - C_2R_B + L} \tag{2.3}$$

where G, C1, C2 and L are constants. The coefficients adopted in the MODIS-EVI algorithm are; L=1, $C_1 = 6$, $C_2 = 7.5$, and G (gain factor) = 2.5. In the case where only two spectral bands are available (NIR and red), the EVI can be calculated using $C_1 = 2.4$:

$$EVI2 = G\frac{R_{NIR} - R_R}{R_{NIR} + C_1R_R + L} \tag{2.4}$$

Using the earlier examples from Figure 2.2, the EVI2 for the blue sample is approximately 0.91 while the EVI2 for the grey sample is approximately 0.55. The NDVI is chlorophyll sensitive; however the EVI is more responsive to canopy structural, including leaf area index (LAI), canopy type, plant physiognomy, and canopy architecture.

These vegetation indexes can differentiate stresses in different parts of a crop, allowing spatially specific management of the crop inputs to optimise production. The sensors can be mounted on machinery, on aircraft or drones, on satellite platforms, or even on small airships (Figure 2.4).

Although there is usually good success with spatially specific input management during the early stages of technology adoption, it is clear that longer term influences, such as system inertia, can mitigate potential improvements in agricultural systems. Achieving better system responses requires high resolution temporal (time based) data as well as high resolution spatial data.

Figure 2.4: (left) Duel camera system with IR and true colour cameras (right) mounted on a transportable airship (Photographs of the system in operation over the vineyard at Dookie campus of the University of Melbourne).

2.8 Temporal Data

Understanding how a system changes over time is critical to better system management. Data acquisition is simply the gathering of information about a system or process over an extended period of time. It is a core tool to the understanding, control and management of complex systems or processes. As with most systems, complexity becomes more apparent as monitoring frequency increases; therefore high resolution temporal data usually depends on automatic data acquisition (Vandoren 1982).

Information such as temperature, pressure or flow is gathered by sensors that convert measurements into electrical signals. Sometimes only one sensor is needed, such as when recording local rainfall. Sometimes hundreds or even thousands of sensors are needed, such as when monitoring a complex industrial process. The signals from sensors are transferred by wire, optical fibre or wireless links to an instrument which conditions, amplifies, scales, processes, displays and stores the sensor signals (Brodie 2009).

In the past data acquisition equipment was largely mechanical, using clock work and chart recorders. Later, electrically powered chart recorders and magnetic tape recorders were used. Today, powerful microprocessors and computers perform data acquisition faster, more accurately, more flexibly, with more sensors, more complex data processing, and elaborate presentation of the final information.

Data acquisition can be divided into two broad classifications – real time data acquisition and data logging. Real time data acquisition is when data acquired from sensors is used either immediately or within a short period of time, such as when controlling a process (Frey and Williams 1994). An example of this kind of data acquisition and control system is an automatic irrigation system that responds to output from a soil moisture sensor. Data logging on the other hand is when data acquired from sensors is stored for later use (Frey and Williams 1994). In reality, there is a continuum of devices between real time data acquisition and data logging that share the attributes of both of these classifications.

All data acquisition requires proper sampling of the system. In terms of time based sampling, the Nyquist-Shannon sampling theorem states that reconstruction of a continuous signal from its samples is only possible if the sampling frequency is greater than twice the bandwidth of the monitored system (Nyquist 2002). A similar principle applies to spatial sampling. Therefore appropriate sampling rates depend on how quickly the phenomenon of interest is changing with respect to both time and location.

2.9 Conclusions

Transformational innovations have allowed agricultural production to increase as rapidly as population, forestalling the dire predictions of Malthus; however this sustained innovation has meant that developed societies have become dependent on a small portion of the population for its food security. Adoption of high resolution agriculture has allowed agricultural production to increase while reducing or maintaining system inputs; however this can only be sustained by ongoing research and investment into novel technologies that may allow greater agricultural productivity or improvements in the quality of what is currently being produced. Although they have not been mentioned in this chapter, microwave and radio frequency technologies that can contribute to agricultural production are currently being explored. The next chapter will highlight some of the potential developments in this domain.

References

Anonymous. 2009. Researcher shortage could mean empty plates. *Times Higher Education*. (1892): 10-10.

Australian Bureau of Statistics 2000, *Year Book Australia*, Canberra: Australian Bureau of Statistics.

Blondé, B. 2010. At the cradle of the transport revolution?: Paved roads, traffi c flows and economic development in eighteenth-century Brabant. *Journal of Transport History*. 31(1): 89-111.

Brodie, G. and Hazell, L. 2014 Establishing Megalith Transport Routes using Geographic Information Systems. In *Geographic Information Systems (GIS): Techniques, Applications and Technologies*, 137-150. Nielson, D. ed. Nova Publishing: Hauppauge, USA.

Brodie, G. I. 2009, *Ingenious Devices and Systems: Engineering for Landscape Managers*, Saarbruecken, Germany: VDM Verlag.

Canadian Council of Professional Engineers. 2003. *History of Engineering*. July 2006. http://www.new-sng.com/maintemplate.cfm

Cao, Q., Cui, Z., Chen, X., Khosla, R., Dao, T. and Miao, Y. 2012. Quantifying spatial variability of indigenous nitrogen supply for precision nitrogen management in small scale farming. *Precision Agriculture*. 13(1): 45-61.

Chauhan, B. S. 2006. Ecology and management of weeds under no-till in southern Australia. Unpublished PhD thesis. Roseworthy: University of South Australia,

Culpin, C. 1976, *Farm Machinery*, 9th edn, London: Granada Publishing.

Davidson, B. R. 1981, *European Farming in Australia: An Economic History of Australian Farming*, Amsterdam: Elsevier.

Demeny, P. and McNicoll, G. 2006. World Population 1950-2000: Perception and Response. *Population and Development Review*. 32: 1-51.

Diao, X., Hazell, P., Resnick, D. and Thurlow, J. 2007. *The Role of Agriculture in Development: Implications for Sub-Saharan Africa*. International Food Policy Research Institute

Frey, R. and Williams, D. 1994, *PC Instrumentation for the 90s*, 4th edn, Perth: Boston Technical Books Pty Ltd.

Gelbard, A. and Haub, C. 1999. Population growth before 1900.(World Population Beyond Six Billion). *Population Bulletin*. (1): 4.

Goering, C. E. 2008. Celebrating a century of tractor development. *Resource*. 15(7): 5-6.

Gollin, D., Parente, S. and Rogerson, R. 2002. The role of agriculture in development. *American Economic Review*. 92(2): 160-164.

Hazell, L. C. and Brodie, G. 2005. Investigating megalithic transport by preclassical Olmec society in Mesoanerica using GIS analysis of environmental and geographical elements of central Mexico to determine possible land route corridors. *Proc. Chacmool Conference*. Calgary, Canada.

Hazell, L. C. and Brodie, G. 2012. Applying GIS tools to define prehistoric megalith transport route corridors: Olmec megalith transport routes: a case study. *Journal of Archaeological Science*. 39(11): 3475-3479.

Hazell, L. C. and Fitzpatrick, S. M. 2006. The maritime transport of prehistoric megaliths in Micronesia. *Archæology and Physical Anthropology in Oceania*. 41(1): 12-24.

Heap, I. M. 2008. *International Survey of Herbicide Resistant Weeds*. 25th September, 2008. http://www.weedscience.org/in.asp

International Food Policy Research Institute. 2002. *Green Revolution: Curse or Blessing?* International Food Policy Research Institute

James, C. and Krattiger, A. F. 1996. *Global Review of the Field Testing and Commercialization of Transgenic Plants: 1986 to 1995*. The International Service for the Acquisition of Agri-biotech Application

Malthus, T. 1798, *An Essay on the Principle of Population*, London: J. Johnson, in St. Paul's Church-Yard.

Marsh, J. 2009. Railway History. *The Canadian Encyclopedia*.

Nyquist, H. 2002. Certain topics in telegraph transmission theory. *Proceedings of the IEEE*. 90(2): 280-305.

Perkins, A. J. 1929. A critical glance at some aspects of of tractor farming in Australia. *Journal of the Department of Agriculture of South Australia*. 33: 224-236.

Peterson, R. W. 1995. The growers. (agricultural scientists)(includes related article)(Masters of Invention). (9): 38.

Poddar, A. n.d. *Transportation Revolution*. 10th July, 2014. http://firstindustrialrevolution.weebly.com/transportation-revolution.html

Sayre, L. B. 2010. The pre-history of soil science: Jethro Tull, the invention of the seed drill, and the foundations of modern agriculture. *Physics and Chemistry of the Earth, Parts A/B/C*. 35(15-18): 851–859.

Schuh, G., Gottschalk, S. and Hohne, T. 2007. High Resolution Production Management. *CIRP Annals - Manufacturing Technology*. 56(1): 439-442.

Scrimshaw, N. S. 1987. The Phenomenon of Famine. *Annual Review of Nutrition*. 7(1): 1-22.

Short, J. 2010. Transport innovations: the development of transport and society are inescapably interlinked. *OECD Observer*. (279): 40.

Stringer, R. 2001. *How important are the 'non-traditional' economic roles of agriculture in development?* Centre for International Economic Studies

Troudi, A., Sefi, M., Ben Amara, I., Soudani, N., Hakim, A., Zeghal, K. M., Boudawara, T. and Zeghal, N. 2012. Oxidative damage in bone and erythrocytes of suckling rats exposed to 2,4-dichlorophenoxyacetic acid. *Pesticide Biochemistry and Physiology*. 104(1): 19-27.

Tull, J. 1733, *The Horse-Hoing Husbandry: Or, an Essay on the Principles of Tillage and Vegetation. Wherein is Shewn a Method of Introducing a Sort of Vineyard-culture into the Corn-fields, in Order to Increase their Product, and Deminish the Common Expence; by the use of Instruments Described in Cuts*, London: Self Published.

Ubbelohde, A. R. 1963, *Man and Energy*, Harmondsworth, Middlesex: Penguin Books Ltd.

Vandoren, A. 1982, *Data Acquisition Systems*, Reston, Virginia: Reston Publishing.

3 A Brief Overview of Radio Frequency and Microwave Applications in Agriculture

There is great potential for using radio frequency and microwave technologies to solve problems associated with agricultural production. Studies have been undertaken to use radio frequency and microwave energy: to improve crop handling, storage and preservation; to provide pest and weed control for agricultural production; for food preservation and quarantine purposes; for land survey; for automatic data acquisition and communication; and for preconditioning of products for better quality and more energy efficient processing. This chapter is concerned with radio frequency and microwave applications in the agricultural industries for purposes other than human food processing. Many of these applications will be more fully explored in subsequent chapters.

3.1 Heating Applications

3.1.1 Crop Drying

Many studies have investigated the application of radio frequency and microwave energy to speed up crop and wood drying (Manickavasagan, et al. 2006, Setiady, et al. 2009). Microwave drying provides an alternative to traditional drying methods. Polar molecules are affected by radio frequency and microwave radiation; therefore polar molecule, such as free water, in a given matrix can be directly heated (Beary 1988). Bound water molecules are more difficult to volatilize because the fixed bond inhibits rotation (Beary 1988).

Microwave drying is a rapid drying technique that can be applied to specific foods, particularly high value products such as fruits and vegetables (Zhang, *et al.* 2006). Increasing concerns over product quality and production costs have motivated industry to adopt radio frequency and microwave drying technologies. The advantages of these systems include: shorter drying time, improved product quality, and flexibility in producing a wide variety of dried products (Zhang, *et al.* 2006); however current applications are limited to small categories of fruits and vegetables due to high start-up costs and relatively complicated technology as compared to conventional convection drying (Zhang, *et al.* 2006).

3.1.2 Quarantine

Dried timber, nuts and fruits are commonly treated by chemical fumigation to control field and storage pests before being shipped to domestic and international markets.

Because chemical fumigants such as methyl bromide are no longer available (Carter, *et al.* 2005), there is a heightened interest in developing non–chemical pest control. An important key to developing successful thermal treatments is to balance the need for complete insect mortality with minimal impact on the product quality. A common difficulty in using conventional hot–air disinfestation is the slow heating rate, non–uniform temperature distribution, and possible heat damage to heat–sensitive commodities (Wang, *et al.* 2003). A more promising approach is to heat the commodity rapidly using radio frequency (RF) or microwave dielectric heating to control insects (Nelson 2001, Wang, *et al.* 2003).

Interest in controlling insects, using electromagnetic energy, dates back nearly 70 years. Headlee (1929, 1931), cites one earlier report of experiments determining lethal exposures for several insect species to 12 MHz electric fields and the body temperatures produced in honey bees due to dielectric heating. Nelson (1996) has shown that microwaves can kill insects in grain; however one of the challenges for microwave insect control is to differentially heat the insects in preference to the grain that surrounds them. Nelson (1996) shows that differential heating depends on microwave frequency. It appears that using a 2.45 GHz microwave system, which is the frequency used in domestic microwave ovens, heats the bulk grain material, which then transfers heat to the insects; however lower frequencies heat the insects without raising the temperature of the surrounding material beyond 50 °C (Nelson 1996).

Nzokou et al (2008) investigated the use of kiln and microwave heat treatments for the sanitisation of emerald ash borer (*Agrilus planipennis* Fairmaire) infested logs. Their microwave treatment method was conducted in a 2.8 GHz microwave oven (volume: 0.062 m^3, power: 1250 W) manufactured by Panasonic (Panasonic Co., Secaucus, New Jersey). Due to the limited volume of the microwave oven, two runs were necessary to treat logs assigned to each microwave treatment temperature. Their results showed that a temperature of 65 °C was successful at sanitising the infested logs. Microwave treatment was not as effective as kiln treatment, probably because of the uneven distribution of the microwave fields and temperature inside the treated logs. This uneven temperature distribution is partly due to the nature of microwave heating, but may also be due to their choice of microwave chamber used during their experiments.

Park, *et al.* (2006) studied the survival of microorganisms after heating in a conventional microwave oven. Kitchen sponges, scrubbing pads, and syringes were deliberately contaminated with wastewater and subsequently exposed to microwave radiation. The heterotrophic plate count of the wastewater was reduced by more than 99 percent within 1 to 2 minutes of microwave heating. Coliform and *E. coli* in kitchen sponges were completely inactivated after 30 seconds of microwave heating. Bacterial phage MS2 was totally inactivated within 1 to 2 minutes, but spores of *Bacillus cereus* were more resistant than the other microorganisms tested, requiring 4 minutes of irradiation for complete eradication.

Microwave heating for quarantine control of pests in dry materials, such as wood, has been accepted internationally. This technology is now recognised by the Food and Agriculture Organisation (FAO) and implemented in the "International Standards for Phytosanitary Measures" (ISPM 15) (Bisceglia, *et al.* 2009).

A prototype for continuous pasteurisation of liquids and fruit preparations using radio frequency heating techniques has been available for several years. The product is pumped inside Teflon pipes and then heated up when it passes through the electromagnetic field generated between two facing metallic plates. The product is uniformly and quickly heated at the rate of 1°C/sec. As with many radio frequency and microwave heating applications, these systems provide faster product processing, better temperature control, and better energy efficiency than conventional pasteurisation processes (Meggiolaro 2014).

3.1.3 Effect of Microwave Heating on Seeds and Plants

Interest in the effects of high frequency electromagnetic waves on biological materials dates back to the late 19th century, while interest in the effect of high frequency waves on plant material began in the 1920's (Ark and Parry 1940). In many cases, short exposure of seeds to radio frequency and microwave radiation resulted in increased germination and vigour of the emerging seedlings (Tran 1979, Tran and Cavanagh 1979); however, long exposure usually resulted in seed death (Bebawi, *et al.* 2007).

Davis *et al.* (Davis, *et al.* 1971, Davis 1973) were among the first to study the lethal effect of microwave heating on seeds. They treated seeds, with and without any soil, in a microwave oven and showed that seed damage was mostly influenced by a combination of seed moisture content and the energy absorbed per seed. Other findings from their studies suggested that both the specific mass and specific volume of the seeds were strongly related to seed mortality (Davis 1973). This could be due to the "*radar cross-section*" (Wolf, *et al.* 1993) presented by seeds to propagating microwaves. Large radar cross-sections allow the seeds to intercept, and therefore absorb, more microwave energy. The geometry of many seeds can be regarded as ellipsoids or even spheres, so the microwave fields are focused into the centre of the seed. Therefore larger seeds focus more energy into their core, which results in higher temperatures at the centre of the seed, leading to higher mortality rates. Seeds whose geometry can be approximated as being cylindrical will also focus more energy into their core as their dimensions increase.

Microwaves can kill a range of weed seeds in the soil (Davis, *et al.* 1971, Davis 1973, Brodie, *et al.* 2009), however fewer studies have considered the efficacy of using microwave energy to manage already emerged weed plants. Davis et al. (1971) considered the effect of microwave energy on bean (*Phaseolus vulgaris*) and Honey Mesquite (*Prosopis glandulosa*) seedlings. They discovered that plant aging had little effect on the susceptibility of bean plants to microwave damage, but honey mesquite's

resistance to microwave damage increased with aging. They also discovered that bean plants were more susceptible to microwave treatment than honey mesquite plants.

Bigu-Del-Blanco, *et al.* (1977) exposed 48 hour old seedlings of *Zea mays* (var. Golden Bantam) to 9 GHz radiation for 22 to 24 hours. The power density levels were between 10 and 30 mW cm^{-2} at the point of exposure. Temperature increases of only 4 °C, when compared with control seedlings, were measured in the microwave treated specimens. The authors concluded that the long exposure to microwave radiation, even at very low power densities, was sufficient to dehydrate the seedlings and inhibit their development. On the other hand, recent studies on fleabane (*Conyza bonariensis*) and paddy melon (*Cucumis myriocarpus*) (Brodie, *et al.* 2012a, b) have revealed that a very short (less than 5 second) pulse of microwave energy, focused onto the plant stem, was sufficient to kill these plants.

In weed control, microwave radiation is not affected by wind, which extends the application periods compared with conventional herbicide spraying. Energy can also be focused onto individual plants without affecting adjacent plants (Brodie, *et al.* 2012b). This would be very useful for in-crop or spot weed control activities. Microwave energy can also kill the roots and seeds that are buried to a depth of several centimetres in the soil (Diprose, *et al.* 1984, Brodie, *et al.* 2007).

3.1.4 Microwave Treatment of Animal Fodder

Hay is an important feed source for ruminant animals so every effort should be made to improve its feed conversion efficiency and reduce the risk of importing weed seeds as hay is transported from one location to another. Similarly, cereal grains are the base of most horse rations, because they are a valuable source of digestible energy; however their use is always associated with some risk.

The major concern when feeding cereal grains to horses is the risk of incomplete starch digestion in the small intestine, which enables significant amounts of starch to pass through to the caecum and colon. When starch is able to reach these organs it rapidly ferments producing an accumulation of acidic products, which place the horse at risk of developing serious and potentially fatal illnesses such as laminitis, colic and ulcers (Bird, *et al.* 2001).

Dong *et al.* (2005) discovered that organic matter degradability of wheat straw in the rumen of yaks was increased by around 20% after 4 min of treatment in a 750 W, 2.54 GHz, microwave oven. Sadeghi and Shawrang (2006a) showed that microwave treatment of canola meal increased *in vitro* dry matter disappearance, including substances that were deemed to be ruminally undegradable. Sadeghi and Shawrang (2006b) also showed that microwave treatment reduced the rumen degradable starch fraction of corn grain and decreased crude protein degradation of soya-bean meal (Sadeghi, *et al.* 2005) compared with untreated samples. No studies of microwave treatment of horse feeds could be found in the available literature.

Small scale *in vitro* pepsin-cellulase digestion experiments (Brodie, *et al.* 2010), similar to the technique developed by McLeod and Minson (1978, 1980), demonstrated that microwave treatment: increased dry matter percentage with increasing microwave treatment time; increased *in vitro* dry matter disappearance with increasing microwave treatment time; but had no significant effect on post-digestion crude protein content.

When 25 kg bags of lucerne fodder were treated in an experimental 6 kW, 2.45 GHz, microwave heating chamber (Harris, *et al.* 2011) were subjected to a similar *in vitro* pepsin-cellulase digestion study, dry matter disappearance significantly increased compared to the untreated samples; however there was no significant difference attributable to the duration of microwave treatment. Feeding 12-14 month old Merino sheep on a "maintenance ration" of microwave treated Lucerne resulted in a significant increase in body weight instead of the relatively constant body weight that would be expected from a maintenance ration. By the end of the 5 week feeding trial the control group was only 0.4 % heavier than when they started, which would be expected from a maintenance ration. However the group being fed the microwave treated lucerne gained 7 % of their initial body weight in the second week of the trial and maintained this body weight until the end of the trial. Their finishing weight after 5 weeks was 8.1 % higher than their starting weight (Brodie, *et al.* 2010).

3.1.5 Microwave Assisted Extraction

During microwave assisted extraction (MAE), plant materials such as wood, seeds and leaves are suspended in solvents and the mixture is exposed to microwave heating instead of conventional heating. Enhanced rates of plant oil extraction have been observed for a range of plant materials. Chen and Spiro (1994) examined the extraction of the essential oils of peppermint and rosemary from hexane and ethanol mixtures and found that yields were more than one third greater in the microwave assisted extractions. Saoud et al. (2006) studied MAE of essential oils from tea leaves and achieved higher yields (26.8 mg/g) than conventional steam distillation (24 mg/g).

Chemat et al. (2005) studied the extraction of oils from limonene and caraway seeds and found that MAE led to more rapid extraction as well as increased yields. Scanning electron microscopy of the microwave treated and untreated seeds revealed significantly increased rupture of the cell walls in the treated seeds. MAE also led to a more chemically complex extract, which was thought to be a better representation of the true composition of the available oils in caraway seed.

Industrial scale microwave assisted extraction systems have been developed and used in several countries. Several approaches to industrial microwave-assisted extraction techniques have been developed. These include: continuous-flow reactors; small-scale batch stop-flow protocols; or large-scale single-batch reactors (Hoz, *et al.* 2011).

One of the limitations of microwave scale-up technology is the restricted penetration depth of microwave irradiation into absorbing materials (Hoz, *et al.* 2011). This means that solvent or reagents in the centre of large reaction vessel are heated by convection and not by direct 'in core' microwave dielectric heating (Brodie 2008a).

Although less well described in the literature, an alternative approach for utilizing microwave heating of plant based materials has been to treat the materials with microwave energy prior to conventional extraction processes (Miletic, et al. 2009). Microwave preconditioning of sugar cane prior to juice diffusion studies led to significant decreases in colour and significant increases in juice yield, Brix %, purity and Pol % (Brodie, et al. 2011). Microwave treatment significantly reduced the compression strength of the sugar cane samples (Brodie, et al. 2011), especially while the cane was still hot from the microwave treatment. This treatment option reduced the compressive strength of the cane to about 18 % of its original strength, implying that much less energy would be required to crush the cane for juice extraction.

3.1.6 Microwave Assisted Pyrolysis and Bio-fuel Extraction

Three different thermo-chemical conversion processes are possible, depending on the availability of oxygen during the process: combustion (complete oxidation), gasification (partial oxidation) and pyrolysis (thermo-chemical degradation without oxygen). Among these, combustion is the most common option for recovering energy. Combustion is also associated with the generation of carbon oxides, sulphur, nitrogen, chlorine products (dioxins and furans), volatile organic compounds, polycyclic aromatic hydrocarbons, and dust (Fernandez, et al. 2011); however gasification and pyrolysis offer greater efficiencies in energy production, recovery of other compounds and less pollution.

Most studies of pyrolysis behaviour have considered lingo-cellulosic materials, which comprise of a mixture of hemicellulose, cellulose, lignin and minor amounts of other organic compounds. While cellulose and hemicelluloses form mainly volatile products during pyrolysis due to the thermal cleavage of the sugar units, lignin mainly forms char since it is not readily cleaved into lower molecular weight fragments (Fernandez, et al. 2011). Wood, crops, agricultural and forestry residues, and sewage sludges (Dominguez, et al. 2005) can be subjected to pyrolysis processes to recover valuable chemicals and energy.

Conventional heating transfers heat from the surface towards the centre of the material by convection, conduction and radiation; however microwave heating is a direct conversion of electromagnetic energy into thermal energy within the volume of the material (Metaxas and Meredith 1983). In microwave heating, the material is at higher temperature than its surroundings, unlike conventional heating where it is necessary for the surrounding atmosphere to reach the desired operating temperature before heating the material (Fernandez, et al. 2011). Consequently, microwave heating

favours pyrolysis reactions involving the solid material, while conventional heating improves the reactions that take place in surroundings, such as homogeneous reactions in the gas-phase (Fernandez, et al. 2011). In microwave heating, the lower temperatures in the microwave cavity can also be useful for condensing the final pyrolysis vapours on the cavity walls.

Microwave assisted pyrolysis yields more gas and less carbonaceous (char) residue, which demonstrate the efficiency of microwave energy (Fernandez, et al. 2011). The conversion rates in microwave assisted pyrolysis are always higher than those observed in conventional heating at any temperature. The differences between microwave heating and conventional heating seems to be reduced with temperature increase, which points to the higher efficiency of microwave heating at lower temperatures (Fernandez, et al. 2011).

Bio-fuel extraction is facilitated when microwave energy is used to thermally degrade various organic polymers to facilitate extraction of sugars for fermentation (Tsubaki and Azuma 2011). These sugars can then be fermented and distilled to create fuel alcohols. Woody plant materials are commonly subjected to microwave assisted bio-fuel extraction; however other materials such as discharge from food processing industries, agriculture and fisheries can also be processed using these techniques. Other materials that have been subjected to microwave assisted bio-fuel extraction include: soybean residue; barley malt feed; tea residues; stones from Japanese apricots; corn pericarp, which is a by-product from corn starch production; and Makombu (*Laminaria japonica*), which is a kind of brown sea algae.

3.2 Sensor Applications

3.2.1 Assessment of Wood

Early non-destructive detection of biological degradation in wood, such as decay or termite attack, is important if remedial treatments are to be effective. Wood and wood based materials are relatively transparent at microwave frequencies (Torgovnikov 1993, Daian, *et al*. 2005); however their level of transparency decreases as moisture or other materials are added to the wood. Conversely, wood's transparency increases as wood material is softened due to fungal decay or other biological degradation.

When microwaves are transmitted through wood (Figure 3.1), the wave will be partially reflected, attenuated and delayed compared to a wave traveling through free space (Lundgren 2005, Brodie 2008b). Wave attenuation; reflections from the surface; and internal scattering from embedded objects or cavities causes a "shadow" on the opposite side of the material from the microwave source. An x-ray image is a good example of the information that can be derived from wave attenuation and phase delay measurement.

The transparency of wood, or any other material, to electromagnetic waves is linked to the complex dielectric properties of the material under study (James 1975, Torgovnikov 1993, Olmi, *et al.* 2000). The real part of the complex dielectric properties determines the wave length of the electromagnetic wave inside the object and therefore influences the speed of wave propagation through the object. The imaginary part of the complex dielectric properties determines the amount of energy that the material will absorb from the wave as it travels into or through the object.

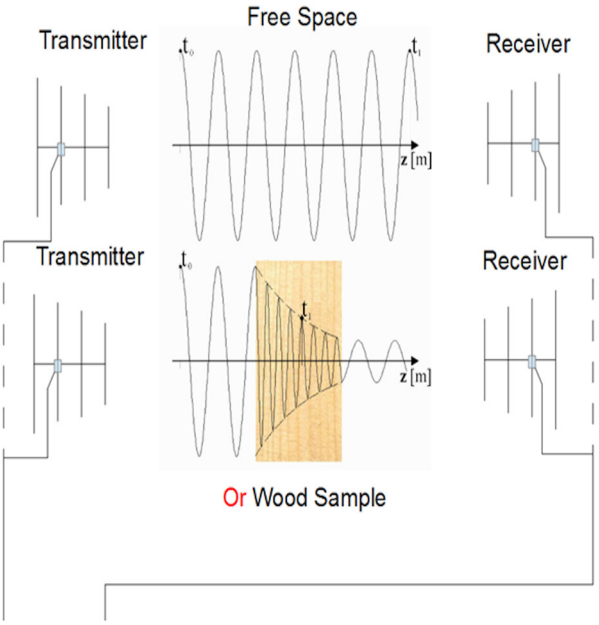

Figure 3.1: Schematic of a simple "look through" system for assessing wood status using microwave energy (Source: Brodie, *et al.* 2014).

3.2.2 Radar Systems

Active sensors provide their own source of energy to illuminate the target. Active sensors are generally divided into two distinct categories: imaging and non-imaging. The most common form of active imaging sensor is RADAR.

Non-imaging sensors include altimeters and scatterometers. Radar altimeters transmit short microwave pulses and measure the round trip time to targets to determine their distance from the sensor (Canadian Centre for Remote Sensing 2003). Scatterometers are used to make precise quantitative measurements of the amount of energy reflected from targets. The amount of reflected energy is dependent on the

surface properties (roughness) and the angle at which the energy strikes the target (Canadian Centre for Remote Sensing 2003).

RADAR is an acronym for **RA**dio **D**etection **A**nd **R**anging (Connor 1972). Radar is essentially a ranging or distance-measuring device. It consists of a transmitter, a receiver, an antenna, and an electronics system to process and record the data (Connor 1972). The transmitter generates successive short bursts (or pulses) of microwave energy at regular intervals, which are focused by the antenna into a beam (Connor 1972).

In the case of terrain imaging radar, the radar beam is projected at right angles to the motion of the aircraft or satellite platform at an oblique angle to the terrain and reflects back to the source. This is similar to the flash of a camera. The antenna receives a portion of the reflected energy (or backscatter) from various objects within the illuminated beam (Sabins 1987, Drury 1998, Canadian Centre for Remote Sensing 2003). By measuring the time delay between the transmission of a pulse and the reception of the echo from different targets, their distance from the radar and thus their location in the resulting image can be determined (Sabins 1987, Drury 1998, Canadian Centre for Remote Sensing 2003).

One of the more useful features of radar is that the speed of moving objects can be determined with considerable accuracy. Doppler shift is the apparent change in wavelength (or frequency) of an electromagnetic or acoustic wave when there is relative movement between the transmitter and the receiver. This effect is commonly noticeable when a whistling train or police siren passes by. An observer in front of the moving car or train hears a higher pitch than a passenger in the vehicle. Similarly, the passenger hears a higher pitch than an observer behind the vehicle. Doppler can also affect the frequency of a radar carrier wave, the time between pulses of a radar signal, or even light waves causing an apparent shift of colour.

Ground penetrating radar (GPR) has been used for over twenty years at chemical and nuclear waste disposal sites as a non-invasive technique for site characterization. Standard GPR surveys are conducted from the surface of the ground providing geotechnical information from the surface to depths of 2 to 15 m, depending on GPR's operating frequency and soil conductivity. Commercially available GPR systems operate over the frequency range from 50 MHz to 1,000 MHz.

Lower frequencies provide better penetration into the soil but poor resolution, while the higher frequencies give poor penetration but good resolution. There are many critical environmental monitoring situations where surface GPR does not provide the depth of penetration or necessary resolution. Borehole radar can place the sensor closer to the region of interest, overcoming the high signal attenuation near the surface.

3.3 Communication Systems

Agriculture is facing new and severe challenges due to the growing global population, which is expected to reach 9 billion by 2050. Feeding that population will require a 70 percent increase in food production (McNamara, *et al.* 2012). Modern production systems rely as much on good dissemination of Information as they do on physical systems that directly contribute to production. Communication has always mattered in agriculture. Updated information allows farmers to: keep up to date with markets; maintain contact with family, colleagues and workers; automate many aspects of their production systems; and provide important knowledge about new production systems.

The arrival of information communication technology (ICT) is well timed (McNamara, *et al.* 2012). The benefits of the green revolution greatly improved agricultural productivity; however, there is a demonstrable need for a new revolution that will contribute to "smart" agriculture that can increase production (McNamara, *et al.* 2012) and potentially ward off Malthus' predicted catastrophe (Malthus 1798). Available technology has allowed access to unprecedented amounts of agricultural and scientific data and mobile telephony, wireless data transmission, and the Internet have found a foothold, even in poor small farms (McNamara, *et al.* 2012).

3.4 Conclusion

Microwave and radio frequency energy has many potential applications in the agricultural and forestry industries. This chapter has discussed a few of these, but there are many more that have not been included. The purpose of this chapter was to encourage practitioners within the microwave engineering and agricultural and forestry industries to explore the many possibilities of applying radio frequency and microwave energy to address many problems and opportunities within primary industries. Clearly, the interaction between electromagnetic fields and materials is critical. The next chapter will explore these interactions more thoroughly.

References

Ark, P. A. and Parry, W. 1940. Application of High-Frequency Electrostatic Fields in Agriculture. *The Quarterly Review of Biology*. 15(2): 172-191.

Beary, E. S. 1988. Comparison of microwave drying and conventional drying techniques for reference materials. *Analytical Chemistry*. 60(8): 742-746.

Bebawi, F. F., Cooper, A. P., Brodie, G. I., Madigan, B. A., Vitelli, J. S., Worsley, K. J. and Davis, K. M. 2007. Effect of microwave radiation on seed mortality of rubber vine (*Cryptostegia grandiflora* R.Br.), parthenium (*Parthenium hysterophorous* L.) and bellyache bush (*Jatropha gossypiifolia* L.). *Plant Protection Quarterly*. 22(4): 136-142.

Bigu-Del-Blanco, J., Bristow, J. M. and Romero-Sierra, C. 1977. Effects of low-level microwave radiation on germination and growth rate in corn seeds. *Proceedings of the IEEE*. 65(7): 1086-1088.

Bird, S., Brown, W. and Rowe, J. 2001. *Safe and Effective Grain Feeding for Horses*. Rural Industries Research and Development Corporation

Bisceglia, B., De Leo, R. and Diaferia, N. 2009. MW PALLETS DISINFESTATIONS. *Journal of Microwave Power & Electromagnetic Energy*. 43(4): 1-13.

Brodie, G. 2008a. The influence of load geometry on temperature distribution during microwave heating. *Transactions of the American Society of Agricultural and Biological Engineers*. 51(4): 1401-1413.

Brodie, G., Hamilton, S. and Woodworth, J. 2007. An assessment of microwave soil pasteurization for killing seeds and weeds. *Plant Protection Quarterly*. 22(4): 143-149.

Brodie, G., Harris, E., Farrell, P., Tse, N. A., Roberts, A. and Kvansakul, J. 2014. In-situ, noninvasive investigation of an outdoor wooden sculpture. *Proc. ICOM-CC 17th Triennial Conference*. 1-9. ICOM-CC 17th Triennial Conference Preprints, Melbourne, 15–19 September 2014

Brodie, G., Harris, G., Pasma, L., Travers, A., Leyson, D., Lancaster, C. and Woodworth, J. 2009. Microwave soil heating for controlling ryegrass seed germination. *Transactions of the American Society of Agricultural and Biological Engineers*. 52(1): 295-302.

Brodie, G., Jacob, M. V., Sheehan, M., Yin, L., Cushion, M. and Harris, G. 2011. Microwave modification of sugar cane to enhance juice extraction during milling. *Journal of Microwave Power and Electromagnetic Energy*. 45(4): 178-187.

Brodie, G., Rath, C., Devanny, M., Reeve, J., Lancaster, C., Harris, G., Chaplin, S. and Laird, C. 2010. Effect of microwave treatment on lucerne fodder. *Animal Production Science*. 50(2): 124–129.

Brodie, G., Ryan, C. and Lancaster, C. 2012a. The effect of microwave radiation on Paddy Melon (Cucumis myriocarpus). *International Journal of Agronomy*. 2012: 1-10.

Brodie, G., Ryan, C. and Lancaster, C. 2012b. Microwave technologies as part of an integrated weed management strategy: A Review. *International Journal of Agronomy*. 2012: 1-14.

Brodie, G. I. 2008b, *Innovative wood drying: Applying microwave and solar technologies to wood drying*, Saarbruecken, Germany: VDM Verlag.

Canadian Centre for Remote Sensing. 2003. *Fundamentals of Remote Sensing*. February 6, 2004. http://www.ccrs.nrcan.gc.ca/ccrs/learn/tutorials/fundam/fundam_e.html

Carter, C. A., Chalfant, J. A., Goodhue, R. E., Han, F. M. and DeSantis, M. 2005. The Methyl Bromide Ban: Economic Impacts on the California Strawberry Industry. *Review of Agricultural Economics*. 27(2): 181-197.

Chemat, S., Aït-Amar, H., Lagha, A. and Esveld, D. C. 2005. Microwave-assisted extraction kinetics of terpenes from caraway seeds. *Chemical Engineering and Processing*. 44(12): 1320-1326.

Chen, S. S. and Spiro, M. 1994. Study of microwave extraction of essential oil constituents from plant materials. *Journal of Microwave Power and Electromagnetic Energy*. 29(4): 231-241.

Connor, F. R. 1972, *Antennas*, London: Edward Arnold.

Daian, G., Taube, A., Birnboim, A., Shramkov, Y. and Daian, M. 2005. Measuring the dielectric properties of wood at microwave frequencies. *Wood Science and Technology*. 39(3): 215 -223.

Davis, F. S., Wayland, J. R. and Merkle, M. G. 1971. Ultrahigh-Frequency Electromagnetic Fields for Weed Control: Phytotoxicity and Selectivity. *Science*. 173(3996): 535-537.

Davis, F. S., Wayland, J. R. and Merkle, M. G. 1973. Phytotoxicity of a UHF Electromagnetic Field. *Nature*. 241(5387): 291-292.

Diprose, M. F., Benson, F. A. and Willis, A. J. 1984. The Effect of Externally Applied Electrostatic Fields, Microwave Radiation and Electric Currents on Plants and Other Organisms, with Special Reference to Weed Control. *Botanical Review*. 50(2): 171-223.

Dominguez, A., Menendez , J. A., Inguanzo, M. and Pis, J. J. 2005. Investigations into the characteristics of oils produced from microwave pyrolysis of sewage sludge. *Fuel Processing Technology*. 86(9): 1007 -1020.

Dong, S., Long, R., Zhang, D., Hu, Z. and Pu, X. 2005. Effect of microwave treatment on chemical composition and in sacco digestibility of wheat straw in yak cow *Asian-Australasian Journal of Animal Sciences*. 18(1): 27-31.

Drury, S. A. 1998, *Images of the Earth: A guide to Remote Sensing*, 2nd edn, Oxford University Press.

Fernandez, Y., Arenillas, A. and Menendez, J. A. 2011 Microwave heating applied to pyrolysis. In *Advances in Induction and Microwave Heating of Mineral and Organic Materials*, 723-752. Grundas, S. ed. InTech: Rijeka, Croatia.

Harris, G. A., Brodie, G. I., Ozarska, B. and Taube, A. 2011. Design of a Microwave Chamber for the Purpose of Drying of Wood Components for Furniture. *Transactions of the American Society of Agricultural and Biological Engineers*. 54(1): 363-368.

Headlee, T. J. 1931. The difference between the effect of radio waves on insects and on plants. *Journal of Economic Entomology*. 24(2): 427-437.

Headlee, T. J. and Burdette, R. C. 1929. Some Facts Relative to the Effect of High Frequency Radio Waves on Insect Activity. *Journal of the New York Entomological Society*. 37(1): 59-64.

Hoz, A. D. L., Alcázar, J., Carrillo, J., Herrero, M. A., Muñoz, J. D. M., Prieto, P., Cózar, A. D. and Diaz-Ortiz, A. 2011 Reproducibility and Scalability of Microwave-Assisted Reactions. In *Microwave Heating*, 137-162. InTech.

James, W. L. 1975. *Dielectric properties of wood and hardboard: Variation with temperature, frequency, moisture content, and grain orientation*. U.S. Department of Agriculture

Lundgren, N. 2005. Modelling Microwave Measurements in Wood. Unpublished thesis. Luleå University of Technology, Department of Skellefteå Campus, Division of Wood Science and Technology

Malthus, T. 1798, *An Essay on the Principle of Population*, London: J. Johnson, in St. Paul's Church-Yard.

Manickavasagan, A., Jayas, D. S. and White, N. D. G. 2006. Non-Uniformity of Surface Temperatures of Grain after Microwave Treatment in an Industrial Microwave Dryer. *Drying Technology*. 24(12): 1559–1567.

McLeod, M. N. and Minson, D. J. 1978. The accuracy of the pepsin-cellulase technique for estimating the dry matter digestibility in vivo of grasses and legumes. *Animal Feed Science and Technology*. 3(4): 277-287.

McLeod, M. N. and Minson, D. J. 1980. A note on Onozuka 3S cellulase as a replacement for Onozuka SS (P1500) cellulase when estimating forage digestibility in vitro. *Animal Feed Science and Technology*. 5(4): 347-350.

McNamara, K., Belden, C., Kelly, T., Pehu, E. and Donovan, K. 2012, *ICT in Agriculture Sourcebook*.

Meggiolaro, F. 2014. *In-line Pasteurisation of Fluidized Products by Means of Radio Frequency Heating*. AMPERE

Metaxas, A. C. and Meredith, R. J. 1983, *Industrial Microwave Heating*, London: Peter Peregrinus.

Miletic, P., Grujic, R. and Marjanovic-Balaban, Z. 2009. The application of microwaves in essential oil hydro-distillation processes. *Chemical Industry and Chemical Engineering Quarterly*. 15(1): 37-39.

Nelson, S. O. 1996. Review and assessment of radio-frequency and microwave energy for stored-grain insect control. *Transactions of the ASAE*. 39(4): 1475-1484.

Nelson, S. O. 2001. Radio-frequency and microwave dielectric properties of insects. *Journal of Microwave Power and Electromagnetic Energy*. 36(1): 47-56.

Nzokou, P., Tourtellot, S. and Kamdem, D. P. 2008. Kiln and microwave heat treatment of logs infested by the emerald ash borer (Agrilus planipennis Fairmaire) (Coleoptera: Buprestidae). *Forest Products Journal*. 58(7/8): 68.

Olmi, R., Bini, M., Ignesti, A. and Riminesi, C. 2000. Dielectric properties of wood from 2 to 3 GHz. *Journal of Microwave Power and Electromagnetic Energy*. 35(3): 135-143.

Park, D., Bitton, G. and Melker, R. 2006. Microbial inactivation by microwave radiation in the home environment. *Journal of Environmental Health*. 69(5): 17-24.

Sabins, F. F. 1987, *Remote Sensing, Principles and Interpretation*, New York: W. H. Freeman and Co.

Sadeghi, A. A., Nikkhaha, A. and Shawrang, P. 2005. Effects of microwave irradiation on ruminal degradation and in vitro digestibility of soya-bean meal. *Animal Science*. 80(3): 369-375.

Sadeghi, A. A. and Shawrang, P. 2006a. Effects of microwave irradiation on ruminal degradability and in vitro digestibility of canola meal. *Animal Feed Science and Technology*. 127(1-2): 45-54.

Sadeghi, A. A. and Shawrang, P. 2006b. Effects of microwave irradiation on ruminal protein and starch degradation of corn grain. *Animal Feed Science and Technology*. 127(1-2): 113-123.

Saoud, A. A., Yunus, R. M. and Aziz, R. A. 2006. Yield study for extracted tea leaves essential oil using microwave-assisted process. *American Journal of Chemical Engineering*. 6(1): 22-27.

Setiady, D., Tang, J., Younce, F., Swanson, B. A., Rasco, B. A. and Clary, C. D. 2009. Porosity, Color, Texture, and Microscopic Structure of Russet Potatoes Dried Using Microwave Vacuum, Heated Air, and Freeze Drying *Applied Engineering in Agriculture*. 25(5): 719-724.

Torgovnikov, G. I. 1993, *Dielectric Properties of Wood and Wood-Based Materials*, Springer Series in Wood Science, Berlin: Springer-Verlag.

Tran, V. N. 1979. Effects of Microwave Energy on the Strophiole, Seed Coat and Germination of Acacia Seeds. *Australian Journal of Plant Physiology*. 6(3): 277-287.

Tran, V. N. and Cavanagh, A. K. 1979. Effects of microwave energy on Acacia longifolia. *Journal of Microwave Power*. 14(1): 21-27.

Tsubaki, S. and Azuma, J.-i. 2011 Application of microwave technology for utilization of recalcitrant biomass. In *Advances in Induction and Microwave Heating of Mineral and Organic Materials*, 697-722. Grundas, S. ed. InTech: Rijeka, Croatia.

Wang, S., Tang, J., Cavalieri, R. P. and Davis, D. C. 2003. Differential heating of insects in dried nuts and fruits associated with radio frequency and microwave treatment. *Transactions of the ASAE*. 46(4): 1175–1182.

Wolf, W. W., Vaughn, C. R., Harris, R. and Loper, G. M. 1993. Insect radar cross-section for aerial density measurement and target classification. *Transactions of the American Society of Agricultural and Biological Engineers*. 36(3): 949-954.

Zhang, M., Tang, J., Mujumdar, A. S. and Wang, S. 2006. Trends in microwave-related drying of fruits and vegetables. *Trends in Food Science & Technology*. 17(10): 524-534.

4 Microwaves and their Interactions with Materials

The earth has three important fields associated with it. Two of these fields are obvious and taken for granted, the other is important, but not so obvious to the casual observer. The obvious fields are: the gravitational field and the magnetic field. The not so obvious one is the electrical field that exists between the surface of the earth and the ionosphere, which is high in the atmosphere. Interestingly, the gravitational field is the weakest of all field forces. The main reason that gravitational fields are so obvious is because planets and stars are so massive and therefore manifest large gravitational fields. The magnetic field is strong and protects the earth by deflecting charged particles away from the earth and provides orientation for many creatures including humanity; however magnetic fields are much weaker than an electrical field.

Experiments since very early times demonstrate that there are two types of matter. When two particles of the same type of matter are brought into close proximity to each other, a force grows between them that push them apart. The closer these particles come to each other, the stronger this force becomes. When two particles of different types are brought into close proximity to each other, a force grows between them that pulls them together. These two types of matter are designated as positive or negative and the property that differentiates between the two types of matter is called charge. When charges are static (i.e. not moving) these forces act radially from the centre of the charged particle. This radially acting force is caused by an electrical field.

When charge moves, a magnetic field comes into existence. When current (moving charges) flows through a wire, a magnetic field begins to circulate around the wire. If the wire is wound into a coil, the individual magnetic fields from each turn in the coil add to the magnetic field of its neighbour and so the magnetic field becomes stronger. This of course is an electro-magnetic coil. When the electrical current is turned off and the charges stop flowing, the magnetic field decays and disappears.

In a similar way, if a magnetic field exists in some volume of space and a charged particle travels into that volume, the charged particle experiences a phenomenon that forces it to follow a curved (or even circular) path through this space where as in the absence of any magnetic field it follows a straight path through space. Therefore it is apparent that electric fields and magnetic fields are linked. It also becomes apparent that torsion (or twisting action) is involved in these interactions between electric and magnetic fields.

The idea of a field is really an abstract thought that is used to better describe the effect of one object on another without being in contact with it. It is a little unclear, even in this modern era, what a field really is. If the field around a charged particle can be imagined like spokes on a wheel, it is clear that the spokes are closer together near the hub of the wheel and further apart from one another at the rim. In a similar way, field lines can be imagined to be closer together immediately near a charged particle and become further apart with distance from the particle. In a similar thought,

there is a curling effect of magnetic fields on moving charged particles and there is also a curling effect of moving charged particles on magnetic fields. There are two nice mathematical tools that can calculate how quickly field lines diverge from one another with distance from a charged particle and how much of a curling influence a field may have. It is no surprise that these are called the "divergence" and the "curl" operators. These operators must be applied to quantities called Vectors.

4.1 Electric and Magnetic Field Vectors

Because electric and magnetic fields exert forces on charged particles, they must be regarded as vector quantities. They have both a magnitude and direction of action. It is possible to perform various mathematical operations on vector quantities, including the application of calculus. Most of these mathematical operations will yield vector quantities; however some will yield non-vector quantities; which are called scalars. A scalar only has magnitude; there is no direction of operation associated with a scalar. Therefore any normal number is a scalar.

Changes in scalar quantities in space can be mapped using contours. For example, land elevation is a scalar quantity and is usually designated as some height above a datum. These values are designated by contours on a map. As another example, a synoptic weather map has contour lines to depict air pressure.

The steepness of a hill side can be determined by measuring how close together the contour lines are. This calculation is called the gradient; however the gradient has a particular direction, which is up the steepest part of the slope. Therefore the gradient of a scalar field is actually a vector quantity.

Gradient has a mathematical definition. The gradient of some scalar field f(x, y, z), which has a defined value at every point (x, y, z) is given by:

$$\nabla f\left(x,y,z\right)=\hat{i}\,\frac{\partial f}{\partial x}+\hat{j}\,\frac{\partial f}{\partial y}+\hat{k}\,\frac{\partial f}{\partial z} \tag{4.1}$$

In this case the unit (or basis) vectors in the x, y, and z directions $\left(\hat{i},\hat{j},\ and\ \hat{k}\right)$ are used to define the final direction of the vector of fastest change for the scalar quantity.

As mentioned earlier, electric and magnetic phenomenon depend on how quickly the electric and magnetic fields diverge from one another. This divergence value is simply a number, without any particular direction associated with it; therefore it is a scalar value.

Divergence also has a mathematical definition. The divergence of some vector field $\vec{f}(x,y,z)$, which has a defined value at every point (x, y, z) is given by:

$$\nabla \cdot \vec{f}(x,y,z) = \frac{\partial f_x}{\partial x} + \frac{\partial f_y}{\partial y} + \frac{\partial f_z}{\partial z} \tag{4.2}$$

So the divergence is a measure of the tendency for a field to converge or repel from within a given volume of space. Because there are no basis vectors involved in the calculation, the final result is a scalar quantity.

The other feature of vector fields is their rotational tendencies. This is particularly true of electromagnetic phenomenon. The degree of rotation in a given space can be determined by calculating the curl of the vector field.

Curl also has a mathematical definition. The curl of some vector field $\vec{f}(x,y,z)$, which has a defined value at every point (x, y, z) is given by:

$$\nabla \times \vec{f}(x,y,z) = \hat{i}\left(\frac{\partial f_z}{\partial y} - \frac{\partial f_y}{\partial z}\right) + \hat{j}\left(\frac{\partial f_x}{\partial z} - \frac{\partial f_z}{\partial x}\right) + \hat{k}\left(\frac{\partial f_y}{\partial x} - \frac{\partial f_x}{\partial y}\right) \tag{4.3}$$

Because there are basis vectors involved in the calculation, the final result is a vector quantity.

4.2 Maxwell's Equations for Electro-magnetism

James Clerk Maxwell combined the fundamental properties of electrical and magnetic behaviour into a mathematical model of electromagnetism, which he based on earlier work carried out by Faraday, Ampere and Gauss. Maxwell published this work in "A Treatise on Electricity and Magnetism", 1873. Others have refined Maxwell's original equations, using the ideas of divergence and curl. The final result is four fundamental equations that when used in their proper combinations can describe every electrical or magnetic phenomenon.
Maxwell's equations can be defined as:

$$\nabla \times \vec{E} = -\mu \frac{\partial \vec{H}}{\partial t} \tag{4.4}$$

$$\nabla \times \vec{H} = \varepsilon \frac{\partial \vec{E}}{\partial t} + \sigma \vec{E} + \vec{J}_s \tag{4.5}$$

$$\nabla \cdot \vec{E} = \frac{\rho}{\varepsilon} \tag{4.6}$$

$$\nabla \cdot \vec{H} = 0 \tag{4.7}$$

where ε is the electrical permittivity of the space in which the electrical field E exists; μ is the magnetic permeability of the space in which the magnetic field H exists; σ is the conductivity of the space in which the electrical field exists; Js accounts for any source current densities in the space of interest; and ρ accounts for any stationary charges in the space of interest.

In anisotropic media, where the orientation of the electric or magnetic fields is critical to the electrical behaviour of the material: the dielectric permittivity; magnetic permeability; and electrical conductivity are tensors (having different values depending on the orientation of the field vectors) rather than single values. In vacuum, which is isotropic, the dielectric permittivity and the magnetic permeability are constants and the conductivity is zero. In this case $\varepsilon_o = 8.854187817 \times 10^{-12}$ (F/m) and $\mu_o = 4\pi \times 10^{-7}$ (H/m).

One of the most important contributions made by Maxwell was to clarify that light was actually electromagnetic waves.

Although it takes a while to go through the mathematical derivation, Maxwell's equations can be combined and manipulated to ultimately yield the following relationship:

$$\nabla^2 \vec{E} = \mu\varepsilon \frac{\partial^2 \vec{E}}{\partial t^2} + \mu\sigma \frac{\partial \vec{E}}{\partial t} + \mu \frac{\partial \vec{J}_s}{\partial t} + \nabla\left(\frac{\rho}{\varepsilon}\right) \tag{4.8}$$

This is called a wave equation, because the solution to this type of equation behaves like a wave. A similar wave equation for the magnetic field can also be derived from Maxwell's equations.

In particular, equation (4.8) is called a "forced, damped wave equation". It is made up of three components:

1. $$\nabla^2 \vec{E} = \mu\varepsilon \frac{\partial^2 \vec{E}}{\partial t^2} + \mu\sigma \frac{\partial \vec{E}}{\partial t}$$

   , which is wave response that diminishes as the wave travel along due to energy being absorbed by the space due to the conductivity properties of the space (usually the wave energy is transformed into heat energy in the space of interest);

2. $$\mu \frac{\partial \vec{J}_s}{\partial t},$$

   which is a time varying current that "forces" (or creates) the damped wave; and

3.

$$\nabla\left(\frac{\rho}{\varepsilon}\right),$$

which is a static component to the electrical field, associated with any stationary charges.

Waves of various kinds transfer energy through space and time. Waves in water and sound waves in air are two examples of mechanical waves. Mechanical waves are caused by a disturbance or vibration in matter, whether solid, gas, liquid, or plasma. Electromagnetic waves differ from mechanical waves in that they do not require a medium through which to propagate. This means that electromagnetic waves can travel not only through gasses, liquids or solids, but they can also travel through a vacuum. This implies that space-time itself has inherent electromagnetic properties. As mentioned in chapter 1, it has even been suggested that electromagnetic phenomena may be a space-time phenomenon, with electromagnetic behaviour being the result of space-time torsion (Evans 2005).

Maxwell was the first to formalise the concept of electromagnetic waves when he combined the fundamental properties of electrical and magnetic behaviour into a mathematical model of electromagnetism. Heinrich Hertz, a German physicist, applied Maxwell's theories to the production and reception of radio waves (Seitz 1996, Ramsay 2013). His experiment with radio waves solved two problems. Firstly, he had demonstrated in practice, what Maxwell had only theorised, that the velocity of radio waves was equal to the velocity of light. This proved that radio waves were a form of light. Secondly, Hertz demonstrated that: electric and magnetic fields can generated from electrical currents in wires (antennae); propagated as electromagnetic waves through open space; and be received by other wires (antennae) and turned back into electrical currents.

If rectangular coordinates are used and propagation is assumed to be in the $\hat{z}$ direction with the electric field vector is polarized in the $\hat{y}$ direction, then equation (4.9) is a useful solution (Sadiku 2001a, Sadiku 2001b) to equation (4.8). This solution applies a Fourier series to represent any complex wave patterns induced by the source currents.

$$\vec{E} = \sum_{n=1}^{\infty} \Re\left\{E_n \cdot e^{j\varsigma_n x} \cdot e^{j\xi_n y} \cdot e^{j(\omega_n t - \beta_n z)}\right\} \cdot e^{-\alpha_n z} \cdot \hat{y} + \Phi \tag{4.9}$$

where

$$\alpha_n = \omega_n \sqrt{\mu_o \varepsilon_o} \sqrt{\frac{\kappa'}{2}\left(\sqrt{1+\left(\frac{\kappa''}{\kappa'}\right)^2} - 1\right)} \ (\mathrm{m}^{-1}) \tag{4.10}$$

and

$$\beta_n = \omega_n \sqrt{\mu_o \varepsilon_o} \sqrt{\frac{\kappa'}{2}\left(\sqrt{1+\left(\frac{\kappa''}{\kappa'}\right)^2} + 1\right)} \ (\mathrm{m}^{-1}) \tag{4.11}$$

Where k' is the real part of the relative dielectric constant $\left[\kappa' = \Re\left(\frac{\varepsilon}{\varepsilon_o}\right)\right]$ of the space through which the wave travels and k" is the imaginary part of the relative dielectric constant $\left[\kappa'' = \Im\left(\frac{\varepsilon}{\varepsilon_o}\right)\right]$.

The constants ς and ξ are determined by the boundary conditions imposed onto the wave by any structures the wave may encounter. The magnitude (E_n) and frequency (w_n) of each wavelet are related to the source current density $\vec{J}_s$ and the distance from the source where the wave is detected, while Φ represents a static component of the electric field associated with any stationary charge density ρ.

In the case where $\varsigma = \xi = \kappa'' = \alpha = \rho = 0$, equation (4.9) reduces to the equation for a plane wave:

$$\vec{E} = \sum_{n=1}^{\infty} E_n \cdot Cos\left(\omega_n t - \beta_n z\right) \cdot \hat{y} \tag{4.12}$$

Light is an oscillating electromagnetic phenomenon. The behaviour of the wave depends on whether it is propagating through free-space or some material. Although equations (4.9) and (4.12) are solutions to Maxwell's wave equation, they do not directly link to the actual electrical current that creates the waves; therefore it is convenient to define a further vector quantity called the Magnetic Vector Potential $\left(\vec{A}\right)$, which is directly linked to course currents.

4.3 Magnetic Vector Potential

Vector potential, which is often perceived as a somewhat abstract idea, has a relatively simple interpretation, something that makes it appear quite intuitive. The path of deriving the vector potential from Maxwell's equations is not simple; however the result is very useful. The vector potential is constantly proportional to the field momentum contained within a system.

The complete derivation of the magnetic vector potential is a complex process; however it essentially depends on the mathematical properties that $\nabla \cdot \vec{H} = 0$, $\nabla \cdot \nabla \times \vec{A} = 0$, $\nabla \times \vec{A} = \mu \vec{H}$, and $\nabla \times \nabla \Phi = 0$. When these are substituted into Maxwell's equations and manipulated, they ultimately lead to three important equations:

$$\vec{E} = -\frac{\partial \vec{A}}{\partial t} - \nabla \Phi \tag{4.13}$$

$$\nabla \cdot \vec{A} = -\mu\varepsilon \frac{\partial \Phi}{\partial t} \tag{4.14}$$

and

$$\vec{A} = \sum_{n=0}^{\infty} M_n \int_v \frac{\mu \cdot d\vec{J}_s}{4\pi} \cdot \frac{e^{-j\omega_n \sqrt{\mu\varepsilon} \cdot r}}{r} \cdot dv \tag{4.15}$$

where M_n is the magnitude of the n^{th} harmonic term, r is the distance from the current source that created the magnetic potential, and w_n is the angular frequency of the n^{th} harmonic term. Note that the angular frequency is related to standard frequency (f) by:

$$\omega = 2\pi f \tag{4.16}$$

These equations allow the electrical field to be calculated from any known distribution of source currents and charges.

4.4 Continuity

It is useful to know the relationship between currents and charges. This implies that net charge is conserved throughout any electrical phenomenon. More specifically, it implies that electrical currents crossing a closed surface of a fixed volume of space must be equal to the rate of change of the charge within the volume.
Taking the divergence of equation (4.5) gives:

$$\nabla \cdot \left(\nabla \times \vec{H} \right) = \varepsilon \frac{\partial \left(\nabla \cdot \vec{E} \right)}{\partial t} + \sigma \left(\nabla \cdot \vec{E} \right) + \left(\nabla \cdot \vec{J}_s \right) \tag{4.17}$$

Mathematically, $\nabla \cdot \left(\nabla \times \vec{H} \right) = 0$, and $\nabla \cdot \vec{E} = \frac{\rho}{\varepsilon}$. Therefore:

$$\frac{\partial \rho}{\partial t} = -\sigma \left(\nabla \cdot \vec{E} \right) - \left(\nabla \cdot \vec{J}_s \right) \tag{4.18}$$

Therefore the divergence of all currents (including conductivity currents caused by an electrical field) is balanced by a change in charge with respect to time. More simply, currents are moving charges and total charge is conserved.

4.5 Conservation of Electromagnetic Energy

A natural extension of the continuity equation is Poynting's Theorem. Poynting's theorem is a powerful statement of energy conservation. It can be used to relate the power absorption in an object to the electromagnetic fields that are incident on the surface of that object.
After another lengthy derivation from Maxwell's equations, it can be shown that:

$$-\oint_s \left(\vec{E}\times\vec{H}\right)\cdot ds = \frac{1}{2}\frac{\partial}{\partial t}\int_v \left(\varepsilon E^2 + \mu H^2\right)\cdot dv + \int_v \sigma E^2 \cdot dv + \int_v \vec{E}\cdot\vec{Js}\cdot dv \qquad (4.19)$$

Each term in equation (4.19) represents a component of the total electromagnetic energy in a fixed volume of space:

1. $\vec{E}\times\vec{H}$ is the instantaneous Poynting Vector. This term represents the instantaneous power flow across a closed surface s into the enclosing volume of interest (v);
2. $\frac{1}{2}\varepsilon E^2$ is the instantaneous stored electrical energy density inside the enclosed volume;
3. $\frac{1}{2}\mu H^2$ is the instantaneous stored magnetic energy density inside the enclosed volume;
4. σE^2 is the instantaneous power dissipated inside the enclosed volume by electrical currents generated in the material by resistive losses (this component of the equation equals the heat that can be generated inside objects by electromagnetic energy); and
5. $\vec{E}\cdot\vec{Js}$ is the instantaneous electromagnetic power generated inside the volume by any current sources.

By way of explanation, a closed surface is any surface that completely encloses a fixed volume (perhaps the surface of a 3-dimensional object). The integral over the volume inside the closed surface corresponds to a sum of the terms in the integrand over all the points inside the volume.

Effectively, Poynting's theorem is a power balance equation. It implies that the electromagnetic power that goes across the surface of an object must either be stored as electromagnetic energy or be converted to heat. When real objects are being considered, the amount of electromagnetic power that crosses the surface into the contained volume of the object will depend on what happens at the surface of the object.

4.6 Boundary Conditions

Consider an electromagnetic field at the boundary between two materials with different properties. The tangent and the normal component of the fields must be examined separately, in order to understand the effects of the boundary on the behaviour of the electromagnetic wave.

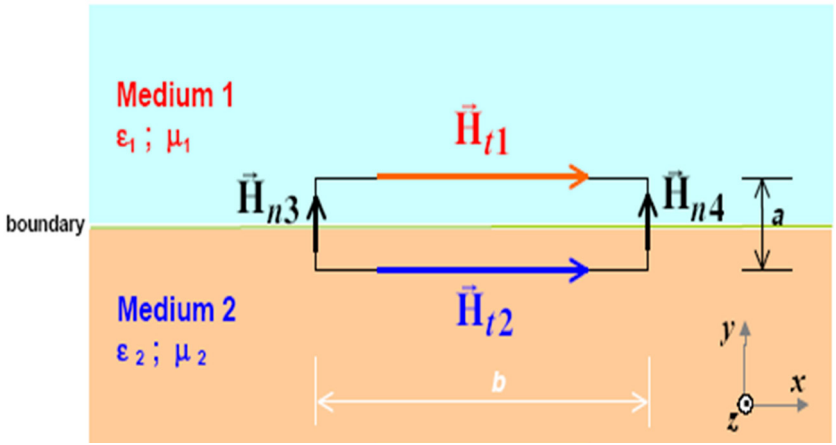

Figure 4.1: Magnetic fields at the boundary of two different materials (Source: Georgieva 2001).

Consider the situation shown in Figure 4.1, where the magnetic fields, both inside and outside the boundary, are being studied. From equation (4.5) it follows that:

$$.\nabla\times\vec{H}=\left(\frac{\partial H_y}{\partial x}-\frac{\partial H_x}{\partial y}\right)\cdot\hat{z}=\varepsilon\frac{\partial\vec{E_z}}{\partial t}+\vec{J_z} \tag{4.20}$$

The curl part of this equation can be expressed in a difference form as:

$$\left(\frac{H_{n4}-H_{n3}}{b}-\frac{H_{t1}-H_{t2}}{a}\right)\cdot\hat{z}=\varepsilon\frac{\partial\vec{E_z}}{\partial t}+\vec{J_z} \tag{4.21}$$

where the components of the magnetic field are shown in Figure 4.1.

If the boundary region shrinks, with dimension “a” going to zero faster than dimension “b”, then:

$$H_{t1}-H_{t2}=\lim_{a\to 0}\left(a\varepsilon\frac{\partial\vec{E_z}}{\partial t}+a\vec{J_z}-\frac{a\left(H_{n4}-H_{n3}\right)}{b}\right)=0 \tag{4.22}$$

If there is a surface current at the interface so that no matter how small the dimension "a" becomes, this current is still evident, then equation (4.22) needs to be modified to become:

$$H_{t1} - H_{t2} = \lim_{a \to 0} \left(a\varepsilon \frac{\partial \vec{E}_z}{\partial t} + a\vec{J}_z + \vec{J}_{zs} - \frac{a\left(H_{n4} - H_{n3}\right)}{b} \right) = \vec{J}_{zs} \tag{4.23}$$

where $\vec{J}_s$ is the surface current immediately on the interface itself.

Equation (4.22) reveals that for many materials, such as insulators, the tangential components of the magnetic fields are continuous across the boundary between two materials; however in the case of conducting materials, where a surface current may be possible, Equation (4.23) reveals surface currents modify the magnetic field as it crosses the material boundary.

Now considering the electric fields:

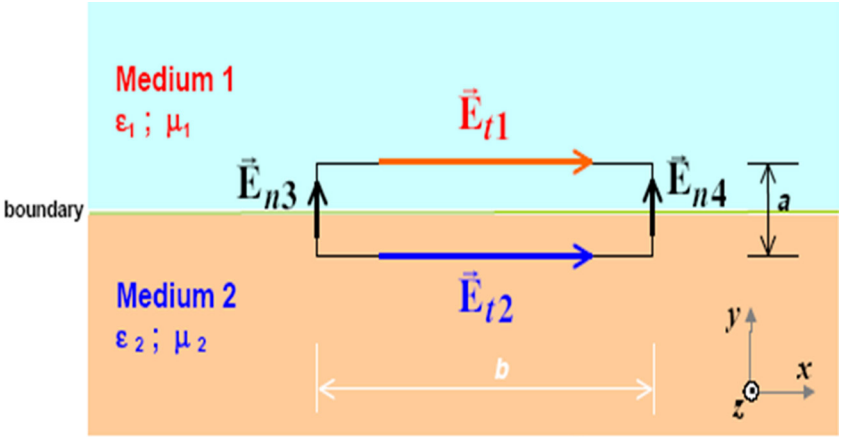

Figure 4.2: Electric fields at the boundary of two different materials (Source: Georgieva 2001).

Consider the situation shown in Figure 4.2, where the electric fields, both inside and outside the boundary, are being studied. From equation (4.4) it follows that:

$$E_{t1} - E_{t2} = \lim_{a \to 0} \left(a\varepsilon \frac{\partial \overrightarrow{H_z}}{\partial t} - \frac{a\left(E_{n4} - E_{n3}\right)}{b} \right) = 0 \tag{4.24}$$

Equation (4.24) implies that tangential electrical fields are continuous across the boundary of any object.

Now consider a small box that encloses an area with surface charge ρ_s:

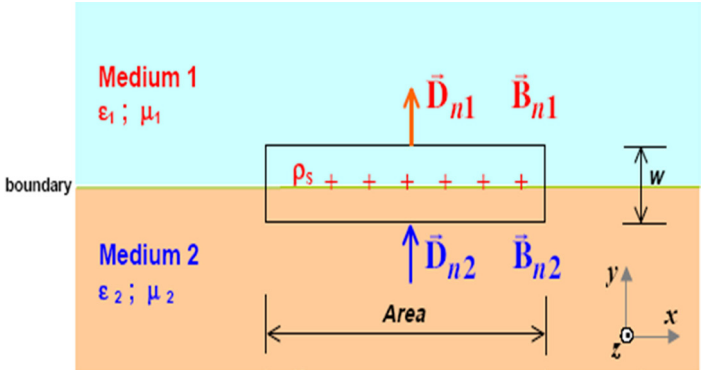

Figure 4.3: Fields at the boundary of two different materials (Source: Georgieva 2001).

From equations (4.6) and (4.7) it follows that:

$$\varepsilon_1 E_{1n} - \varepsilon_2 E_{2n} = \rho_s \tag{4.25}$$

$$\mu_1 H_{1n} - \mu_2 H_{2n} = 0 \tag{4.26}$$

These equations imply that magnetic fields that are perpendicular to the surface are modified by any change in permeability as they cross the material's surface, while electric fields that are perpendicular to the surface are modified by changes in the permittivity of the two spaces on either side of the surface and by any surface charges that may be on the interface.

Because the electric and magnetic fields change in response to a material, it is useful to define a single parameter that can describe the behaviour of the space through which the electromagnetic wave may propagate.

4.7 Wave Impedance

If the simplest solution of the electrical field wave, equation (4.12) with $\beta = \omega\sqrt{\mu_o \kappa' \varepsilon_o}$, is directly substituted into equation (4.4), then the only non-zero term in $\nabla \times \vec{E}$ is: $-\frac{\partial E_y}{\partial z}\hat{x}$, therefore:

$$-\frac{\partial\left[E_o Cos\left(\omega t-\beta z\right)\right]}{\partial z}\cdot\hat{x}=-\mu\frac{\partial\vec{H}}{\partial t} \tag{4.27}$$

This implies that:

$$\vec{H}=\frac{\int\beta E_o\cdot Sin\left(\omega t-\beta z\right)\cdot dt}{\mu}\cdot\hat{x} \tag{4.28}$$

This yields:

$$\vec{H}=\frac{\beta E_o\cdot Cos\left(\omega t-\beta z\right)}{\mu\omega}\cdot\hat{x} \tag{4.29}$$

Therefore

$$\vec{H}=\sqrt{\frac{\kappa'\varepsilon_o}{\mu}}\cdot E_o\cdot Cos\left(\omega t-\beta z\right)\cdot\hat{x} \tag{4.30}$$

Equation (4.22) implied that the magnetic field is at right angles to the electric field. Equation (4.30) can be simplified to:

$$\left|\vec{H}\right|=\left|\vec{E}\right|\sqrt{\frac{\kappa'\varepsilon_o}{\mu}}\equiv\frac{\left|\vec{E}\right|}{\eta} \tag{4.31}$$

This can be rearranged to yield:

$$\frac{\left|\vec{E}\right|}{\left|\vec{H}\right|}=\eta=\sqrt{\frac{\mu}{\varepsilon}} \tag{4.32}$$

Equation (4.32) defines the wave impedance of the space through which the electromagnetic wave is propagating. The wave impedance determines how difficult it is for the wave to propagate. When there is a sudden change in the wave impedance, such as at the surface of a material, the wave behaviour abruptly changes.

4.8 Reflection and Transmission at an Interface

When a plane wave propagating in a homogenous medium encounters an interface with a different medium, a portion of the wave is reflected from the interface while the remainder of the wave is transmitted. The reflected and transmitted waves can be determined by enforcing the electromagnetic field boundary conditions described earlier.

When the wave is propagating perpendicular to the interface between the two materials, the total tangential electric field on the incident side of the interface is the sum of the tangential components of the incident and reflected waves. The electric field on the transmission side of the interface is simply the tangential component of the transmitted wave. If the reflection coefficient for the interface is defined as:

$$\Gamma = \frac{E_r}{E_i} \tag{4.33}$$

Where: Γ is the reflection coefficient of the surface; Er is the reflected wave; and Ei is the incident wave. The transmission coefficient is defined as:

$$\tau = \frac{E_t}{E_i} \tag{4.34}$$

These can be applied to the boundary condition for the tangential electric fields yields:

$$E_i + E_r = E_t \quad or \quad +\Gamma = \tag{4.35}$$

When the magnetic fields are being considered, the total perpendicular magnetic field on the incident side of the interface is the difference between the components of the incident and reflected waves.

The magnetic field on the transmission side of the interface is simply the perpendicular component of the transmitted wave.

$$H_i - H_r = H_t \quad or \quad H_i - \Gamma H_i = H_t \quad or \quad \frac{E_i}{\eta_1} - \Gamma \frac{E_i}{\eta_1} = \tau \frac{E_i}{\eta_2} \tag{4.36}$$

This yields:

$$\frac{1-\Gamma}{\eta_1}=\frac{\tau}{\eta_2} \tag{4.37}$$

If equation (4.37), multiplied by η_2, and equation (4.35) are combined and simplified, then:

$$\Gamma=\frac{\eta_2-\eta_1}{\eta_2+\eta_1} \tag{4.38}$$

From equation (4.35) it immediately follows that:

$$\tau=\frac{2\eta_2}{\eta_2+\eta_1} \tag{4.39}$$

From equations (4.38) and (4.39) it is clear that the wave impedances of the spaces on either side of an interface determine how much of the wave is transmitted and how much is reflected. This analysis has so far only considered when a wave is propagating perpendicular to the interface. In the case where the incident wave is not perpendicular to the interfacial surface, two extreme cases exist: the electrical field may be oriented perpendicular to the plane of incidence to the surface, as shown in Figure 4.4; or the electric field may be oriented to be parallel to the plane of incidence to the surface as shown in Figure 4.5.

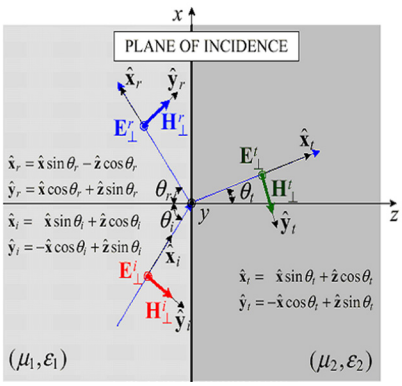

Figure 4.4: Analysis of electromagnetic waves at medium interface for perpendicular polymerization (Source: Georgieva 2001.)

In analysing this problem, continuity of the magnetic components must be modified to account for the angle of incidence:

$$\begin{aligned} & H_i Cos\theta_i - H_r Cos\theta_r = H_t Cos\theta_t \\ \Rightarrow & \frac{E_i}{\eta_1} Cos\theta_i - \Gamma \frac{E_i}{\eta_1} Cos\theta_r = \tau \frac{E_i}{\eta_2} Cos\theta_t \\ \Rightarrow & \frac{Cos\theta_i}{\eta_1} - \Gamma \frac{Cos\theta_r}{\eta_1} = \tau \frac{Cos\theta_t}{\eta_2} \end{aligned} \tag{4.40}$$

Where θ_i is the incident angle of the wave, θ_r is the reflection angle of the wave and θ_t is the transmission angle of the wave. Equation (4.40) can be manipulated to eventually yield:

$$\Gamma_\perp = \frac{\eta_2 Cos\theta_i - \eta_1 Cos\theta_t}{\eta_2 Cos\theta_r + \eta_1 Cos\theta_t} \tag{4.41}$$

It follows that:

$$\tau_\perp = \frac{2\eta_2 Cos\theta_i}{\eta_2 Cos\theta_r + \eta_1 Cos\theta_t} \tag{4.42}$$

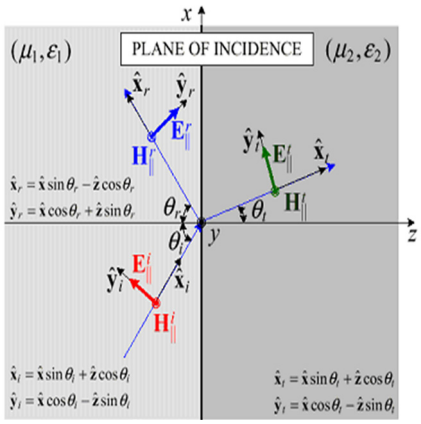

Figure 4.5: Analysis of electromagnetic waves at medium interface for parallel polymerization (Source: Georgieva 2001).

Applying a similar analysis to the parallel polarization case yields:

$$\Gamma_{\parallel} = \frac{\eta_2 Cos\theta_t - \eta_1 Cos\theta_i}{\eta_2 Cos\theta_t + \eta_1 Cos\theta_i} \tag{4.43}$$

It follows that:

$$\tau_{\parallel} = \frac{2\eta_2 Cos\theta_i}{\eta_2 Cos\theta_t + \eta_1 Cos\theta_i} \tag{4.44}$$

4.9 Electromagnetic Behaviour of Materials

Material can be categorized as transparent, absorbing or reflective, according to their electromagnetic behaviour at any given frequency. If the attenuation factor (α) defined in equation (4.10) is negligible, then the material can be regarded as transparent at the electromagnetic frequency of interest. If the attenuation factor is not negligible, then the material can be regarded as absorbing at the electromagnetic frequency of interest. Finally, if the reflection coefficient for the surface of the material (Γ) is very high, the material can be regarded as reflective.

4.10 Conclusions

In summary, Maxwell's equations can be used to describe the wave behaviour of electromagnetic phenomenon. These waves propagate through space; transport energy from one part of space to another; consist of orthogonal electric and magnetic vector fields; are reflected from and refracted through interfacial boundaries of materials; and are attenuated in materials that have non-zero electrical conductivity. There must be an energy balance associated with these waves, so as electromagnetic waves are attenuated, heat energy is generated in a material.

This chapter has introduced many of the key concepts associated with radio frequency and microwave propagation through space. Many of these concepts are complex and therefore required more than a cursory presentation of the facts. The remainder of this book will explore how these propagating waves can be used to do useful things in an agricultural context.

References

Evans, M. W. 2005. The Spinning and Curving of Spacetime: The Electromagnetic and Gravitational Fields in the Evans Field Theory. *Foundations of Physics Letters*. 18(5): 431-454.

Georgieva, N. 2001. *Modern Antennas in Wireless Telecommunications*. http://www.ece.mcmaster.ca/faculty/georgieva/

Ramsay, P. S. 2013. Heinrich Hertz, the Father of Frequency. *Neurodiagnostic Journal*. 53(1): 3-26.

Sadiku, M. 2001a Wave Propagation in Free Space. Golio, M. ed. CRC Press: Boca Raton.

Sadiku, M. N. O. 2001b, *Elements of Engineering Electromagnetics*, New York: Oxford University Press.

Seitz, F. 1996. The Tangled Prelude to the Age of Silicon Electronics. *Proceedings of the American Philosophical Society*. 140(3): 289-337.

Section 2: **Non-destructive Characterisation using Electromagnetic Waves**

5 Section Introduction

From the previous section it is clear that modern agriculture depends on continuing innovation. This will become even more important as human populations grow and demand for food and fibre increases. Radiofrequency and microwave technologies have much to offer in most industries, but this is particularly so for modern agriculture.

It is also clear from the previous section that the transparency of any other material to electromagnetic waves is linked to the complex dielectric properties of the material under study (James 1975, Torgovnikov 1993, Olmi, *et al.* 2000). The real part of the complex dielectric properties determines the wave length of the electromagnetic wave inside the object and therefore influences the speed of wave propagation through the object. The imaginary part of the complex dielectric properties determines the amount of energy that the material will absorb from the wave as it travels into or through the object.

For example, when microwaves are transmitted through a material such as wood, the wave will be partially reflected, attenuated and delayed compared to a wave travelling through free space (Lundgren 2005, Brodie 2008a, Brodie 2008b). Wave attenuation, reflections from the surface, and internal scattering from embedded objects or cavities in the wood causes a "shadow" on the opposite side of the material from the electromagnetic source. An x-ray image is a good example of how shadows associated with phase delay and attenuation can be used to interpret the internal structures of objects.

Effectively the combination of attenuation and phase delay, which are directly linked to the dielectric properties of the material, provide information about the material through which the wave travels; therefore this section of the book will consider how the dielectric properties are measured and how systems can be developed to use these properties to detect and monitor various materials of importance to agriculture and forestry.

References

Brodie, G. 2008a. The influence of load geometry on temperature distribution during microwave heating. *Transactions of the American Society of Agricultural and Biological Engineers*. 51(4): 1401-1413.

Brodie, G. I. 2008b, *Innovative wood drying: Applying microwave and solar technologies to wood drying*, Saarbruecken, Germany: VDM Verlag.

James, W. L. 1975. *Dielectric properties of wood and hardboard: Variation with temperature, frequency, moisture content, and grain orientation*. U.S. Department of Agriculture

Lundgren, N. 2005. Modelling Microwave Measurements in Wood. Unpublished thesis. Luleå University of Technology, Department of Skellefteå Campus, Division of Wood Science and Technology

Olmi, R., Bini, M., Ignesti, A. and Riminesi, C. 2000. Dielectric properties of wood from 2 to 3 GHz. *Journal of Microwave Power and Electromagnetic Energy*. 35(3): 135-143.

Torgovnikov, G. I. 1993, *Dielectric Properties of Wood and Wood-Based Materials*, Springer Series in Wood Science, Berlin: Springer-Verlag.

6 Techniques for Measuring Dielectric Properties

In general materials can be classified into conductors, semiconductors and insulators or dielectric materials. Dielectric materials play an important role in our daily life especially every electronic circuit, which needs a dielectric medium to build the circuit. Typically high frequency electronics circuits are built on dielectric materials and the operation of all high frequency circuits depends on the dielectric properties of the material. In order to design high frequency circuits it is essential to have vital understanding of the properties of the dielectric materials especially the dielectric constant (real part of complex permittivity) and loss tangent at the operating conditions. Dielectric property is also a characteristic of plant materials and fruits mainly due to the structure of the biomaterials and the large amount of water content. A 'dielectric material' (or dielectric) is an electrically insulating material that will be polarized under an electric field and the phenomenon is called dielectric polarization. The dielectric properties of the material provides valuable information about the storage and dissipation of electric and magnetic fields in materials and also provides insight into the feasibility of using the material in potential applications. The polarizability of the material is expressed by permittivity. The permittivity is a complex number and the real part is often called as dielectric constant. Though a "perfect dielectric" is a material with zero electrical conductivity, all insulators are not dielectrics.

6.1 Dielectric Properties

The two parameters which determine electromagnetic field propagation in any space are the electrical permittivity and magnetic permeability of the space. Except in the case of ferromagnetic materials, the magnetic permeability of space is usually unaltered by the presence of objects; however the dielectric properties of the material profoundly affect the electrical permittivity of the space occupied by any material object.

The dielectric properties of materials, namely permittivity, are typically measured as a function of frequency and are called dielectric/ impedance spectroscopy. The permittivity values show the interaction of an external field with the electric dipole moment of the sample (Griffiths 1999, Baker-Jarvis, *et al.* 2010, Yaw 2012). Dielectric measurement is an important tool to understand the material behavior especially at high frequencies because it can provide the electrical or magnetic characteristics of the materials, which is a critical parameter required to implement the material in many applications. The measurement of complex dielectric properties of materials at radio frequency (RF) and microwave frequency is very relevant especially in the research fields, such as material science, communication, microwave circuit design

and biological research (Burdette, *et al.* 1980, F.H.Wee, *et al.* 2009). A number of methods have been developed to measure the complex permittivity of materials in time domain or frequency domain using transmission (2 port) or reflection (1 port) methods. Each technique is limited to specific frequencies, materials and applications and has its own limitations. Often, data obtained by dielectric spectroscopy is expressed graphically in a Bode plot or a Nyquist plot.

Maxwell's equations can be used to understand and explain the dielectric properties of materials. Four differential equations proposed by James Clerk Maxwell in 1864 form the basis of the theory of electromagnetic waves (Griffiths 1999). They may be written, in vector notation, as:

$$\nabla \times E = -\frac{\partial B}{\partial t} \qquad \oint_c E \cdot dl = -\frac{\partial \Phi}{\partial t} \text{ Faraday's law}$$

$$\nabla \times H = J + \frac{\partial D}{\partial t} \qquad \oint_c H \cdot dl = J + \oint_s \frac{\partial D}{\partial t} \cdot ds \text{ Ampére's law} \tag{6.1}$$

$$\nabla \cdot D = \rho \qquad \oint_s D \cdot ds = Q \text{ Gauss's law}$$

$$\nabla \cdot B = 0 \qquad \oint_s B \cdot ds = 0 \text{ No isolated magnetic charge}$$

where **D** is the electric displacement, **B** the magnetic flux density, **E** the electric field strength or intensity, **H** the magnetic field strength or intensity, ρ the charge density, and **J** the current density.

In addition to Maxwell's base equations, the Lorentz condition is:

$$\nabla \cdot \vec{A} + \mu\varepsilon \frac{\partial V}{\partial t} = 0 \tag{6.2}$$

$$\nabla \times \vec{B} = \mu \vec{J} + \mu \frac{\partial \vec{D}}{\partial t} = \nabla \times \nabla \times \vec{A} \tag{6.3}$$

$$= \mu \vec{J} + \mu\varepsilon \frac{\partial}{\partial t}(-\nabla V - \frac{\partial \vec{A}}{\partial t}) \tag{6.4}$$

$$= \nabla(\nabla \cdot \vec{A}) - \nabla^2 \vec{A} \tag{6.5}$$

$$= \mu \vec{J} - \nabla(\mu\varepsilon \frac{\partial V}{\partial t}) - \mu\varepsilon \frac{\partial^2 \vec{A}}{\partial t^2}$$

$$\Rightarrow \nabla^2 \vec{A} - \mu\varepsilon \frac{\partial^2 \vec{A}}{\partial t^2} = -\mu \vec{J} + \nabla(\nabla \cdot \vec{A} + \mu\varepsilon \frac{\partial V}{\partial t}) \tag{6.6}$$

If the Lorentz Condition holds, then:

$$\nabla^2 \vec{A} - \mu\varepsilon \frac{\partial^2 \vec{A}}{\partial t^2} = -\mu \vec{J} \tag{6.7}$$

$$\nabla \cdot \vec{D} = \rho = \nabla \cdot \varepsilon \vec{E} = \rho = \nabla \cdot \varepsilon(-\nabla V - \frac{\partial}{\partial}) \tag{6.8}$$

$$\Rightarrow \nabla^2 V + \frac{\partial}{\partial t}(\nabla \cdot \vec{A}) = \nabla^2 V + \frac{\partial}{\partial t}(-\mu\varepsilon \frac{\partial V}{\partial t}) = -\frac{\rho}{\varepsilon} \tag{6.9}$$

$$\nabla^2 V - \mu\varepsilon \frac{\partial^2 V}{\partial t^2} = -\frac{\rho}{\varepsilon} \tag{6.10}$$

From the above set of equations effective permittivity can be derived:

$$\nabla \times \vec{H} = \vec{J} + \varepsilon \frac{\partial \vec{E}}{\partial t} = \sigma \vec{E} + j\omega\varepsilon \vec{E} \tag{6.11}$$

$$\nabla \times \vec{H} = j\omega(\varepsilon + \frac{\sigma}{j\omega})\vec{E} = j\omega\varepsilon_C \vec{E} \tag{6.12}$$

$$\Rightarrow \varepsilon_r = \varepsilon - j\frac{\sigma}{\omega} = \varepsilon' - j\varepsilon'' \Rightarrow \sigma = \omega\varepsilon'' \tag{6.13}$$

Measurement of dielectric properties involves measurements of the complex relative permittivity (ε), which consists of a real part and an imaginary part. As mentioned earlier, the real part of the complex permittivity, also known as the dielectric constant is a measure of the amount of energy from an external electrical field stored in the material. The imaginary part is zero for lossless materials and is also known as loss factor. It is a measure of the amount of energy loss from the material due to an external electric field.

Loss tangent:

$$\tan\delta_C = \frac{\varepsilon''}{\varepsilon'} = \frac{\sigma}{\omega\varepsilon} \tag{6.14}$$

The term tanδ is called loss tangent (dissipation factor or loss factor) and it represents the ratio of the imaginary part to the real part of the complex permittivity.

6.2 Polarization

Polarization is an ordering in space of an electrically charged unit under the influence of an external electric field. The charges become polarized to compensate for the electric field such that the opposite charges move in opposite directions. The external field causes the formation of an electric moment in the entire volume of the dielectric material in each polarizing units namely atom, ion or molecule. Linear dielectrics show a direct proportionality between the induced electric dipole moment p acquired by the polarizable unit during the process of polarization and the intensity E of the field acting on it as given by $p = \alpha E$, where α is the polarizability, which reflects the properties of individual polarizable units. Polarizability is independent of the dielectric volume and this parameter is very important to define the electrical properties of a dielectric material. As a result of polarization the charges that are displaceable will accumulated at physical barriers like the grain boundary and hence interfacial polarization or space charge polarization occurs. At the microscopic level, several dielectric mechanisms can contribute to dielectric behavior. At different frequency regions the mechanism of polarization, which gives the dielectric constant, is different. For example, dipole orientation and ionic conduction interact strongly at microwave frequencies like the dipole of water molecules, which rotate to follow an alternating electric field. Atomic and electronic mechanisms are relatively weak. Each dielectric mechanism has a characteristic "cutoff frequency".

As frequency increases, the slow mechanisms drop out in turn, leaving the faster ones to contribute to ε'. The loss factor (ε_r'') will correspondingly peak at each critical frequency. The magnitude and "cutoff frequency" of each mechanism is unique for different materials. Based on the dipolar effect the dielectric constant changes significantly at certain frequencies or will remain stable. For example the dielectric constant of water decreases significantly at 22 GHz where as Teflon exhibits constant dielectric properties. Figure. 6.1 depicts the different frequency region and different polarization mechanism.

6.2.1 DIPOLAR POLARIZATION

The formation of a molecule due to the combination of atoms by sharing electrons will cause an imbalance in charge distribution and hence a permanent dipole moment is created. When an electric field is applied due to the torque on the electric dipole, the dipole will rotate to align with the electric field causing dipolar (orientation) polarization to occur. The friction accompanying the orientation of the dipole will contribute to the dielectric losses. The ε_r' and ε_r" changes due to dipolar rotation. Below 1 kHz, dipolar polarization occurs due to the molecules containing permanent dipole moment or by the rotation of dipoles between two equilibrium positions, and this relaxation is around 10 kHz to 10 MHz.

6.2.2 IONIC POLARIZATION

The ionic polarization occurs due to the displacement of the positive and negative ions against each other, and it relaxes in the frequency range of 10^{12} to 10^{13} Hz. The different types of atoms in a molecule (or crystal) create a positive or negative charge and the centres of these charges can be displaced. The locations of the centre of charges are affected by the symmetry of the displacements. When the centres do not correspond, polarizations arise in molecules. This polarization is called ionic polarization.

6.2.3 ELECTRONIC AND ATOMIC POLARIZATION

Electronic polarization occurs due to the displacement of electrons with respect to the atomic nucleus, and it relaxes at high frequencies ~ 10^{15} Hz. Atomic polarization occurs when adjacent positive and negative ions "stretch" under an applied electric field. For many dry solids, electronic and atomic polarizations are the dominant polarization mechanisms especially at microwave frequencies, although the actual resonance occurs at a much higher frequency. The amplitude of the oscillations will be small for any frequency other than the resonant frequency. Far below resonance, the electronic and atomic mechanisms contribute only a small constant amount to ε_r' and are almost lossless. The resonant frequency is identified by a resonant response in ε_r' and a peak of maximum absorption in ε_r''. Above the resonance, the contribution from these mechanisms disappears.

6.2.4 INTERFACIAL OR SPACE CHARGE POLARIZATION

Electronic, atomic, and dipolar polarization occur when charges are locally bound in atoms or molecules. Charge carriers also exist that can migrate over a distance through the material when a low frequency electric field is applied. Interfacial or space charge polarization occurs when the charge carriers moving over a distance through the material interfaces under electric field and the motion of these migrating charges are impeded. This is the space charge polarization. The charges can become trapped within the interfaces of a material. Motion may also be impeded when charges cannot be freely discharged or replaced at the electrodes. This can also results in charge accumulation and hence higher capacitance effect.

6.2.5 DIELECTRIC LOSS

Dielectric loss (loss tangent or tan δ) quantifies a dielectric material's inherent dissipation of electromagnetic energy (for example as heat due to the charging

and discharging of capacitor). Dielectric losses depend on frequency and the dielectric material. Heating through dielectric loss is widely employed industrially for heating thermosetting glues, for drying lumber and other fibrous materials, for preheating plastics before moulding, and for fast jelling and drying of foam rubber. In communication systems, higher the dielectric loss means higher the attenuation and hence it is a limitation for long range transmission. At low frequencies, the overall conductivity can be made up of many different conduction mechanisms, but ionic conductivity is the most prevalent in moist materials. The ionic conductivity of materials will contribute to the dielectric loss.

6.2.6 RELAXATION TIME

Relaxation time τ is a measure of the mobility of the molecules (dipoles) that exist in a material. The dielectric relaxation is caused by the delay in molecular polarization with respect to a changing electric field in a dielectric medium. The movement of dipoles under the field causes collisions and hence internal friction so that the molecules turn slowly until it reaches the final state of orientation polarization with relaxation time constant τ. When the field is switched off, the sequence is reversed and random distribution is restored with the same time constant. The relaxation frequency fc is inversely related to relaxation time. The dielectric loss is proportional to the frequency up to fc. Above the relaxation frequency both ε_r' and ε_r'' decreases as the electric field is too fast to influence the dipole rotation and the orientation polarization disappears.

6.3 Cole-Cole diagram

The complex permittivity may also be shown on a Cole-Cole diagram by plotting the real part (ε_r') on the horizontal axis and the imaginary part (ε_r'') on the vertical axis with frequency as the independent parameter.

6.3.1 Bode' plots and Nyquist Plots

There are several ways of displaying frequency response data, including Nyquist plots, which is invented by Nyguist and Bode' plots. Bode' plots use frequency as the horizontal axis and use two separate plots to display amplitude and phase of the frequency response (Figure 6.1). A Nyquist plot is a polar plot of the frequency response function of a linear system. Nyquist plots display both amplitude and phase angle on a single plot, using frequency as a parameter in the plot.

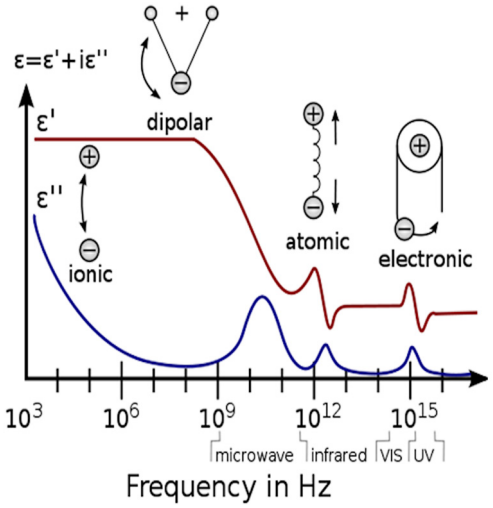

Figure 6.1: The various phenomenon at different frequencies (Technologies 2010, Yaw 2012).

6.4 Microwave Measurement Methods

There were number of dielectric characterization technique developed over the last couple of decades. This is mainly due to:

Communication technologies have grown to unprecedented heights during the last decade. Increased popularity rising due to mobile communications, wireless data transfers and instant access technologies – such as the internet, has given rise for the need for faster data rates and more data channels for an increased number of users. To cater for the increasing number of users, demanding more data in a shorter period of time, circuits must be made smaller, and perform faster than ever before. In order to facilitate this requirement, materials with good dielectric properties (Complex permittivity) must be used in the circuit. Manufacturers will give a value of permittivity for the materials, which is often at low-frequency however this measure is not adequate for use in RF (microwave frequency) applications. Dielectric characterization of biomaterials could provide information about the quality of agricultural produces and the information can be collected non-destructively. This information can be used for determining the quality of wood, fruits and vegetables, especially for wood, which is commonly used in electric poles. Degradation or termite infestation can be determined before critical damage to the system occurs.

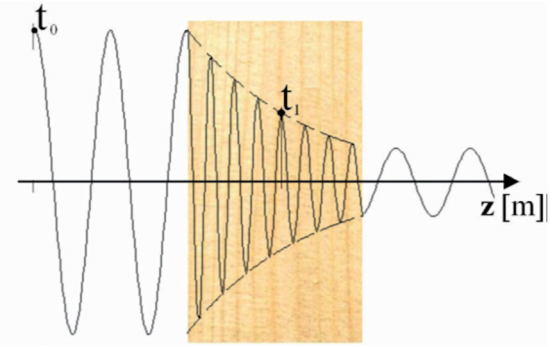

Figure 6.2: Propagation of microwave energy through wood showing the attenuation.

Decay in the tissue can cause severe damage to all biological samples including any type of wood or plant materials. Early non-destructive detection of biological degradation in wood is important if remedial treatments are to be effective. Wood and wood based materials are relatively transparent at microwave frequencies. The microwave transmission through the material depends on the moisture content. For example, when microwaves are transmitted through wood, the wave will be partially reflected, attenuated and delayed (Figure 6.2). Wave attenuation; reflections from the surface; and internal scattering from embedded objects or cavities in the wood causes a "shadow" on the opposite side of the material from the microwave source. Phase delay also depends on the bulk properties of the material through which the wave travels.

Many methods exist for determining the dielectric constant and loss tangent of a sample. Typically the methods used for the microwave characterisation of dielectric materials are classified into different groups based on the measurement structure implemented, namely Free Space Methods, Transmission Line and Reflection Methods, Resonant Techniques. These include one port coaxial and waveguide cells, open-ended probes, free-space transmission and/ or reflection methods, microwave microscope methods, microwave cavity methods, stripline and microstrip methods (Afsar, *et al*. 1986, Baker-Jarvis, *et al*. 1990, Courtney 1998, Yue, *et al*. 1998, Courtney and Motil 1999, Wang, *et al*. 2002, Murata, *et al*. 2005, Krupka 2006b). Most of these techniques are widely used. Each technique has its own limitations including the frequency at which the measurements can be performed and the type of material that can be measured. Frequency-domain methods are however preferred when measurement resolution is of concern, which is of importance for low-loss materials (Afsar, et al. 1986). Coaxial and waveguide methods are commonly used for determining the electromagnetic properties of materials, however rely on additional measurement fixtures and specific geometric dimensions of the sample to obtain accurate results. The accuracy of characterization is much higher for resonant techniques especially the modified cavity techniques (Janezic and Williams 1997, Baker-Jarvis, *et al*. 2010).

Transmission line techniques, including reflection techniques utilize transmission line concepts, where a piece of dielectric material is placed inside a transmission line, and an electromagnetic wave is directed at the sample. The disadvantage of this technique is that frequencies above 10 GHz are usually immeasurable, due to parasitic losses at higher frequencies. Majority of microwave devices operate at frequencies significantly higher than 10 GHz, hence, these techniques are not popular for characterizing PCB materials at microwave frequencies (Krupka, *et al.* 2000, Technologies 2010)

Resonant techniques are widely used to determine the permittivity and loss tangent of low loss PCB materials operating at microwave frequencies. Cavities are used to shield the dielectric, and to perform the measurement process. Cavities resonate specific to the mode for which they were manufactured. Most cavities are defined by their mode of operation. In TE_{01n} mode for example, electromagnetic field lines are tangential to the surface of the dielectric material. Resonant techniques encompass five main families of resonant metrology techniques: Microstrip, Dielectric probe, cavity, dielectric resonators and Open resonators. Cavities can be either TM_{0n0} mode, or TE_{01n} mode, while open resonators include the fabry-perot resonator. Dielectric Resonators were used for these experiments and consist of: TE_{0111} mode, Whispering Gallery Mode, $TE_{01\delta}$ Mode, and Split Post Dielectric Resonator. (Sheen 2005, Technologies 2006, Sheen 2007)

Parallel Plate Holder, is an accurate and popular method of measuring permittivity and dielectric loss of solid materials for the 8 GHz – 40 GHz operating range. The advantage of these methods lies in accessing the material from the resonator, as it is much simpler than in other devices, meaning the material is less likely to become damaged via insertion or removal. Operating range is from 50 MHz, while the permittivity measurement uncertainties are at 0.3%. (Krupka 1999)

Dielectric probes are advantageous given their ease of use, and non-invasive measurement technique. While easy to use, 3 sources of error; Air gaps, cable stability and sample thickness, can affect the measurement such that uncertainty in the technique is +/- 3% for larger specimens.

Two measurement techniques namely; Split Post Dielectric Resonator (SPDR) and Dielectric Probe, were used (Krupka 1999, 2006a). SPDR is a very accurate measurement which can be performed as a function of temperature, however as it is a resonant technique it can only be measured at one frequency. The second technique used, was the dielectric probe, even though the error in measurement is high, it allows the measurement to be carried out over a wide range of frequencies.

In general the different methods developed for complex permittivity measurement can be classified into (Baker-Jarvis, *et al.* 2010, Technologies 2010):

- Transmission/reflection line method,
- Open ended coaxial probe method,
- Free space method,
- Resonant method.

6.4.1 Transmission/Reflection Line Method

The Transmission/Reflection line method (Janezic and Williams 1997) is a popular broadband measurement method. In this method, only the fundamental waveguide mode (TEM mode in coaxial line and TE mode in waveguides) is assumed to propagate. Transmission line techniques, including reflection techniques utilize transmission line concepts, where a piece of dielectric material is placed inside a transmission line, and an electromagnetic wave is directed at the sample. The disadvantage of this technique is that frequencies above 10 GHz are usually immeasurable, due to parasitic losses at higher frequencies. The majority of microwave devices operate at frequencies significantly higher than 10 GHz, hence, these techniques are not popular for characterizing PCB materials at microwave frequencies.

A measurement using the Transmission/Reflection line method involves placing a sample in a section of waveguide or coaxial line and measuring the two ports complex scattering parameters with a vector network analyzer (VNA). The method involves measurement of the reflected (S_{11} or S_{22}) and transmitted signal (S_{21} or S_{12}). The relevant scattering parameters relate closely to the complex permittivity and permeability of the material by equations. The conversion of s-parameters to complex dielectric parameter is computed by solving the equations using a computer program. In many cases, the method requires sample preparation so that the samples fit tightly into the structure, typically waveguide or coaxial line. For accurate dielectric measurement, the maximum electric field is required within the sample. Calibrations in transmission line measurements use various terminations (standards such as open, short or 50 ohm load) that produce different resonant behavior in the transmission line.

Advantages of Transmission/Reflection line method (Yaw 2012)

- Coaxial lines and waveguides are commonly used to measure samples with medium to high loss.
- It can be used to determine both the permittivity and permeability of the material under test.
- Disadvantages of Transmission/Reflection line method
- Measurement accuracy is limited by the air-gap effects.
- It is limited to low accuracy when the sample length is the multiple of one-half wavelength in the material.

6.4.2 Resonant Technique

The resonant method provides high accuracies and assumes the TE or TM propagation mode. Resonant techniques are widely used to determine the permittivity and loss tangent of low loss PCB materials operating at microwave frequencies (Jacob, *et al.* 2002, Jacob, *et al.* 2005, Baker-Jarvis, *et al.* 2010). Cavities are used to shield the dielectric, and to perform the measurement process. Cavities resonate specific to the

mode for which they were manufactured. Most cavities are defined by their mode of operation. In TE_{01n} mode for example, electromagnetic field lines are tangential to the surface of the dielectric material.

Resonant techniques encompass five main families of resonant metrology techniques: Dielectric probe (Burdette, *et al*. 1980, Ellison and Moreau 2008, Technologies 2010), cavity /dielectric resonators and Open resonators. Cavities can be either TM_{0n0} mode, or TE_{01n} mode. Dielectric Resonators were used for these experiments and consist of: TE_{0111} mode, Whispering Gallery mode resonator $TE_{01\delta}$ Mode, and Split Post Dielectric Resonator.

Resonant measurement is one of the most accurate dielectric characterisation methods but at the expense of the limited frequencies and low loss characteristics of the materials. There are many types of resonant methods available such as reentrant cavities, split cylinder resonators, cavity resonators, Fabry-Perot resonators etc. There are two types of resonant measurements commonly used. Perturbation methods are suitable for all permittivity measurements, magnetic materials and medium to high loss material measurements. Low loss measurement method is a measurement on low loss materials using larger samples. However, the perturbation method is more popular especially using a TM cavity geometry. With resonance characteristics depending on the MUT in a cavity its, quality factor and resonance frequency can be monitored to determine the dielectric parameters. The dielectric properties can be determined by first measuring the resonant frequency and quality factor of an empty cavity. The second step is to repeat the measurement after filling the cavity with the MUT. The permittivity or permeability of the material can then be computed using the frequency, volume and q-factor.

Advantages of resonant method

- Ability to measure very small MUT.
- Use of approximate expression for fields in sample and cavity.

Disadvantages of resonant method

- Need high frequency resolution VNA.
- Limited to narrow band of frequencies only.

6.4.3 Dielectric Resonator

The dielectric resonator typically consists of a metallic cavity and a dielectric material of cylindrical shape (Figure 6.3). The measured loss consists of loss from the metallic walls and dielectric loss. By properly designing the cavity, the loss from the lateral walls can be eliminated. Also by using low loss materials like superconducting materials as the end plate, all the losses associated with the cavity can be substantially reduced and hence the measured loss will be from the material under test. The Dielectric resonator technique with High Temperature Superconducting (HTS) plates

is a modification of the metallic dielectric resonator and the cavity perturbation techniques used in the past to characterize dielectric materials. The dielectric sample to be measured was enclosed in a copper cylindrical cavity between metallic (or two High Temperature Superconducting films). As the dielectrics under test exhibit low relative permittivity, the diameter 'd' of the samples was chosen to be sufficiently large to ensure that electromagnetic fields are evanescent in the air region.

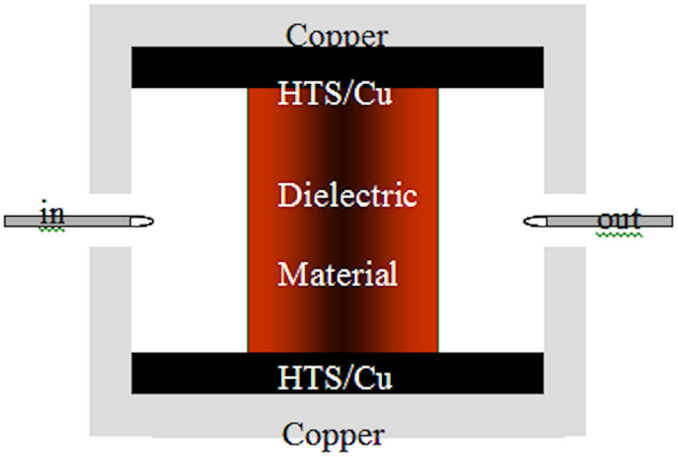

Figure 6.3 Schematic of a TE_{011} mode dielectric resonator.

Since the materials under test are isotropic, the TE_{011} mode of operation was employed in the measurements. The real part of relative permittivity ε_r of a dielectric was determined as the first root of the following transcendental equation (Jacob, *et al.* 2002):

$$k_{\rho 1} J_0(k_{\rho 1} b) F_1(b) + k_{\rho 2} J_1(k_{\rho 1} b) F_0(b) = 0 \tag{6.15}$$

where:

$$\begin{aligned} F_0(\rho) &= I_0(k_{\rho 2}\rho) + K_0(k_{\rho 2}\rho)\frac{I_1(k_{\rho 2}a)}{K_1(k_{\rho 2}a)} \\ F_1(\rho) &= -I_1(k_{\rho 2}\rho) + K_1(k_{\rho 2}\rho)\frac{I_1(k_{\rho 2}a)}{K_1(k_{\rho 2}a)} \\ k_{\rho 1}^2 &= \frac{\omega^2 \varepsilon_r}{c^2} - k_z^2, \quad k_{\rho 2}^2 = k_z^2 - \frac{\omega^2}{c^2}, \quad k_z = \pi / L \end{aligned} \tag{6.16}$$

and ω is the angular frequency ($2\pi f$), c is velocity of light, ε_o is free space permeability, ε_r is real relative permittivity of the sample and J_0, J_1, I_0, I_1, K_0, K_1, denote corresponding Bessel and Hankel functions.

The loss tangent of a dielectric under test is found on the basis the loss equation of the resonator and measured values of the Q_0-factor of the resonator, namely:

$$\tan\delta = \frac{1}{\rho_e}\left[\frac{1}{Q_0} - \frac{R_{SS}}{A_S} - \frac{R_{SM}}{A_M}\right] \tag{6.17}$$

where Q_0 is measured unloaded Q-factor of the entire resonant structure, R_{SS} and R_{SM} are the surface resistance of the end and lateral metallic walls of the cavity respectively, A_S and A_M are the geometric factors of the end and lateral metallic walls of the cavity and r_e is the electric energy filling factor.

Geometric factors A_S, A_M, and r_e to be used in were computed using incremental frequency rules as follows:

$$A_S = \frac{\omega^2\mu_0}{4} / \frac{\partial\omega}{\partial L} \tag{6.18}$$

$$A_M = \frac{\omega^2\mu_0}{2} / \frac{\partial\omega}{\partial a} \tag{6.19}$$

$$p_e = 2\left|\frac{\partial\omega}{\partial\varepsilon_r}\right|\frac{\varepsilon_r}{\omega} \tag{6.20}$$

6.4.4 Dielectric Post Resonator

The accuracy of measurements using HCDR (Jacob, *et al.* 2002, Jacob, *et al.* 2005) is high but the main difficulty is to machine samples precisely to realize the same height as that of the copper cavity. Also the linear thermal expansion coefficient of the metallic wall is different from that of the dielectric material. This constitutes a problem especially during low temperature measurement. Hence a TE_{01d} mode post dielectric resonator is suitable. The dielectric under test is placed over a low loss support material. The DP resonator can be used for characterizing the material at different frequencies by exciting the higher order modes. The electromagnetic field distribution of TE_{011} mode is shown in Figure 6.4. The field distribution studies will assist to estimate the permittivity of the material at different frequencies. This technique also needs machining of the sample but the height of the sample is more

flexible. This technique can be used for timber or fresh biological samples machined in cylindrical shape.

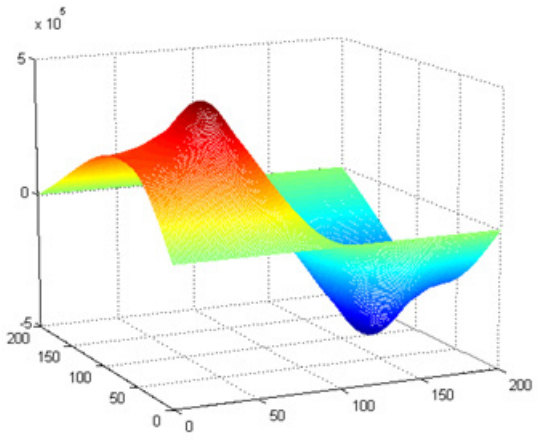

Figure 6.4: H_r Fields for different quasi TE_{0mn} modes in MgF_2 loaded DP resonator (Jacob, et al. 2005).

6.4.5 Whispering Gallery Mode Resonator

The Whispering Gallery Mode (WGM) Resonators (Krupka, *et al.* 1999) enable the most accurate measurements of very low loss dielectric materials. The WGM technique is a very complex one and requires large dielectric samples of specific shapes. WGM describes the electromagnetic wave that circulates around the inner surface of a dielectric sphere or cylinder as the result of total internal reflection. At millimeter wavelengths, the conventional dielectric resonators (as listed above) operate in their TE or TM modes have quite small dimensions, lower Q-factor and are difficult to machine. The WGM operates at higher frequencies and the Q-factor is very high. But it is difficult to identify the correct modes and hence it is advisable to know the approximate value of the permittivity before using WGM resonators for microwave characterization using another technique.

6.4.6 Open-ended co-axial probe method

The open ended co-axial probe method (Gabriel, *et al.* 1996, Ellison and Moreau 2008, Technologies 2010, Yaw 2012) is a non-destructive method and the method assumes only the TEM or TE mode is propagating. In this method the probe is pressed against a specimen or immersed into the liquids and the reflection coefficient is measured

and used to determine the permittivity. Since the sample must be in contact with the probe, it is critical to have the sample polished to avoid air gaps for solid specimens. In many cases it is not possible to machine or prepare the samples so that we can use some techniques such as dielectric resonator or waveguide. This is especially important in the case of biological specimens to perform in-vivo measurements because the material characteristics may change. Therefore, with this method the sample can be placed in close contact with the probe without causing any changes in the material properties.

The reflection coefficient is measured using a vector network analyzer (VNA). The VNA with a probe system is first calibrated so that the reflection coefficient measurements are referenced to the probe's aperture plane. This can be done by using reference liquids for direct calibration at the open end of the probe. Though simple, the uncertainties in the measurement are due to the uncertainties in the characterization of the reference liquids and the selection of reference liquids as calibration standard. In this method, all measurements are performed by placing the standards (a short, an open and a referenced liquid) at the end of the probe. The referenced liquid is used as a calibration standard and must be a liquid with known dielectric properties. Water, saline and methanol are usually selected as the reference liquids. Standard one port full calibration is then applied. The s-parameters measured on the MUT can be post-processed to obtain the dielectric parameters using a program.

Advantages of open ended coaxial probe method

- Require no machining of the sample, easy sample preparation.
- After calibration, the dielectric properties of a large number of samples can be routinely measured in a short time.
- Measurement can be performed in a temperature controlled environment.
- Disadvantages of open ended coaxial probe method
- Only reflection measurement available.
- Affected by air gaps for measurement on specimen.

6.4.7 Dielectric Probe (Coaxial probe)

The open-ended coaxial probe is a cut off section of transmission line (Figure 6.5). This technique is ideal for a variety of materials including solids and liquids, and also for broadband measurement. Over all, the design is rugged and can withstand many physical conditions especially a wide range of temperatures.

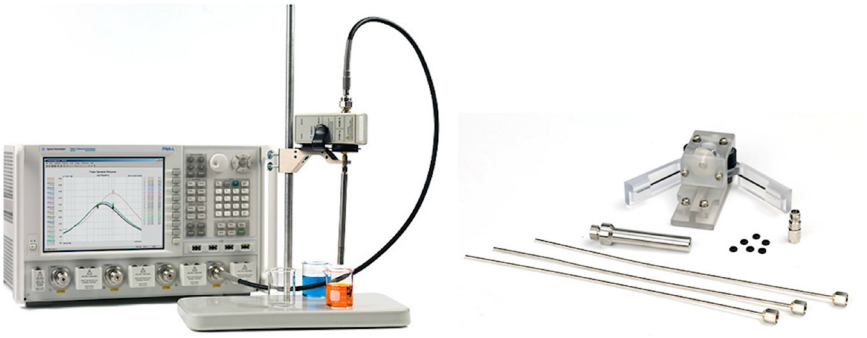

Figure 6.5: Dielectric Probe Setup (Agilent).

Most of the characterization techniques discussed so far are very good for a single frequency. In order to evaluate the sample over a wide range of frequencies wave guide techniques or dielectric probe (Agilent) techniques could be used. The open-ended coaxial probe is a cut off section of transmission line. The material is measured by touching the flat face of a solid material to the probe. The EM fields at the probe end penetrate into the material under test and the reflected signal (S_{11}) can be measured. The complex permittivity is computed from the reflected signal. However the accuracy and repeatability of the dielectric probe technique is very poor.

The Dielectric Probe (Figure 6.6) was used to measure the complex permittivity over a wide range of frequencies, thereby allowing the response over various frequencies for a particular dielectric to be viewed. It is a convenient measurement technique as it does not require manipulating the geometry of the dielectric material to be tested, however, the accuracy in the permittivity measurement is poor.

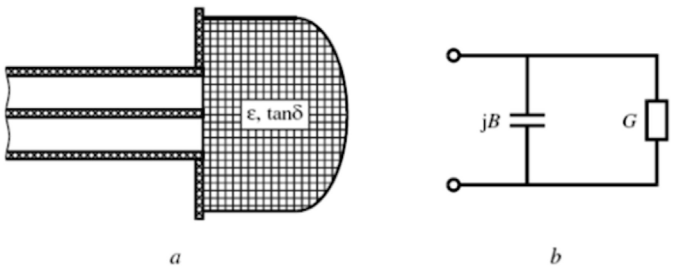

Figure 6.6: a – Schematic of a dielectric probe with open end, b – equivalent circuit of dielectric probe (Mekhannikov, et al. 2007).

The principle of operation involves the propagation of a TEM travelling wave, launching fringing EM fields from the open end, into the dielectric material. The reflection coefficient can be related to the complex permittivity by using; modal analysis of the fields in the transmission line, or by analyzing the fields in the dielectric material. Equations below govern the determination of permittivity and loss tangent for a dielectric probe. (Mekhannikov, *et al.* 2007)

$$\varepsilon = \frac{2T\sin\left[2B + \frac{4\pi(L_2 - L_1)}{\lambda}\right]}{B\left\{1 + T^2 + 2T\cos\left[2B + \frac{4\pi(L_2 - L_1)}{\lambda}\right]\right\}} \tag{6.21}$$

$$\tan\delta = \frac{1 - T^2}{2T\sin\left[2B + \frac{4\pi(L_2 - L_1)}{\lambda}\right]} \tag{6.22}$$

where:

T - Is magnitude of reflection coefficient of the probe with sample.

B - Standing wave ratio.

The dielectric probe technique calculates the dielectric properties from the phase and amplitude of the reflected signal at the end of an open-ended coaxial line inserted into a sample to be measured. The coaxial probe has a tip used for sensing the signal reflected from the material. The tip is brought into contact with the substance by touching the probe to a flat face of a solid or by immersing it in a liquid. This method is easy to use and makes it possible for the dielectric properties to be measured over a wide range of frequencies (500 MHz – 110 GHz). The operations of the open-ended coaxial lines to measure the dielectric constant of unknown materials is documented in papers by Athey, Stuchly, & Stuchly. The input reflection coefficient at the probe tip is given by:

$$\rho = \frac{Z_L - Z_o}{Z_L + Z_o} = \frac{Y_o - Y_L}{Y_o + Y_L} \tag{6.23}$$

where Z_0 is the line impedance and Z_L is the load impedance. When placed in contact with a homogenous material whose thickness is sufficient to simulate a slab of infinite electrical thickness, an open coaxial line has an admittance, Y_L, of:

$$Y_L(\omega, \varepsilon) = Y_i(\omega) + Y_e(\omega, \varepsilon) \tag{6.24}$$

This admittance value is comprised of two terms; the first is the internal admittance, Y_i, corresponding to the fringing capacitance that accounts for the fringing field in the Teflon region between the inner and outer conductors of the line. The second term is the external admittance, Y_e, which is a function of the frequency and the dielectric constant of the material being examined. A calibration is required when operating the measurement probe in order to define values concerned with the capacitance, conductance and geometry of the probe. This enables an iterative process to find a value for the dielectric constant, ϵ.

Ulaby and El-Rayes operated the dielectric probe over a wide frequency range extending from 0.1 GHz up to 20 GHz, which requires a small radii probe, and also there is a need to have strong sensitivities to variations in the dielectric properties, which require a probe with a large radii.

One of the typical issues is to obtain good surface contact and hence the measured reflection may not represent full reflectance from the sample. Surface preparation of solid samples must be done very carefully to insure that no air gaps remain where the probe is applied. The change in reflected signal is dependent on the electrical properties of the impedance which terminates the line. In the case of the coaxial probe, the sample material terminates the line and its properties are mirrored in the reflection coefficient.

6.4.8 Free Space Method

The free space method (Courtney 1970, Athey, *et al.* 1982, El-Rayes and Ulaby 1987, Ghodgaonkar, *et al.* 1990, Amiet and Jewsbury 2000, Trabelsi and Nelson 2003, F.H.Wee, *et al.* 2009, Juan-García and Torrents 2010, Cataldo, *et al.* 2011) is for broadband applications and assumed only the TEM propagation mode. Free space technique is good for materials that can remain unmodified for characterization purposes. Free space metrology is used for characterizing materials in an un-enclosed environment (Figure 6.7). Reflective mirrors are set up, such that diverging beams are directed onto a piece of dielectric material. Though surface modification or separate enclosure is not required, measurements performed in open space will increase possibility of obtaining inaccurate results.

Free space measurement allows measurements on MUT under many environmental or physical conditions such as high temperatures and wide band frequencies. The measurement requires the MUT to be large and flat. It usually utilizes two antennas placed facing each other and the antennas are connected to a network analyzer. Before starting the measurement, the VNA must first be calibrated. There are a number of calibration methods that can be used, such as the through-reflect-line (TRL), the through-reflect-match (TRM) and the line-reflect-line (LRL). However, the LRL calibration method can produce the highest calibration quality. The line standard can be achieved by separating the focal plane of the two antennas to approximately a

quarter of wavelength. The reflect standard can be obtained by placing a metal plate on the sample holder in between the antennas. Once calibrated, the s-parameters of an empty sample holder are measured by placing the sample holder midway between the two antennas. The MUT is then placed on the sample holder between the antennas and the s-parameter measurement is performed again. Using the de-embedding function of the VNA, the influence of the sample holder can be cancelled out and only the s-parameter of the MUT can be determined. The s-parameter for both the reflection and transmission coefficients can be determined.

Time domain gating should also be applied to ensure there are no multiple reflections in the sample itself, though appropriate thickness should able to avoid this. It also eliminates the diffraction of energy from the edge of the antennas. The dielectric properties can be determined by post processing the measured reflection and transmission coefficient using a program.

Advantages of free space method

- Can be used for high frequency measurement.
- Allows non-destructive measurement.
- Measure MUT in hostile environment.
- Both the magnetic and electric properties can be evaluated.

Disadvantages of free space method

- Need large and flat MUT.
- Multiple reflections between antenna and surface of sample.
- Diffraction effects at the edge of sample.

6.4.9 Antenna

In the case of many materials it is hard to use dielectric probe or cavity resonators because the probes cannot be kept in contact. For materials such as vegetables or soils etc, a non-destructive technique involving a pair of horn antennae can be used; this is a free-space method operating in the far-field region employing spot-focusing horn lens antennae. This technique measures reflection coefficients and from the measured data dielectric constants, loss factors, and complex permeability as a function of frequency (microwaves) can be estimated.

This technique is suitable for precise, accurate and reproducible microwave measurements on materials under various environmental conditions and complex electromagnetic environmental conditions due to contactless feature of free-space measurements. Composite materials such as timber, vegetable and soil which are lossy and anisotropic cause a linearly polarized electromagnetic field to be depolarized (i. e. elliptically polarized) upon transmission through the material.

The measurement system consists of a pair of spot-focusing horn lens antennas, mode transitions, coaxial cables and a vector network analyzer. The inaccuracies in

free-space measurements are due to two main sources of errors. The spot-focusing antennae are used for minimizing diffraction effects and free-space LRL (line, reflect, line) calibration method implemented on VNA eliminates errors due to multiple reflections. The time domain gating or smoothing feature of VNA is used to reduce post calibration errors in reflection and transmission measurements. The main errors are due to:

i. Diffraction effects at the edges of the material specimen/sample.
ii. Multiple reflections between horn lens antennas and mode transitions via the surface of the sample.

The sample is kept in between the two focused antennas, which are connected to the two ports of the vector network analyzer by using precision coaxial cables, rectangular-to-circular waveguide adapters and coaxial-to-rectangular waveguide adapters.

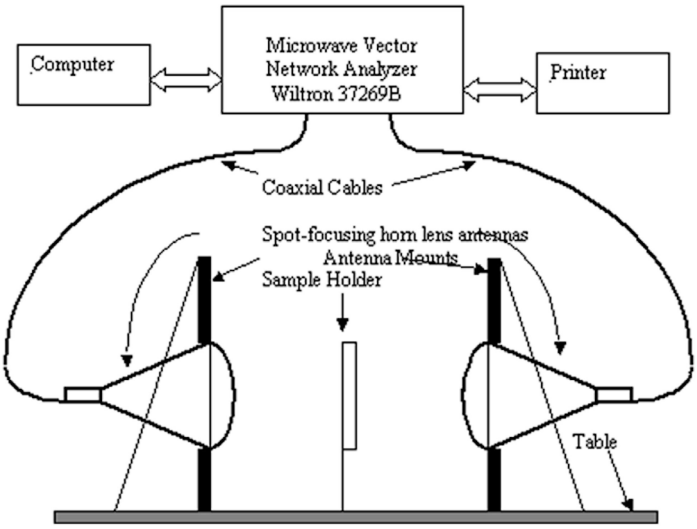

Figure 6.7: Microwave Nondestructive Testing using Free-Space Microwave Measurement Techniques (Ghodgaonkar, et al. 1990).

6.4.10 Near-field Microwave Probe

Local properties of thin films can be measured by focusing the EM fields on to the film surface. This can be done by using a near field microwave probe (Gao and Xiang 1998), which scans thin films or measures submicron materials because the resolution can be much smaller than $\lambda/2$. The near-field microwave probe usually consists of

a resonator connected to a probe on the bottom, so that as the probe approaches a material, it shifts the cavity resonance. The measurement requires measurement of resonant frequency and Q with and without the specimen and analysis of the shift in measured parameters. In order to obtain precise accuracy in measurement a theoretical and numerical model that relates shifts in the system's cavity resonator to the material under test is needed.

6.4.11 Reentrant Cavity

The reentrant cavity consists of a coaxial line or other transmission line with a gap in the inner electrode. The specimen is inserted into this gap. The cavity is then resonated and the capacitance of the gap produces a frequency shift. Depends on the specimen gap region the cavity can be a singly reentrant cavity or a doubly reentrant cavity. The resonant reentrant cavity typically estimates the permittivity component normal to the face of the material. This Technique is ideal for low microwave frequency region.

6.4.12 Fabry-Perot Resonator

Fabry-Perot Resonators (Courtney 1970, Clarke and Rosenberg 1982) are characterised by very high Q factors (typically around 200,000) and are ideal for characterisation of low loss materials in the millimetre range region. Fabry-Perot Resonators, a form of open resonator, uses two sufficiently large mirrors to direct a Gaussian beam of light at a sample material to determine the complex permittivity. In the confocal setup both mirrors are concave, whereas in the semi-confocal arrangement only one of the mirrors is concave and the other is flat Since they are open structures they suffer from leakage of radiation. This can be reduced by large samples such that the Gaussian beam incidents the sample at full strength which is usually taken to be an integral multiple of ½ the wavelength (λ). The tensor permittivity values can be obtained by measuring at different angles of incidence. When combined with a 'Bragg Reflector' these resonators become excellent at measuring complex permittivity of gasses.

6.5 Conclusions

Figure 6.8 shows the different types of measurement technique used and the feasibility of methods as a function of frequency. Based on the nature of samples required for this project, dielectric probe and free-space measurement using transmitting and reflecting antenna are ideal measurement systems for biological samples and plant materials. Table 6.1 shows the dielectric constant of many materials.

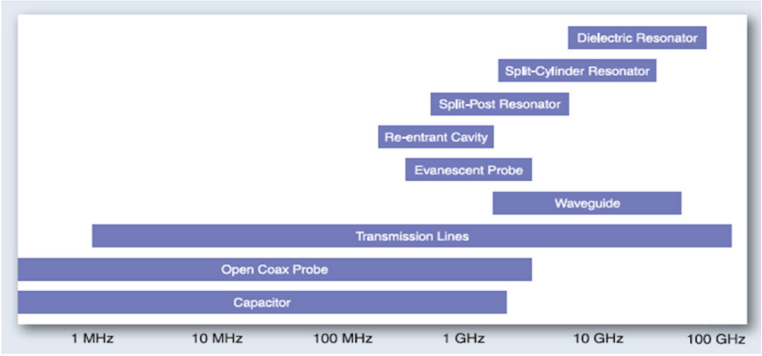

Figure 6.8: Different microwave characterization techniques used as a function of frequency (Baker-Jarvis, et al. 2010, Yaw 2012).

Table 6.1: The real part of the Dielectric Constant of Various Materials.

Material Name	Relative Dielectric Constant	Material Name	Relative Dielectric Constant
Acetic acid	6.2	Fat	16
Air	1	Fibre	5
Alcohol, ethyl (grain)	24.55	Flour (dry)	4.1 - 6.2
Alcohol, methyl (wood)	32.7	Formica	3.6
Amber	2.6 - 2.7	Freon 12 (vapour)	2.4
Asbestos	4	Freon 12 (liquid)	3.5
Asbestos fibre	3.1 - 4.8	Germanium	16
Asphalt	2.6	Glass	5.0 - 10.0
Bakelite	5	Glass pyrex	4.6
Barium titanate	100	Glycerine	42.5
Beeswax	2.4	Gutta percha	2.4
Benzene	2.284	Isolantite	6.1
Bone, cancellous	26	Jet fuel (jet a)	1.7
Bone, cortical	14.5	Kevlar	3.5 - 4.5
Brain, gray matter	56	Lead magnesium niobate	100
Brain, meninges	58	Lead oxide	25.9
Brain, white matter	43	Lead sulfide (galena)	200
Calcite	8	Lead titanate	200
Calcium carbonate	8.7	Liquid ammonia(-78°C)	25

Continued **Table 6.1:** The real part of the Dielectric Constant of Various Materials.

Material Name	Relative Dielectric Constant	Material Name	Relative Dielectric Constant
Cambric	4	Lithium deuteride	14
Carbon tetrachloride	2.17	Lucite	2.5
Cartilage, ear	47	Mica	4
Cartilage, general	22	Mica, canadian	6.9
Celluloid	4	Mica, muscovite	5.4
Cellulose	3.7 - 7.5	Micarta	3.2 - 5.5
Cellulose acetate	2.9 - 4.5	Muscle, smooth	56
Cement	~2	Muscle, striated	58
Cocaine	3.1	Mycalex	7.3
Cotton	1.3	Mylar	3.1
Diamond, type I	5.87	Neoprene	4
Diamond, type iia	5.66	Nylon	3.4 - 22.4
Durite	4.7 - 5.1	Oil, linseed	3.4
Ebonite	2.7	Oil, mineral	2.1
Epoxy resin	3.4 - 3.7	Oil, olive	3.1
Ethyl alcohol	6.5 - 25	Oil, petroleum	2.0 - 2.2
Eye, aqueous humor	67	Oil, silicone	2.5
Eye, cornea	61	Oil, sperm	3.2
Eye, sclera	67	Oil, transformer	2.2
Paper	3.3, 3.5	Slate	7
Paraffin	2	Soil	44
Plexiglas	3.4	Soil dry	2.4
Plexiglass	2.6 - 3.5	Steatite	5.2
Polycarbonate	2.9 - 3.2	Strontium titanate	332
Polyester	3.2 - 4.3	Styrofoam	1.03
Polyethylene	2.25 - 2.5	Sulfur	3.7
Polyimide	3.4	Tantalum pentoxide	27
Polypropylene	2.2 - 2.3	Teflon	2.1
Polystyrene	2.55	Tin antimonide	147
Polystyrene	2.4	Tin telluride	70
Polyvinyl chloride	3.18 - 4.5	Titanium dioxide (rutile)	114

Continued **Table 6.1:** The real part of the Dielectric Constant of Various Materials.

Material Name	Relative Dielectric Constant	Material Name	Relative Dielectric Constant
Porcelain	4.0 - 8.0	Tobacco	1.6 - 1.7
Potassium niobate	700	Tongue	38
Potassium tantalate niobate, 20°C	6000	Uranium dioxide	24
Quartz	5	Vacuum	1
Quartz, crystalline	4.5 - 4.6	Vaseline	2.16
Quartz, fused	3.8	Vinylite	2.7 - 7.5
Rubber	2	Water	80.4
Rubber, butyl	2.4	Water distilled	34
Rubber, neoprene	6.6	Water, ice, –30°C	99
Rubber, silicone	3.2	Water, liquid, 0°C	87.9
Rubber, vulcanized	2.9	Water, liquid, 100°C	55.5
Ruby mica	5.4	Water, liquid, 20°C	80.2
Salt	5.9	Water, liquid, 40°C	73.2
Selenium	6	Water, liquid, 60°C	66.7
Shellac	2.9 - 3.9	Water, liquid, 80°C	60.9
Silicon	11.8	Wax, beeswax	2.7 - 3.0
Silicon carbide (αsic)	10.2	Wax, carnuba	2.9
Silicon dioxide	4.5	Wax, paraffin	2.1 - 2.5
Silicone	3.2	Waxed paper	3.7
Silicone oil	2.7 - 2.8	Waxes, mineral	2.2
Skin	33 - 44	Wood dry	1.4 - 2.9

References

Afsar, M. N., Birch, J. R. and Clarke, R. N. 1986. The Measurement of the Properties of Materials. *Proceedings of the IEEE*. 74(1):

Amiet, A. and Jewsbury, P. 2000. Free space microwave permittivity and permeability measurements. *Proc. Microwave Conference, 2000 Asia-Pacific*. 445-448.

Athey, T. W., Stuchly, M. A. and Stuchly, S. S. 1982. Measurement of Radio Frequency Permittivity of Biological Tissues with an Open-Ended Coaxial Line: Part I. *Microwave Theory and Techniques, IEEE Transactions on*. 30(1): 82-86.

Baker-Jarvis, J., Janezic, M. D. and DeGroot, D. C. 2010. High-Frequency Dielectric Measurements. *Part 24 in a Series of Tutorials on Instrumentation and Measurement.*

Baker-Jarvis, J., Vanzura, E. J. and Kissick, W. A. 1990. Improved Technique for Determining Complex Permittivity with the Transmission/Reflection Method. *IEEE Transactions on Microwave Theory and Techniques*. 38(8):

Burdette, E. C., Cain, F. L. and Seals, J. 1980. In Vivo Probe Measurement Technique for Determining Dielectric Properties at VHF through Microwave Frequencies. *Microwave Theory and Techniques, IEEE Transactions on*. 28(4): 414-427.

Cataldo, A., Benedetto, E. D. and Giuseppe Cannazza. 2011. Broadband Reflectometry for Enhanced Diagnostics and Monitoring Applications. *Spinger*.

Clarke, R. N. and Rosenberg, C. B. 1982. Fabry-Perot and open resonators at microwave and millimetre wave frequencies, 2-300 GHz. *Journal of Physics E: Scientific Instruments*. 15(1): 9.

Courtney, C. C. 1998. Time-Domain Measurement of the Electromagnetic Properties of Materials. *IEEE Transactions on Microwave Theory and Techniques*. 46(5): 517-522.

Courtney, C. C. and Motil, W. 1999. One-Port Time-Domain Measurement of the Approximate Permittivity and Permeability of Materials. *IEEE Transactions on Microwave Theory and Techniques*. 47(5): 551-555.

Courtney, W. E. 1970. Analysis and Evaluation of a Method of Measuring the Complex Permittivity and Permeability Microwave Insulators. *Microwave Theory and Techniques, IEEE Transactions on*. 18(8): 476-485.

El-Rayes, M. A. and Ulaby, F. T. 1987. Microwave Dielectric Spectrum of Vegetation-Part I: Experimental Observations. *Geoscience and Remote Sensing, IEEE Transactions on*. GE-25(5): 541-549.

Ellison, W. J. and Moreau, J. M. 2008. Open-Ended Coaxial Probe: Model Limitations. *Instrumentation and Measurement, IEEE Transactions on*. 57(9): 1984-1991.

F.H.Wee, PJ.Soh, Suhaizal, A. H. M., H.Nornikman and Ezanuddin, A. A. M. 2009. Free Space Measurement Technique on DielectricProperties of Agricultural Residues at Microwave Frequencies

SBMO/IEEE MTT-S International Microwave & Optoelectronics Conference Proceedings.

Gabriel, S., Lau, R. W. and Gabriel, C. 1996. The dielectric properties of biological tissues: II. Measurements in the frequency range 10 Hz to 20 GHz. *Physics in Medicine and Biology*. 41(11): 2251.

Gao, C. and Xiang, X. D. 1998. Quantitative microwave near-field microscopy of dielectric properties. *Review of Scientific Instruments*. 69(11): 3846-3851.

Ghodgaonkar, D. K., Varadan, V. V. and Varadan, V. K. 1990. Free-space measurement of complex permittivity and complex permeability of magnetic materials at microwave frequencies. *Instrumentation and Measurement, IEEE Transactions on*. 39(2): 387-394.

Griffiths, D. J. 1999. Introduction to electrodynamics (Third ed.). *Prentice Hall*. pp. 559–562.

Jacob, M. V., Mazierska, J. and Krupka, J. 2005. Dielectric properties of Yttrium Vanadate crystals from 15 K to 295 K. *Journal of Electroceramics*. 15(3): 237-241.

Jacob, M. V., Mazierska, J., Leong, K. and Krupka, J. 2002. Microwave properties of low-loss polymers at cryogenic temperatures. *Ieee Transactions on Microwave Theory and Techniques*. 50(2): 474-480.

Janezic, M. D. and Williams, D. F. 1997. Permittivity characterization from transmission-line measurement. *Proc. Microwave Symposium Digest, 1997., IEEE MTT-S International*. 3: 1343-1346 vol.3.

Juan-García, P. and Torrents, J. M. 2010. Measurement of mortar permittivity during setting using a coplanar waveguide. *Measurement Science and Technology*. 21(4): 045702.

Krupka, J. 1999. Comparrison of split post dielectric resonator and ferrite disc resonator techniques for microwave permittivity measurements of plycrystalline yttrium iron garnet.

Krupka, J. 2006a. Frequency domain complex permittivity measurements at microwave frequencies. *Measurement Science and Technology*. (6): R55.

Krupka, J. 2006b. Frequency domain complex permittivity measurements at microwave frequencies. *Meas. Sci. Technol.* 17: R55 - R70.

Krupka, J., Clarke, R. N., Rochard, O. C. and Gregory, A. P. 2000. Split post dielectric resonator technique for precise measurements of laminar dielectric specimens-measurement uncertainties. *Proc. Microwaves, Radar and Wireless Communications. 2000. MIKON-2000. 13th International Conference on*. 1: 305-308 vol.1.

Krupka, J., Derzakowski, K., Abramowicz, A., Tobar, M. E. and Geyer, R. G. 1999. Use of whispering-gallery modes for complex permittivity determinations of ultra-low-loss dielectric materials. *Microwave Theory and Techniques, IEEE Transactions on*. 47(6): 752-759.

Mekhannikov, A., Myl'nikov, A. and Maslennikova, L. 2007. Calibration of a coaxial antenna-probe for microwave dielectric measurements. *Measurement Techniques*. 50(4): 425-428.

Murata, K., Hanawa, A. and Nozaki, R. 2005. Broadband complex permittivity measurement techniques of materials with thin configuration at microwave frequencies. *Journal of Applied Physics*. 98(8): 084107-1 to 084107-8.

Sheen, J. 2005. Study of microwave dielectric properties measurements by various resonance techniques. *Measurement*. 37(2): 123-130.

Sheen, J. 2007. Microwave measurements of dielectric properties using a closed cylindrical cavity dielectric resonator. *Ieee Transactions on Dielectrics and Electrical Insulation*. 14(5): 1139-1144.

Technologies, A. 2006. Split Post Dielectric Resonators for Dielectric Measurements of Substrates 1(1): 11.

Technologies, A. 2010. Technical Overview: 85070E Dielectric Probe Kit 200 MHz to 50 GHz, *online*.

Trabelsi, S. and Nelson, S. O. 2003. Free-space measurement of dielectric properties of cereal grain and oilseed at microwave frequencies. *Measurement Science and Technology*. 14(5): 589.

Wang, Z. Y., Kelly, M. A., Shen, Z. X., Wang, G., Xiang, X. D. and Wetzel, J. T. 2002. Evanescent microwave probe measurement of low-k dielectric films. *Journal of Applied Physics*. 92(2): 808-811.

Yaw, K. C. 2012. Measurement of Dielectric Material Properties Application Note. *Rhode and Shawrtz Technical Publication*.

Yue, H., Virga, K. L. and Prince, J. L. 1998. Dielectric Constant and Loss Tangent Measurement Using a Stripline Fixture. *IEEE Transactions on Components, Packaging and Manufacturing Technology - Part B*. 21(4):

7 Dielectric Properties of Organic Materials

Interest in the dielectric properties of various organic materials stems from the array of potential engineering applications these studies can support. Various food products have been studied to better understand microwave heating potential for food processing (Ohlsson and Risman 1978). The potential for RF and microwave drying of organic materials have also been explored (Chuah, *et al.* 1997, Cui, *et al.* 2005). Other studies have been undertaken with RF and microwave sensing systems in mind (Ulaby and Jedlicka 1984, van Dam 2005), while others have explored to potential for differentiating and detecting different organic materials in a mixed environment. These latter studies have wide interest for biosecurity and pest detection (Donskoy and Sedunov 2002).

The interactions between electromagnetic waves and materials in the radio frequency to microwave range of the spectrum largely depend on: electrical conductivity at lower frequencies; and dipole movement at higher frequencies. The behaviour of dipoles in a material is defined by a material parameter known as the complex dielectric constant. Several studies have demonstrated that the complex dielectric constant is dependent on the physical and chemical properties of the material (Tiitta, *et al.* 2003, Dinulović and Rašuo 2011, Sung, *et al.* 2011). This chapter presents information about the dielectric characterisation of organic materials and the development of a Debye-Cole multi-dispersion dielectric mixing model to predict these dielectric properties from simple physical parameters.

Most organic materials can be considered as a mixture of air, water and solid materials (Ulaby and El-Rayes 1987). When the moisture content of an organic material is high, some of the water in the cellular structure of organic matter will be in a relatively free liquid state; however some of the water will be bound to the solid material by hydrogen or chemical bonds (Youngman, *et al.* 1999, Brodie 2008). The dipole molecules in this bound water component are not as free to move as in free water; therefore the dielectric response of bound water will be very different to that of free water.

As organic materials dry, air fills the cellular voids vacated by the free water and the water which remains in the material is bound to the organic polymers (Youngman, *et al.* 1999, Brodie 2008). Therefore the dielectric properties of organic materials change significantly with moisture content. Dissolved salts also affect the dielectric properties of organic materials. The dielectric properties of water and organic polymers are also temperature dependent (Nelson 1991). This temperature dependence is a function of the dielectric relaxation processes operating under the particular conditions existing in the material and the frequency being used (Nelson 1991).

In some cases, such as in plant stems, cellular orientation affects the dielectric properties of the organic material. Generally the dielectric properties are higher when the electromagnetic wave's electric field is oriented parallel to the cellular orientation

and less when the electric field is oriented perpendicular to the cellular orientation (Torgovnikov 1993).

Material density also affects the dielectric properties of organic materials. The density of a dry organic material depends on the three dimensional geometry of the underlying organic cell structure, which will determine the volume-fraction of voids that can be filled with air or water. Therefore material density will also affect the dielectric properties of organic materials.

7.1 Frequency Dependency of Dielectric Properties

With the exception of some almost transparent materials that hardly absorb any energy from RF and microwave fields, the dielectric properties of most materials vary with the frequency of the applied electric fields (Nelson 1991). This frequency dependence is associated with the ability of dipolar molecules to move in time with any applied electromagnetic fields. Materials usually have a characteristic response (or relaxation) time that depends on the molecular structure of the dipolar molecules and any surrounding structures in the bulk organic material (Calderwood 1992).

Debye (1929) was among the first to study relaxation in polar molecules. From the instant that a constant electric field is applied to a polar material, the polarization caused by the permanent dipoles (i.e. the orientation polarization) rises exponentially with a time constant τ to its final steady-state value P. When this external field is removed, this polarization decays exponentially with the same time constant τ (Calderwood 1992). This is termed the relaxation time of the process.

When an alternating electromagnetic field is applied to a dipolar material, the dipole may move in time with the field, lag behind the applied field or remain relatively unaffected (Chaplin 2007). The ability of the dipolar molecule to keep up with the applied electromagnetic field depends on the relaxation time of the dipole.

Debye (1929) defined the complex dielectric constant, including the electrical conductivity of the material, by equation (7.1):

$$\varepsilon = \varepsilon_{\infty} + \frac{\varepsilon_s - \varepsilon_{\infty}}{1 + j\omega\tau} - j\frac{\sigma}{\omega\varepsilon_o} \tag{7.1}$$

where ε_{∞} is the dielectric constant at very high frequencies; ε_s is the dielectric constant at very low frequencies; ω is the angular frequency (rad s^{-1}); τ is the relaxation time of the dipoles (s); σ is the conductivity of the material (Siemens m^{-1}) ; j is the complex operator (i.e. $j = \sqrt{-1}$), and ε_o is the dielectric permittivity of free space.

This dielectric constant is a complex number, which can be decomposed into a real and an imaginary component after some manipulation. The real part of this number is:

$$\varepsilon' = \varepsilon_\infty + \frac{\varepsilon_s - \varepsilon_\infty}{1 + \omega^2\tau^2} \tag{7.2}$$

While the imaginary part becomes:

$$\varepsilon'' = \frac{(\varepsilon_s - \varepsilon_\infty)\omega\tau}{1 + \omega^2\tau^2} + \frac{\sigma}{\omega\varepsilon_o} \tag{7.3}$$

The dielectric constant ε' expresses the material's ability to store electrical energy (Singh and Heldman 1993) and thus represents the reactive nature of the material's dielectric properties (Smith 1976, Giancoli 1989); in particular ε' influences the wave impudence of the space occupied by the dielectric material, causing reflections at the inter-facial boundary between the air and the dielectric material. Changes in wave impedance also cause refraction of the wave due to the change in the propagation velocity of the wave within the dielectric material compared with its velocity in air or vacuum (Montoro, *et al.* 1999).

The dielectric loss ε" represents the resistive nature of the material's electrical properties (Smith 1976, Giancoli 1989). Resistive losses within the medium reduce the amplitude of the microwave field and generate heat inside the material.

It is common practice to express the dielectric properties of a material in terms of the relative dielectric constants κ' and κ", which are defined such that: $\varepsilon' = \kappa'\varepsilon_o$ and $\varepsilon'' = \kappa''\varepsilon_o$. Most materials have a complex frequency response; however the general form of the dielectric properties of polar materials resembles the normalised example shown in Figure 7.1.

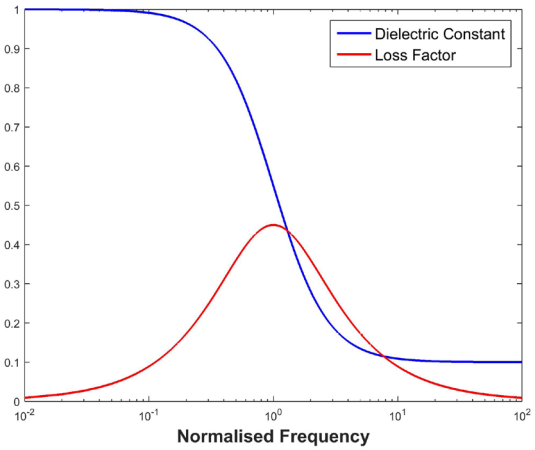

Figure 7.1: Normalised Dielectric Properties of a Polar Material.

The dielectric properties of most materials are directly associated with its molecular structure. Debye's basic relationship assumes that the molecules in a material are homogeneous in structure and can be described as "polar". Since few materials can be described in this way, many other equations have been developed to describe frequency-dependent dielectric behaviour.

In many cases, the material may be regarded as a composite or mixture and will exhibit multiple relaxation times. If this is the case then the complex dielectric constant may be represented by a variation of Debye's original equation (Kuang and Nelson 1997):

$$\kappa = \kappa_{\infty} + a\left(\frac{\kappa_s - \kappa_1}{1 + j\omega\tau_1}\right) + b\left(\frac{\kappa_1 - \kappa_2}{1 + j\omega\tau_2}\right) + .. - j\frac{\sigma}{\omega\varepsilon_o} \tag{7.4}$$

Where κ_1 and κ_2 are intermediate values of the dielectric constant between the various relaxation periods of τ_1 and τ_2, and a and b are constants related to how much of each component is precent in the total material.

7.2 Temperature Dependence of the Dielectric Properties

As temperature increases, the relaxation time usually decreases, and the loss-factor peak, illustrated in Figure 7.1, will shift to higher frequencies. For many materials, this means that at dispersion frequencies the dielectric constant will increase while the loss factor may either increase or decrease depending on whether the operating frequency is higher or lower than the relaxation frequency (Nelson 1991). For example, Table 7.1 shows how the dielectric properties of some food stuffs vary with temperature.

Some food stuffs in Table 7.1 follow the predicted trend of increasing dielectric constant as temperature increases; however it is apparent that the dielectric constant of other entries in Table 7.1 decline with increasing temperature rather than increasing with temperature. This is linked to their water content, because the dielectric constant of water at a fixed frequency decreases with increasing temperature (Figure 7.2).

Table 7.1: Dielectric properties of some common foods at 2.8 GHz as a function of temperature (Source: Ohlsson and Bengtsson 1975).

Food Product	Moisture Content	Fat Content	Temperature					
			50		75		100	
			ε'	ε"	ε'	ε"	ε'	ε"
Peanut Butter	-	48.5	3.1	4.1	3.2	4.5	3.5	5.0
Ground Beef	50.7	31.9	39.0	10.4	32.2	11.5	31.7	12.6
Ham	69.1	4.7	66.6	47.0	87.4	57.0	101.0	60.0
Concentrated Orange Juice	57.6	-	54.1	15.7	53.5	15.2	52.0	15.7
Mashed Potatoes	81.3	0.9	60.6	17.4	56.3	16.5	52.9	15.8
Peas, cooked	778.6	-	60.8	12.6	50.5	9.7	46.6	9.1

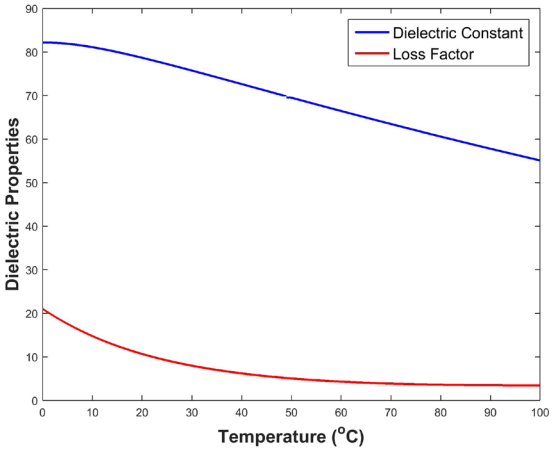

Figure 7.2: Dielectric properties of pure water as a function of temperature at 2.45 GHz.

7.3 Density and Field Orientation Dependence of Dielectric Properties

Because a dielectric material's influence over electromagnetic waves depends on the amount of the material, it follows that the density of the material must influence the bulk dielectric properties of organic materials. This is especially true of particulate materials, such as soil, grains or flours (Nelson 1991).

As an example, Torgovnikov's (1993) work with wood polymers demonstrates that the dielectric properties of oven dried wood depends on the wood density (ρ). The dielectric properties of wood also depend on whether the electromagnetic wave's electric field is oriented parallel or perpendicular to the wood grain (James 1975, Torgovnikov 1993). For example, Table 7.3 shows the dielectric properties of Blue Gum (*Eucalyptus globulus*) wood of different densities and moisture content, with the electric field parallel or perpendicular to the wood grain.

Table 7.2: Dielectric properties of Blue Gum samples as a function of density, moisture content and field orientation (Source: Daian and Shramkov 2005).

Density (kg/m³)	Moisture Content (%)	Field Orientation	κ'	κ"
718	0.0	Perpendicular	1.9	0.1
		Parallel	2.3	0.3
	10.8	Perpendicular	2.4	0.4
		Parallel	3.5	0.7
	68	Perpendicular	13.4	3.2
		Parallel	21.9	4.1
601	95	Perpendicular	15.3	3.8
		Parallel	27.0	5.1
	100	Perpendicular	16.1	3.8
		Parallel	28.1	5.1

The dielectric properties of oven dry wood, with the electric field perpendicular to the wood grain, are described by:

$$\kappa' = \kappa_\infty + \frac{\left(\kappa_o - \kappa_\infty\right)\left[1 + \omega\tau^{(1-\alpha)} Cos\left(\pi\frac{1-\alpha}{2}\right)\right]}{\left[1 + \omega\tau^{2(1-\alpha)} + 2\omega\tau^{(1-\alpha)} Cos\left(\pi\frac{1-\alpha}{2}\right)\right]} \tag{7.5}$$

and

$$\kappa'' = \frac{\left(\kappa_o - \kappa_\infty\right)\left[1 + \omega\tau^{(1-\alpha)} Cos\left(\pi\frac{1-\alpha}{2}\right)\right]}{2\left[1 + \omega\tau^{2(1-\alpha)} + 2\omega\tau^{(1-\alpha)} Cos\left(\pi\frac{1-\alpha}{2}\right)\right]} \tag{7.6}$$

Table 7.3 shows values of κ_0 and κ_∞ as a function of wood density. These relationships can be expressed as:

$$\kappa_\infty = 1.2696e^{1.1149\rho} \tag{7.7}$$

and

$$\kappa_o = 1.0805e^{0.6884\rho} \tag{7.8}$$

where ρ is the density of the dry material (kg m^{-3}).

Table 7.3: Values of κs and κ∞ for oven dried wood of various densities when the electric field is perpendicular to the wood grain (Based on data from: Torgovnikov 1993).

Wood Density (g/cm3)	κ_0	κ_∞	Wood Density (g/cm3)	κ_0	κ_∞
0.13	1.4	1.16	1.0	4.0	2.3
0.2	1.6	1.2	1.2	4.8	2.5
0.4	2.0	1.4	1.4	6.0	2.8
0.6	2.5	1.65	1.53	6.8	2.9
0.8	3.2				

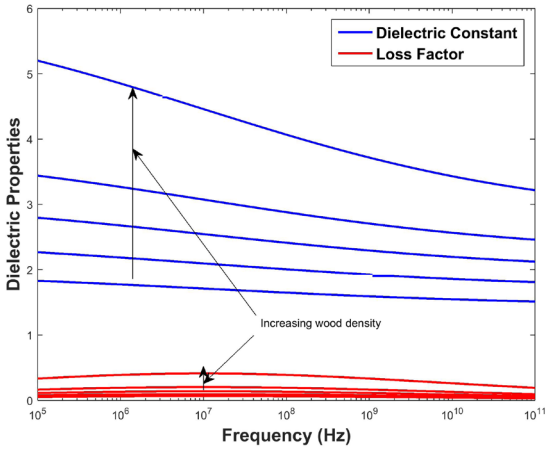

Figure 7.3: Estimated relative dielectric properties of oven dried wood, with the electric field perpendicular to the wood grain, as a function of frequency and wood density (ρ = 400 kg m^{-3} to 1,400 kg m^{-3}).

7.4 Dielectric Modelling of Organic Materials

Equipment for the direct measurement of dielectric properties is usually expensive and requires specialist techniques to determine the dielectric properties. Therefore many studies have focused on developing useful models for estimating the dielectric properties of agricultural and forestry products from parameters that are much easier to measure, such as moisture content, density and electrical conductivity.
Some models are based on empirical assessment of the material under test, while other models can be developed by assessing the contribution from separate components of the mixture. For example, organic materials are usually composed of various polymers, bound water, free water and air. The dielectric properties of air are close to that of free space and can be regarded as such in most calculations, while the dielectric properties of free and bound water have been well studied over many years (Ellison, *et al.* 1996, Buchner, *et al.* 1999, Boyarskii, *et al.* 2002). The dielectric properties of organic materials must be understood in terms of equation (7.4), were the dielectric properties of the bulk material can be estimated from the contribution of each constituent material.

Ulaby and El-Rayes (1987) developed a dielectric mixture model for plant leaf material based on a non-dispersive residual value combined with the volume-fraction weighted dielectric properties of free and bound water. Using their work as a guide, a dielectric mixing model for organic materials can be based on the volume weighted fractions for: oven dried organic material; free water; and bound water. This can be expressed as:

$$\kappa = v_s \kappa_s + v_{fw} \kappa_{fw} + v_{bw} \kappa_{bw} \tag{7.9}$$

where v_s is the volume fraction for total solids, k_s is the complex dielectric constant for dry organic materials; v_{fw} is the volumetric fraction of free water in the sample; k_{fw} is the complex dielectric constant of free water; v_{bw} is the volumetric fraction of bound water in the sample; and k_{bw} is the complex dielectric constant of bound water.

While several models have been proposed to distinguish bound water from free water, none of these models are easily verifiable (Ulaby and El-Rayes 1987). Ulaby and El-Rayes (1987) have proposed that the volume fraction for bound water is:

$$v_{bw} = \frac{4.64m^2}{3\left(1+7.36m^2\right)} \tag{7.10}$$

where m is the gravimetric moisture content of the material. As a starting point for the proposed model, the volume fraction for free water was assumed to be:

$$v_{fw} = 1 - m_s \tag{7.11}$$

where m_s is the total solids fraction of the sample on a gravimetric basis.

7.4.1 Modelling the Dielectric Properties of Free Water

Although the simple molecular structure of water (i.e. H_2O) has been known for some time, it is only recently that the complex structures of water have been more carefully studied (Chaplin 2000). Water molecules cling to one another by a mechanism called hydrogen bonding. In its liquid phase, this hydrogen bonding creates a network of water molecules throughout the fluid. Chaplin (2000) proposes that liquid water consists of fluctuating three-dimensional networks of water molecules, with localised icosahedral symmetry, derived from spheroidal clusters containing up to 280 fully hydrogen-bonded molecules that interconvert between lower and higher density forms. The resulting three-dimensional structure somewhat resembles a geodetic sphere; therefore, dipole movement in water depends on the strength and extent of these hydrogen bonded clusters within the liquid phase (Chaplin 2004, 2007).

In the free liquid state, the strength and extent of the hydrogen bonding determines the relaxation time of water molecules (Buchner, *et al.* 1999). As the temperature increases, the strength of the hydrogen bonding decreases, causing the relaxation time to reduce (Chaplin 2004, 2007). The relaxation time for bound water is longer than the relaxation time of free water, because the water molecules are more restricted (Tikhonov 1997). This implies that the frequency at which dipole movement of the water molecules occurs in bound water is usually lower than for free water. Tikhonov (1997) and Boyarskii et al. (2002) suggest that relaxation time for bound water decreases as the number of mono-molecular layers in the bound water film increases.

Meissner and Wentz (2004) suggest that a double Debye equation for the complex dielectric constant is needed to describe the dielectric behaviour of water in the RF and microwave range:

$$\kappa_{fw} = \kappa_\infty + \frac{\kappa_s - \kappa_1}{1 + j\,f/f_1} + \frac{\kappa_1 - \kappa_\infty}{1 + j\,f/f_2} - j\frac{\sigma}{2\pi f \varepsilon_o} \tag{7.12}$$

The various parameters are defined as:

$$\kappa_\infty = \left(3.6143 + 0.0028841 \times T\right)\left[1 + S\left(\text{-}0.00204265 + 0.000157883 \times \text{T}\right)\right] \tag{7.13}$$

$$\kappa_s = \left\{\frac{37088.6\text{-}82.168\times \mathrm{T}}{421.854+\mathrm{T}}\right\} \mathrm{e}^{\left(-0.00356417\times \mathrm{S}+0.00000474868\times \mathrm{S}^2+0.0000115574\times \mathrm{S}\times \mathrm{T}\right)} \tag{7.14}$$

$$\kappa_1 = \left\{\begin{matrix}5.723+\\0.022379\times \mathrm{T}\\-0.00071237\times \mathrm{T}^2\end{matrix}\right\} \mathrm{e}^{\left(-0.00628908\times \mathrm{S}+0.000176032\times \mathrm{S}^2-0.0000922144\times \mathrm{S}\times \mathrm{T}\right)} \tag{7.15}$$

$$f_1 = \left\{\frac{45+\mathrm{T}}{5.0478\text{-}0.070315\times \mathrm{T}+0.00060059\times \mathrm{T}^2}\right\}\times \left\{1+\mathrm{S}\times\left(\begin{matrix}0.00239357\\-0.000031353\times \mathrm{T}\\+0.000000252477\times \mathrm{T}^2\end{matrix}\right)\right\} \quad \text{GHz} \tag{7.16}$$

$$f_2 = \left\{\frac{45+\mathrm{T}}{0.13652\text{-}0.0014825\times \mathrm{T}+0.00024166\times \mathrm{T}^2}\right\}\times \left\{1+\mathrm{S}\times\left(\begin{matrix}-0.0199723\\+0.000181176\times \mathrm{T}\end{matrix}\right)\right\} \quad \text{GHz} \tag{7.17}$$

$$\sigma = a\sigma_{35}\mathrm{S}\frac{37.5109+5.45216\times \mathrm{S}+0.014409\times \mathrm{S}^2}{1004.75+182.283\times \mathrm{S}+\mathrm{S}^2} \tag{7.18}$$

$$a = 1+\frac{\left[\frac{\left(6.9431+3.2841\times \mathrm{S}\text{-}0.099486\times \mathrm{S}^2\right)}{\left(84.85+69.024\times \mathrm{S}+\mathrm{S}^2\right)}\right]\left(\mathrm{T}\text{-}15\right)}{49.843\text{-}0.2276\times \mathrm{S}+0.00198\times \mathrm{S}^2+\mathrm{T}} \tag{7.19}$$

$$\sigma_{35} = 2.903602+0.08607\times \mathrm{T}+0.0004738817\times \mathrm{T}^2 \text{-}0.000002991\times \mathrm{T}^3+0.0000000043047\times \mathrm{T}^4 \tag{7.20}$$

where T is the temperature (°C) and S is the salinity of the sample (parts per thousand). Salinity can be determined from electrical conductivity (EC) measurements, made at 25 °C under standard pressure using (Wagner, *et al.* 2006):

$$S = 0.012-0.2174\left(\frac{EC}{53087}\right)^{0.5}+25.3283\left(\frac{EC}{53087}\right)+13.7714\left(\frac{EC}{53087}\right)^{1.5}- 6.4788\left(\frac{EC}{53087}\right)^{2.0}+2.5842\left(\frac{EC}{53087}\right)^{2.5} \tag{7.21}$$

where EC is the electrical conductivity (mS cm^{-1}) of the sample.

Figure 7.4 shows the frequency and temperature dependency of the dielectric properties of free liquid water. It is interesting to note that the maximum dielectric loss occurs at much higher frequencies than those which are normally reserved for industrial microwave heating; however the loss factor significantly increases with increasing concentrations of dissolved solids in the water - particularly salts. This is shown in Figure 7.5.

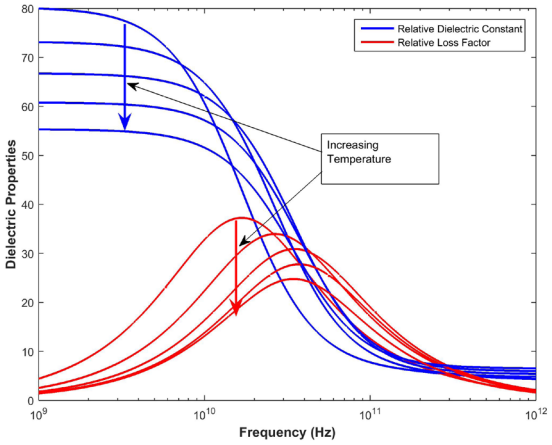

Figure 7.4: Estimated relative dielectric constant (κ') and loss factor (κ'') of pure water between 0°C and 100°C, the arrows showing the direction of increasing temperature.

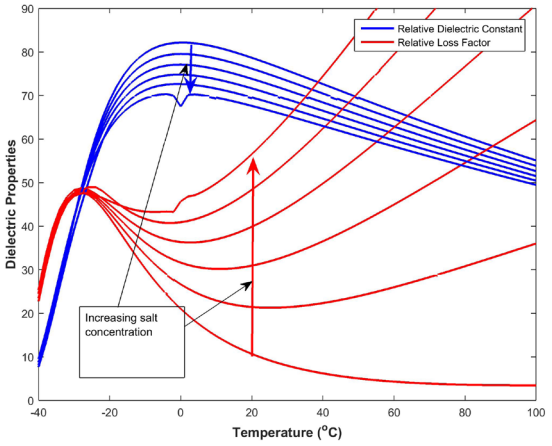

Figure 7.5: Estimated relative constant (κ') and loss factor (κ'') at 2.45 GHz for different levels of water salinity in parts per thousand w/w (ppt) for the temperature range for -40°C ~ +100°C.

This model for the dielectric properties of water is accurate between temperatures of – 2 °C and + 29 °C (Meissner and Wentz 2004); however it provides a good estimate of the dielectric properties between – 40 °C and + 100 °C.

7.4.2 Modelling the Dielectric Properties of Bound Water

Several dielectric models have been proposed for bound water. Early studies suggested that bound water should be regarded as having similar behaviour to ice (Ulaby and El-Rayes 1987); however there is no physical basis for this assumption and it is consequently inaccurate in its estimation of the dielectric properties of bound water. Tikhonov (1997) proposed a model that depended on the molecular thickness of the bound water layer; however estimating the number of molecules in a bound water layer is difficult. Ulaby and El-Rayes (1987) propose a model for bound water; however their equation does not seem to differentiate between bound water and the wet substrate.

Serdyuk (2008) proposed a much more comprehensive model for the dielectric properties of bound water. In many organic materials, when the moisture content rises above 25 to 30 %, moisture begins to appear as free water in the structural voids rather than bound water on the organic molecules. As mentioned earlier, the relaxation frequency of bound water is much lower than that of free water (Figure 7.6)

$$\kappa_{bw} = 3.2 + \frac{\ln\left(\frac{f}{1\times10^{9}}\right)}{\ln(10)} + j\frac{\ln\left(\frac{f}{1\times10^{8}}\right)}{180\ln(10)} + \left[12 + \frac{52-12}{1-j\frac{f}{0.18\times10^{9}}} + j\frac{\sigma_1}{f}\right]\left[\frac{2.65\sqrt{16m^2+0.09}-0.3}{64m^3+1}\right] + \left[2 + \frac{20-2}{1-j\frac{f}{0.18\times10^{9}}} + j\frac{\sigma_2}{f}\right]\left[\frac{5.25\left(\frac{m}{0.09}\right)^2}{1+\left(\frac{m}{0.09}\right)^8}\right] + \left[\frac{320}{1-j\frac{f}{1.5\times10^{4}}}\right]0.65\left(\frac{u_1}{\sqrt{1+u_1^{\,2}}} - \frac{u_2}{\sqrt{1+u_2^{\,2}}}\right) \tag{7.22}$$

where:

$$u_1 = \frac{m-0.15}{0.02},\ u_2 = \frac{m-0.21}{0.03}$$

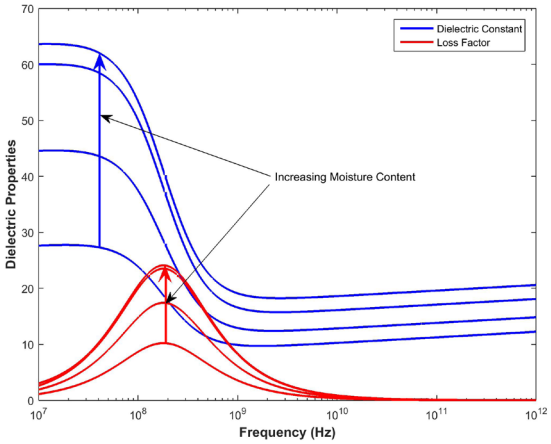

Figure 7.6: Estimated relative constant (κ') and loss factor (κ'') for bound water as a function of frequency and increasing moisture content from 1% moisture to 20 % moisture.

7.4.3 Modelling the Dielectric Properties of Moist Wood

Moist wood is essentially a heterogeneous mixture of solid, liquid and gaseous materials. Wood cells are built up as a honeycomb like structure oriented along the stem, except in the case of ray cells. The cell wall is a composite material consisting of partly crystalline cellulose micro-fibrils embedded in an amorphous matrix made up of hemicelluloses and lignin (Torgovnikov 1993, Forest Products Laboratory 1999). At the micro-structural level, wood can be described in terms of longitudinal tracheids, pit pairs, which connect between tracheids, the primary cell walls and the secondary cell walls (Meyland and Butterfield 1972, Hofstetter, *et al.* 2007). Hardwoods contain vessel elements (Jackson and Day 1989, Forest Products Laboratory 1999) while softwoods often contain resin channels (Jackson and Day 1989). The orientation of wood cells profoundly affects all the measurable properties of wood (Torgovnikov 1993).

At the molecular level, wood must be described in terms of polymers, free and bound water, extractives, minor amounts (5% to 10%) of extraneous materials contained in a cellular structure and air (Meyland and Butterfield 1972, Jackson and Day 1989, Torgovnikov 1993, Forest Products Laboratory 1999, Hofstetter, *et al.* 2007). The polymers of wood can be classified into three major types: cellulose, hemicellulose, and lignin. The proportion of these three polymers varies between species (Society of Wood Science and Technology 2001). Variations in the characteristics and volume of these components and differences in cellular structure make woods heavy or light, stiff or flexible, and hard or soft (Forest Products Laboratory 1999, Society of Wood Science and Technology 2001).

The dielectric properties of moist wood can be modelled on equation (7.9), where the dielectric properties of the various components of oven dried wood, bound water and free water have all been developed throughout this chapter. Although the wood polymers contribute to the dielectric properties of wood, the dielectric properties of moist wood (Figure 7.7) depend strongly on moisture content and temperature (Daian, *et al.* 2005).

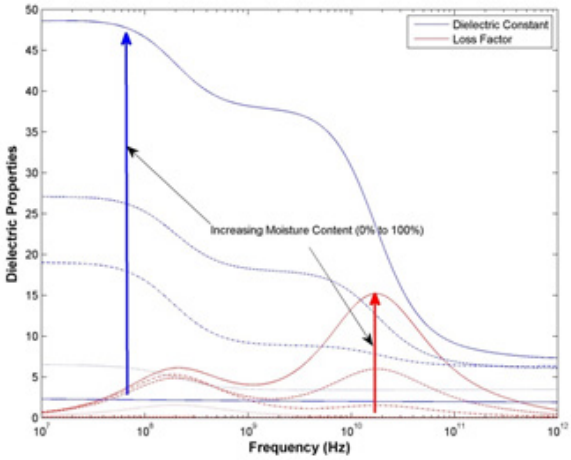

Figure 7.7: Estimated relative dielectric constant (κ') and loss factor (κ'') for moist wood as a function of frequency and increasing moisture content from 0% moisture to 100 % moisture (on and dry weight basis) with the electric field oriented perpendicular to the wood grain.

As moisture increases from oven dry to fibre saturation, the bound water dominates the dielectric properties (i.e. lower frequency peak in the loss factor); however above fibre saturation free water dominates the dielectric properties (i.e. higher frequency peak in the loss factor).

7.4.4 Modelling the Dielectric Properties of Grains

The dielectric properties of grains and seeds have been studied for many decades. Nelson and Trabelsi (2011) have used these measured and published data to develop models for predicting the dielectric properties of several important crop grains and oil seeds.

The general form of these models are presented in equations (7.23) and (7.24). The parameter values for various grains and seeds are listed in Table 7.4.

The models predict dielectric constants with standard errors of 1% to 2% with some up to about 4% for grain and seed at frequencies in the range from 5 to 15 GHz

over given moisture ranges. Loss factors are predicted with standard errors of a few percent, but much larger errors can naturally result when loss factors are very small (Nelson and Trabelsi 2011). The dielectric properties of grains in storage are low because of their low moisture content (Figure 7.8).

$$\kappa' = \kappa'_o + a \cdot \log(f) + b \cdot m \tag{7.23}$$

And

$$\kappa'' = \kappa''_o + c \cdot f + d \cdot m \tag{7.24}$$

Where f is the frequency (GHz) and m is the moisture content on a wet mass basis (%).

Table 7.4: Parameter values for use in equations (7.23) and (7.24) (Source: Nelson and Trabelsi 2011).

Grain or seed type	κ'_o	κ''_o	a	b	c	d
Wheat	2.5075	-0.1330	-0.4198	0.0406	-0.0021	0.0360
Maze	2.5546	-0.4488	-0.6035	0.0598	0.0146	0.0579
Barley	2.2685	-0.1984	-0.4549	0.0316	0.0042	0.0285
Oats	1.6547	-0.0942	-0.2277	0.0279	0.0011	0.0171
Soybeans	2.0411	-0.5344	-0.5087	0.0877	0.0071	0.0659
Canola	2.0824	-0.2174	-0.5938	0.0837	-0.0052	0.0499
Grain sorghum	2.1388	-0.3338	-0.6753	0.0866	-0.0011	0.0514
Shelled peanuts	2.0029	-0.4524	-0.3966	0.0764	0.0099	0.0691
Pod peanuts	1.7246	-0.9290	-0.6661	0.0580	0.0454	0.0666

7.4.5 Modelling the Dielectric Properties of Soils

Based on the work of Wang (1980), a useful model for predicting the dielectric properties of sand or clay can be developed. If the soil is predominantly clay based, equations (7.25) and (726) should be used to estimate the dielectric properties; however if the soil is predominantly sand based, equations (7.27) and (7.28) should be used to estimate the dielectric properties.
For clay:

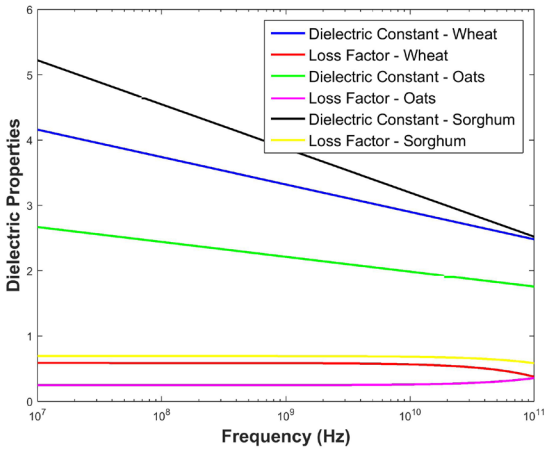

Figure 7.8: Estimated relative dielectric constant (κ') and loss factor (κ'') for various grains at 12 % moisture content, which is the maximum moisture content suitable for storage.

$$f_m = 49.254m^2 - 12.965m + 2.3635 \tag{7.25}$$

$$\beta = 170.16m^3 - 172.26m^2 + 54.749m + 0.9167 \tag{7.26}$$

For sand:

$$f_m = 20958.0m^4 - 17046.0m^3 + 4346.3m^2 - 296.02m + 11.343 \tag{7.27}$$

$$\beta = 3.0 \tag{7.28}$$

Where f_m is the relaxation frequency (GHz) and m is the moisture content on a dry volume basis. These parameters can be used in the following equations to model the dielectric properties.

$$\tau = \frac{1}{2\pi f_m} \tag{7.29}$$

$$\xi = e^{-\beta} \tag{7.30}$$

$$\varepsilon_\infty = \varepsilon_r(1-P) + \varepsilon_a(P-m) + 4m \tag{7.31}$$

$$\varepsilon_s = 3.14 + 23.83m + 91.58m^2 \tag{7.32}$$

$$\kappa' = \varepsilon_\infty + \frac{\left(\varepsilon_s - \varepsilon_\infty\right)}{2\ln\left(\xi^{-1}\right)} \ln\left[\frac{\xi^{-1} + \omega^2\tau^2}{\xi + \omega^2\tau^2}\right] \tag{7.33}$$

$$\kappa'' = \frac{\left(\varepsilon_s - \varepsilon_\infty\right)}{\ln\left(\xi^{-1}\right)} \tan^{-1}\left[\frac{\left(1-\xi\right)\omega\tau}{\sqrt{\xi}\left(1+\omega^2\tau^2\right)}\right] + 60\lambda\sigma \tag{7.34}$$

Where λ is the wavelength in free space (in cm) and σ is the conductivity of the soil water solution.

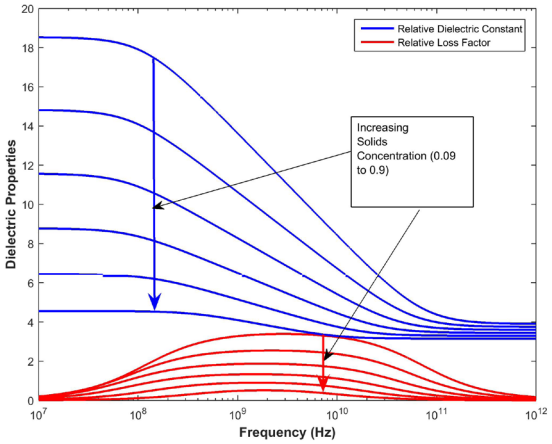

Figure 7.9: Estimated relative dielectric constant (κ') and loss factor (κ'') for moist clay as a function of frequency and moisture content (m varying between 5% and 30%).

7.4.6 Dielectric Properties of Insects

Insect infestations are a serious biosecurity hazard; therefore reliable detection of insects inside other bulk materials and non-chemical disinfestation are a high priority. Dielectric properties of insects vary with frequency, species and temperature, as illustrated in Tables 7.5 and 7.6. Generally insects have a higher dielectric constant than stored grain (Figure 7.8) or dry wood in service (Figure 7.3).

Table 7.5: Dielectric data for two grain storage insect pests (Data from: Nelson 2001).

Frequency (MHz)	Rice weevil (*Sitophilus oryzae*)		Confused flour beetle (*Triolium confusum*)	
	ε'	ε"	ε'	ε"
1.0	81	17		
3.0	62	22		
10.0	45	19	62	22
30.0			51	21
40.0	31	18	46	19
50.0	30	18		
200.0	48	38		
2,450.0	37	11		
9,400.0	28	14		
20,000.0	20	14		

Table 7.6: Dielectric properties of four insect larvae at five temperatures and four frequencies (Data from: Wang 2003).

Species	Temperature (°C)	Frequency (MHz)							
		ε'				ε"			
		27	40	915	1800	27	40	915	1800
Codling moth	20	71.5	64.9	47.9	44.5	238.1	163.3	11.7	12.0
	30	71.5	63.9	45.9	42.9	277.8	190.2	12.5	11.7
	40	73.8	64.5	44.6	41.6	332.4	227.5	13.9	11.9
	50	79.3	68.5	45.6	42.7	422.5	288.6	16.5	13.2
	60	84.5	71.5	45.0	41.9	511.3	349.1	19.1	14.2
Indian meal moth	20	81.3	69.1	39.9	37.5	210.9	149.0	13.4	10.6
	30	85.8	72.0	39.2	36.9	244.1	172.4	14.3	10.6
	40	94.4	77.3	37.6	35.5	268.7	190.9	15.2	10.6
	50	103.7	83.7	37.2	35.3	314.0	223.1	16.9	11.4
	60	113.0	90.4	37.8	35.6	397.4	280.7	19.9	12.8
Mexican fruit fly	20	90.3	71.2	48.5	47.0	343.9	230.9	17.5	13.3
	30	105.1	87.2	47.3	45.5	384.7	272.2	21.3	13.9

Continued **Table 7.6:** Dielectric properties of four insect larvae at five temperatures and four frequencies (Data from: Wang 2003).

Species	Temperature (°C)	Frequency (MHz)							
		ε'				ε"			
		27	40	915	1800	27	40	915	1800
	40	117.4	95.4	46.4	44.7	446.1	316.5	24.2	14.5
	50	128.7	102.9	45.7	44.1	521.8	370.7	26.8	15.4
	60	141.2	111.5	44.5	43.0	582.2	414.5	29.4	16.5
Navel orange worm	20	80.2	68.6	44.5	42.2	307.8	212.6	16.1	12.7
	30	83.6	70.4	43.6	41.5	359.7	248.0	17.5	12.9
	40	87.7	72.7	42.8	40.7	419.4	288.8	19.2	13.4
	50	92.8	75.9	42.3	40.2	480.3	330.8	21.2	14.1
	60	99.4	80.1	42.2	40.0	562.7	386.7	24.0	15.5

7.5 Conclusions

This chapter has explored the important factors that influence the dielectric properties of organic and agricultural materials. In most cases, moisture content is the most important factor in determining the dielectric properties; therefore RF and microwave systems for monitoring moisture or detecting moist objects, like insects, in otherwise dry materials are becoming common. These will be explored in the following chapters.

References

Boyarskii, D. A., Tikhonov, V. V. and Komarova, N. Y. 2002. Modeling of dielectric constant of bound water in soil for applications of microwave remote sensing. *Progress In Electromagnetics Research*. 35: 251–269.

Brodie, G. I. 2008, *Innovative wood drying: Applying microwave and solar technologies to wood drying*, Saarbruecken, Germany: VDM Verlag.

Buchner, R., Barthel, J. and Stauber, J. 1999. The dielectric relaxation of water between 0° C and 35° C. *Chemical Physics Letters*. 306(1-2): 57-63.

Calderwood, J. H. 1992. The Interpretation of Debye Relaxation by Means of a Classical Vibrational Model. *Conf. Dielectric Materials, Measurements and Applications, IEE, No. 636 B2 - Conf. Dielectric Materials, Measurements and Applications, IEE, No. 636*. 249-252.

Chaplin, M. 2004. *Water Structure and Behavior*. December, 2004. http://www.lsbu.ac.uk/water/index.html

Chaplin, M. 2007. *Water Structure and Science*. 7th June, 2007. http://www.lsbu.ac.uk/water/

Chaplin, M. F. 2000. A proposal for the structuring of water. *Biophysical Chemistry*. 83(3): 211-221.

Chuah, H. T., Kam, S. W. and Chye, Y. H. 1997. Microwave dielectric properties of rubber and oil palm leaf samples: measurement and modelling. *International Journal of Remote Sensing*. 18(12): 2623 - 2639.

Cui, Z., Xu, S., Sun, D. and Chen, W. 2005. Temperature changes during microwave-vacuum drying of sliced carrots. *Drying Technology*. 23(5): 1057 -1074.

Daian, G., Taube, A., Birnboim, A., Shramkov, Y. and Daian, M. 2005. Measuring the dielectric properties of wood at microwave frequencies. *Wood Science and Technology*. 39(3): 215 -223.

Daian, G., Taube, A., Birnboim, A., Daian, M., and and Shramkov, Y. 2005. Modeling the dielectric properties of wood. *Wood Science and Technology*. 40(3): 237-246.

Debye, P. 1929, *Polar Molecules*, New York: Chemical Catalog.

Dinulović, M. and Rašuo, B. 2011. Dielectric modeling of multiphase composites. *Composite Structures*. 93(12): 3209-3215.

Donskoy, D. and Sedunov, N. 2002. *Method and Apparatus for Detection of Wood Destroying Insects and Damage Evaluation Using Microwaves*. Patent No. 20020180607

Ellison, W. J., Lamkaouchi, K. and Moreau, J. M. 1996. Water: a dielectric reference. *Journal of Molecular Liquids*. 68(2–3): 171-279.

Forest Products Laboratory 1999, *Wood Handbook—Wood as an engineering material*, Madison, Wisconsin: U.S. Department of Agriculture, Forest Service, Forest Products Laboratory.

Giancoli, D. C. 1989, *Physics for Scientists and Engineers*, 2nd edn, New Jersey: Prentice Hall.

Hofstetter, K., Hellmich, C. and Eberhardsteiner, J. 2007. Micromechanical modeling of solid-type and plate-type deformation patterns within softwood materials. A review and an improved approach. *Holzforschung*. 61(4): 343-351.

Jackson, A. and Day, D. 1989, *Wood Worker's Manual*, Sydney: William Collins Sons & Co. Ltd.

James, W. L. 1975. *Dielectric properties of wood and hardboard: Variation with temperature, frequency, moisture content, and grain orientation*. U.S. Department of Agriculture

Kuang, W. and Nelson, S. O. 1997. Dielectric relaxation characteristics of fresh fruits and vegitables from 3 to 20 GHz. *Journal of Microwave Power and Electromagnetic Energy*. 32(2): 114-122.

Meissner, T. and Wentz, F. J. 2004. The Complex Dielectric Constant of Pure and Sea Water From Microwave Satellite Observations. *IEEE Transactions on Geoscience and Remote Sensing*. 42(9): 1836-1849.

Meyland, B. A. and Butterfield, B. G. 1972, *Three-dimensional Structure of Wood: A Scanning Electron Microscope Study*, Reed Education.

Montoro, T., Manrique, E. and Gonzalez-Reviriego, A. 1999. Measurement of the refracting index of wood for microwave radiation. *Holz als Roh- und Werkstoff*. 57(4): 295 -299.

Nelson, S. O. 1991. Dielectric properties of agricultural products: measurements and applications. *IEEE Transactions on Electrical Insulation*. 26(5): 845-869.

Nelson, S. O. 2001. Radio-frequency and microwave dielectric properties of insects. *Journal of Microwave Power and Electromagnetic Energy*. 36(1): 47-56.

Nelson, S. O. and Trabelsi, S. 2011. Models for the Microwave Dielectric Properties of Grain and Seed. *Transactions of the ASABE*. 54(2): 549-553.

Ohlsson, T. and Bengtsson, N. E. 1975. Dielectric food data for microwave sterilization processing. *J Microw Power*. 10(1): 93-108.

Ohlsson, T. and Risman, P. O. 1978. Temperature distributions of microwave heating - spheres and cylinders. *Journal of Microwave Power and Electromagnetic Energy*. 13(4): 303–310.

Serdyuk, V. M. 2008. Dielectric properties of bound water in grain at radio and microwave frequencies. *Progress In Electromagnetics Research*. 84: 379-406.

Singh, R. P. and Heldman, D. R. 1993, *Introduction to Food Engineering*, 2nd edn, New York: Academic Press.

Smith, R. J. 1976, *Circuits, Divices and Systems*, 3rd edn, New York: Wiley International.

Society of Wood Science and Technology. 2001. *Structure of Wood*. Society of Wood Science and Technology

Sung, P.-F., Hsieh, Y.-L., Angonese, K., Dunn, D., King, R. J., Machbitz, R., Christianson, A., Chappell, W. J., Taylor, L. S. and Harris, M. T. 2011. Complex dielectric properties of microcrystalline cellulose, anhydrous lactose, and α-lactose monohydrate powders using a microwave-based open-reflection resonator sensor. *Journal Of Pharmaceutical Sciences*. 100(7): 2920-2934.

Tiitta, M., Kainulainen, P., Harju, A. M., Venäläinen, M., Manninen, A., Vuorinen, M. and Viitanen, H. 2003. Comparing the effect of chemical and physical properties on complex electrical impedance of Scots pine wood. *Holzforschung*. 57(4): 433 -439.

Tikhonov, V. V. 1997. Dielectric model of bound water in wet soils for microwave remote sensing. *Proc. IEEE International Geoscience and Remote Sensing Symposium, 1997*. 3: 1108 - 1110. Singapore International Convention and Exhibition Centre, Singapore

Torgovnikov, G. I. 1993, *Dielectric Properties of Wood and Wood-Based Materials*, Springer Series in Wood Science, Berlin: Springer-Verlag.

Ulaby, F. T. and El-Rayes, M. A. 1987. Microwave Dielectric Spectrum of Vegetation - Part II: Dual-Dispersion Model. *IEEE Transactions on Geoscience and Remote Sensing*. GE-25(5): 550-557.

Ulaby, F. T. and Jedlicka, R. P. 1984. Microwave Dielectric Properties of Plant Materials. *Geoscience and Remote Sensing, IEEE Transactions on*. GE-22(4): 406-415.

van Dam, R. L., Borchersb, B., and Hendrickx, J. M. H. 2005. Methods for prediction of soil dielectric properties: a review. *Proc. SPIE Defense and Security Symposium 2005*. 188-197.Orlando, Florida

Wagner, R. J., Boulger, R. W., Oblinger, C. J. and Smith, B. A. 2006. *Guidelines and Standard Procedures for Continuous Water-Quality Monitors: Standard Operation, Record Computation, and Data Reporting*. U.S. Geological Survey

Wang, J. R. 1980. The dielectric properties of soil-water mixtures at microwave frequencies. *Radio Science*. 15(5): 977-985.

Wang, S., Tang, J., Johnson, J.A., Mitcham, E., Hansen, J.D., Hallman, G., Drake, S.R., and Wang, Y. 2003. Dielectric Properties of Fruits and Insect Pests as related to Radio Frequency and Microwave Treatments. *Biosystems Engineering*. 85(2): 201-212.

Youngman, M. J., Kulasiri, D., Woodhead, I. M. and Buchan, G. D. 1999. Use of a combined constant rate and diffusion model to simulate kiln-drying of Pinus radiata Timber. *Silva Fennica*. 33(4): 317-325.

8 Insect and Decay Detection

One of the major challenges in agriculture and forestry is pest control. Insects constitute one of the major threats to agricultural production and stored food spoilage. Ever since ancient times, insects such as locusts have been a major cause of crop damage (Roberts 2010). Insects, such as termites and borers, also damage wood products as well. Decay causing fungi can also damage wood, stored fodder and stored grain. This chapter will explore how RF and microwave systems are employed to detect insects and decay.

8.1 Radar Entomology

Nikola Tesla foreshadowed the idea of remote detection of objects using radio waves; however radar was not fully developed until the mid-twentieth century. Most early applications of radar were associated with military activities. More recently, radar has been used in civilian applications. During the last thirty years there has been a growing interest in consumer applications of radar, especially with the development of tiny single-chip radar systems that can be purchased for just a few dollars (Evans, *et al*. 2013). These chips contain a complete RF transceiver system. For example, The University of Melbourne has developed a complete radar-on-a-chip system operating at 76–77 GHz (Evans, *et al*. 2013). Therefore radar technology will become more accessible for a wider range of applications.

Radar entomology has become a practical long-term monitoring technique since its initial development in the 1970's (Hobbs and Aldhous 2006). Radar can be applied to the detection of insects in two ways: firstly it can be used to remotely monitor larger flying insects (Riley 1992, Hobbs and Aldhous 2006), such as locusts; and secondly it can be used to detect the motion of insects, such as termites and borers, in other relatively dry materials such as wood-in-service (Donskoy and Sedunov 2002, Mankin 2004).

Radar's ability to remotely monitor flying insect flight provides valuable insights into insect behaviour. Current operational systems use a vertically pointing, linearly polarised beam and marine X-band transceivers, and rotate the plane of polarisation about the vertical axis at several Hertz (Hobbs and Aldhous 2006). The beam is slightly offset from the vertical axis and scanned around the vertical at the same rate. The combination of modulations due to the beam motion and polarisation rotation is used to measure the target's trajectory and radar cross-section (RCS) parameters (Hobbs and Aldhous 2006). Species weighing about a gram can be individually detected at ranges up to 2 km away with quite modest radar equipment (Riley 1992); however radar is subject to range limitations, depending on the antenna used to focus the radar energy.

8.1.1 Antennas

Antennas are the fundamental components of any radar system. Different systems transmit and receive different wavelengths, so the operational characteristics of the system are designed according to the properties of the antennas. There must be two types of antennas in any system: a transmitting and a receiving antenna. The ideal transmitting antenna is one that will radiate all the power delivered to it in the desired direction and with the desired polarisation, while the ideal receiving antenna is one that will obtain the maximum possible signal voltage from the passing electromagnetic wave while reducing the noise input into the receiver system.

Several antenna configurations are possible, but most radar antennae have an aperture through which the electromagnetic fields propagate. These apertures are generally either rectangular or circular.

8.1.2 Rectangular Apertures

Consider a plane wave propagating in the z direction encountering an aperture of height a and width b, as shown in Figure 8.1:

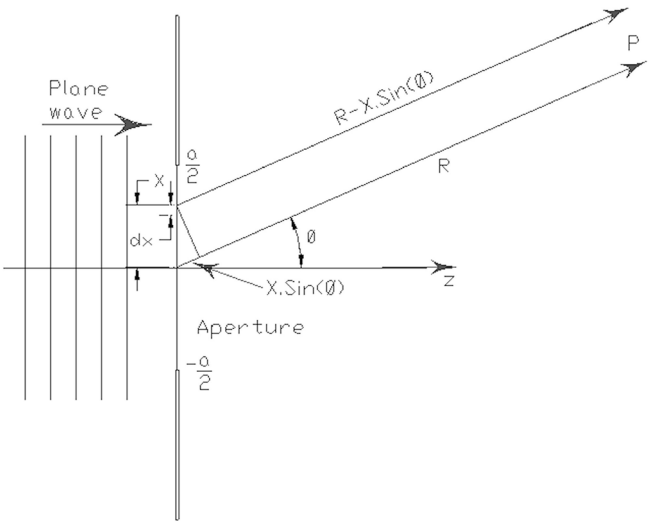

Figure 8.1: Rectangular aperture .

The plane wave can be represented as:

$$E = E_o e^{j(wt-\beta z)} \tag{8.1}$$

where $\beta = \frac{2\pi}{\lambda}$

By Huygen's principle (Connor 1972), the field radiated from the aperture must be considered as a number of isotropic point source radiators distributed across the aperture. Therefore the field intensity at some point P is obtained by integrating the radiation from all the individual point sources.

For a point source at some location (x,y) in the aperture the field intensity *dE* at point P is given by:

$$dE = E_o e^{j(\omega t-\beta(R-x\cdot Sin(\phi)-y\cdot Sin(\theta)))} \cdot dx \cdot dy \tag{8.2}$$

The total field is therefore given by:

$$E = \int_{-b/2}^{b/2}\int_{-a/2}^{a/2} E_o e^{j(\omega t-\beta(R-x\cdot Sin(\phi)-y\cdot Sin(\theta)))} \cdot dx \cdot dy \tag{8.3}$$

This can be rewritten as:

$$E = E_o e^{j(\omega t-\beta R)} \int_{-b/2}^{b/2} e^{j\beta(y\cdot Sin(\theta))} \cdot dy \int_{-a/2}^{a/2} e^{j\beta(x\cdot Sin(\phi))} \cdot dx \tag{8.4}$$

$$E = E_o e^{j(\omega t-\beta R)} \frac{e^{j\beta(y\cdot Sin(\theta))}}{j\beta Sin(\theta)}\Bigg|_{-b/2}^{b/2} \frac{e^{j\beta(x\cdot Sin(\phi))}}{j\beta Sin(\phi)}\Bigg|_{-a/2}^{a/2} \tag{8.5}$$

$$E \quad abE\ e^{j(\omega t\ \ \beta R)} \frac{e^{j\beta bSin(\theta)/2} - e^{-j\beta bSin(\theta)/2}}{2j\beta bSin(\theta)/2} \frac{e^{j\beta aSin(\phi)/2} - e^{-j\beta aSin(\phi)/2}}{2j\beta aSin(\phi)/2} \tag{8.6}$$

$$E = abE_o e^{j(\omega t-\beta R)} \frac{Sin\left(\beta bSin(\theta)/2\right)}{\beta bSin(\theta)/2} \frac{Sin\left(\beta aSin(\phi)/2\right)}{\beta aSin(\phi)/2} \tag{8.7}$$

Substituting for β yields:

$$E = abE_o e^{j(\omega t-\beta R)} \frac{Sin\left(\pi bSin(\theta)/\lambda\right)}{\pi bSin(\theta)/\lambda} \frac{Sin\left(\pi aSin(\phi)/\lambda\right)}{\pi aSin(\phi)/\lambda} \tag{8.8}$$

Note: The integral expression in equation (8.4) is similar to a double Fourier transformation. In practice the far-field radiation pattern is often calculated by measuring the aperture field and performing a Fast-Fourier Transform on the data. The aperture illumination, which was assumed to be uniform in this analysis, is usually more complex because of variations in amplitude and phase across the aperture.

8.1.3 Open Ended Wave-Guide

In the case of an open ended wave-guide, the field distribution in the x-z plane is described by:

$$E = E_o Cos\left(n\pi x/a\right) \tag{8.9}$$

In this case the equivalent integral for equation (8.4) becomes:

$$E = E_o e^{j(wt-\beta R)} \int_{-b/2}^{b/2} e^{j\beta(y\cdot Sin(\theta))} \cdot dy \int_{-a/2}^{a/2} Cos\left(n\pi x/a\right) e^{j\beta(x\cdot Sin(\phi))} \cdot dx \tag{8.10}$$

From standard tables:

$$\int_{-a/2}^{a/2} Cos\left(n\pi x/a\right) e^{j\beta(x\cdot Sin(\phi))} \cdot dx = \frac{e^{j\beta(x\cdot Sin(\phi))}\left[j\beta Sin(\phi) Cos\left(n\pi x/a\right) + n\pi/a\, Sin\left(n\pi x/a\right)\right]}{\left(n\pi/a\right)^2 - \beta^2 Sin^2(\phi)}\Bigg|_{-a/2}^{a/2}$$

$$= \frac{2n\pi/a\, Cos\left(\beta aSin(\phi)/2\right)}{\left(n\pi/a\right)^2 - \beta^2 Sin^2(\phi)} \tag{8.11}$$

Therefore, substituting for β, the electric field distribution at some point P is:

$$E = \frac{2n\pi bE_o e^{j(wt-\beta R)}}{a} \frac{Sin\left(\pi bSin(\theta)/\lambda\right)}{\pi bSin(\theta)/\lambda} \cdot \frac{Cos\left(\pi aSin(\phi)/\lambda\right)}{\left(n\pi/a\right)^2 + \left(2\pi Sin(\phi)/\lambda\right)^2} \tag{8.12}$$

The biggest problem with open ended wave-guides is that much of the microwave energy is reflected back into the wave-guide because of the abrupt change in wave impedance at the mouth of the aperture. The reflection coefficient is:

$$\Gamma_{TE} = \frac{\sqrt{1-\left(\frac{n\lambda_o}{2a}\right)^2-\left(\frac{m\lambda_o}{2b}\right)^2}-1}{\sqrt{1-\left(\frac{n\lambda_o}{2a}\right)^2-\left(\frac{m\lambda_o}{2b}\right)^2}+1} \tag{8.13}$$

If the wave-guide is propagating in a TM mode the impedance in the guide is:

$$\eta_g = \eta_o\sqrt{1-\left(\frac{n\lambda_o}{2a}\right)^2-\left(\frac{m\lambda_o}{2b}\right)^2} \tag{8.14}$$

So the reflection coefficient is:

$$\Gamma_{TM} = \frac{1-\sqrt{1-\left(\frac{n\lambda_o}{2a}\right)^2-\left(\frac{m\lambda_o}{2b}\right)^2}}{1+\sqrt{1-\left(\frac{n\lambda_o}{2a}\right)^2-\left(\frac{m\lambda_o}{2b}\right)^2}} \tag{8.15}$$

To reduce the reflection coefficient as much as possible, it is desirable to provide some gradual transition between the wave-guide and the external space.

8.1.4 Horn Antennas

Horn antennas are extremely popular in the microwave region (above 1 GHz). Horns provide high gain, low reflection (with waveguide feeds), relatively wide bandwidth, and they are easy to make. The rectangular horns are ideally suited for rectangular waveguide feeders. The horn acts as a gradual transition from a waveguide mode to a free-space mode of the EM wave. Horn antennas are somewhat more difficult to analyse because there is a phase error in the aperture due to the difference in travel distance from the horn's apex to the aperture as illustrated in Figure 8.2.

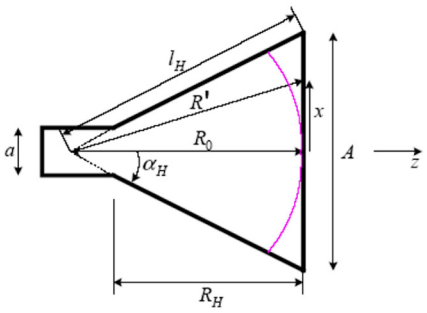

Figure 8.2: Geometry of the wave front in a horn antenna.

In this case the wave front in the aperture can not be described as a plane wave. It approaches the form of a spherical wave centred on the apex of the horn's pyramid. In this case, if the horn only flares in the H-Plane, the equivalent integral for equation (8.4) must be calculated with an additional phase shift between the spherical surface and the aperture:

$$E = \int_{-b/2}^{b/2} \int_{-a/2}^{a/2} E_o Cos\left(\frac{n\pi x}{a}\right) e^{j\left(wt-\beta\left(R-(R'-R_o)-x\cdot Sin(\phi)-y\cdot Sin(\theta)\right)\right)} \cdot dx \cdot dy \tag{8.16}$$

Now $R'-R_o = R_o\sqrt{1+\left(\frac{x}{R_o}\right)^2} - R_o \approx \frac{1}{2}\left(\frac{x}{R_o}\right)^2$, therefore:

$$E = \int_{-b/2}^{b/2} \int_{-a/2}^{a/2} E_o Cos\left(\frac{n\pi x}{a}\right) e^{j\left\{wt-\beta\left[R-\frac{1}{2}\left(\frac{x}{R_o}\right)^2-x\cdot Sin(\phi)-y\cdot Sin(\theta)\right]\right\}} \cdot dx \cdot dy \tag{8.17}$$

This is quite a complex integration that eventually yields:

$$E = \frac{b}{2} E_o e^{j(wt-\beta R)} \sqrt{\frac{\lambda R_o}{2}} I \cdot \frac{Sin\left(\pi b Sin(\theta)/\lambda\right)}{\pi b Sin(\theta)/\lambda} \tag{8.18}$$

where:

$$I = \begin{cases} e^{j\frac{R_o\lambda}{4\pi}\left(2\pi Sin\theta/\lambda+\frac{\pi}{A}\right)^2}\left[C(s_2)-jS(s_2)-C(s_1)+jS(s_1)\right]+ \\ e^{j\frac{R_o\lambda}{4\pi}\left(2\pi Sin\theta/\lambda-\frac{\pi}{A}\right)^2}\left[C(t_2)-jS(t_2)-C(t_1)+jS(t_1)\right] \end{cases} \tag{8.19}$$

and:

$$
\begin{aligned}
s_1 &= \sqrt{\frac{\lambda}{2\pi^2 R_o}}\left(-\frac{\pi A}{\lambda} - 2\pi R_o Sin\theta \Big/ \lambda - \frac{\pi R_o}{A}\right) \\
s_2 &= \sqrt{\frac{\lambda}{2\pi^2 R_o}}\left(\frac{\pi A}{\lambda} - 2\pi R_o Sin\theta \Big/ \lambda - \frac{\pi R_o}{A}\right) \\
t_1 &= \sqrt{\frac{\lambda}{2\pi^2 R_o}}\left(-\frac{\pi A}{\lambda} - 2\pi R_o Sin\theta \Big/ \lambda + \frac{\pi R_o}{A}\right) \\
t_2 &= \sqrt{\frac{\lambda}{2\pi^2 R_o}}\left(\frac{\pi A}{\lambda} - 2\pi R_o Sin\theta \Big/ \lambda + \frac{\pi R_o}{A}\right)
\end{aligned}
\tag{8.20}
$$

C(x) and *S(x)* are Fresnel integrals, which are defined as:

$$
\begin{aligned}
C(x) &= \int_0^x Cos\left(\frac{\pi}{2}\tau^2\right)\cdot d\tau \\
S(x) &= \int_0^x Sin\left(\frac{\pi}{2}\tau^2\right)\cdot d\tau
\end{aligned}
\tag{8.21}
$$

8.1.5 Circular Apertures

Applying the same analysis to a circular aperture of radius a, the integral becomes:

$$
E = \int_0^{2\pi}\int_0^a E_o e^{j\left(wt-\beta\left(R-\rho\cdot Sin(\phi)Cos(\theta)\right)\right)}\cdot\rho\cdot d\rho\cdot d\theta \tag{8.22}
$$

This becomes:

$$
E = E_o e^{j(wt-\beta R)}\int_0^{2\pi}\int_0^a e^{j\rho\cdot Sin(\phi)Cos(\theta)}\cdot\rho\cdot d\rho\cdot d\theta \tag{8.23}
$$

From standard tables:

$$
\begin{aligned}
e^{j\rho\cdot Sin(\phi)Cos(\theta)} &= J_o\left(\beta\rho Sin(\phi)\right) - 2\left[J_2\left(\beta\rho Sin(\phi)Cos(\theta)\right) - J_4\left(\beta\rho Sin(\phi)Cos(\theta)\right)\ldots\right] + \\
&2j\left[J_3\left(\beta\rho Sin(\phi)Cos(\theta)\right) - J_5\left(\beta\rho Sin(\phi)Cos(\theta)\right)\ldots\right]
\end{aligned}
\tag{8.24}
$$

As the integral of Cos(θ) over 2π is zero, equation (8.24) becomes:

$$E = E_o e^{j(wt-\beta R)} \int_0^{2\pi} \int_0^{a} J_o\left(\beta\rho \cdot Sin(\phi)\right) \cdot \rho \cdot d\rho \cdot d\theta \tag{8.25}$$

This becomes:

$$\begin{aligned} E &= E_o e^{j(wt-\beta R)} \int_0^{2\pi} d\theta \cdot \int_0^{a} J_o\left(\beta\rho \cdot Sin(\phi)\right) \cdot \rho \cdot d\rho \\ &= 2\pi E_o e^{j(wt-\beta R)} \int_0^{a} J_o\left(\beta\rho \cdot Sin(\phi)\right) \cdot \rho \cdot d\rho \end{aligned} \tag{8.26}$$

To evaluate this integral, let:
$x = \beta\rho \cdot Sin(\phi)$
$dx = \beta \cdot Sin(\phi) \cdot d\rho$
x = 0 when ρ = 0
$x = \beta a \cdot Sin(\phi)$ when ρ = a

Therefore:

$$E = \frac{2\pi a^2 E_o e^{j(wt-\beta R)}}{\left[\beta a \cdot Sin(\phi)\right]^2} \int_0^{\beta a \cdot Sin(\phi)} x J_o(x) \cdot dx \tag{8.27}$$

From standard tables:

$$\int_0^{\alpha} x J_o(x) \cdot dx = \alpha J_1(\alpha) \tag{8.28}$$

Therefore:

$$E = 2\pi a^2 E_o e^{j(wt-\beta R)} \frac{J_1\left(\beta a \cdot Sin(\phi)\right)}{\beta a \cdot Sin(\phi)} \tag{8.29}$$

Substituting for β and remembering that the diameter is twice the radius, equation (8.29) becomes:

$$E = 2\pi a^2 E_o e^{j(wt-\beta R)} \frac{J_1\left(\pi DSin(\phi)/\lambda\right)}{\pi DSin(\phi)/\lambda} \tag{8.30}$$

Many practical circular aperture antennas are not uniformly illuminated. In these cases the antennas can be often regarded as radially symmetric apertures with field amplitude that is tapered from the centre toward the aperture edge. The aperture field distribution can often be approximated using the parabolic taper of order n:

$$E_a(\rho') = E_o\left[1-\left(\frac{\rho'}{a}\right)^2\right]^n \tag{8.31}$$

Thus the normalized principle plane pattern is described by:

$$E = 2^{n+1}\pi a^2 E_o e^{j(wt-\beta R)} \frac{J_{n+1}\left(\pi DSin(\phi)/\lambda\right)}{\left(\pi DSin(\phi)/\lambda\right)^{n+1}} \tag{8.32}$$

Figure 8.3 shows that these approximations can be quite useful at times.

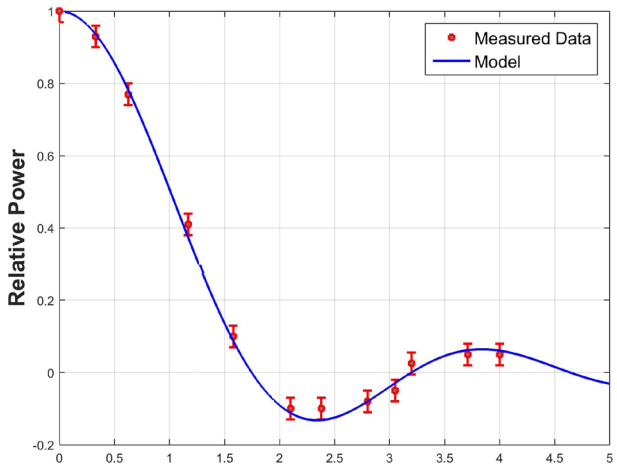

Figure 8.3: Comparison of radiation pattern predicted by equation (8.33) with measured data for a 1.0 m diameter dish antenna (Original data from: Brodie 1981).

8.1.6 Antenna Gain

The antenna is the transition between a guiding device (transmission line, waveguide) and open space. Its main purpose is to convert the energy of a guided wave into the energy of an open-space wave (or vice versa) as efficiently as possible. It also acts as a focusing device to project the wave in the desired direction through space. The gain of an antenna is an effective measure of this focusing ability.
There are two measurements of gain, namely directive gain and power gain. Directive gain is the ratio of the power density radiated in a particular direction compared to the power density radiated to the same point by a reference antenna, assuming both antennas are radiating the same amount of power. Usually the reference antenna is assumed to radiate power equally in all directions; therefore, directive gain is a direct indication of the focusing effect of the antenna.

The power gain is almost the same as directive gain except that antenna efficiency is taken into account and the total power fed to the antenna is used in the calculations. It is assumed that the antenna and the reference have the same input power and that the reference antenna is a perfect radiator. The power gain is equal to the directive gain if an antenna radiates 100% of the input power. In reality, no antenna will ever radiate 100 % of its input power, so the power gain is usually less than the directive gain. The gain of an antenna is often used as a figure of merit.

While gain is the most useful parameter to describe the transmitted signal, a receiving antenna is best described by its receiving cross section. A signal at the location of the receiving antenna will have a certain power density. This can be thought of as the amount of power passing through the plane perpendicular to the receiving antenna. This power will excite a current (and voltage) in the antenna, which can be delivered to a receiver circuit. The power received at this point is called the received signal power. The receiving cross section of the antenna is the ratio of the received signal power to the power density at the receiver.

The receiving cross section, however, is not necessarily equal to the physical cross-section of the antenna. However, for some antennas with high gains these areas may be almost equal, while some small antennas may even have much larger receiving cross sections than their physical dimension would indicate. The receiving cross section of an antenna is linked to its radiation pattern.

The radiation pattern of an antenna is a polar diagram representing the spatial distribution of the radiated energy. There are four common radiation patterns used (Silver 1949):

1. Omni-directional (broadcast-type) pattern
2. Pencil-beam patterns
3. Fan-beam patterns
4. Shaped-beam patterns

Omni-directional radiation patterns are created from a single linear element such as a broadcast tower for television or radio communication. These types of antennas can

often be found on the tops of tall hills and mountains. On the other hand, Pencil-beam patterns are usually created using reflector antennas, like the Parkes radio telescope. The other radiation patterns are created using sophisticated antenna designs, which are not commonly used in simple data transmission systems. In spite of their simple appearance, antennas are actually quite complex electrical systems and their design requires some very sophisticated mathematics to analyse them.
Pencil-beam radiation patterns imply that the antenna has a greater focusing effect. This focusing effect is called gain. Gain has an amplifying effect on transmitted or received signals, just like a magnifying glass that can focus (or amplify) the sun's rays to the point where they can start a fire.

The gain of an antenna is related to its efficiency, its physical aperture area and the wavelength of the carrier wave it is transmitting. A nice rule of thumb for a typical reflector antenna is that:

$$G = \frac{4\pi\eta A}{\lambda^2} \tag{8.33}$$

where G is the gain, η is the efficiency, A is the aperture area (m^2) and λ is the wavelength of the carrier wave (m).

Some other important antenna parameters include bandwidth, polarisation and impedance. The bandwidth depends on a number of factors including the shape of the radiation pattern, gain, impedance and polarisation. An adequate definition of bandwidth would be the frequency range over which the antenna performs suitably for a given application (Connor 1972). Polarisation indicates the orientation of the electric field radiated from the antenna (Connor 1972). For example, a horizontally polarized antenna radiates energy with the electric field oriented into the horizontal direction, while a vertically polarised antenna radiates energy with the electric field oriented into the vertical direction (Georgieva 2001).

The input impedance of an antenna affects its transmitting or receiving efficiency. The total input impedance depends not only on the antenna elements, but also on the mutual impedance between the elements and the transmission line components used to connect the antenna elements (Georgieva 2001).

8.1.7 Radar Range

For a given receiver antenna size the capture area is constant no matter how far it is from the transmitter, as illustrated in Figure 8.4. Effectively the signal power is being spread out over the surface of an ever enlarging sphere. The effect is analogous to the reduction in wave height as ripples on the surface of a pond move out from the centre of the disturbance.

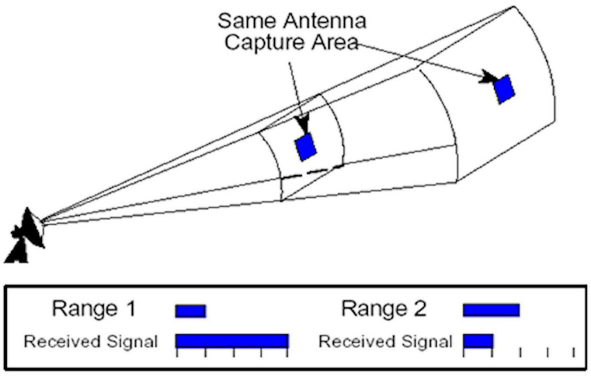

Figure 8.4: Effect of distance on proportion of transmitted signal received (Source: US Naval Air Systems Command 1999).

Suppose a radar transmitter has a gain G_T and is transmitting a power P_T. Allowing for wave attenuation (α) as defined in Equation (4.11) through the intervening media, the power density P_d at an object located a distance r is:

$$P_d = \frac{P_T G_T}{4\pi r^2} \times e^{-2\alpha r} \tag{8.34}$$

The target area of the object is defined as δ m²; therefore the power reflected isotropically from the target is $P_d \times \delta$. It therefore produces a power density at the transmitter of:

$$P_d^1 = \frac{P_T G_T \delta}{\left(4\pi r^2\right)^2} \times e^{-4\alpha r} \tag{8.35}$$

If a receiving antenna has an effective area $A = \frac{\lambda^2}{4\pi\eta} G_R$, then the power received is:

$$P_R = P_d^1 \cdot A = \frac{P_T G_T \delta}{\left(4\pi r^2\right)^2} \cdot \frac{G_R \lambda^2}{4\pi\eta} \cdot e^{-4\alpha r} \tag{8.36}$$

Therefore the ratio of received to transmitted power will be:

$$\frac{P_R}{P_T} = \frac{G_T G_R \delta \lambda^2}{(4\pi)^3 \eta r^4} \cdot e^{-4\alpha r} \tag{8.37}$$

This is the basic radar equation, relating transmitted to received power. The minimum detectable signal to noise ratio is S, where the noise in the system is given by $N = kTB$, N is the noise power (W), k is Boltzman's constant (1.38 x 10^{-23} J K^{1}), T is the absolute noise temperature of the antenna (K) and B is the band width of the system (Hz), then the radar range of the system will be:

$$r = \sqrt[4]{\frac{P_T G_T G_R \delta \lambda^2}{(4\pi)^3 \eta kTBS}} \cdot e^{-\alpha r} \tag{8.38}$$

So the effective range of a radar system depends on the fourth root of P_T. This is why radar systems need such high power output. Generally, the attenuation factor (α) of air is negligible; therefore the radar range in the atmosphere is proportional to $\frac{1}{r^4}$; however other materials such as wood, grains, soil and water have very high attenuation factors at radar frequencies, consequently radar range in these media is very limited.

8.1.8 Radar Cross Section

Radar cross section is the measure of a target's ability to reflect radar signals in the direction of the radar receiver, i.e. it is a measure of the ratio of backscatter power per steradian (unit solid angle) in the direction of the radar (from the target) to the power density that is intercepted by the target (Wolf, *et al.* 1993).

Radar targets may exhibit Rayleigh, Mie, or optical scattering depending on whether their greatest circumference is much smaller than, approximately equal to, or much larger than the radar wavelength. For Mie scattering, the exact size, shape, and alignment of the target dramatically affect the RCS due to interference effects between the incident electromagnetic waves and electromagnetic fields reflected from the target (Mie 1908). For example, water spheres with diameters of 0.5, 1.0, and 1.2 cm have the same RCS (1 cm^2) for a radar wavelength of 3.2 cm.

A larger "optical" target has a RCS related to its projected area (as viewed by the radar), as well as radar polarization, target composition, and alignment. The optical Radar Cross Section (RCS) of a target can be viewed as a comparison of the strength of the reflected signal from a target to the reflected signal from a perfectly smooth sphere of cross sectional area of 1 m^2, as shown in Figure 8.5.

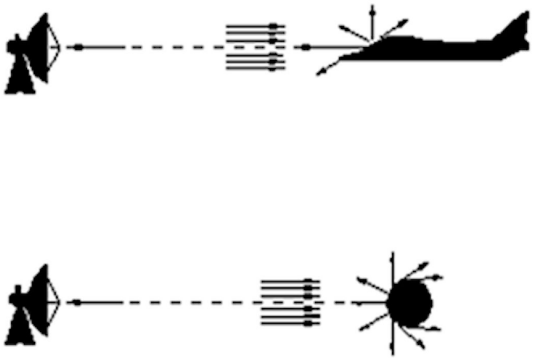

Figure 8.5: Concept of radar cross section (Source: US Naval Air Systems Command 1999).

The conceptual definition of optical RCS includes the fact that not all of the radiated energy falls on the target. A target's RCS (δ) is:

$$\delta = A \cdot \Gamma \cdot D \tag{8.39}$$

where A is the projected cross sectional area (m^2), Γ is the reflectivity (i.e. The percent of intercepted power scattered by the target) and D is the directivity (i.e. The ratio of the power scattered back in the radar's direction to the power that would have been backscattered had the scattering been uniform in all directions) (US Naval Air Systems Command 1999).

Experimentally, reflections from a target are compared to the reflections from a sphere, which has a projected area of one square metre. Using the spherical shape aids in field or laboratory measurements since orientation or positioning of the sphere will not affect radar reflection intensity measurements (US Naval Air Systems Command 1999). Mathematical derivation of the RCS of a target is complex and results in different mathematical expressions for Rayleigh, Mie, and optical sized targets. A crude approximation to the RCS of an insect is a water ellipsoid with the same weight as the insect (Wolf, *et al.* 1993).

Insects that are smaller than 200 mg exhibit Rayleigh scattering for 3.2 cm radar wavelength (Wolf, et al. 1993), while most larger flying insects exhibit Mie scattering. Because of their geometry, the radar cross section of flying insects depends on their orientation relative to the radar system and the polarisation of the microwave fields (Table 8.1). In many cases of radar entomology, swarms are detected rather than individual insects and motion detection is more useful than positional accuracy.

Table 8.1: Radar cross section of selected insects for different orientations (front or side) to the radar system, with different polarisations of the microwave fields (operating frequency of radar: 8 GHz to 12 GHz) (Source: Wolf, et al. 1993).

Insect Species	Front	Side
Horizontal Polarisation		
Honeybee drone	0.0072	2.00
Honeybee queen	0.0043	3.02
Honeybee worker	0.0011	0.30
Stink bug	0.054	2.24
Boll weevil	0.0010	0.0079
Vertical Polarisation		
Honeybee drone	0.062	0.41
Honeybee queen	0.0071	0.40
Honeybee worker	0.0012	0.032
Stink bug	0.038	0.18
Boll weevil	0.0013	0.0021

The surface roughness of an object also controls how the microwave energy interacts with that target. Surface roughness refers to the average height variations in the surface compared with a plane surface. Whether a surface appears rough or smooth to radar depends on the wavelength and incidence angle of the microwave fields. A surface will appear smooth if the height of any features is less than the Rayleigh criterion, which is defined as:

$$h_r = \frac{\lambda}{8Sin\theta} \tag{8.40}$$

Where λ is the microwave wavelength and θ is the depression angle.

8.1.9 Close Range Radar

In the case of a radar system with separate transmitting and receiving antennae, the detected signal is a combination of reflected energy and mutually coupled energy that travels directly from the transmitting antenna to the receiving antenna. Bird (1996) has shown that coupling occurs between various elements, such as wave-

guides and coaxial cables, terminated in a ground plane. The same coupling occurs between antennae in the same plane. Based on the analysis of mutual coupling between rectangular wave-guides by Bird (1990), the elements of the mutual coupling admittance matrix (y) can be described by:

$$y_{il}(m,n/m',n') = \frac{jk_eY_e}{4\pi\sqrt{Y_{m,n}Y_{m',n'}}} \iint H_{m,n} \cdot dS \times \iint H_{m',n'} \cdot G(R) \cdot dS' \tag{8.41}$$

where $G(R) = \frac{e^{-jk_e|R|}}{|R|}$ is the Green's function, $k_e = k_o\sqrt{\kappa}$, $Y_e = Y_o\sqrt{\kappa}$, $k_o = 2\frac{\pi}{\lambda}$, k is the dielectric constant of the space in front of the radar system, and $Y_o = \frac{1}{376.7}$.

Similarly, studies by Ishimaru *et al.* (2004) show that the reflected field from a discontinuity in the material that is some distance from the radar source is given by:

$$H_r = 2\iint G(R_1) \cdot G(R_2) \cdot \Gamma\left(H_{m',n'} \cdot \hat{\xi}\right) \cdot dS'' \tag{8.42}$$

where R_1 represents the outward path of the microwave fields, R_2 represents the return path, H_I is the initial magnetic field , G is the reflection coefficient of the object, and $\hat{\xi}$ is the normal to the reflective object's surface. Therefore the combined effect of mutual coupling directly from input to output and reflections from the target will be:

$$y_{il}(m,n/m',n') = \frac{jk_eY_e}{4\pi\sqrt{Y_{m,n}Y_{m',n'}}} \iint H_{m,n} \cdot dS \times \left\{\iint H_{mut} + 2\iint H_{ref}\right\} \tag{8.43}$$

Where $H_{mut} = H_{m',n'} \cdot G(R) \cdot dS'$, and $H_{ref} = G(R_1) \cdot G(R_2) \cdot \Gamma \cdot \left(H_{m',n'} \cdot \hat{\xi}\right) \cdot dS'$

The effective dielectric properties of the space in front of the radar system will be a combination of the dielectric properties of air and the dielectric properties of the target object. As the gap between the radar system and the target object reduces the k_e and Y_e terms in equation (8.43) become more sensitive to the dielectric properties of the target. Therefore very close range radar can respond to subtle changes in the dielectric behaviour of the target material.

8.1.10 Motion Detection - Doppler Shift

One of the more useful features of radar is that the speed of moving objects can be determined with considerable accuracy. Doppler shift is the apparent change

in wavelength (or frequency) of an electromagnetic or acoustic wave when there is relative movement between the transmitter and the receiver.

$$f = \left(\frac{c + v_r}{c + v_s} \right) f_o \tag{8.44}$$

Where f_o is the frequency of the system (Hz), f is the frequency perceived by the receiver (Hz), c is the speed of the carrier wave (m s^{-1}), v_r is the relative velocity of the receiver (m s^{-1}), and v_s is the relative velocity of the source (m s^{-1}).

This effect is noticeable when a whistling train or police siren passes by. An observer in front of the moving car or train hears a higher pitch than a passenger in the vehicle. Similarly, the passenger hears a higher pitch than an observer behind the vehicle. Doppler shift can also affect the frequency of a radar carrier wave, the time between pulses of a radar signal, or even light waves causing an apparent shift of colour. The frequency shift associated with moving objects is illustrated in Figure 8.4; therefore the speed and relative motion of moving objects, such as insects can be determined from radar. This is especially useful when the medium surrounding the insect is not air (for example wood or stored grain). In these cases Doppler shift is a useful parameter to monitor.

Several variants on Doppler radar systems have been developed for insect detection. For example, Termatrac® is a 24 GHz Doppler radar termite detector, developed by Scientific Technology. The original radar system consisted of a Gunn diode and mixer coupled to a horn antenna; however the current system uses an automotive fixed dual array sensor (Rankin, *et al.* 2012). In these systems the scattered field is mixed with the generated radar signal to produce a "beat" frequency that can be isolated using appropriate filtering.

Termite detection is difficult due to the very low signal to noise ratio and high attenuation and scattering from the wood material (Rankin, *et al.* 2012); therefore the Termatrac system separates the Doppler shift due to termite movement from the stationary background clutter using a 0.1 to 10 Hz band pass filter (Rankin, *et al.* 2012). Accidental movement of the instrument results in relative movement of the background clutter in the radar signal and reduces the effectiveness of this filtering. From the Nyquist criterion, the minimum frame rate is 20 Hz in order to capture termite motion within the filter bandwidth (Nyquist 2002, Rankin, *et al.* 2012).

Controlled field tests, using the Termatrac system, resulted in at least 90 % accuracy (Evans 2002). In some cases, motion of non-termite insects was detected even though termites were not present in the samples. The great advantage of radar detection is that it is non-destructive, while older methods of insect detection in materials such as wood relied on strategic drilling into the material to confirm infestations.

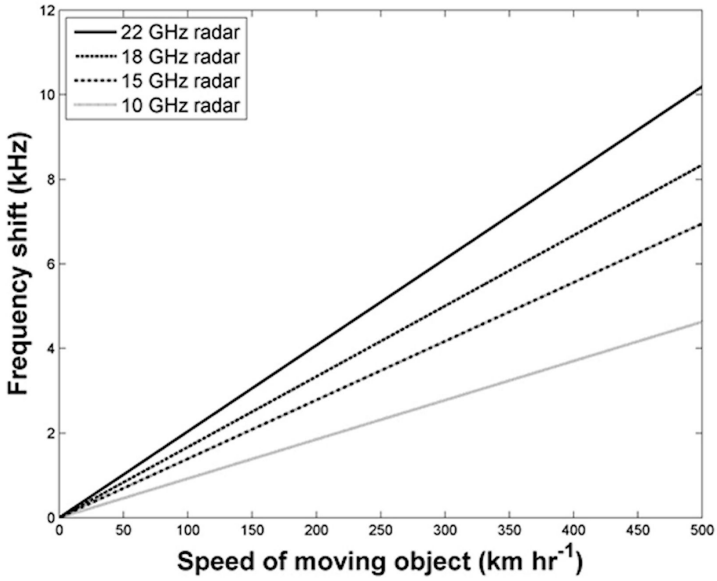

Figure 8.6: Doppler frequency shift as a function of object speed and radar operating frequency for fast moving objects.

Doppler systems, such as Termatrac, can also be used to detect insects in stored grain or flour. Mankin (2004) demonstrated that movement of individual adults or groups of insects [*Lasioderma serricorne* (F.), *Oryzaephilus surinamensis* (L.), *Attagenus unicolor* (Brahm), and *Tribolium castaneum* (Herbst)] were easily detected over distances up to 30 cm in air using the Termatrac system. Mankin (2004) then demonstrated that insect movement of between 5 to 100 insects could be detected in boxes of corn meal mix and flour mix; however detection was only possible in the grain or flour at very short range.

Although radar is effective for detecting insects in the air and in some materials such as wood, nuts and stored grain, the effective range in many media is very small [see equation (8.8)]; therefore it is often useful to use a free-space technique to assess the shadows cast by insects rather than depending on radar reflections.

8.2 Free-Space Microwave Systems

When microwaves are transmitted through a material, the wave will be partially reflected from the surface of the material, attenuated and delayed compared to a wave travelling through free space (Figure 8.7), depending on the bulk dielectric properties of all the materials in the space between the antennae. The combination of wave

attenuation and wave delay provides useful information about the material through which the wave passed. An x-ray image is a good example of the information that can be derived from wave attenuation and delay.

In chapter 4, the concept of the magnetic vector potential was introduced. The total magnetic vector potential at some distance from the transmitting antenna is determined by integrating all contributions within a volume of interest:

$$\vec{A} = \int_v \frac{\mu \cdot d\vec{J}}{4\pi} \cdot \frac{e^{j\omega\sqrt{\mu\varepsilon}\cdot r}}{r} \cdot dv \tag{8.45}$$

Now $\omega\sqrt{\mu\varepsilon}$ is a complex number that can be described by:

$$\omega\sqrt{\mu\varepsilon} = \omega\sqrt{\mu\varepsilon_o\left(\kappa' + j\kappa''\right)} = \omega\sqrt{\mu\varepsilon_o\kappa'\left(1 + j\frac{\kappa''}{\kappa'}\right)} \tag{8.46}$$

where k' is the relative dielectric constant of the material and k" is the relative dielectric loss factor of the material through which the electromagnetic wave passes. After some manipulation, equation (8.46) can finally be expressed as: $\omega\sqrt{\mu\varepsilon} = \alpha + j\beta$, where:

$$\alpha = \omega\sqrt{\frac{\mu\varepsilon_o\kappa'\sqrt{\left(1+\left(\frac{\kappa''}{\kappa'}\right)^2\right)}+1}{2}} \tag{8.47}$$

and

$$\beta = \omega\sqrt{\frac{\mu\varepsilon_o\kappa'\sqrt{\left(1+\left(\frac{\kappa''}{\kappa'}\right)^2\right)}-1}{2}} \tag{8.48}$$

Therefore equation (8.45) becomes:

$$\vec{A} = \int_v \frac{\mu \cdot d\vec{J}}{4\pi} \cdot \frac{e^{j\alpha\cdot r}}{r} \cdot e^{-\beta\cdot r} \cdot dv \tag{8.49}$$

Because the magnetic vector potential is directly linked to the electric field of an electromagnetic wave, changes in the magnetic vector potential are also manifested as changes in the electric field. The Green's function $\frac{e^{j\alpha\cdot r}}{r}$ term in equation (8.49)

accounts for the phase delay illustrated in Figure 8.7, while the $e^{-\beta \cdot r}$ term in equation (8.49) accounts for the attenuation. Both terms are directly linked to the bulk dielectric properties of the space between the antennae. These bulk dielectric properties will depend on static materials in the space and will change as other materials, such as insects, move between the antennae.

Various systems have been developed that use the free-space technique to detect insects in stored grain. As was highlighted in Chapter 7, the dielectric properties of insects are much higher than that of dry grain or nuts (Nelson 1996, Wang 2003); therefore insects can dramatically change the bulk dielectric properties of the space between the antennae of a free-space system and therefore increase the attenuation and phase delay of the microwave fields as they pass between the antennae. This is analogues to casting a shadow in the visible portion of the light spectrum.

This technique for detecting insects is particularly effective when several microwave frequencies are used simultaneously. For example, Ding et al (2008) had greater success at detecting and identifying eight species of pest insects in grain when using three separate frequencies (180.3, 1020, and 1032 MHz) rather than a single frequency.

8.2.1 Decay Detection

The dielectric properties of wood depend on: the frequency of the microwave fields; the density of the wood; the orientation of the microwave's electrical field with respect to the wood grain; the uniformity of the wood structure (Torgovnikov 1993, Daian, et al. 2005); and especially the moisture content of the wood (Torgovnikov 1993). Digestion of wood by decay causing fungi significant reduces the number of tracheids from the wood; thus creating voids in the wood's micro-structure. These voids affect the bulk dielectric properties of the wood, which in turn affect the microwave scattering and the field coupling response of wood. Ultimately these changes in the bulk dielectric properties allow decay detection with microwave fields.

Wood density is reduced due to digestion of wood polymers by decay causing fungi (Figure 8.8). Orienting the antennae of a look though microwave system so that the microwave's electrical field was parallel to the wood grain can easily differentiated between the different levels of decay exposure in both hardwood and softwood samples; however orienting the antennae so that the electrical field was perpendicular to the grain could not differentiate between the levels of decay exposure (Figure 8.9).

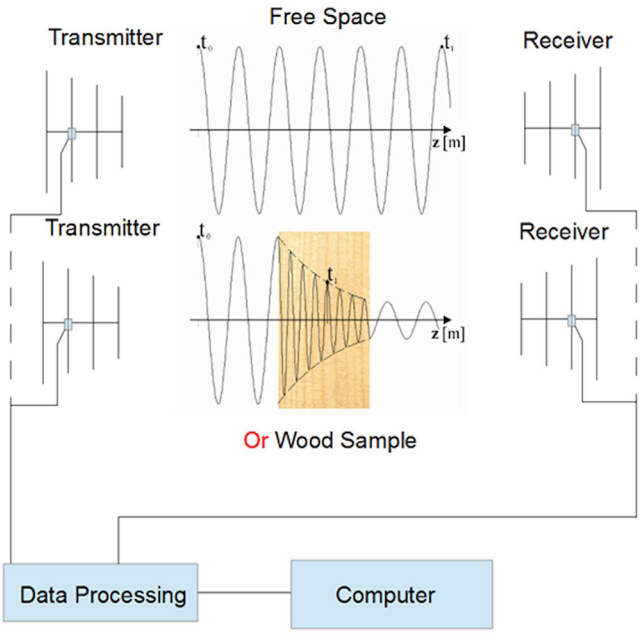

Figure 8.7: Propagation of microwave energy through wood compared to propagation through open space.

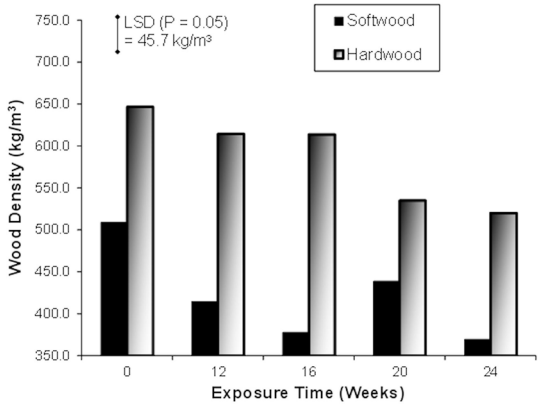

Figure 8.8: Mean wood density of hardwood (Eucalyptus regnans) and softwood (Pinus radata) samples as a function of exposure to decay causing fungi.

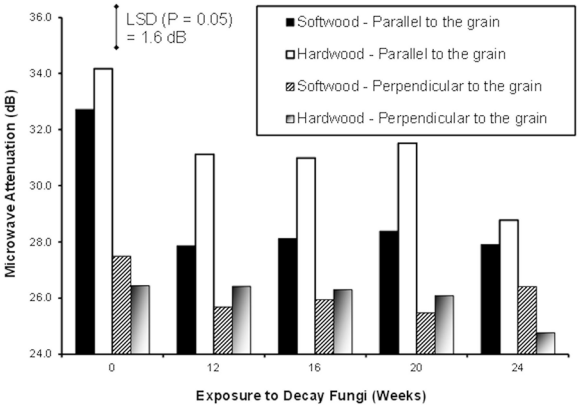

Figure 8.9: Mean microwave field attenuation as a function of antenna orientation, wood species and decay exposure time.

8.3 Conclusions

This chapter has explored the use of RF and microwave systems for detecting insects and decay in other materials such as air, wood and grains. In most cases, movement and the high moisture content of the insects is the most important factor in determining their detectability; therefore RF and microwave systems can be used for monitoring moisture. This will be briefly explored in the following chapter.

References

Bird, T. S. 1990. Analysis of mutual coupling in finite arrays of different-sized rectangular waveguides. *IEEE Transactions on Antennas and Propagation*. 38(2): 166-172.

Bird, T. S. 1996. Cross-coupling between open-ended coaxial radiators. *Microwaves, Antennas and Propagation, IEE Proceedings* -. 143(4): 265-271.

Brodie, G. 1981. Design of an antenna for the Homestead and Community Broadcast Satellite Service. Unpublished Honours thesis. Townsville: James Cook University, Electrical and Electronic Engineering

Connor, F. R. 1972, *Antennas*, London: Edward Arnold.

Daian, G., Taube, A., Birnboim, A., Shramkov, Y. and Daian, M. 2005. Measuring the dielectric properties of wood at microwave frequencies. *Wood Science and Technology*. 39(3): 215 -223.

Ding, F., Jones, C. L. and Weckler, P. 2008. Detection and Identification of Stored Grain Insects with RF/Microwave and Neural Network Technology. *ASABE*. (082343):

Donskoy, D. and Sedunov, N. 2002. *Method and Apparatus for Detection of Wood Destroying Insects and Damage Evaluation Using Microwaves*. Patent No. 20020180607

Evans, R. J., Farrell, P. M., Felic, G., Hoa Thai, D., Hoang Viet, L., Li, J., Li, M., Moran, W., Morelande, M. and Skafidas, E. 2013. Consumer radar: Technology and limitations. *Proc. Radar (Radar), 2013 International Conference on*. 21-26.

Evans, T. A. 2002. Assessing efficacy of Termatrac (TM): a new microwave based technology for non-destructive detection of termites (Isoptera). *Sociobiology*. 40(3): 575 -583.

Georgieva, N. 2001. Modern Antennas in Wireless Telecommunications.

Hobbs, S. E. and Aldhous, A. C. 2006. Insect ventral radar cross-section polarisation dependence measurements for radar entomology. *IEE Proceedings -- Radar, Sonar & Navigation*. 153(6): 502-508.

Ishimaru, A., Jaruwatanadilok, S. and Kuga, Y. 2004. Multiple scattering effects on the radar cross section (RCS) of objects in a random medium including backscattering enhancement and shower curtain effects. *Waves in Random Media*. 14(4): 499-512.

Mankin, R. W. 2004. Microwave radar detection of stored-product insects. *Journal of Economic Entomology*. 97(3): 1168-1173.

Mie, G. 1908. Contributions on the optics of turbid media, particularly colloidal metal solutions. *Annalen der Physik*. 25(3): 377-445.

Nelson, S. O. 1996. Review and assessment of radio-frequency and microwave energy for stored-grain insect control. *Transactions of the ASAE*. 39(4): 1475-1484.

Nyquist, H. 2002. Certain topics in telegraph transmission theory. *Proceedings of the IEEE*. 90(2): 280-305.

Rankin, G. A., Tirkel, A. Z., Bui, L. Q. and Marshall, N. W. D. L. 2012. Radar Imaging: Conventional and MIMO. *Proc. The International Conference on Communications and Electronics*. 171-176.

Riley, J. R. 1992. A millimetric radar to study the flight of small insects. *Electronics & Communication Engineering Journal*. 4(1): 43-48.

Roberts, K. 2010. *Locust damage in crops and pastures*. Department of Industry and Investment, New South Wales

Silver, S. 1949, *Microwave Antenna Theory and Design*, New York.: McGraw-Hill Book Company.

Torgovnikov, G. I. 1993, *Dielectric Properties of Wood and Wood-Based Materials*, Springer Series in Wood Science, Berlin: Springer-Verlag.

US Naval Air Systems Command 1999, *Electronic Warfare and Radar Systems Engineering Handbook*, Avionics Department, Naval Air Systems Command, US Navy.

Wang, S., Tang, J., Johnson, J.A., Mitcham, E., Hansen, J.D., Hallman, G., Drake, S.R., and Wang, Y. 2003. Dielectric Properties of Fruits and Insect Pests as related to Radio Frequency and Microwave Treatments. *Biosystems Engineering*. 85(2): 201-212.

Wolf, W. W., Vaughn, C. R., Harris, R. and Loper, G. M. 1993. Insect radar cross-section for aerial density measurement and target classification. *Transactions of the American Society of Agricultural and Biological Engineers*. 36(3): 949-954.

9 Moisture Monitoring

Microwave techniques have been considered for moisture sensing in many food processing and agriculture-related industries (Trabelsi, *et al.* 1998b). Chapter 7 highlighted the strong dependence of dielectric properties for organic materials on the moisture content of the material. Both bound water and free water have much higher dielectric properties than dry organic materials; therefore RF and microwave technologies have been used to automatically monitor moisture content.

9.1 Free-Space Moisture Detection

The previous chapter introduced the idea of using a free-space transmission technique for detecting decay in wood. The same technique can be used for measuring moisture in various materials. As the microwaves propagate through a layer of organic material, they will be attenuated and experience a phase shift (Kim, *et al.* 2002, Kim, *et al.* 2006), as illustrated in Figure 8.5 in the previous chapter. The attenuation and phase shift can be compared to an empty sample holder between two antennae (Kim, *et al.* 2002, Kim, *et al.* 2006).

The change in RF and microwave field attenuation is given by (Kim, *et al.* 2002, Kim, *et al.* 2006):

$$\Delta A = \frac{8.686\pi}{\lambda_o} \cdot \frac{\kappa''}{\sqrt{\kappa'}} \cdot d \tag{9.1}$$

where ΔA is the difference between the attenuation, with and without samples, in dB, λ_o is the free space wave length, κ' and κ" are the real and imaginary parts of the relative permittivity of the material, and d is the thickness of the material under test. The phase delay is given by (Trabelsi, *et al.* 1998a, Kim, *et al.* 2006):

$$\Delta\Phi = \left(\sqrt{\kappa'} - 1\right)\frac{360}{\lambda_o} \cdot d \tag{9.2}$$

Where ΔΦ is the difference between the phase, with and without samples, in degrees. As illustrated in equation (9.1), the change in attenuation depends on the dielectric properties of the samples under test when the frequency and sample thickness are constant. Because the dielectric properties are closely linked to moisture content, it is possible to measure the moisture content by detecting the peak voltage of the microwave signal from the receiving antenna (Kim, *et al.* 2002); however, with

particulate materials, bulk density fluctuations cause significant errors in moisture content determination (Trabelsi, *et al.* 1998b).

Trabelsi et al. (1998b) demonstrated that plotting $\frac{\kappa''}{\rho}$ against $\frac{\kappa'}{\rho}$ for varying moisture content, where ρ is the bulk density of the material, resulted in a straight line of the form:

$$\frac{\kappa''}{\rho} = a\left(\frac{\kappa'}{\rho} - b\right) \tag{9.3}$$

Slope (a) and intercept (b) values for hard red winter wheat of different moisture contents are listed in Table 9.1. All the lines cross the axis at a common point, which corresponds to the coordinates, in the complex plane, of the dielectric properties of a totally dry kernel mixture (Trabelsi, *et al.* 1998b).

The slope factor (a) depends solely on frequency (in GHz) such that (Trabelsi, *et al.* 1998a):

$$a = 0.0184f + 0.3826 \tag{9.4}$$

Table 9.1: Slope and intercept values for hard red winter wheat of different moisture contents as a function of frequency (Source: Trabelsi, et al. 1998b).

Frequency (GHz)	11.3	12.3	13.3	14.2	15.2	16.8	18.0
a - measured	0.5960	0.6060	0.6255	0.6474	0.6596	0.6905	0.7187
a – calculated from equation (9.3)	0.59052	0.60892	0.62732	0.64388	0.66228	0.69172	0.7138
b - measured	2.765	2.776	2.776	2.758	2.747	2.756	2.773
r^2	0.9907	0.9875	0.9888	0.9900	0.9884	0.9891	0.9868

Provided a and b are known for any given material, the bulk density can be determined from the dielectric properties at any given moisture content and temperature (Trabelsi, et al. 1998a):

$$\rho = \frac{a\kappa' - \kappa''}{ab} \tag{9.5}$$

The slope and intercept values (a and b) must be determined experimentally for each material to be tested.

A density-independent function can also be defined (Trabelsi, *et al.* 1998a):

$$\xi = \frac{\kappa''}{\kappa'\left(a\kappa' - \kappa''\right)} \tag{9.6}$$

The square root of ξ varies linearly with moisture and is ultimately independent of bulk density:

$$\sqrt{\xi} = \alpha m + \beta \tag{9.7}$$

where α and β are constants, and m is the moisture content of the sample.

9.1.1 Practical Applications

Various free-space systems moisture detection systems have been developed for use in agriculture for monitoring the moisture of grains and hay going into storage (Figure 9.1). For example, a commercially available moisture detection system for quickly measuring the moisture content of hay bales has been developed (Figure 9.1). Analysis of this commercial microwave hay moisture meter showed a close relationship of the meter's readings compared to the lab results ($R^2 = 0.867$) (Keith, *et al.* 2013).

Similar RF and microwave based free-space systems are available for measuring moisture of other agricultural products that are susceptible to moisture related degradation, including: grain, sugar, and cotton. In all cases, the dielectric properties of the dry material are very low compared with the dielectric properties of bound and free water; therefore moisture detection is moderately easy to achieve.

Free-space moisture monitoring relies on transmitting a RF or microwave field through a material under test. Although this arrangement is ideal for monitoring many agricultural and forestry products, such as grains and sawn timber, it is not always possible to have access to both sides of a material. Under these circumstances, microwave emissions from the material or radar assessments are better.

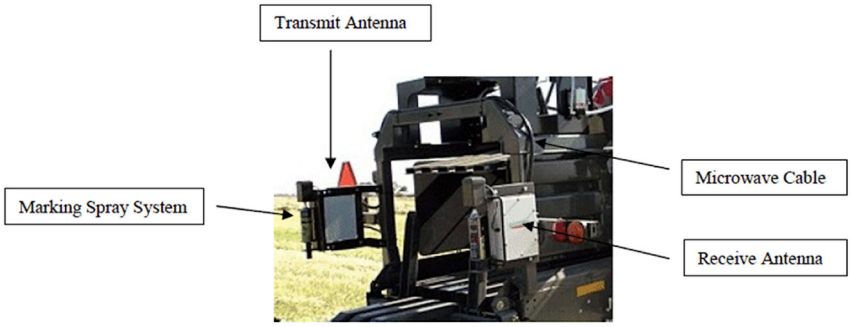

Figure 9.1: Microwave system for monitoring moisture in hay bales mounted on the outlet of a large square baler (Source: Anonymous 2013).

Other moisture monitoring techniques rely on close range radar analysis. These also respond to changes in the dielectric properties due to changes in the moisture content of the material being monitored. In particular these changes in the dielectric properties change the reflectivity of the material, which therefore enhances the reflections that the radar system detects.

One commercial example of a radar-based moisture detection system was developed for the measurement of moisture and temperature in rotating pan, static and planetary mixers (Hydronix Limited 2004). The main sensor has a simple temperature sensor and a compact modular microwave radar system mounted on an arm. This can be inserted into a mixer system, such as an animal feed mixer, and monitors the moisture content of the material as it passes by the radar module. Changes in the moisture content correspond to changes in the output voltages from the radar module.

9.2 Microwave Emissions as a Measure of Moisture

Heat is transferred through space by conduction, convection and radiation. Radiative heat transfer refers to the transfer of energy by broad spectrum electromagnetic radiation from some adjacent hot object (or from a hot environment) to the heated object. Any object that is above zero degrees Kelvin will radiate energy in the form of electromagnetic photons. The German physicist, Max Planck (1858 – 1947), deduced that the ideal radiation spectral density (ρ_{ideal}) given off from a hot object depended on the wavelength of interest and the temperature of the object. This spectral density can be described by:

$$\rho_{ideal} = \frac{2\pi hc}{\lambda^5 \left(e^{\frac{hc}{\lambda kT}} - 1 \right)} \tag{9.8}$$

Where h is Planck's constant (6.6256×10^{-34} J s), c is the speed of light, λ is the electromagnetic wavelength of interest, k is Boltzmann's constant (1.38054×10^{-23} J K^{-1}), and T is the temperature in Kelvin. A typical set of spectral distributions is shown for different temperatures are shown in Figure 9.2. Although the peak emissions occur in the infra-red part of the spectrum for ambient temperatures, some energy is emitted in the RF and microwave bands.

Real objects radiate slightly less energy in different parts of the spectrum. The ratio of the real emission at any given wavelength and the ideal emission is defined as the emissivity (e) of the surface:

$$e = \frac{\rho_{ideal}}{\rho_{real}} \tag{9.9}$$

The spectral emissivity of a material is directly related to its reflection coefficient (Γ) at the wavelength of interest (Lakshmi 2013):

$$e = 1 - \Gamma \tag{9.10}$$

This is the same as the transmission coefficient defined in equation (4.40) in Chapter 4. Combining and manipulating equations (4.33) and (4.40) yields:

$$e = \frac{2\sqrt{\kappa}}{1 + \sqrt{\kappa}} \tag{9.11}$$

where κ is the complex relative dielectric constant of the material.

It has already been demonstrated in Chapter 7 that the relative dielectric constant of organic materials and soils in the RF and microwave bands is strongly linked to the moisture content of the material while the influence of moisture on the dielectric properties of these materials in the infra-red part of the spectrum is negligible; therefore monitoring natural electromagnetic emissions from organic materials and soils using duel band sensors (thermal infra-red and microwave) can remotely determine the moisture content of these materials (Lakshmi 2013), as illustrated in Figure 9.3.

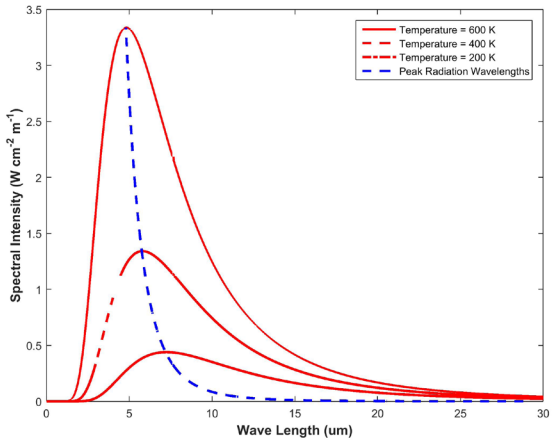

Figure 9.2: Ideal radiative spectral density at different temperatures as a function of temperature and wavelength.

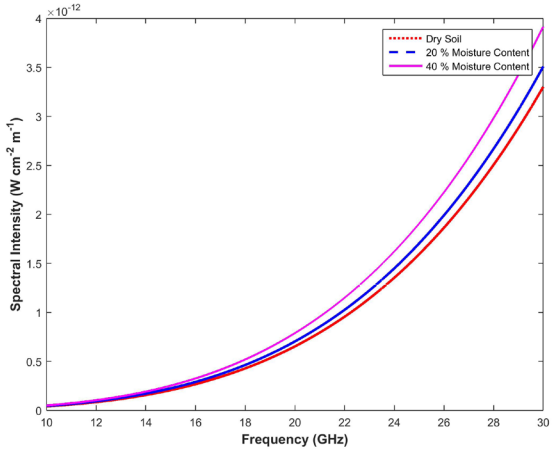

Figure 9.3: Estimated microwave emissions from bare clay soil as a function of frequency and soil moisture content at 25 °C.

Although the electromagnetic power emissions from soil at microwave are very small, radiometers that measure microwave emission brightness from the earth's surface have been deployed in satellites for some time and are routinely used to determine the moisture content of soils on a large scale (Lakshmi 2013). Close range systems, mounted on farm machinery, could also be developed; however the requirement for dual band monitoring makes these systems expensive.

9.3 Radar Moisture Measurement

The reflection coefficient of surface is also dependent on the dielectric properties of the material:

$$\Gamma = \frac{1-\sqrt{\kappa}}{1+\sqrt{\kappa}} \tag{9.12}$$

Therefore the radar cross section of an object, which was introduced in Chapter 8, also depends on the dielectric properties of the surface material of an object. If radar is directed at an organic material or the soil, changes in moisture content will affect the reflection coefficient of the surface (Figure 9.4).

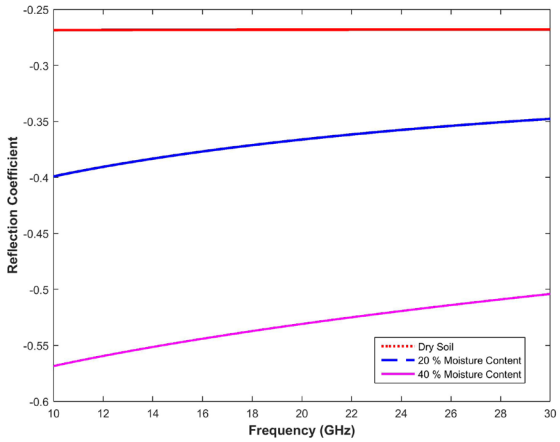

Figure 9.4: Reflection coefficient of bare clay soil as a function of frequency and soil moisture content at 25 °C.

Comparing figures (9.3) and (9.4) suggests that reflection provides better discrimination between soil moisture status than emissions, therefore research into remote moisture measurements using radar is being actively pursued (Zhan, *et al.* 2006).

Mass produced radar modules at fixed frequencies have been available for some time. These can be deployed on agricultural machinery to measure the moisture content of soil and produce in real time. Aerial and satellite radar systems can also be employed to assess large areas of the landscape. These large scale radar systems will be explored in the next chapter.

References

Anonymous. 2013. *Gazeeka Moisture Gauge*. International Stock Foods

Hydronix Limited. 2004. *Hydro-Probe Orbiter User Guide*

Keith, E. W., Mathew, D., Jeff, A. and Drew, S. 2013. Production Scale Single-pass Corn Stover Large Square Baling Systems. *Proc. 2013 Kansas City, Missouri, July 21 - July 24, 2013*. 1.

Kim, K., Kim, J., Lee, S. S. and Noh, S. H. 2002. Measurement of Grain Moisture Content Using Microwave Attenuation at 10.5 GHz and Moisture Density. *IEEE Transactions on Instrumentation and Measurement*. 51(1): 72-77.

Kim, K. B., Kim, J. H., Lee, C. J., Noh, S. H. and Kim, M. S. 2006. Simple instrument for moisture measurement in grain by free-space microwave transmission. *Transactions of the American Society of Agricultural and Biological Engineers*. 49(4): 1089-1093.

Lakshmi, V. 2013. Remote Sensing of Soil Moisture. *ISRN Soil Science*. 2013: 1-33.

Trabelsi, S., Kraszewski, A. W. and Nelson, S. O. 1998a. A Microwave Method for On-line Determination of Bulk Density and Moisture Content of Particulate Materials. *IEEE Transactions on Instrumentation and Measurement*. 47(1): 127-132.

Trabelsi, S., Krazsewski, A. W. and Nelson, S. O. 1998b. New Density-Independent Calibration Function for Microwave Sensing of Moisture Content in Particulate Materials. *IEEE Transactions on Instrumentation and Measurement*. 47(3): 613-622.

Zhan, X., Houser, P. R., Walker, J. P. and Crow, W. T. 2006. A Method for Retrieving High-Resolution Surface Soil Moisture From Hydros L-Band Radiometer and Radar Observations. *IEEE Transactions on Geoscience and Remote Sensing*. 44(6): 1534-1544.

10 Radar Imaging

Active sensors provide their own source of energy to illuminate the target. Active sensors are generally divided into two distinct categories: imaging and non-imaging. The most common form of active imaging sensor is RADAR.

Non-imaging sensors include altimeters and scatterometers. Radar altimeters transmit short microwave pulses and measure the round trip time to targets to determine their distance from the sensor (Canadian Centre for Remote Sensing 2004). Scatterometers are used to make precise quantitative measurements of the amount of energy reflected from targets (Canadian Centre for Remote Sensing 2004). The amount of reflected energy is dependent on the surface properties (roughness) and the angle at which the energy strikes the target.

Radar consists of a transmitter, a receiver, an antenna, and an electronics system to process and record the data (Sabins 1987, Tikhonov 1997, Navalgund, *et al.* 2007, Lakshmi 2013). The transmitter generates successive short bursts (or pulses) of microwave energy at regular intervals, which are focused by the antenna into a beam. The radar beam illuminates the surface obliquely at a right angle to the motion of the platform and reflects back to the source, similar to the flash of a camera. The antenna receives a portion of the reflected energy (or backscatter) from various objects within the illuminated beam (Sabins 1987). By measuring the time delay between the transmission of a pulse and the reception of the echo from different targets, their distance from the radar and thus their location can be determined (Sabins 1987, Canadian Centre for Remote Sensing 2004).

10.1 Radar Imaging

When discussing microwave energy, the polarisation of the radiation is important. Polarisation refers to the orientation of the electric field. Most radar systems are designed to transmit microwave radiation either horizontally polarised or vertically polarised. Similarly, the antenna receives either the horizontally or vertically polarised echoed energy. There can be four combinations of both transmitted and received polarizations:

1. HH - for horizontal transmit and horizontal receive,
2. VV - for vertical transmit and vertical receive,
3. HV - for horizontal transmit and vertical receive, and
4. VH - for vertical transmit and horizontal receive.

The first two polarisation combinations are referred to as like polarised because the transmitted and receive polarisations are the same. The last two combinations are referred to as cross-polarised because the transmitter and receiver polarisations are opposite of one another.

Both wavelength and polarisation affect how radar interacts with the surface. Therefore, radar imagery collected using different polarization and wavelength combinations may provide different and complementary information about the targets on the surface (Canadian Centre for Remote Sensing 2004).

The imaging geometry of a radar system is different from the framing and scanning systems commonly employed for optical remote sensing. The microwave beam is transmitted obliquely at right angles to the direction of flight illuminating a swath (Avery and Berlin 1992). Range refers to the across-track dimension perpendicular to the flight direction, while azimuth refers to the along-track dimension parallel to the flight direction. This side-looking geometry is typical of imaging radar systems.

The portion of the image swath closest to the flight track of the radar platform is called the near range while the portion of the swath farthest from the flight track is called the far range. Figure 10.1 shows the geometry of an imaging radar system. The incidence angle is the angle between the radar beam and ground surface (A), which increases, moving across the swath from near to far range. The look angle (B) is the angle at which the radar "looks" at the surface (Canadian Centre for Remote Sensing 2004). At all ranges the radar antenna measures the radial line of sight distance between the radar and each target on the surface. This is the slant range distance (C). The ground range distance (D) is the true horizontal distance along the ground corresponding to each point measured in slant range (Canadian Centre for Remote Sensing 2004).

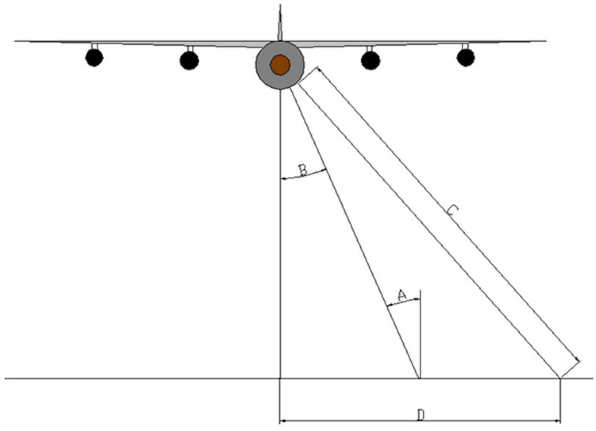

Figure 10.1: Incident angles.

Unlike optical systems, radar's spatial resolution is a function of the specific properties of the microwave radiation and geometrical effects. If a Real Aperture Radar (RAR) is used, a single transmit pulse and the echoed signal are used to form the image (Avery and Berlin 1992). In this case, the resolution is dependent on the effective length of

the pulse in the slant range direction and the width of the illumination in the azimuth direction (Canadian Centre for Remote Sensing 2004). The range or across-track resolution is dependent on the length of the pulse (P). Therefore:

$$R_s = \frac{P}{2} \tag{10.1}$$

Therefore, two distinct targets on the surface will be distinguished from one another if their separation is greater than half the pulse length as seen in Figure 10.2. However, when projected into ground range coordinates, the resolution in ground range will depend on the incidence angle. Thus, for fixed slant range resolution, the ground range resolution will decrease with increasing range.
Range resolution is defined as:

$$P_r = \frac{P \cdot c}{2\cos\theta} \tag{10.2}$$

where P is the pulse length in seconds, c is the speed of light and θ is the depression angle, which is the angle between horizontal and bottom of radar beam (ie. 90° – B). The azimuth or along-track resolution is determined by the angular width of the radiated microwave beam and the slant range distance, as shown in Figure 10.2. This beam-width is a measure of the width of the illumination pattern and depends on the radiation pattern and gain of the radar antenna. As the radar pulse travels away from the sensor, the azimuth resolution becomes worse. Azimuth resolution is defined as:

$$R_a = \frac{0.7S\lambda}{D} \tag{10.3}$$

Where S is the slant range distance in metres, D is the antenna length and λ is the microwave wavelength.

Finer range resolution can be achieved by using a shorter pulse length. Finer azimuth resolution can be achieved by increasing the antenna dimensions; however, the actual length of the antenna is limited by what can be carried on an airborne or space-borne platform. For airborne radars, antennas are usually limited to one or two metres in size while for satellites they can be from 10 to 15 metres in length (Canadian Centre for Remote Sensing 2004).

To overcome this size limitation, the forward motion of the platform and Doppler analysis of the echoes are used to simulate a very long antenna and thus increase

azimuth resolution (Avery and Berlin, 1992). This process is called Synthetic Aperture Radar (SAR).

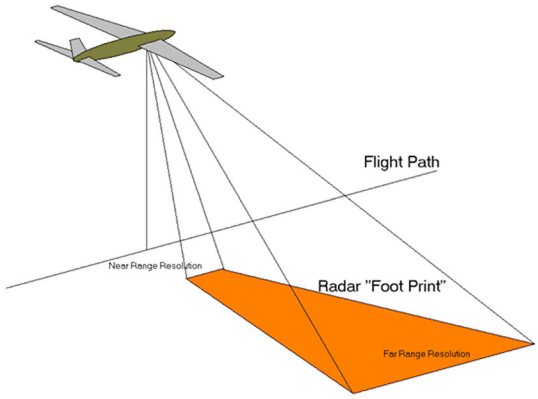

Figure 10.2: Azimuth resolution.

10.2 Image Distortion

As with all remote sensing systems, the viewing geometry of radar results in certain geometric distortions in the resultant image. However, there are key differences for radar imagery, which are due to the side-looking geometry, and the fact that the radar is fundamentally a distance-measuring device (Canadian Centre for Remote Sensing 2004).

Slant-range scale distortion occurs because the radar is measuring the distance to features in slant-range rather than the true horizontal distance along the ground. This results in a varying image scale, moving from near to far range (Figure 10.3). This causes targets in the near range to appear compressed relative to the far range. Using trigonometry, ground-range distance can be calculated from the slant-range distance and platform altitude to convert to the proper ground-range format.

Similar to the distortions encountered when using cameras and scanners, radar images are also subject to geometric distortions due to relief displacement. As with scanner imagery, this displacement is one-dimensional and occurs perpendicular to the flight path; however, the displacement is reversed with targets being displaced towards, instead of away from the radar flight path (Canadian Centre for Remote Sensing 2004). Radar foreshortening and radar layover are two consequences, which result from relief displacement. Layover occurs when the radar beam reaches the top of a tall feature before it reaches the base. The return signal from the top of the feature will be received before the signal from the bottom (Canadian Centre for Remote Sensing 2004).

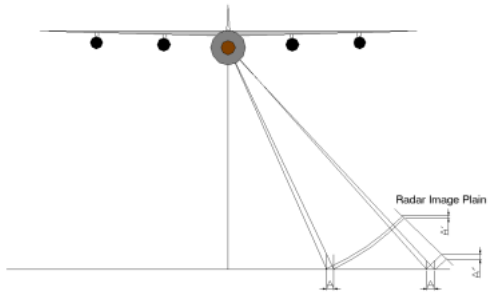

Figure 10.3: Slant distance distortion.

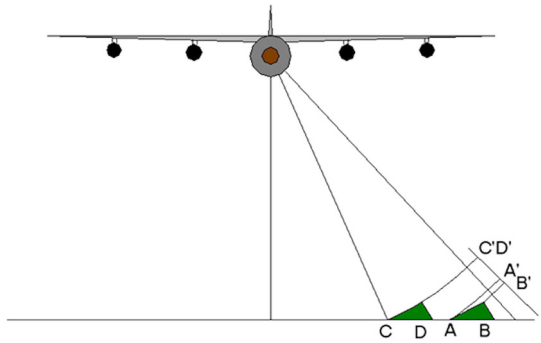

Figure 10.4: Radar image foreshortening, where elevation points on an object appear to coincide.

Both foreshortening and layover result in radar shadow. Radar shadow occurs when the radar beam is not able to illuminate the ground surface (Canadian Centre for Remote Sensing 2004). Shadows occur in the down range dimension (i.e. towards the far range), behind vertical features or slopes with steep sides.

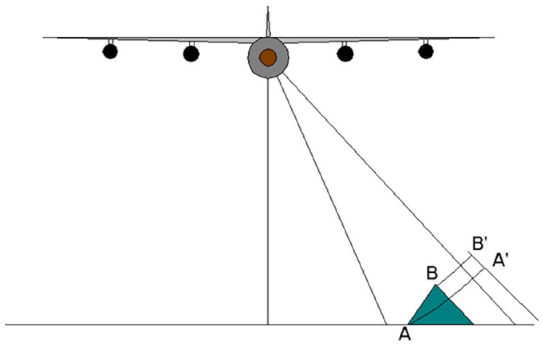

Figure 10.5: Radar image layover.

10.3 Target Interaction and Image Appearance

The brightness of features in a radar image is dependent on the portion of the transmitted energy that is returned back to the radar from targets on the surface. The magnitude or intensity of this echoed energy is dependent on how the radar energy interacts with the surface. This depends on the particular characteristics of the radar system (frequency, polarization, viewing geometry, etc.) as well as the characteristics of the surface (land cover type, topography, relief, dielectric properties etc.). Because many of these characteristics are interrelated, it is impossible to separate out each of their individual contributions to the appearance of features in a radar image.

For the purposes of discussion, these characteristics can be grouped into three areas, which fundamentally control radar energy/target interactions. They are:

1. Surface roughness of the target
2. Radar viewing and surface geometry relationship
3. Moisture content and dielectric properties of the target

The surface roughness of a feature controls how the microwave energy interacts with that surface or target and is generally the dominant factor in determining the tones seen on a radar image. Surface roughness refers to the average height variations in the surface cover from a plane surface. Whether a surface appears rough or smooth to radar depends on the wavelength and incidence angle. A surface will appear smooth if the height of any features is less than the Rayleigh criterion, which is defined as:

$$h_r = \frac{\lambda}{8 \sin \theta} \tag{10.4}$$

Where λ is the microwave wavelength and θ is the depression angle.

Incidence or look angle in relation to viewing geometry and how changes in this angle affect the signal returned to the radar have already been discussed. However, in relation to surface geometry, and its effect on target interaction and image appearance, the local incidence angle is a more appropriate concept. The local incidence angle is the angle between the radar beam and a line perpendicular to the surface at the point of incidence. Thus, local incidence angle takes into account the local slope of the terrain in relation to the radar beam. With flat terrain, the local incidence angle is the same as the look angle of the radar. For terrain with any type of vertical relief, this is not the case. Generally, slopes facing towards the radar will have small local incidence angles, causing relatively strong echoes, which results in a bright-toned appearance within an image (Canadian Centre for Remote Sensing 2004). Conversely, slopes facing away from the radar will appear to be darker.

The presence (or absence) of moisture affects the dielectric properties of objects (Sabins 1987). Changes in the dielectric properties influence the absorption,

transmission, and reflection of microwave energy; therefore, the moisture content will influence how targets and surfaces reflect energy from radar and how they will appear in an image (Sabins 1987). Generally, reflectivity (image brightness) increases with increased moisture content (Canadian Centre for Remote Sensing 2004).

If the radar energy does manage to penetrate through the topmost surface, then volume scattering may occur (Canadian Centre for Remote Sensing 2004). Volume scattering is the scattering of radar energy within a volume rather than from an outer surface, and usually consists of multiple bounces and reflections from different components within the volume. For example, in a forest, scattering may come from the leaf canopy at the tops of the trees, the leaves and branches further below, and the tree trunks and soil at the ground level. Volume scattering may decrease or increase image brightness, depending on how much of the energy is scattered out of the volume and back to the radar (Canadian Centre for Remote Sensing 2004).

10.4 Airborne versus Space-borne Radar

Like other remote sensing systems, an imaging radar sensor may be carried on-board either an airborne or space-borne platform. There are trade-offs between the two. Regardless of the platform used, a significant advantage of using a Synthetic Aperture Radar (SAR) is that the spatial resolution is independent of platform altitude (Canadian Centre for Remote Sensing 2004); therefore fine resolution can be achieved from both airborne and space-borne platforms.

Although spatial resolution is independent of altitude, viewing geometry and swath coverage can be greatly affected by altitude variations. At aircraft operating altitudes, an airborne radar system must operate over a wide range of incidence angles, perhaps as much as 60 or 70 degrees, in order to achieve relatively wide swaths; therefore foreshortening, layover, and shadowing will be subject to wide variations, across a large incidence angle range (Canadian Centre for Remote Sensing 2004). On the other hand, space-borne radar operating at altitudes of several hundred kilometres has a much narrower range of incidence angles, typically ranging from 5 to 15 degrees (Canadian Centre for Remote Sensing 2004). This provides for more uniform illumination and reduces undesirable image variations across the swath due to viewing geometry.

Although airborne radar systems may be more susceptible to imaging geometry problems, they are flexible in their capability to collect data from different angles and directions. Space-borne radar does not have this degree of flexibility, as its viewing geometry and data acquisition schedule is controlled by the pattern of its orbit.

As with any aircraft, airborne radar will be susceptible to variations in velocity and other motions of the aircraft. Thus the radar system must use sophisticated positioning equipment to compensate for these variations. Space-borne radar is not affected by motion of this type. Indeed, the geometry of their orbits is usually very

stable and their positions can be accurately calculated; however, geometric correction of imagery from space-borne platforms must take into account other factors, such as the rotation and curvature of the Earth (Sabins 1987).

10.5 Ground Penetrating Radar

Ground penetrating radar (GPR) has been used for over twenty years at chemical and nuclear waste disposal sites as a non-invasive technique for site characterization. More recently GPR is being used in the horticultural industry to map the distribution of tree roots for better orchard and landscape management. Standard GPR surveys are conducted from the surface of the ground providing geotechnical information from the surface to depths of between 2 and 15 m, depending on GPR frequency of operation and soil conductivity. Commercially available GPR systems operate over the frequency range 50 MHz to 1000 MHz. Lower frequencies provide better penetration but poor resolution, while the higher frequencies give poor penetration but good resolution.

Soil water content is a key control for plant growth and health. Recent studies have shown that careful irrigation management can have beneficial effects on many crops, including almonds, citrus, prunes, pistachios and wine grapes. In particular, moderate water stress on grapevines early in the growing season can have a positive impact on grape quality. Hubbard et al. (2005) used 900 MHz GPR ground-wave travel time data, to estimated soil water content distribution in the top 15 cm of soil in a Californian Vineyard. Comparison with conventional 'point' soil moisture measurements, obtained using time domain reflectometry (TDR) and gravimetric techniques revealed that the estimates of GPR-obtained volumetric water content estimates were accurate to within 1 % by volume (Hubbard, *et al.* 2005).

Barton *et al* (2009) have used GPR to investigate tree roots (Barton and Montagu 2004) and wood decay (Butnor, *et al.* 2009) in living trees. They found that tree roots could be successfully mapped using GPR operating at 500 MHz (Barton and Montagu 2004). When using GPR to assess wood quality, they also demonstrated that near-surface wood decay, air-filled voids and desiccated boles had unique electromagnetic signatures, which could be separated from other defects. GPR successfully estimated the percent area of air-filled cavities and was not significantly different than results from destructive sampling (Butnor, *et al.* 2009).

GPR can also be used to map soil properties around agricultural landscapes; however GPR systems are not common and can be expensive. The next chapter will explore the use of electromagnetic survey systems for mapping soils.

References

Avery, T. E. and Berlin, G. L. 1992, Fundamentals of Remote Sensing and Airphoto Interpretation, New York:: Prentice Hall.

Barton, C. V. M. and Montagu, K. D. 2004. Detection of tree roots and determination of root diameters by ground penetrating radar under optimal conditions. Tree Physiology. 24(12): 1323–1331.

Butnor, J. R., Pruyn, M. L., Shaw, D. C., Harmon, M. E., Mucciardi, A. N. and Ryan, M. G. 2009. Detecting defects in conifers with ground penetrating radar: applications and challenges. Forest Pathology. 39(5): 309-322.

Canadian Centre for Remote Sensing. 2004. Fundamentals of Remote Sensing. December, 2004. http://www.ccrs.nrcan.gc.ca/ccrs/learn/tutorials/fundam/fundam_e.html

Hubbard, S., Jinsong, C., Williams, K., Rubin, Y. and Peterson, J. 2005. Environmental and agricultural applications of GPR. Proc. Advanced Ground Penetrating Radar, 2005. IWAGPR 2005. Proceedings of the 3rd International Workshop on. 45-49.

Lakshmi, V. 2013. Remote Sensing of Soil Moisture. ISRN Soil Science. 2013: 1-33.

Navalgund, R. R., Jayaraman, V. and Roy, P. S. 2007. Remote sensing applications: An overview. Current Science. 93(12): 1747-1766.

Sabins, F. F. 1987, Remote Sensing, Principles and Interpretation, New York: W. H. Freeman and Co.

Tikhonov, V. V. 1997. Dielectric model of bound water in wet soils for microwave remote sensing. Proc. IEEE International Geoscience and Remote Sensing Symposium, 1997. 3: 1108 - 1110. Singapore International Convention and Exhibition Centre, Singapore

11 Electromagnetic Survey Techniques

Electromagnetic induction technology (EMI or EM) and other soil conductive technologies (e.g. resistivity) have been used for decades to map ground conductivities in mineral exploration (Keller and Frischknecht 1966). Early application in agriculture was for salinity management in irrigated systems (Dejong, *et al.* 1979). There is now great interest from dry-land farming enterprises, particularly the grains industry, where the management of crops at a greater spatial resolution is now achievable (Corwin and Lesch 2003).

EM sensors only measure bulk soil electrical conductivity. Other soil properties may be inferred using EM data; however calibration of EM readings against other observed data is necessary. For agricultural applications the most common variables that have been found to correlate well with EM data are: soil water content, soil clay content and soil salinity (Johnson, *et al.* 2001). Unfortunately, temperature (air and soil) effects make universal calibrations complex. Additionally, the mineral type and content of the soil will also affect the calibration. As a result, universal calibrations, whilst theoretically attractive, prove very difficult in practice (Corwin and Lesch 2003).

The lack of a workable universal calibration to relate ECa to other soil properties makes it necessary to establish these correlations for each individual survey site. This may be achieved through analysis of soil cores taken at the same time as the soil conductivity survey (Corwin and Lesch 2003). Other variables, like potential rooting depth, that are functions of water, clay and salt content may also be applicable in some places. The detection of specific elements or compounds (e.g. phosphorous) can only be accommodated to the extent of the strength of the ECa co-correlation with water, salt and clay (Kitchen, *et al.* 2005). Other variables like drainage cannot be measured directly with EM because of the complex relationship between other components of the water balance equation and time. Thus, customised calibrations must be derived after a survey to establish what can and can not be measured with EM sensors. It is very site specific (Kitchen, *et al.* 2005).

11.1 Electromagnetic Induction

The electromagnetic (EM) geophysical survey method determines electrical properties of earth materials by inducing electromagnetic currents in the ground and measuring the secondary magnetic field produced by these currents. An alternating current is generated in a wire loop or coil above the ground's surface. This alternating magnetic field generates circular eddy current loops in the soil below the coil. Each current loop generates a secondary electromagnetic field that is proportional to the current flowing in the eddy current loop. A fraction of this secondary electromagnetic field is intercepted by a second coil and the sum of these signals is amplified and formed into an output voltage, which is related to a depth-weighted bulk soil conductivity.

The receiver coil measures amplitude and phase of the secondary electromagnetic field. The amplitude and phase differ from the primary coil fields as a result of the soil properties, spacing of the coils, orientation of the coils with respect to the soil surface, and distance from the soil surface (Corwin and Lesch 2003). After compensating for the primary field, both the magnitude and relative phase (in-phase and quadrature-phase) of the secondary field are measured. The quadrature-phase component is converted to a value of apparent soil electrical conductivity (EC). This value represents an estimate of the local average soil EC. The depth of measurement is dependent on the instrument's coil spacing, orientation, operating frequency, and the actual subsurface EC variations. The EC measurement for soils with EC < 100 mS m^{-1} is given by (Corwin and Lesch 2003):

$$EC = \frac{2}{\pi \mu_o f^2 s}\left(\frac{H_s}{H_p}\right) \tag{11.1}$$

where H_p and H_s are the intensities of the primary and secondary magnetic fields (A m^{-1}), f is the frequency of the system (Hz), μ_o is the magnetic permeability of free-space (4π x 10^{-7} H m^{-1}), and s is the inter-coil spacing (m).

EM systems have been developed using a number of standard coil spacings and frequencies. Commonly used systems include EM31, EM34, EM38 and EM39.

11.1.1 EM31

The EM31 system uses a frequency of 9.8 kHz, with an inter-coil spacing of 3.66 m. The EM31 systems maps geological variations, groundwater contaminants or any subsurface feature associated with changes in the ground conductivity using an electromagnetic inductive technique that makes the measurements without electrodes or ground contact. With this inductive method, surveys can be carried out under most geological conditions including those of high surface resistivity such as sand, gravel and asphalt. The effective depth of exploration is about six meters, making it ideal for many geotechnical and groundwater contaminant surveys.

Important advantages of the EM31 over conventional resistivity methods include:

1. the speed with which surveys can be conducted.
2. the precision with which small changes in conductivity can be measured.
3. the continuous readout and data collection (logging) while traversing a survey area.

The in-phase component is especially useful for detecting shallow ore bodies and buried metal waste.

11.1.2 EM34

The EM34-3 has been particularly successful for mapping deeper groundwater contaminant plumes and for groundwater exploration. Using the same inductive method as the EM31, the EM34-3 uses 3 inter-coil spacings with separate operating frequencies (Table 11.1) to give variable depths of exploration down to 60 meters. With the 3 spacings and 2 dipole modes, vertical EC soundings can also be obtained.

Table 11.1: Inter-coil spacing and Operating Frequencies for EM34 system.

Inter-coil Spacing (m)	Operating Frequency (kHz)
10	6.4
20	1.6
40	0.4

11.1.3 EM39

The EM39 system uses a frequency of 39.2 kHz. The EM39 provides measurement of the electrical conductivity of the soil and rock surrounding a borehole or monitoring well, using the inductive electromagnetic technique. The unit employs coaxial coil geometry with an inter-coil spacing of 50 cm to provide a substantial radius of exploration into the formation while maintaining excellent vertical resolution. Measurement is unaffected by a conductive borehole fluid or the presence of plastic casing. The instrument operates to a depth of 500 metres.

11.1.4 EM38

The EM38 system uses a frequency of 14.6 kHz, with an inter-coil spacing of 1.0 m. These systems are designed to be particularly useful for agricultural surveys measuring soil salinity. The EM38 system, shown in Figure 11.1, can cover large areas quickly.

Figure 11.1: EM38 apparatus.

In a relatively homogeneous soil profile, the EM readings from both the vertical and horizontal dipole modes are given by (Huth and Poulton 2007):

$$EC = \int_0^\infty EC(z)\phi_v(z)\cdot\partial z \tag{11.2}$$

$$EC = \int_0^\infty EC(z)\phi_H(z)\cdot\partial z \tag{11.3}$$

where z is the ratio of depth into the soil to inter-coil spacing, EC(z) is the electrical conductivity at depth z and:

$$\phi_v(z) = 4z\left(4z^2+1\right)^{-3/2} \tag{11.4}$$

$$\phi_H(z) = 2-4z\left(4z^2+1\right)^{-1/2} \tag{11.5}$$

The vertical and horizontal mode responses of an EM38 instrument are shown in Figure 11.2.

Soil water is a major driver of EM38 response. As moisture content changes and water redistributes within the soil profile the EM response will change (Johnson, *et al.* 2001). There can often be a direct correlation between soil volumetric water content

and the EM data in soils with uniform profiles; however the EM38 instrument also responds to dissolved ions, charged clay particles, soil structure, and organic matter. The EM38 system is particularly well suited to being mounted on a sled for towing behind an all-terrain vehicle with a Differential GPS and automatic data logger to acquire EM data at regular intervals as the vehicle travels back and forth across the area of interest. This process captures point data (Figure 11.3) that can be interpolated using tools such as a Geographic Information System (GIS).

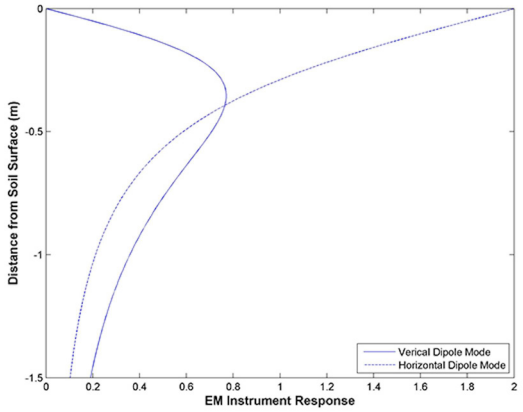

Figure 11.2: EM instrument response as a function of soil depth and dipole orientation.

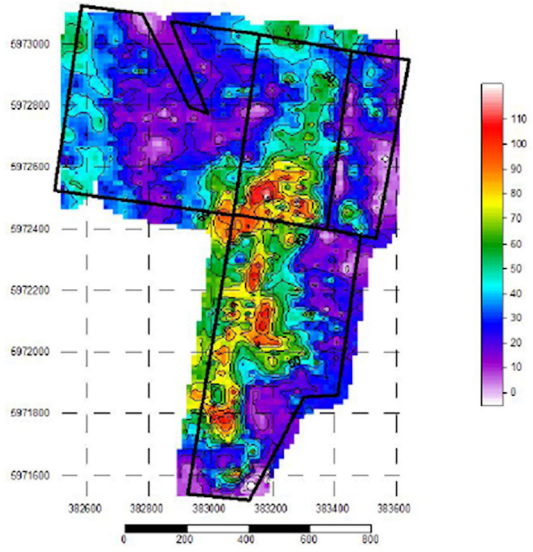

Figure 11.3: EM point data from a survey at Dookie Campus of the University of Melbourne.

Because GPS and GIS play a critical role in the capture and interpretation of EM data, it is useful to understand some basic concepts of these supporting technologies as well.

11.2 Global Positioning System

The Global Positioning System (GPS) is a worldwide radio-navigation system based on a constellation of at least 24 satellites, as shown in Figure 11.4, and their ground stations (El-Rabbany 2002). Often there have been more than 24 fully operational satellites. GPS uses these satellites as reference points to calculate positions. To ensure world-wide coverage, these satellites are deployed into six orbital planes with four satellites in each plane (El-Rabbany 2002). With this geometry, at least four satellites will be visible in the sky from anywhere in the world at any time (El-Rabbany 2002).

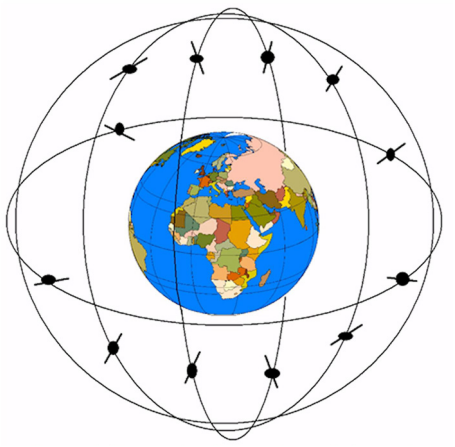

Figure 11.4: An illustration of the constellation of GPS satellites in orbit around the earth.

At the other end of the system, GPS receivers have been miniaturised to just a few integrated circuits. Currently GPS is finding its way into cars, boats, planes, construction equipment, movie making gear, farm machinery and even hand held computers.

The global positioning system (GPS) makes use of medium altitude satellites to determine position, velocity and time at the receiver. GPS receivers can access the L1 (1.575 GHz), L2 (1.227 GHz), and L5 (1.176 GHz) bands (Falade, *et al.* 2012). Antennae on GPS receivers vary in their configuration, but micro-strip patch antennae are becoming more common because of their low profile, light weight, low cost, ruggedness, and

conformability (Chang, *et al.* 1986). Patch antennae provide variable bandwidths. For example the stacked patch antenna, designed by Falade, et al. (2012), provides negative 10 dB attenuation outside its operating bandwidths for GPS L1, L2, and L5 frequency bands are 1.160–1.182 (2.0%), 1.214–1.232 (1.5%), and 1.568–1.598 GHz (2.0%), respectively.

11.2.1 Principles of GPS Operation

GPS works by following five logical steps:

1. The basis of GPS is "triangulation" from satellites.
2. To "triangulate," a GPS receiver measures distance using the travel time of radio signals.
3. To measure travel time, GPS needs very accurate timing which it achieves with some tricks.
4. Along with distance, the exactly location of the satellites in space must be known. High orbits and careful monitoring are the secret.
5. Finally corrections for any delays the signal experiences as it travels through the atmosphere must be made.

11.2.2 Step 1: Triangulating from Satellites

The idea behind GPS is to use satellites in space as reference points for locations on earth. GPS satellites generate two signals, one at 1,575.42 MHz and the other at 1,227.60 MHz (El-Rabbany 2002). Calculating distances from three satellites using these signals results in a series of intersecting spheres, whose radii are equal to the distances from the satellites. The calculations narrow the final position down to two points, one of which is so obviously wrong that it can be ignored.

11.2.3 Step 2: Measuring distance from a satellite

Distances from the satellites are calculated using accurate timing and by knowing how fast the radio signal travels between the satellite and the receiver. To help clarify this a little, if a car travels along a highway at exactly 100 km/h for 2.5 hours, it is clear that the car has travelled 250 km in that time. In the case of GPS the signal velocity is the speed of light which is roughly 300,000 km/s. By determining how long it has been since the signal left the satellite determining the distance between the satellite and the receiver becomes a relatively simple calculation.

The problem is measuring the travel time. If a satellite were right overhead the time taken for the signal to travel in intervening 20,200 km between the satellite and

the receiver (El-Rabbany 2002) would be approximately 0.07 seconds. So a very precise clock is needed. Assuming precise clocks are available the process of measuring travel time is done by comparing the phase shift due to travel time between the signals sent from the satellite and an equivalent signal at the receiver.

To make sure that the receiver does not accidentally lock onto some other satellite transmitter and allow information theory to amplify the signals, the GPS satellites generate a signal, which is so complex that it almost looks like random electrical noise. This signal is called a Pseudo Random Code (PRC). Another reason for using such a complex signal is that it makes it more difficult for a hostile force to jam the system.

11.2.4 Step 3: Getting perfect timing

Accurate timing is the key to GPS; therefore the clocks used in the system must be very good. On the satellite side, timing is provided by atomic clocks. However the receivers are not equipped with atomic clocks. The key to good positioning is that three perfect measurements can locate a point in 3-dimensional space however four imperfect measurements can do the same thing. By using an extra satellite measurement and some algebra a GPS receiver can eliminate any clock inaccuracies by comparing the four calculated locations generated from imperfectly timed signals from the four satellites. It is important to remember two important principles:

1. If perfect timing were available there would only be two possible positions as the positions calculated from all satellite combinations would coincide. Imperfect timing results in four locations, arranged in closely located pairs.
2. After discarding two positions because they are so obviously wrong the difference between the remaining two positions must be due to clock timing error.

Since any clock error will affect all the measurements simultaneously, the receiver calculates a single correction factor that can be subtracted from all its timing measurements to cause them to intersect at a single point. This correction brings the receiver's clock back into synchronization with universal time. Thus it is possible to produce atomic clock accuracy in a hand held device. This particular attribute of GPS technology has some profound field applications. Being able to measure time accurately to millionths of a second in the field could revolutionize many monitoring experiments. Unfortunately space constraints do not permit a full exploration of this at the moment.

11.2.5 Step 4: Knowing where a satellite is in space

On the ground, all GPS receivers have an almanac programmed into their computers that indicates where each satellite is, moment by moment. The basic orbits are quite stable, but just to make sure, the GPS satellites are constantly monitored by the US Department of Defence. It uses radar to confirm each satellite's altitude, position and speed. Errors due to the gravitational pulls from the moon and sun or the pressure of the solar wind on the satellites are calculated and broadcast via the GPS satellites to all receivers.

11.2.6 Step 5: Correcting errors

GPS satellite signals, like any form of light, are refracted, reflected and attenuated by the atmosphere and other objects around the receivers. Refraction slows the light and can be observed on hot days as a "shimmering" effect, which is so commonly observed when looking out over a distant landscape. Reflections cause double images of the signal sources and often result in "ghosting" of the signals similar to that observed on some television sets. Consequently, accuracy can be compromised. Another critical factor in determining accuracy is the policy called Selective Availability (SA) introduced by the US government (El-Rabbany 2002). The idea behind it is to make sure that no hostile force or terrorist group can use GPS to make accurate weapons. Fortunately all of these inaccuracies usually provide a position within 100 m of the true location and a form of GPS called "Differential GPS" can significantly reduce these problems.

11.2.7 Differential GPS

Differential GPS involves the cooperation of two receivers. One is a stationary receiver located over a precisely know point on the earth's surface while the other moves around making position measurements. The stationary receiver is the key. It ties the satellite based measurements into a known local reference (El-Rabbany 2002).

Because the reference receiver can compare its true location to the location expressed by the satellite signals, the error can be calculated. The reference receiver then transmits this error information to the roving receiver so it can correct its own measurements. The roving receivers get a complete list of errors for each available satellite and apply these corrections for the particular satellites being used. Using differential GPS can provide positions on the earth's surface to within 0.02 m of the true location.

El-Rabbany (2002) rightly points out that a real time differential GPS with a single reference station has the disadvantage of only being able to provide corrections for

a small number of roving receivers located close to the station. To overcome this, a system based on a number of widely separated reference stations connected together by land lines or communication satellites has been developed. To reduce the cost of these systems, GPS correctional data is sometimes broadcast as a sub-carrier on the normal broadcasting frequency of commercial FM radio stations (El-Rabbany 2002).

11.3 Geographic Information Systems

An information system is a computer program that manages data. A Geographic Information System (GIS), then, is a type of information system that deals specifically with geographic or spatial data.

By convention, most GIS systems express Latitude and Longitude as decimal degrees. This implies that latitudes which are south of the equator are expressed as negative numbers. Similarly, longitudes which are west of Greenwich are expressed as negative numbers. Latitudes and longitudes are usually expressed as a single number in GIS software coordinates rather than as degrees, minutes and seconds. Conversion to a single number from field notes and GPS receivers may be necessary before entering data into a GIS.

Like other information systems, a GIS is a data base and should be treated as such. The distinguishing feature of a GIS is its ability to interpret and display geographic information in a user-friendly form. The geo-location of objects can be expressed as latitude and longitude coordinates, but in most cases more complex grid systems are used.

GIS has a wide range of capabilities, but it also has some limitations. Contrary to popular belief, GIS is not simply a map-making tool. While the most common product of a GIS is often presented in map form, the real power of GIS lies in its ability to *analyse*. A GIS manages data. Knowing how to extract that data and apply it in a meaningful way is the key to GIS analysis.

11.3.1 Integration

One of the most powerful and fundamental tools of GIS is *integrating* the data (Longley, *et al.* 2005) in new ways. One example is overlaying different data sets.

GIS can integrate data mathematically by performing operations on certain attributes of the data. For example, streams could be categorised by comparing the population near the stream to its water quality. Poor quality streams with a large population nearby should probably receive more attention than others. This simple example could be performed with a set of mathematical operations.

However, visual integration, rather than mathematical, is sometimes more subtle and effective. For instance, Figure 11.5 shows a satellite image of some farming land,

overlaid with contour data. It becomes evident that the lower land has been cleared for agricultural purposes while the hilly areas are still forested. Although this is a rather trivial example, techniques such as this provide quick and usable information to decision makers.

The power to integrate data is one of the cornerstones of GIS use. It enables GIS to take the data to a new level of complexity and meaning.

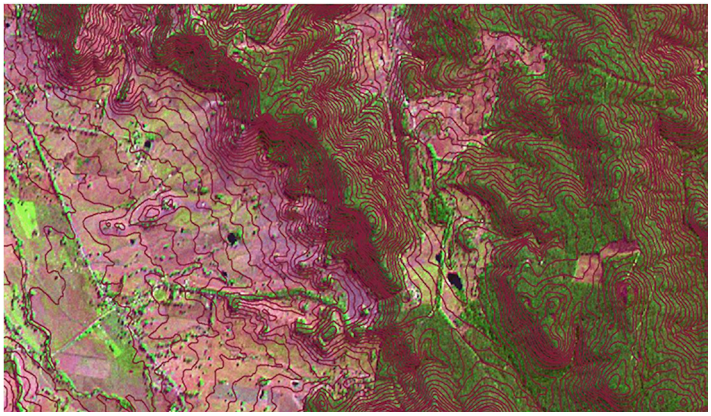

Figure 11.5: Satellite image overlaid with contour data.

11.3.2 Limitations

Despite these powerful applications, GIS does have some limitations. GIS software companies are focusing on these limitations, because if they can be overcome, GIS will enter a new era that increases its power many fold.

For instance, it is currently impossible to account for temporal changes in GIS. Although it is obvious that a dataset such as the weather and climate may change over time, existing GIS technology is not able to incorporate those changes for analysis purposes. Although there are ways to "fake it", real time analysis is still in the developmental phase. Temporal analysis could be used to track urban growth, monitor changes in water quality over time, and many other powerful applications.

Another priority in the GIS field is the support of three dimensional analyses in GIS. Three-dimensional GIS would allow analysts to see how vertical layers interact with each other. This could include layers of air, soil, rock, or water. As with temporal analysis, some programs are able to simulate a "pseudo-3-D" mode, but no real 3-D applications are available. This would have tremendous applications for geology, air and weather, which, in turn, would affect groundwater and air pollution control, to name just a few.

References

Chang, E., Long, S. A. and Richards, W. F. 1986. An Experimental Investigation of Electrically Thick Rectangular Microstrip Antennas. *IEEE Transactions on Antennas and Propogation*. AP-34(6): 767-772.

Corwin, D. L. and Lesch, S. M. 2003. Application of Soil Electrical Conductivity to Precision Agriculture: Theory, Principles, and Guidelines. *Agronomy Journal*. 95(3): 455–471.

Dejong, E., Ballantyne, A. K., Cameron, D. R. and Read, D. W. L. 1979. MEASUREMENT OF APPARENT ELECTRICAL-CONDUCTIVITY OF SOILS BY AN ELECTROMAGNETIC INDUCTION PROBE TO AID SALINITY SURVEYS. *Soil Science Society of America Journal*. 43(4): 810-812.

El-Rabbany, A. 2002, *Introduction to GPS: The Global Positioning System*, Boston: Artech House.

Falade, O. P., Rehman, M. U., Gao, Y., Chen, X. and Parini, C. G. 2012. Single Feed Stacked Patch Circular Polarized Antenna for Triple Band GPS Receivers. *IEEE Transactions on Antennas & Propagation*. 60(10): 4479-4484.

Huth, N. I. and Poulton, P. L. 2007. An electromagnetic induction method for monitoring variation in soil moisture in agroforestry systems. *Soil Research*. 45(1): 63-72.

Johnson, C. K., Doran, J. W., Duke, H. R., Wienhold, B. J., Eskridge, K. M. and Shanahan, J. F. 2001. Field-scale electrical conductivity mapping for delineating soil condition. *Soil Science Society of America Journal*. 65(6): 1829-1837.

Keller, G. V. and Frischknecht, F. C. 1966, *Electrical methods in geophysical prospecting*, New York: Pergamon Press.

Kitchen, N. R., Sudduth, K. A., Myers, D. B., Massey, R. E. and et al. 2005. Development of a conservation-oriented precision agriculture system: Crop production assessment and plan implementation. *Journal of Soil and Water Conservation*. 60(6): 421-430.

Longley, P. A., Goodchild, M. F., Maguire, D. J. and Rhind, D. W. 2005, *Geographical Information Systems and Science*, John Wiley & Sons.

Section 3: **Dielectric Heating**

12 Section Introduction

Before World War II, there is little evidence of work on radio frequency or microwave heating; however Kassner (1937b) mentions industrial applications of microwave energy in two of his patents on spark-gap microwave generators (Kassner 1937a, b, 1938). Unfortunately early studies in radio frequency heating concluded that microwave heating of food stuffs would be most unlikely because the calculated electric field strength required to heat biological materials would approach the breakdown voltage of air (Shaw and Galvin 1949).

A fortuitous discovery by Spencer that microwave energy could heat food (Murray 1958) lead to a series of patents (Spencer 1947, 1949, 1952) and the development of microwave cooking equipment. Radiofrequencies and microwaves interact with all organic materials. As was discussed in the previous section, the strength of this interaction depends on the dielectric properties of the materials. These dielectric properties are strongly influenced by the amount of water in the material. Absorption of radiofrequency or microwave energy by these dialectic materials generates heat in the material.

Microwave magnetic field heating can provide more superior results than electric field heating for materials that include magnetic dielectrics and metal powders (Zhiwei, *et al.* 2012). Several researchers have studied the behaviour of microwave magnetic field heating; however most agricultural and forestry materials are non-magnetic; therefore dielectric heating, which involves interaction between the electromagnetic electric field and the material is the most common mechanism for electromagnetic heating. This interaction is referred to as "dielectric heating".

The major advantages of dielectric heating are its short start-up, precise control and volumetric heating (Ayappa, *et al.* 1991); however dielectric heating suffers from: uneven temperature distributions (Van Remmen, *et al.* 1996, Brodie 2008); unstable temperatures (Vriezinga 1996, 1998, 1999, Vriezinga, *et al.* 2002); and rapid moisture movement (Brodie 2007).

In industry, dielectric heating is used for drying (Ayappa, *et al.* 1991, Zielonka and Dolowy 1998, Antti and Perre 1999, Hasna, *et al.* 2000), oil extraction from tar sands, cross-linking of polymers, metal casting (Ayappa, *et al.* 1991), medical applications (Bond, *et al.* 2003), pest control (Nelson 1972), enhancing seed germination (Nelson and Stetson 1985), and solvent free chemistry (Arrieta, *et al.* 2007). Dielectric heating has been applied to various agricultural and forestry problems and products since the 1960's (Nelson 2003). Studies have been undertaken to use microwave energy: to improve crop handling, storage and preservation; to provide pest and weed control for agricultural production, for food preservation and quarantine purposes; and for preconditioning of products for better quality and more energy efficient processing. This section is concerned with dielectric heating applications in the agricultural and forestry industries for purposes and consists of a review, update, and discussion

of some potential applications that may be of interest to the microwave power and agricultural industries.

References

Antti, A. L. and Perre, P. 1999. A microwave applicator for on line wood drying: Temperature and moisture distribution in wood. *Wood Science and Technology*. 33(2): 123-138.

Arrieta, A., Otaegui, D., Zubia, A., Cossio, F. P., Diaz-Ortiz, A., delaHoz, A., Herrero, M. A., Prieto, P., Foces-Foces, C., Pizarro, J. L. and Arriortua, M. I. 2007. Solvent-Free Thermal and Microwave-Assisted [3 + 2] Cycloadditions between Stabilized Azomethine Ylides and Nitrostyrenes. An Experimental and Theoretical Study. *Journal of Organic Chemistry*. 72(12): 4313-4322.

Ayappa, K. G., Davis, H. T., Crapiste, G., Davis, E. J. and Gordon, J. 1991. Microwave heating: An evaluation of power formulations. *Chemical Engineering Science*. 46(4): 1005-1016.

Bond, E. J., Li, X., Hagness, S. C. and Van Veen, B. D. 2003. Microwave imaging via space-time beamforming for early detection of breast cancer. *IEEE Transaction on Antennas and Propagation*. 51(8): 1690-1705.

Brodie, G. 2007. Simultaneous heat and moisture diffusion during microwave heating of moist wood. *Applied Engineering in Agriculture*. 23(2): 179-187.

Brodie, G. 2008. The influence of load geometry on temperature distribution during microwave heating. *Transactions of the American Society of Agricultural and Biological Engineers*. 51(4): 1401-1413.

Hasna, A., Taube, A. and Siores, E. 2000. Moisture Monitoring of Corrugated Board During Microwave Processing. *Journal of Electromagnetic Waves and Applications*. 14(11): 1563.

Kassner, E. E. W. 1937a. *Apparatus for the generation of short electromagnetic waves*. Patent No. 2094602

Kassner, E. E. W. 1937b. *Process for altering the energy content of dipolar substances*. Patent No. 2089966

Kassner, E. E. W. 1938. *Apparatus for generating and applying ultrashort electromagnetic waves*. Patent No. 2109843

Murray, D. 1958. Percy Spencer and his itch to know. *Reader's Digest*. August:

Nelson, S. O. 1972. Insect-control possibilities of electromagnetic energy. *Cereal Science Today*. 17(12): 377-387.

Nelson, S. O. 2003 Microwave and radio-frequency power applications in agriculture. In *Third World Congress on Microwave and Radio Frequency Applications*, 331-340. Folz, D. C., et al. eds. The American Ceramic Society: Westerville, OH.

Nelson, S. O. and Stetson, L. E. 1985. Germination responses of selected plant species to RF electrical seed treatment. *Transactions of the ASAE*. 28(6): 2051-2058.

Shaw, T. M. and Galvin, J. A. 1949. High-Frequency-Heating Characteristics of Vegetable Tissues Determined from Electrical-Conductivity Measurements. *Proceedings of the IRE*. 37(1): 83-86.

Spencer, P. L. 1947. *Magnetron anode structure*. Patent No. 2417789

Spencer, P. L. 1949. *Prepared food article and method of preparing*. Patent No. 2480679

Spencer, P. L. 1952. *Electronic cooking*. Patent No. 2582174

Van Remmen, H. H. J., Ponne, C. T., Nijhuis, H. H., Bartels, P. V. and Herkhof, P. J. A. M. 1996. Microwave Heating Distribution in Slabs, Spheres and Cylinders with Relation to Food Processing. *Journal of Food Science*. 61(6): 1105-1113.

Vriezinga, C. A. 1996. Thermal runaway and bistability in microwave heated isothermal slabs. *Journal of Applied Physics*. 79(3): 1779 -1783.

Vriezinga, C. A. 1998. Thermal runaway in microwave heated isothermal slabs, cylinders, and spheres. *Journal of Applied Physics*. 83(1): 438 -442.

Vriezinga, C. A. 1999. Thermal profiles and thermal runaway in microwave heated slabs. *Journal of Applied Physics*. 85(7): 3774 -3779.

Vriezinga, C. A., Sanchez-Pedreno, S. and Grasman, J. 2002. Thermal runaway in microwave heating: a mathematical analysis. *Applied Mathematical Modelling*. 26(11): 1029 -1038.

Zhiwei, P., Jiann-Yang, H. and Matthew, A. 2012. Magnetic Loss in Microwave Heating. *Applied Physics Express*. 5(2): 027304.

Zielonka, P. and Dolowy, K. 1998. Microwave Drying of Spruce: Moisture Content, Temperature and Heat Energy Distribution. *Forest Products Journal*. 48(6): 77-80.

13 Dielectric Heating

Heat transfer analysis predicts the energy movement that occurs when there is a spatial temperature gradient. Thermodynamics predicts that energy, in the form of heat, moves along the temperature gradient until all spatial coordinates reach thermal equilibrium. By definition, equilibrium is reached when the temperature gradient disappears from the system.

Heat is transferred by conduction, convection and radiation. Conduction is the transfer of heat between material interfaces. Convection is the transfer of heat between an object and its environment due to fluid motion, i.e. a gas or liquid interface with a solid. Radiation is the transfer of heat between bodies through the emission and absorption of electromagnetic energy, without the need for a fluid interface (i.e. a vacuum).

In most cases, conduction accounts for internal heat transfer within an object, while convection and radiation can be regarded as surface phenomena at the interface between solids and fluids (or empty space). This section will explore some of the key features of conductive, convective and rediative heat transfer.

13.1 Conductive Heat Transfer

Conductive heat transfer (q) per unit area (A) is controlled by the temperature gradient $\left(\frac{\partial T}{\partial x}\right)$ through the thickness of the material and can be defined as (Holman 1997):

$$\frac{q}{A} = k\frac{\partial T}{\partial x} \tag{13.1}$$

Experience shows that some materials can maintain a considerable temperature gradient for much longer than others. For example, the humble thermos can keep water hot or cold for many hours. The thermos vacuum flask was designed to reduce conductive and convective heat transfer by use of a vacuum space between inner and outer shells, and minimal conductive interfaces at the neck.

Thermal conduction is manifested by the propagation of phonons (quantized mechanical vibrations) through the material (Ding and Zhang 2000). Therefore different materials possess different thermal conductivity (k) properties, depending on their micro-structure and mechanical properties. Table 4 shows the thermal conductivity of several common materials; however it should be noted that the thermal properties of most materials are temperature dependent (Torabi and Aziz 2012). Several models have been proposed to account for the temperature dependence of the thermal conductivity of materials. The simplest meaningful model is to assume some linear relationship between temperature and thermal conductivity (Torabi and Aziz 2012):

$$k = k_o\left[1+\lambda\left(T-T_0\right)\right] \tag{13.2}$$

Where λ is the slope of the linear relationship and k_0 is the thermal conductivity of the material measured at a temperature T_0. The value of λ also depends on the material properties; for example the value of λ for still air is approximately 8.0×10^{-8} °C^{-1} (see data for thermal conductivity of air in Table 13.1).

Table 13.1: Thermal conductivity of various materials at room temperature (Studman 1990).

Material	Thermal conductivity (W/m · °C)
Gypsum plasterboard	0.22
Hardboard	0.14
Particle board (medium density)	0.11
Calcium silicate (insulation)	0.05
Foamed vinyl	0.036
Glass fibre blanket	0.04
Glass fibre building bats	0.05
Polystyrene foam	0.025
Cement plaster	0.8
Structural concrete	1.6
Foamed concrete	0.3
Timber (softwood)	0.13
Timber (hardwood)	0.39
Still air (@ 10°C)	0.025
Still air (@ 50°C)	0.028
Still air (@ 100°C)	0.032
Glass	1.05
Aluminium	230
Steel	40
Copper	380

Heat is not the only quantity that moves through a material. Thermal phonons provide energy to volatile components of organic material, including water. This can result in vapour transport through the material as well.

13.2 Convective Heating

In a conventional heating system such as an oven or furnace, heat flows from a hot fluid into the surface of the heated object. The heat flow from a fluid with a temperature of T_∞ to a solid with a temperature of T_s is expressed as:

$$\frac{q}{A} = h\left(T_s - T_\infty\right) \tag{13.3}$$

where h is the convective heat flow coefficient of the material's surface (Holman 1997). When studying thermodynamic processes, temperatures are usually expressed in absolute (Kelvin) values.

This convective heat flow coefficient depends on a number of other parameters and conditions (Welty, *et al.* 2007). For example, the convective heat flow coefficient for a vertical surface where natural convection achieves turbulent flow conditions over the surface is given by (Welty, *et al.* 2007):

$$h = \frac{k}{L}\left\{0.825 + \frac{0.387 Ra_L^{1/6}}{\left[1+\left(\frac{0.492}{\mathrm{Pr}}\right)^{9/16}\right]^{8/27}}\right\}^2 \tag{13.4}$$

The Rayleigh number (Ra_L) in this equation is also based on a complex relationship between temperature and the physical properties of the fluid. It is given by (Welty, *et al.* 2007):

$$Ra_L = \frac{g\beta}{\nu\alpha}\left(T_s - T_\infty\right)L^3 \tag{13.5}$$

Where g is the acceleration due to gravity; β is the thermal expansion coefficient of the fluid; υ is the kinematic viscosity of the fluid medium; α is the thermal diffusivity of the fluid medium; and L is the characteristic length of the surface.

Finally, the Prandtl number used in equation (13.4) is a relationship between the fluid's viscous and thermal diffusion rates given by (Welty, *et al.* 2007):

$$\mathrm{Pr} = \frac{\nu}{\alpha} \tag{13.6}$$

Close examination of these equations shows that the convective heat transfer coefficient is dependent on the temperature differential between the fluid and the surface of the material (see Figure 13.1). An important consequence of this temperature dependence is that heat transfer diminishes rapidly as the temperature differential between the object and the surrounding fluid reduces.

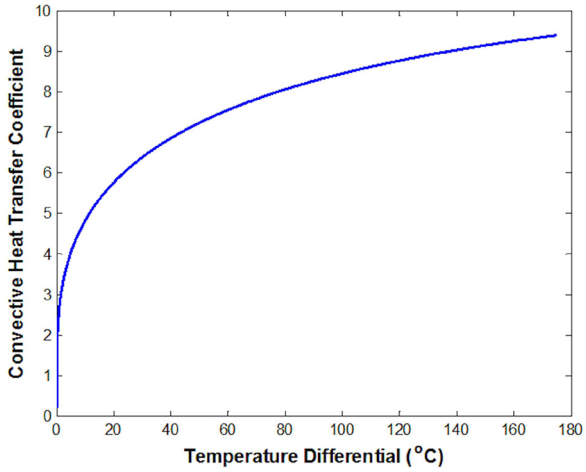

Figure 13.1: Convective heat transfer coefficient (h) for air as a function of temperature differential between an object and the air.

Convective heat transfer requires a hot environment for the heated object. Any hot object or environment will radiate energy in the form of electromagnetic radiation.

13.3 Radiative Heat Transfer

Radiative heat transfer refers to the transfer of energy by broad spectrum electromagnetic radiation from some adjacent hot object (or from a hot environment) to the heated object. Any object that is above zero degrees Kelvin will radiate energy in the form of electromagnetic photons. The German physicist, Max Planck (1858 – 1947), deduced that the radiation spectral density (ρ) given off from a hot object depended on the wavelength of interest and the temperature of the object. This spectral density can be described by:

$$\rho = \frac{2\pi hc}{\lambda^5 \left\{ e^{\frac{hc}{\lambda kT}} - 1 \right\}} \tag{13.7}$$

Where h is Planck's constant (6.6256×10^{-34} J s), c is the speed of light, λ is the electromagnetic wavelength of interest, k is Boltzmann's constant (1.38054×10^{-23} J K^{1}), and T is the temperature in Kelvin. A typical set of spectral distributions is shown for different temperatures are shown in Figure 13.2.

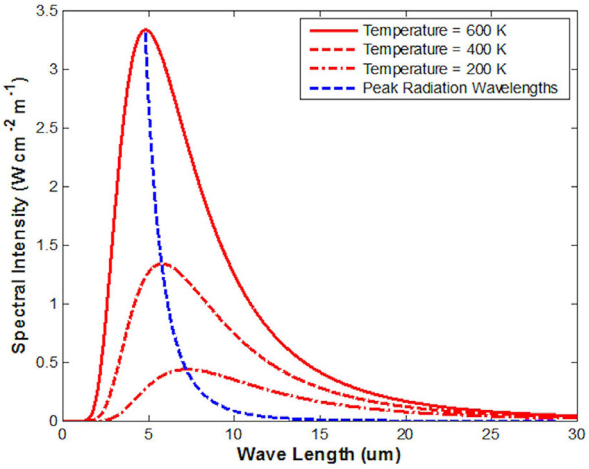

Figure 13.2: Radiative spectral density at different temperatures as a function of temperature and wavelength.

The wavelength at which peak radiation intensity occurs can be found by differentiating Planck's equation and setting the derivative equal to zero. Therefore the wavelength of peak radiation is determined by:

$$\lambda_p = \frac{hc}{5kT} \tag{13.8}$$

At room temperature, or above, the wavelength of peak radiation will be in the micrometer range (~10 μm) or smaller. The penetration depth of electromagnetic energy into materials is limited by the wavelength and the dielectric properties of the material (Vollmer 2004):

$$\delta = \frac{\lambda_p}{4\pi\sqrt{k}} \tag{13.9}$$

where δ is the penetration depth and κ is the relative dielectric constant of the material (This property will be discussed later). The penetration depth of any radiation from objects at room temperature or above will be in the nanometer range. Therefore radiative heat transfer must be regarded as a surface phenomenon where further heat transfer from the surface into the material occurs via internal conduction. The same is also true when short wavelength radiation, such as infrared, visible, ultraviolet etc., are applied to a material.

The total radiated energy can be determined by integrating Planck's equation across all wavelengths for a particular temperature. Ultimately this integration yields the Stefan-Boltzmann equation (Holman 1997):

$$q = \varepsilon \sigma A\left(T_s^4 - T_\infty^4\right) \tag{13.10}$$

Where ε is the surface emissivity of the material; σ is the Stefan-Boltzmann constant (5.6704×10^{-8} J s^{-1} m^{-2} K^{-4}); A is the surface area of the heated object; and T_∞ is the temperature of the environment around the object.

Emissivity determines the efficiency of the heat transfer at the interfacial surface of an object or fluid. The emissivity of air depends on its temperature and humidity (Herrero and Polo 2012):

$$\varepsilon = -0.8384 - 0.7086 W_a + 0.005\, T_\infty - 0.02 W_a^2 + 0.003124 W_a\, T_\infty \tag{13.11}$$

Where W_a is the relative humidity, expressed as a fraction of one. The radiative heat transfer as a function of temperature difference between an object and the air around it is shown in Figure 13.3.

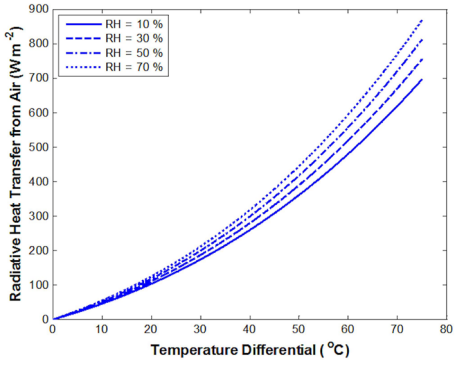

Figure 13.3: Radiative heat transfer from air as a function of temperature differential between an object and the air.

13.4 Microwave Heating

Industrial microwave heating has been used since the 1940's (Metaxas and Meredith 1983). The initial experiments with microwave heating were conducted by Dr. Percy Spencer in 1946, following a serendipitous accident while he was testing a radar magnetron (Gallawa 1998). Since then many heating, drying, thawing and medical applications (Bond, *et al.* 2003) have been developed.

Microwave frequencies occupy portions of the electromagnetic spectrum between 300 MHz to 300 GHz. The full range of microwave frequencies is subdivided into various bands, as indicated in Figure 13.4. Their application falls into two categories, depending on whether the wave is used to transmit information or energy. The first category includes terrestrial and satellite communication links, radar, radio-astronomy, microwave thermography, material permittivity measurements, and so on (Adamski and Kitlinski 2001). The second category of applications is associated with microwave heating and wireless power transmission. In the case of microwave heating, there is usually no signal modulation and the electromagnetic wave interacts directly with solid or liquid materials.

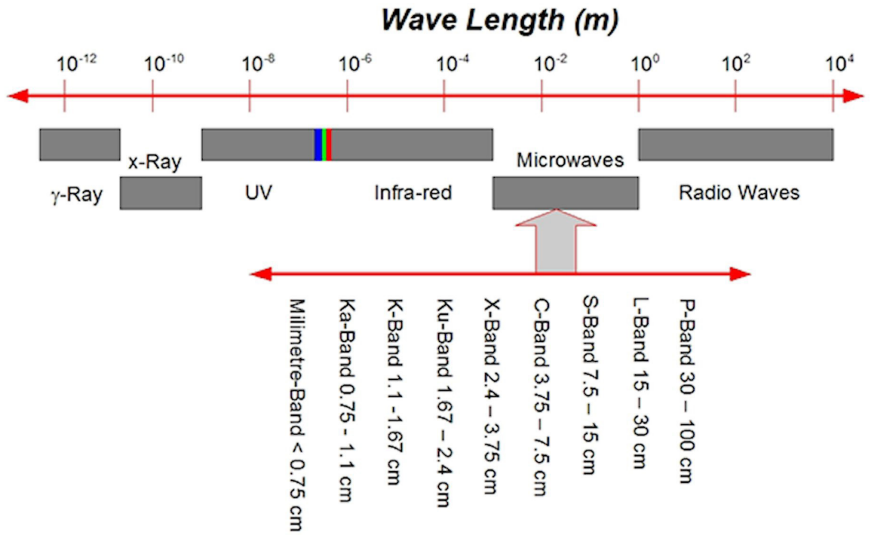

Figure 13.4: The electromagnetic spectrum, highlighting the Microwave range in particular.

Materials can be categorized as conductors, semiconductors and insulators (dielectric materials). "It has long been known that an insulating material can be heated by applying energy to it in the form of high frequency electromagnetic waves" (Metaxas and Meredith 1983).

One key benefit of microwave heating over conventional convective heating is its speed. The origin of this speed is the volumetric interactions between the microwave's electric field and the material. In contrast, convective heat transfer propagates from the surface into the material, with the final temperature profile depending on the material's thermal diffusion properties (Holman 1997) and the influence of moisture transport, which often hinders the convective heating process (Crank 1979). This was discussed in the previous section.

The factors that contribute to microwave heating in materials include their physical and chemical structure, the frequency of the microwaves (Van Remmen, *et al.* 1996), the density of the material (Torgovnikov 1993), the orientation of the electrical field relative to an anisotropic material such as wood grain (Torgovnikov 1993), reflections from the inter-facial surface of the material (Adamski and Kitlinski 2001), electric field strength (Van Remmen, *et al.* 1996), the geometry of the microwave applicator (Metaxas and Meredith 1983), the geometry, size, electrical and thermal properties of the material (Perre and Turner 1997, Zhao, *et al.* 1998, Brodie 2008a), the exposure time, and the coupling of heat and moisture transfer during microwave processing (Brodie 2007b).

13.5 Microwave Frequency and its Influence over Microwave Heating

Because microwaves are also used in the communication, navigation and defence industries, their use in thermal heating is restricted to a small subset of the available frequency bands. In Australia, the commonly used frequencies include 434 ± 1 MHz, 922 ± 4 MHz, 2450 ± 50 MHz and 5800 ± 75 MHz (Commonwealth Department of Transport and Communications 1991, International Telecommunication Union 2004). These frequencies have been set aside for Industrial, Scientific and Medical (ISM) applications. All these frequencies interact to some degree with moist materials. The most common systems for industrial microwave heating use 922 MHz or 2450 MHz. Domestic microwave ovens operate at 2450 MHz, while most large industrial systems operate at 922 MHz. These choices of frequency are based on the dimensions of the oven cavities used to apply the microwave energy to the heated load; higher frequencies have shorter wavelengths and therefore can afford to use oven cavities with smaller dimensions. Therefore domestic microwave ovens use the higher frequency so that their dimensions are acceptable to the public for heating small loads such as individual meals.

The power dissipated per unit volume in a nonmagnetic, uniform material exposed to radio frequency (RF) or microwave fields can be expressed as (Brodie 2012):

$$P = 55.63 \times 10^{-12} f \left(\tau E\right)^2 \kappa" \tag{13.12}$$

Where *f* is the frequency and k" is the dielectric loss factor of the heated material.

13.6 The Influence of Material Geometry on Microwave Heating

After accounting for the microwave field distribution inside the oven, the next most important influence over temperature distributions during microwave heating is the geometry of the work load (Van Remmen, *et al.* 1996). The governing equation for electromagnetic heating is:

$$\nabla^2 \Omega - \frac{1}{\gamma}\frac{\partial \Omega}{\partial t} + \frac{nP}{k} = 0 \tag{13.13}$$

where Ω is a combined heat and moisture term, γ is the combined diffusivity for simultaneous heat and moisture transfer, P is the volumetric heat generated by microwave fields (W m^{-3}), and k is the thermal conductivity of the composite material (W m^{-1} °C^{-1}). The volumetric heating term, P was defined in equation (13.12).

Temperature profiles in thick slabs and blocks usually result in sub-surface heating where the maximum temperature is slightly below the material surface (Van Remmen, *et al.* 1996, Zielonka and Gierlik 1999, Brodie 2008a). It has been shown (Brodie 2008a) that the one-dimensional temperature distribution in rectangular coordinates due to microwave heating is:

$$\Omega(t) = \frac{n\omega\varepsilon_o \varepsilon" \tau^2 E_o^2 \left(e^{4\gamma\beta^2 t} - 1\right)\left(\phi + \varsigma + \eta\right)}{8k\beta^2 \left[1 - 2\Gamma^2 e^{-2\beta W}\cos\left[\delta + 2\alpha W\right] + \Gamma^4 e^{-4\beta W}\right]} \tag{13.14}$$

where

$$\phi = e^{-2\beta z} + \left(\frac{h}{k} + 2\beta\right) z e^{\frac{-z^2}{4\gamma t}}$$

$$\varsigma = 2\Gamma e^{-\beta(W-2z)}\left\{\cos\left[\delta + 2\alpha z\right] + \left[\frac{h}{k}\cos(\delta + 2\alpha W) - 2\beta\sin(\delta + 2\alpha W)\right] z e^{\frac{-z^2}{4\gamma t}}\right\}$$

$$\eta = \Gamma^2 e^{-2\beta W}\left[e^{-2\beta z} + \left(\frac{h}{k} + 2\beta\right) z e^{\frac{-z^2}{4\gamma t}}\right]$$

The solution to multidimensional partial differential equations is a simple product of the single dimensional solutions (Crank 1979, Van Remmen, *et al.* 1996). For example, the temperature distribution within a rectangular block, irradiated equally on all six faces, can be found by multiplying the temperature profiles associated with three slabs of thickness equal to the length, width and height of the rectangular block. Therefore in the case of blocks, the highest temperatures usually occur in the corners of the block, just below the surface (Brodie 2008a) (Figure 13.5). This is due to the superposition of heating effects from microwave energy entering from all sides of the work load. Temperature profiles in thin slabs and small blocks usually have a temperature peak in the core of the material.

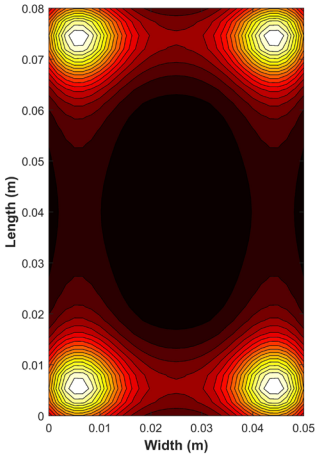

Figure 13.5: Multidimensional temperature distribution in a 50 mm by 50 mm by 80 mm rectangular block with the same thermal properties as agar gel heated for 90 s (Lightest colour represents hottest place) (Source: Brodie 2008a).

The one-dimensional radial temperature distribution in a cylinder is approximately (Brodie 2008a):

$$\Omega(t)=\frac{n\omega\varepsilon_o\kappa''\tau^2E_o^2\left(e^{4\beta^2\gamma t}-1\right)}{4k\beta^2I_o\left(2\beta r_o\right)}\left[\begin{array}{l}\dfrac{4\alpha\gamma t}{\left[J_o\left(\alpha r_o\right)I_o\left(\beta r_o\right)\right]^2}e^{\frac{-r^2}{4\gamma t}}+I_o\left(2\beta r\right)+\\ \left\{2\beta I_1\left(2\beta r_o\right)+\dfrac{h}{k}I_o\left(2\beta r_o\right)\right\}\left(r_o-r\right)e^{\frac{-\left(r_o-r\right)^2}{4\gamma t}}\end{array}\right] \tag{13.15}$$

Therefore temperature profiles in small diameter cylinders usually exhibit pronounced core heating (Ohlsson and Risman 1978, Van Remmen, *et al.* 1996, Brodie 2008a). On the other hand, heating in large cylinders exhibit subsurface heating, with the peak temperature occurring slightly below the surface (Van Remmen, *et al.* 1996, Brodie

2008a). The same is also true when the composition of the heated material is such that the microwave fields do not penetrate very far into the cylinder (Van Remmen, *et al.* 1996, Brodie 2008a) (Figure 13.6).

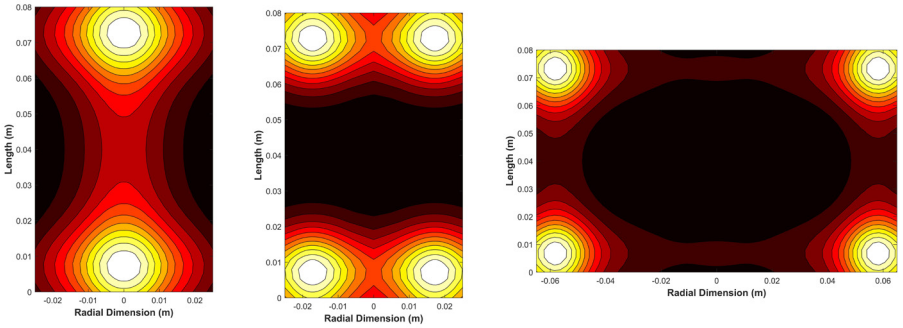

(a) (b) (c)

Figure 13.6: Predicted multidimensional temperature profiles along the longitudinal axis of 80 mm tall cylinders with the same thermal properties as agar gel heated for 90 s: (a) ro = 25 mm, k' = 76.0 and k" = 6.0 (b) ro = 25 mm, k' = 76.0 and k" = 20.0 (c) ro = 65 mm, k' = 76.0 and k" = 6.0 (Lightest colour represents hottest place) (Source: Brodie 2008a).

The temperature distribution in spherical objects is described by (Brodie 2008a):

$$\Omega(t) = \frac{n\omega\varepsilon_o\kappa''\tau^2 E_o^2\left(e^{4\beta^2\gamma t}-1\right)}{k\beta\cdot i_o(2\beta r_o)}\left[\begin{array}{l}\dfrac{\alpha\gamma t}{\beta\left[j_o(\alpha r_o)i_o(\beta r_o)\right]^2}e^{\frac{-r^2}{4\gamma t}}+\dfrac{i_o(2\beta r)}{4\beta}+\\ \left\{2\beta\cdot i_1(2\beta r_o)+\dfrac{h}{k}i_o(2\beta r_o)\right\}\dfrac{(r_o-r)}{4\beta}e^{\frac{-(r_o-r)^2}{4\gamma t}}\end{array}\right] \tag{13.16}$$

Therefore spherical objects respond in a similar way to cylindrical objects in that the temperature profiles in small diameter spheres usually exhibit pronounced core heating (Kritikos, *et al.* 1981, Van Remmen, *et al.* 1996, Brodie 2008a) while larger diameter spheres or spheres made from very absorbent materials exhibit sub-surface heating (Van Remmen, *et al.* 1996, Brodie 2008a) (Figure 13.7).

The temperature distribution also changes with heating time. Figure 13.8 shows a heating sequence for a rectangular block, while Figure 13.9 shows the heating sequence for a cylinder. It is interesting to note in these particular cases, that the temperature profiles in the block and the cylinder have a similar appearance after 400 s of heating.

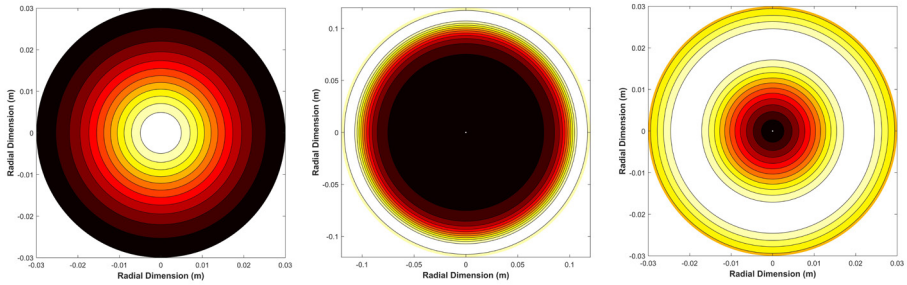

Figure 13.7: Predicted multidimensional temperature profiles in a sphere with the same thermal properties as agar gel heated for 90 s: (a) ro = 30 mm, k' = 76.0 and k" = 6.0 (b) ro = 120 mm, k' = 76.0 and k" = 6.0 (c) ro = 30 mm, k ' = 76.0 and k" = 20.0 (Lightest colour inside the sphere represents hottest place) (Source: Brodie 2008a).

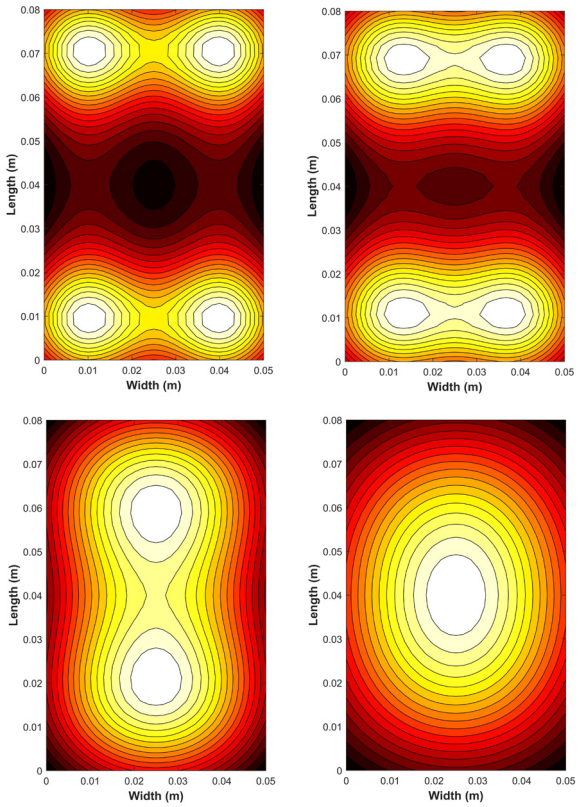

Figure 13.8: Heating sequence for a 50 mm by 50 mm by 80 mm rectangular block of agar gel heated for (from left to right) 90 s, 190 s, 400 s and 800 s (Source: Brodie 2008a).

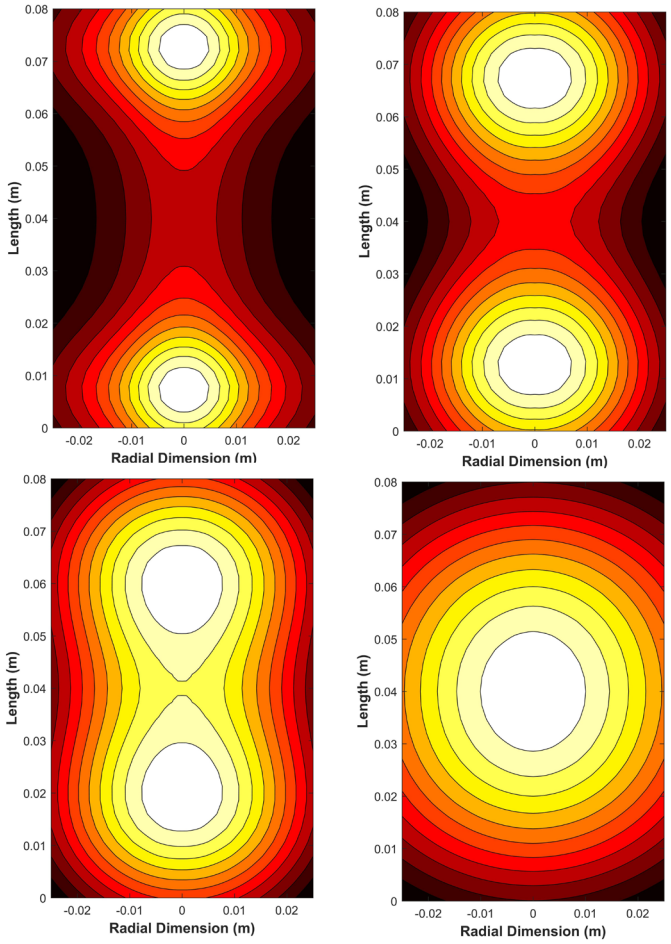

Figure 13.9: Heating sequence for a 80 mm long by 50 mm diameter cylinder of agar gel, heated for (from left to right) 90 s, 190 s, 400 s and 800 s (Source: Brodie 2008a).

In summary, microwave heating is a very complex problem. The final temperature distribution and the location of internal "hot spots" depends on the electric field distribution within the microwave cavity, the geometry of the heated product, the extent of moisture movement through the material during microwave heating and the heating time.

So far it has been assumed that the dielectric and thermal properties of the material are constant during the heating process. This is not the case in practice.

13.7 Comparative Efficiency of Convective and Microwave Heating

Conventional heating systems depend on the temperature differential between the heated object and its surroundings. As this temperature differential reduces the heat transfer reduces also. Thermal conductivity of the material and the complex interactions between heat transfer and moisture transport also influence the thermal transfer in the system. The coupling between heat and moisture transport in a conventional system usually results in slower heating because the water vapour is moving out of the material opposing the transfer of heat into the material. This creates an evaporation surface inside the material (Shaeri, *et al.* 2013) that effectively cools the material until the water source is exhausted.

Microwave heating is a volumetric phenomenon. Although the interactions are complex, the combination of geometry, material properties, microwave field intensities and changes in these parameters induces very rapid heating. There is also a coupling between microwave heating and moisture transport that enhances both heat and moisture transport (Brodie 2007b), rather than diminishing each other as happens in conventional heating systems. Consequently, microwave heating is many times faster than convective heating.

As an easy to understand example of the differences in efficiency between microwave heating and other systems, Table 13.2 compares the energy required for cooking a casserole using different heating systems.

Table 13.2: Comparative energy requirements for cooking a casserole (Source: Jennifer Thorne, et al. 2012).

Appliance	Temperature	Time	Energy
Electric Oven	350	1 hour	2.0 kWh
Electric Convection Oven	325	45 minutes	1.39 kWh
Gas Oven	350	1 hour	3.3 kWh
Electric Frying Pan	420	1 hour	0.9 kWh
Toaster Oven	425	50 minutes	0.95 kWh
Electric Crockpot	200	7 hours	0.7 kWh
Domestic Microwave Oven	“High”	15 minutes	0.36 kWh

It should be noted that, because of the simple, mass-produced, half-wave rectifier used to power the magnetrons in domestic microwave ovens (Gallawa 1998), the electrical power to microwave power efficiency is less than 50 %; however properly designed industrial microwave systems with full rectifying switched mode power supplies can achieve more than 90 % efficiency in electrical to microwave power conversion. Therefore the energy usage, illustrated in Table 5, would be greatly improved and the heating time greatly reduced if an equivalent powered industrial microwave system were used instead of a domestic microwave oven.

13.8 Thermal Runaway

The advantage of radio frequency and microwave heating is its volumetric interaction with the heated material as the electromagnetic energy is absorbed by the material and manifested as heat (Metaxas and Meredith 1983). This means that the heating behaviour is not restricted by the thermal diffusivity of the heated material. The temperature response of the material, other than on the surface, is limited by the coefficient of simultaneous heat and moisture movement g, defined in Chapter 14.
If for any reason the local diffusion rate is much less than the microwave power dissipation rate, the local temperature will increase rapidly. With increasing temperature, the properties of the material change. If such changes lead to the acceleration of microwave power dissipation at this local point, the temperature will increase more rapidly. The result of such a positive feedback is the formation of a hot spot, which is a local thermal runaway (Wu 2002).

Thermal runaway, which manifests itself as a sudden temperature rise due to small increases in the applied microwave power, is very widely documented (Vriezinga 1998, Zielonka and Gierlik 1999). It has also been reported after some time of steady heating at fixed power levels and is usually attributed to temperature dependent dielectric and thermal properties of the material (Vriezinga 1998, Zielonka and Gierlik 1999).

Kriegsmann (1992) developed a one-dimensional model for the heating of a ceramic slab by microwaves. He found the important result that steady-state temperature as a function of the input microwave power gave an S-shaped response curve. In addressing the same phenomenon of thermal runaway, Vriezinga (1998) also used analytical solutions to the differential equations that describe heat diffusion (independent of moisture movement) in isothermal media to obtain similar S-shaped temperature versus microwave power curves.

Hill and Marchant (1996) also developed S-shaped temperature versus microwave power curves during their investigation of microwave heating. They describe these curves as a multi-valued function of microwave power in which the upper and lower arms are stable, but the central arm is unstable. As the power increases from zero, the temperature stays on the lower arm until a critical power level is reached; then an

infinitesimal increase in power will cause the temperature to jump to the upper arm. If the power is decreased the temperature will remain on the upper arm until a second critical power value is reached; then the temperature abruptly falls to the lower arm (Hill and Marchant 1996). Liu *et al.* (2003) reiterate this interpretation of these curves, attributing the sudden jump in temperature to thermal runaway.

Further insight into microwave heating in materials can be provided by a previously derived mathematical model for heating in cylindrical objects (Brodie 2008a). This equation was used in an iterative calculation of the potential temperature in the centre of a cylindrical material. Data from the literature (Ulaby and El-Rayes 1987) and earlier studies (Harris, *et al.* 2011) were used to approximate the drying behaviour and dielectric properties of plant material during microwave treatment. Each of the iterations represented 0.5 second of microwave heating. Following each of these iterations a new moisture content and dielectric permittivity was calculated. These new parameter values were used in the next iteration of the heating calculation.

$$\Omega(t)=\frac{n\omega\varepsilon_o\kappa''\tau^2E_h^2\left(e^{4\beta^2\gamma t}-1\right)}{4k\beta^2I_o\left(2\beta r_o\right)}\left[\frac{4\alpha\gamma t}{\left[J_o\left(\alpha r_o\right)I_o\left(\beta r_o\right)\right]^2}e^{\frac{-r^2}{4\gamma t}}+\right.$$
$$\left.I_o\left(2\beta r\right)+\left\{2\beta I_1\left(2\beta r_o\right)+\frac{h}{k}I_o\left(2\beta r_o\right)\right\}\left(r_o-r\right)e^{\frac{-\left(r_o-r\right)^2}{4\gamma t}}\right] \tag{13.17}$$

The iterative modelling of cylindrical heating, using equation (13.17), revealed that "thermal runaway", manifested as a sudden jump in the calculated temperature, may be occurring in larger diameter cylinders (Figure 13.10 a). Microwave field intensity seems to be an important trigger for this phenomenon (Figure 13.10 b).

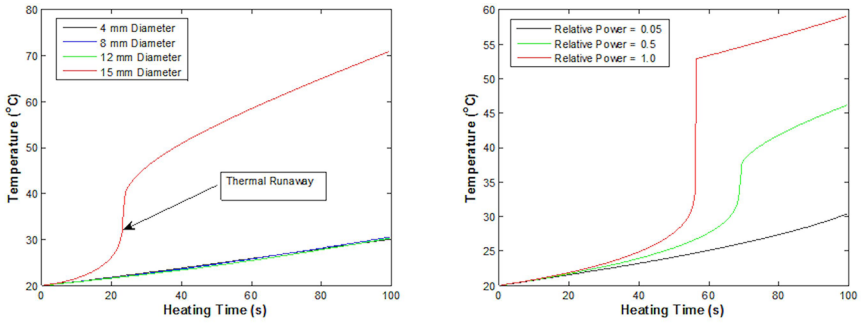

Figure 13.10: Temperature response to microwave treatment at a frequency of 2.45 GHz, in the centre of a cylindrical material (a) as a function of diameter using constant microwave power density and (b) as a function of variable microwave power density in a 15 mm cylinder, calculated using equation (13.28) and assuming moisture content loss during treatment (MC = 0.87 to 0.10).

13.9 Examples of Using Thermal Runaway to Great Advantage

Jerby et al. (Jerby, *et al.* 2002, Jerby 2005) have developed a microwave drill that can drill holes through glass and ceramics by super-heating a very small section of the material using microwave induced thermal runaway at relatively low power levels. The system works by creating very intense microwave fields immediately in front of a needle like probe that extends into the material as the drilling process proceeds.

Vinden and Torgovnikov (2000) have also shown that the controlled application of intense microwave fields to green timber can boil free water inside the wood cells within a few seconds (Vinden and Torgovnikov 2000, XiMing, *et al.* 2002) causing the cells to rupture. Lawrence (2006) has demonstrated that this process can reduce the density of *Eucalyptus obliqua* wood by up to 12 %, as the wood cells are ruptured and the cross section of the wood is expanded due to internal steam explosions. This has been confirmed by other experimental work (Brodie 2007a). This reduction in wood density leads to rapid drying in conventional systems with little loss in wood strength or quality. Wood cell rupture has been linked to thermal runaway (Brodie 2007a, Brodie 2008b) in the timber.

Although there are occasions when thermal runaway is beneficial, in most cases it causes catastrophic damage to the material being heated and must be avoided. The next chapter on crop drying should illustrate this.

13.10 Conclusion

It is evident from this review that microwave heating is different and in many ways better than conventional heating; however being able to predict the outcomes of microwave heating in large scale industrial processing systems depends on knowing the dielectric properties and geometry of the materials to be processed.

Nomenclature

av	Air space fraction in the material
C	Thermal capacity of the composite material (J kg^{-1} °C^{-1})
c	The speed on light (m s^{-1})
Da	Vapor diffusion coefficient of water vapour in air (m^2 s^{-1})
E	Electric field associated with the microwave
ε*	The complex electrical permittivity of the space through which the waves are propagating
E_o	Magnitude of the electric field external to the work load (V m^{-1})
f	The complex wave number of the form $f = \alpha + j\beta$;

γ	Combined diffusivity for simultaneous heat and moisture transfer
H	Convective heat transfer at the surface of a heated object (W m^{-1} K^{1})
H	Magnetic field associated with the microwave
$i_o(x)$	Modified Spherical Bessel Function of the first kind of order zero
$I_o(z)$	Modified Bessel function of the first kind of order zero
J	Complex operator √-1
J_c	The current flux due to internal conduction
$j_o(x)$	Spherical Bessel Function of the first kind of order zero
$J_o(z)$	Bessel function of the first kind of order zero
J_s	Current sources that may be embedded within the region of interest
k	Thermal conductivity of the composite material (W m^{-1} °C^{-1})
κ'	The relative dielectric constant of the material
κ"	The dielectric loss factor of the material
$K_o(z)$	Modified Bessel function of the second kind of order zero
L	Latent heat of vaporization of water (J kg^{-1})
μ	The magnetic permeability of the space through which the waves are propagating
Ms	Moisture content of the solid material (kg kg^{-1})
Mv	Moisture vapor concentration in the pores of the material (kg m^{-3})
q	Volumetric heat generated by microwave fields (W m^{-3})
ρ_c	Charge density within the space through which the waves are propagating
r_o	The external radius of the cylinder (m)
s	The Laplace transformation argument
σ	A constant of association relating moisture vapour concentration to moisture content in a solid
σ_c	Electrical conductivity of the material (S m^{-1})
t	Heating time (s)
τ	Transmission coefficient for incoming microwave
T	Temperature (°C)
W	Thicknesses of the slab (m)
$Y_o(z)$	Bessel function of the second kind of order zero
Γ	Internal reflection coefficient
θ_A	Phase angle associated with forward propagating wave in rectangular coordinate system
θ_B	Phase angle associated with reverse propagating wave in rectangular coordinate system
ρ	Composite material density (kg m^{-3})
ρ_s	Density of the solid material (kg m^{-3})
τ_v	A tortuosity factor
ω	Angular frequency (Radians s^{-1})
υ	A constant of association relating moisture vapour concentration to internal temperature of a solid
$\Re(z)$	Real part of the complex number z

References

Adamski, W. and Kitlinski, M. 2001. On measurements applied in scientific researches of microwave heating processes. *Measurement Science Review*. 1(1): 199-203.

Bond, E. J., Li, X., Hagness, S. C. and Van Veen, B. D. 2003. Microwave imaging via space-time beamforming for early detection of breast cancer. *IEEE Transaction on Antennas and Propagation*. 51(8): 1690-1705.

Brodie, G. 2007a. Microwave treatment accelerates solar timber drying. *Transactions of the American Society of Agricultural and Biological Engineers*. 50(2): 389-396.

Brodie, G. 2007b. Simultaneous heat and moisture diffusion during microwave heating of moist wood. *Applied Engineering in Agriculture*. 23(2): 179-187.

Brodie, G. 2008a. The influence of load geometry on temperature distribution during microwave heating. *Transactions of the American Society of Agricultural and Biological Engineers*. 51(4): 1401-1413.

Brodie, G. 2012 Applications of Microwave Heating in Agricultural and Forestry Related Industries. In *The Development and Application of Microwave Heating*, 45-78. Cao, W. ed. InTech: Rijeka, Croatia.

Brodie, G. I. 2008b, *Innovative wood drying: Applying microwave and solar technologies to wood drying*, Saarbruecken, Germany: VDM Verlag.

Commonwealth Department of Transport and Communications. 1991. *Australian Radio Frequency Spectrum Allocations*. Commonwealth Department of Transport and Communications

Crank, J. 1979, *The Mathematics of Diffusion*, Bristol: J. W. Arrowsmith Ltd.

Ding, W. and Zhang, K. 2000. Energy transfer to polymer materials by microwave radiation. *Proc. Microwave and Millimeter Wave Technology, 2000, 2nd International Conference on. ICMMT 2000*. 188-191.

Gallawa, J. C. 1998, *The Complete Microwave Oven Service Handbook: Operation, Maintenance, Troubleshooting and Repair*, Englewood Cliffs: Prentice Hall.

Harris, G. A., Brodie, G. I., Ozarska, B. and Taube, A. 2011. Design of a Microwave Chamber for the Purpose of Drying of Wood Components for Furniture. *Transactions of the American Society of Agricultural and Biological Engineers*. 54(1): 363-368.

Herrero, J. and Polo, M. J. 2012. Parameterization of atmospheric long-wave emissivity in a mountainous site for all sky conditions. *Hydrology & Earth System Sciences Discussions*. 9(3): 3789-3811.

Hill, J. M. and Marchant, T. R. 1996. Modelling Microwave Heating. *Applied Mathematical Modeling*. 20(1): 3-15.

Holman, J. P. 1997, *Heat Transfer*, 8th edn, New York: McGraw-Hill.

International Telecommunication Union. 2004. *Spectrum Management for a Converging World: Case Study on Australia*. International Telecommunication Union

Jennifer Thorne, A., Katie, A. and Alex, W. 2012, *Consumer Guide to Home Energy Savings*, [N.p.]: New Society Publishers.

Jerby, E., Aktushev, O., and Dikhtyar, V. 2005. Theoretical analysis of the microwave-drill near-field localized heating effect. *Journal of applied physics*. 97(3): 034909-1 - 034909-7.

Jerby, E., Dikhtyar, V., Aktushev, O. and Grosglick, U. 2002. The microwave drill. *Science*. 298(5593): 587-589.

Kriegsmann, G. A. 1992. Thermal runaway in microwave heated ceramics: A one-dimensional model. *Journal of Applied Physics*. 71(4): 1960-1966.

Kritikos, H. N., Foster, K. R. and Schwan, H. P. 1981. Temperature profiles in spheres due to electromagnetic heating. *Journal of Microwave Power and Electromagnetic Energy*. 16(3 and 4): 327–340.

Lawrence, A. 2006. Effect of microwave modification on the density of *Eucalyptus obliqua* wood. *Journal of the Timber Development Association of India*. 52(1/2): 26-31.

Liu, B., Marchant, T. R., Turner, I. W. and Vegh, V. 2003. A comparison of semi-analytical and numerical solutions for the microwave heating of lossy material in a three-dimensional waveguide. *Proc. Third World Congress on Microwave and Radio Frequency Applications*. 331-339.Sydney.

Metaxas, A. C. and Meredith, R. J. 1983, *Industrial Microwave Heating*, London: Peter Peregrinus.

Ohlsson, T. and Risman, P. O. 1978. Temperature distributions of microwave heating - spheres and cylinders. *Journal of Microwave Power and Electromagnetic Energy*. 13(4): 303–310.

Perre, P. and Turner, I. W. 1997. Microwave drying of softwood in an oversized waveguide: Theory and experiment. *AIChE Journal*. 43(10): 2579-2595.

Shaeri, M. R., Beyhaghi, S. and Pillai, K. M. 2013. On applying an external-flow driven mass transfer boundary condition to simulate drying from a pore-network model. *International Journal of Heat and Mass Transfer*. 57(1): 331-344.

Studman, C. 1990, *Agricultural and Horticultural Engineering*, Wellington: Butterworth's Agricultural Books.

Torabi, M. and Aziz, A. 2012. Thermal performance and efficiency of convective–radiative T-shaped fins with temperature dependent thermal conductivity, heat transfer coefficient and surface emissivity. *International Communications in Heat and Mass Transfer*. 39(8): 1018-1029.

Torgovnikov, G. I. 1993, *Dielectric Properties of Wood and Wood-Based Materials*, Springer Series in Wood Science, Berlin: Springer-Verlag.

Ulaby, F. T. and El-Rayes, M. A. 1987. Microwave Dielectric Spectrum of Vegetation - Part II: Dual-Dispersion Model. *IEEE Transactions on Geoscience and Remote Sensing*. GE-25(5): 550-557.

Van Remmen, H. H. J., Ponne, C. T., Nijhuis, H. H., Bartels, P. V. and Herkhof, P. J. A. M. 1996. Microwave Heating Distribution in Slabs, Spheres and Cylinders with Relation to Food Processing. *Journal of Food Science*. 61(6): 1105-1113.

Vinden, P. and Torgovnikov, G. 2000. The physical manipulation of wood properties using microwave. *Proc. International Conference of IUFRO*. 240-247.Tasmania, Australia.

Vollmer, M. 2004. Physics of the microwave oven. *Physics Education*. 39(1): 74-81.

Vriezinga, C. A. 1998. Thermal runaway in microwave heated isothermal slabs, cylinders, and spheres. *Journal of Applied Physics*. 83(1): 438 -442.

Welty, J. R., Wicks, C. E., Wilson, R. E. and Rorrer, G. L. 2007, *Fundamentals of Momentum, Heat and Mass Transfer*, 5th edn, John Wiley and Sons.

Wu, X. 2002. Experimental and Theoretical Study of Microwave Heating of Thermal Runaway Materials. Unpublished thesis. USA: Virginia Polytechnic Institute and State University, Mechanical Engineering

XiMing, W., ZhengHua, X., LiHui, S. and WeiHua, Z. 2002. Preliminary study on microwave modified wood. *China Wood Industry Journal*. 16(4): 16-19.

Zhao, H., Turner, I. and Torgovnikov, G. 1998. An experimental and numerical investigation of the microwave heating of wood. *The Journal of Microwave Power and Electromagnetic Energy*. 33(2): 121-133.

Zielonka, P. and Gierlik, E. 1999. Temperature distribution during conventional and microwave wood heating. *Holz als Roh- und Werkstoff*. 57(4): 247-249.

14 Simultaneous Heat and Moisture Movement

In experiments using wool fibres, described by Cassie, King and Baxter (1940 in Crank 1979), the isothermal moisture diffusion coefficient predicted that moisture equilibrium should be reached within seconds of a sudden change in external humidity. However their experiments demonstrated that equilibrium was only reached after an hour or more of exposure to the new external conditions (Crank 1979).

Any realistic analysis of microwave heating in moist organic materials must account for simultaneous heat and moisture diffusion through the porous material. The coupling between heat and moisture transfer is well known but not very well understood (Chu and Lee 1993). Henry (1948) was one of the first to propose a theory for simultaneous diffusion of heat and moisture into a texture package. Crank (1979) presented a more thorough development of Henry's work. The theory of simultaneous heat and moisture diffusion through porous materials, based on Henry's original work, has been rewritten and used by many authors (Chu and Lee 1993, Vos, *et al.* 1994, Fan, *et al.* 2000, Casada 2002, Fan 2004, Barba 2005, Fan 2005, Frydrych and Ralek 2005).

For a porous material, the amount of water vapour moving into a small section of material is the sum of any net increase in moisture content in the air space and the net increase in moisture content of the material's fibres. Therefore:

$$a_v \tau_v D_a \cdot \nabla^2 M_v = a_v \frac{\partial M_v}{\partial t} + (1 - a_v)\rho_s \frac{\partial M_s}{\partial t} \tag{14.1}$$

Heat is evolved when moisture is absorbed by a material, therefore the thermal diffusion equation, allowing for a volumetric heat source is:

$$C\rho \frac{\partial T}{\partial t} = k\nabla^2 T + L\rho \frac{\partial M_s}{\partial t} + \dot{q}(x) \tag{14.2}$$

If it is assumed that some linear relationship exists between the moisture content of a material, the moisture vapour concentration in the air spaces in the material and the temperature, then:

$$\frac{\partial M_s}{\partial t} = \sigma \frac{\partial M_v}{\partial t} - \omega \frac{\partial T}{\partial t} \tag{14.3}$$

Substituting into equations (14.1) and (14.2) and combining the two equations as described by Henry (1948) yields:

$$\nabla^2\left(pM_v+nT\right)-\frac{\partial}{\partial t}\left\{\begin{bmatrix}\frac{1}{\tau_v D_a}\left(1+\frac{(1-a_v)\sigma\rho_s}{a_v}\right)-\frac{n\rho\sigma L}{pk}\end{bmatrix}pM_v+\right.\\\left.\begin{bmatrix}\frac{C\rho}{k}\left(1+\frac{\omega L}{C}\right)-\frac{p(1-a_v)\omega\rho_s}{n\tau_v D_a a_v}\end{bmatrix}nT\right\}+\frac{n\dot{q(x)}}{k}=0 \tag{14.4}$$

This can be expressed in a simpler form if $\Omega = pM_v + nT$ and p and n are chosen such that:

$$\frac{1}{\gamma}=\left[\frac{1}{\tau_v D_a}\left(1+\frac{(1-a_v)\sigma\rho_s}{a_v}\right)-\frac{n\rho\sigma L}{pk}\right]=\left[\frac{C\rho}{k}\left(1+\frac{\omega L}{C}\right)-\frac{p(1-a_v)\omega\rho_s}{n\tau_v D_a a_v}\right] \tag{14.5}$$

Equation (14.4) can be rewritten as:

$$\nabla^2\Omega-\frac{1}{\gamma}\frac{\partial\Omega}{\partial t}+\frac{n\dot{q(x)}}{k}=0 \tag{14.6}$$

Equation (14.6) is now a diffusion equation in terms of Ω and equation (14.5) is a quadratic polynomial in γ and yields:

$$\gamma=\frac{2\psi\xi}{\psi+\xi\pm\sqrt{\left[\psi-\xi\right]^2+4\psi\xi\chi}} \tag{14.7}$$

where $\psi=\dfrac{k}{C\rho\left(1+\dfrac{L}{C}\omega\right)}$, $\xi=\dfrac{\tau_v D_a}{\left[1+\dfrac{(1-a_v)\rho_s\sigma}{a_v}\right]}$ and $\chi=\dfrac{\sigma\rho_s\omega L}{a_v C^2\left(1+\dfrac{L}{C}\omega\right)^2\left[1+\dfrac{(1-a_v)\rho_s\sigma}{a_v}\right]}$.

Equation (14.7) implies that the combined heat and moisture diffusion coefficient (γ) has two independent values. This is consistent with Henry's (1948) equation for simultaneous heat and moisture diffusion in textiles. The combined processes of heat and moisture diffusion are equivalent to the independent diffusion of two quantities, each of which is a linear function of moisture vapour concentration and temperature. The diffusion coefficients of these two quantities are always such that one is much less and the other much greater than would be observed, were moisture and heat diffusion not coupled together. Therefore the independent solution of the heat and moisture diffusion equations is inadequate to describe their combined influence (Henry 1948). The diffusion coefficient for the slower quantity of the coupled system is always less than either the isothermal moisture diffusion constant or the constant vapour

concentration coefficient for heat diffusion, which ever is less, but never by more than one half (Henry 1948). The faster diffusion coefficient may be many times greater than either of the independent diffusion constants.

Henry (1948) presents a nomogram, shown in Figure 14.1, relating the fast diffusion coefficient to the default diffusion coefficient for the material at 20 °C and 65 % relative humidity. This nomogram can be used to forecast the thermal diffusivity of the system under different conditions. For example, if the relative humidity remains constant and the temperature of some part of the system rapidly rises to 55 °C, Henry's nomogram suggests that the diffusion coefficient for the faster wave will be about 7.5 times higher than the standard thermal diffusivity of the material.

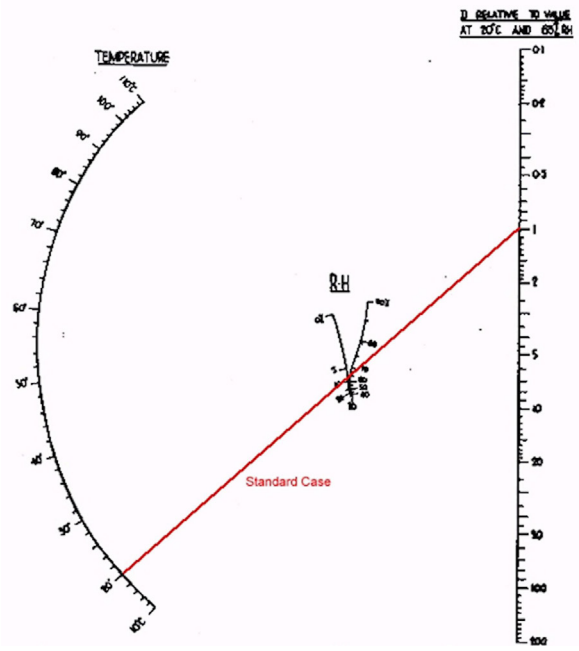

Figure 14.1: Nomogram of variation in g with temperature and relative humidity (Modified from: Henry 1948).

It must be remembered that this data was for cotton packaging in the absence of internal heat sources; however Henry (1948) states that a similarly coupled response should be expected when either moisture or heat are released inside the material in a way that is independent of the diffusion processes. Dielectric heating, from microwave interactions inside the material, is independent of diffusion processes; therefore a rapidly propagating wave of heat and moisture should be expected during microwave heating in any moist materials.

Having now identified some key principles of heat diffusion while heat is being generated inside an object, the specific problem of determining the temperature distribution inside objects during microwave heating can be addressed provided the spatial distribution $q(x)$ can be determined for each microwave heating system configuration. The spatial distribution of heat generated inside the object depends on how microwave energy interacts with the material itself.

Considerable evidence exists in literature for rapid heating and drying during microwave processing (Rozsa 1995, Zielonka, *et al.* 1997, Zielonka and Dolowy 1998); therefore it is reasonable to assume that the faster diffusion wave should dominate microwave heating in moist materials. A slow heat and moisture diffusion wave should also exist; however observing this slow wave during microwave heating may be difficult and no evidence of its influence has been seen in literature so far.

This theory was successfully applied to microwave heating of wood samples (Figure 14.2).

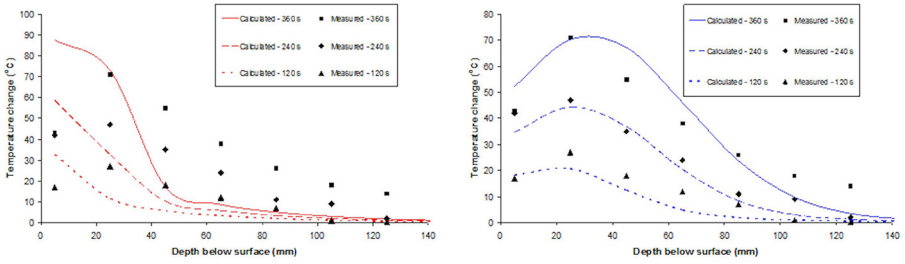

Figure 14.2: Comparison of measured temperature, published by Zielonka and Dolowy (1998), with theoretical temperature, estimated using equation (13.24) - (a) using the published constant vapour concentration thermal diffusivity of wood and (b) using a thermal diffusivity that is 7.8 times larger than the published values, as suggested by Henry's nomogram (Source: Brodie 2007).

In his discussion of simultaneous heat and moisture diffusion, Henry (1948) also stated that thermal diffusion would approach the constant vapour concentration thermal diffusivity of the material as the combined heat and moisture diffusion processes became decoupled. The decline in the multiplying factor, implied by the data shown in Figure 14.3, may be linked to the loss of moisture and subsequent decoupling of the combined heat and moisture transfer mechanisms. This requires further investigation.

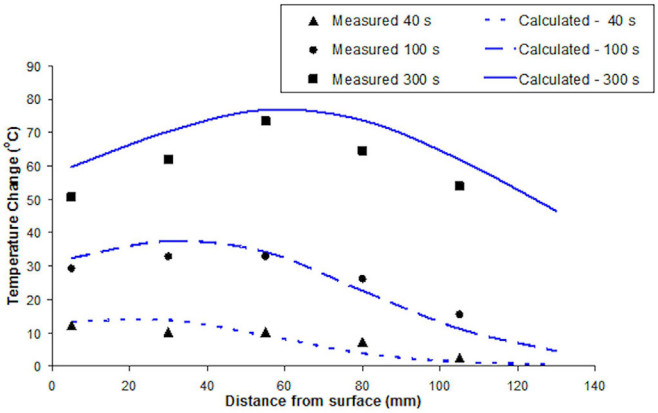

Figure 14.3: Comparison of mean measured temperature with theoretical temperature, estimated using equation (6) when the constant vapour pressure thermal diffusivity of wood was multiplied by 13.1 for 40 s data, 11.5 for 100 s data and 7.8 for 300 s data (Source: Brodie 2007).

14.1 Temperature Sensing in Electromagnetic Fields

Temperature measurement with electromagnetic fields is challenging. Conventional temperature sensors based on thermo-electric effects, such as thermocouples and thermistors, distort the electromagnetic fields in the vicinity of the probes, giving erroneous readings and in some cases causing localised plasma (Tang 2006).

Fibre-optic temperature sensors provide comparable accuracy to thermocouples in a normal heating medium. The probe sizes of fibre-optic sensors are generally small. Fibre-optic temperature sensors are developed based on one of three methods: fluorescence decay time, Fabry–Pe´rot interferometry, and transmission spectrum shift in semiconductor crystals (Tang 2006). These systems can be safely placed into electromagnetic fields because the fibre-optic is transparent at microwave frequencies.

Fluorescence technology uses a fibre-optic cable to connect a phosphor element, which is attached to the tip of a silica fibre and encapsulated in Teflon tube, to an electronic instrument. The phosphor material is excited with a light source, which excites the phosphorescent sensor causing it to emit light. The emitted light returns to the instrument through the same fibre-optic cable. The rate of after-glow decay in this system depends on the temperature of the phosphor material, which is placed in contact with the heated material (Tang 2006).

The Fabry–Pe´rot interferometer consists of two parallel reflective surfaces (mirrors) that form a cavity resonator. These sensors often use a thermally expandable piece of glass between the two reflected surfaces, which cause a perturbation in the resonance of the reflective cavity. These sensors can also respond to pressure changes as well and thermal expansion (Tang 2006).

Semiconductor sensors use the temperature dependent light absorption/transmission characteristics of semiconductor crystals such as gallium arsenide (or GaAs). A unique feature of this crystal is that when temperature increases, the crystal's transmission spectrum shifts to a higher wavelength (Tang 2006). Measuring the position of the absorption shift, using a grating-based near infrared spectrometer, provides information on the temperature of the sensing element.

Another technique for measuring temperature in electromagnetic fields is to use remote infra-red detectors (Chemat, *et al*. 2005, van Dam 2005, Arrieta, *et al*. 2007). These systems respond to increases in the infra-red radiation from materials as the temperature increase; however because the wavelength of thermal infra-red energy is very small, the resulting measurements are limited to surface temperature only.

References

Arrieta, A., Otaegui, D., Zubia, A., Cossio, F. P., Diaz-Ortiz, A., delaHoz, A., Herrero, M. A., Prieto, P., Foces-Foces, C., Pizarro, J. L. and Arriortua, M. I. 2007. Solvent-Free Thermal and Microwave-Assisted [3 + 2] Cycloadditions between Stabilized Azomethine Ylides and Nitrostyrenes. An Experimental and Theoretical Study. *Journal of Organic Chemistry*. 72(12): 4313-4322.

Barba, A. A. 2005. Thermal treatments of foods: a predictive general-purpose code for heat and mass transfer. *Heat and Mass Transfer*. 41(7): 625–631.

Brodie, G. 2007. Simultaneous heat and moisture diffusion during microwave heating of moist wood. *Applied Engineering in Agriculture*. 23(2): 179-187.

Casada, M. E. 2002. Moisture adsorption characteristics of wheat and barley. *Transactions of the ASAE*. 45(2): 361–368.

Chemat, S., Aït-Amar, H., Lagha, A. and Esveld, D. C. 2005. Microwave-assisted extraction kinetics of terpenes from caraway seeds. *Chemical Engineering and Processing*. 44(12): 1320-1326.

Chu, J. L. and Lee, S. 1993. Hygrothermal stresses in a solid: Constant surface stress. *Journal of Applied Physics*. 74(1): 171-188.

Crank, J. 1979, *The Mathematics of Diffusion*, Bristol: J. W. Arrowsmith Ltd.

Fan, J., and Cheng, X. 2005. Heat and Moisture Transfer with Sorption and Phase Change Through Clothing Assemblies. *Textile Research Journal*. 75(2): 99-105.

Fan, J., Cheng, X., Wen, X., and Sun, W. 2004. An improved model of heat and moisture transfer with phase change and mobile condensates in fibrous insulation and comparison with experimental results. *International Journal of Heat and Mass Transfer*. 47(10-11): 2343–2352.

Fan, J., Luo, Z. and Li, Y. 2000. Heat and moisture transfer with sorption and condensation in porous clothing assemblies and numerical simulation. *International Journal of Heat and Mass Transfer*. 43(16): 2989-3000.

Frydrych, D. and Ralek, P. 2005. The Solution of Coupled Heat and Moisture Diffusion with Sorption for Textiles. *Proc. 17th Conference on Scientific Computing*. 53-63.Vysoké Tatry - Podbanské, Slovakia.

Henry, P. S. H. 1948. The diffusion of moisture and heat through textiles. *Discussions of the Faraday Society*. 3: 243-257.

Rozsa, A. 1995. Moisture movement in eucalypt timbers during microwave vacuum drying. *Proc. International Conference on Wood Drying*. 289-294.Slovak Republic.

Tang, J. 2006 Fiber-optic Measurement Systems: Microwave and Radio Frequency Heating Applications. In *Encyclopedia of Agricultural, Food and Biological Engineering*. Marcel Dekker.

van Dam, R. L., Borchers, B., and Hendrickx, J. M. H. 2005. Strength of landmine signatures under different soil conditions: implications for sensor fusion. *International Journal of Systems Science*. 36(9): 573–588.

Vos, M., Ashton, G., Van Bogart, J. and Ensminger, R. 1994. Heat and Moisture Diffusion in Magnetic Tape Packs. *IEEE Transactions on Magnetics*. 30(2): 237-242.

Zielonka, P. and Dolowy, K. 1998. Microwave Drying of Spruce: Moisture Content, Temperature and Heat Energy Distribution. *Forest Products Journal*. 48(6): 77-80.

Zielonka, P., Gierlik, G., Matejak, M. and Dolowy, K. 1997. The comparison of experimental and theoretical temperature distribution during microwave wood heating. *Holz als Roh- und Werkstoff*. 55(6): 395-398.

15 Microwave Drying

Many products must be dried before they can be stored or used. For example, drying of animal fodder helps preserve its quality and avoid spontaneous combustion during storage in hay stacks. Another example is wood, which needs to be dried before use. Many studies have investigated the application of microwave energy to speed up drying (Manickavasagan, *et al.* 2006, Setiady, *et al.* 2009).

The effects of microwave heating must be considered as the simultaneous diffusion of heat and moisture through a material (Brodie 2007). Essentially, the theory of combined heat and moisture diffusion (Henry 1948, Brodie 2007) during microwave heating implies that two independent waves of heat and moisture vapour propagate through the material under the influence of a volumetric heat source created by the interaction of polar molecules and microwave fields (Brodie 2007). According to Henry's theory, the slower of these two waves is always slower than either the isothermal diffusion constant for moisture or the constant vapour concentration diffusion constant for heat diffusion (Henry 1948), whichever is less, but never by more than one half (Henry 1948, Crank 1979). The faster of these two waves is always many times faster than either of the independent diffusion constants (Henry 1948, Crank 1979).

Considerable evidence exists in literature for rapid heating and drying during microwave processing (Zielonka and Dolowy 1998, Torgovnikov and Vinden 2003); therefore it is reasonable to assume that the faster of the two diffusion waves dominates microwave heating in moist materials whereas the slower wave dominates conventional heating (Henry 1948). A slow heat and moisture diffusion wave may also exist during microwave heating; however observing this slow wave during microwave heating experiments is difficult and no evidence of its influence on microwave heating has been seen in literature so far.

Along with the fast heating effect, there is of course fast moisture movement; therefore radio frequency and microwave energy is a logical choice for rapid drying. One of the important features of radio frequency and microwave drying is that heating is directly linked to the dielectric properties of the material being treated. Ulaby and El-Rayes (1987, 1987) and Chuah et al. (1997) have studied the dielectric properties of plant materials at microwave frequencies. Plants with high moisture content have higher dielectric constants (Figure 15.1) and will therefore interact more with the microwave fields, generating more heat; therefore electromagnetic energy preferentially interacts with the moist regions of any material, improving the drying performance of electromagnetic heating. Microwave drying is also self-limiting, because the heating effect reduces as the removal of water from organic materials reduces the dielectric properties of the material (Chen, *et al.* 2014).

15.1 Microwave Drying of Crop Fodder

Higgins and Spooner (1986) investigated alfalfa, which was microwave-dried for 7, 8, 9 or 10 min in a microwave oven, compared with field and convective oven-dried alfalfa. They found no differences in crude protein, *in vitro* dry matter digestibility or acid detergent lignin between the various drying methods. Microwave-dried alfalfa generally retained a higher proportion of the cell-wall constituents (neutral detergent fibre) than did field-dried alfalfa. Microwave dried Alfalfa that was treated for 7 minutes had significantly lower acid detergent fibre values than all other drying treatments.

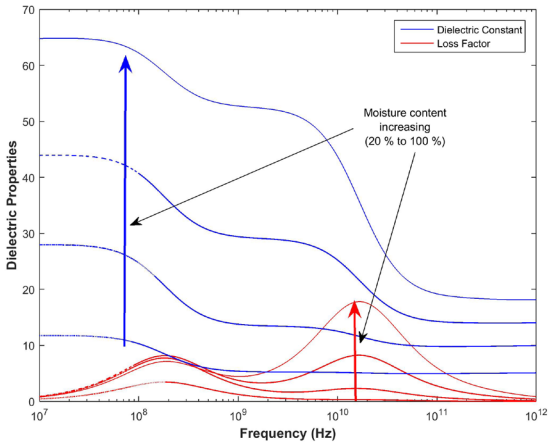

Figure 15.1: Dielectric properties of vegetative material as a function of frequency and moisture content (Based on models presented in: Ulaby and El-Rayes 1987).

Adu and Otten (1996) studied the kinetics of microwave drying of white beans. They found that microwave drying was a falling rate process. When constant power was absorbed, seed temperature increased rapidly to a maximum value during the initial stages of drying and began to decrease gradually during the latter stages of drying. To maintain a constant drying temperature, the microwave power had to be increased progressively as the moisture content of the beans decreased due to drying.

This is linked to reductions in the dielectric properties of the beans as moisture is removed (Nelson 1987). This reduces the interactions between the microwave fields and the beans. The gradual decrease in seed temperature, when the drying rate decreases, is opposite to what is observed during conventional hot air drying. This may be caused by a progressively increasing heat of desorption during the drying

process (Kiranoudis, *et al.* 1993), which is a common phenomenon in hygroscopic solids. Thus, the microwave heating characteristics observed for white beans may apply to other hygroscopic solids, such as soils, wood, and fodder chaff.

As with other heating processes, microwave drying offers better efficiency than conventional drying systems (Chen, *et al.* 2014).

15.2 Modelling Microwave Drying

The rate of change of total moisture content of a treated material with respect to applied microwave energy during microwave drying is proportional to the current moisture content of the material and the already applied microwave energy (Em) such that:

$$\frac{dMC}{dEm} = \frac{-MC \cdot Em}{b} \tag{15.1}$$

Therefore a typical microwave drying curve (Figure 15.2) can be described as a function of initial moisture content (MC_i), final moisture content (MC_f) and the applied microwave energy:

$$\frac{MC - MC_f}{MC_i - MC_f} = e^{\frac{-Em^2}{2b}} \tag{15.2}$$

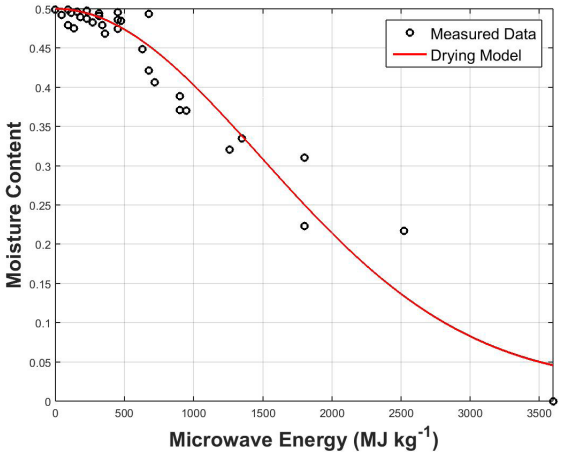

Figure 15.2: Wheat grain moisture content as a function of applied microwave energy.

The microwave drying curve (Figures 15.2 and 15.4) exhibits a short relatively slow drying period, followed by a much faster almost linear relationship between applied microwave energy and moisture loss. This is followed by a more conventional falling rate drying period (Figure 15.2); however prolonged microwave treatment at high power leads to a phenomenon known as "thermal runaway", which causes charring (Figure 15.3). Microwave treatment profoundly affects the germination performance of grains, with any reasonable application of microwave energy totally inhibiting grain germination (Table 15.1); therefore electromagnetic drying should not be considered for seed.

Figure 15.3: Charring of wheat during prolonged microwave treatment.

Problems with thermal runaway during microwave drying can be overcome by using cyclic drying instead of continuous microwave heating (Harris, *et al.* 2011). In this technique, microwave energy is applied for a short time to induce rapid heating and moisture movement and then the product is allowed to equilibrate during a period with no microwave energy applied. This technique has been successfully applied to timber drying (Harris, *et al.* 2011) (Figure 15.4).

Table 15.1: Effect of microwave drying of 700 g samples of wheat in a 750 W, 2.45 GHz, domestic oven on germination percentages of grains.

Microwave Power (%)	Microwave treatment time (minutes)		
	3.5	7.0	10.5
20	88%	42%	4%
50	46%	0%	0%
70	6%	0%	0%
100	0%	0%	0%
Control	90%	88%	94%

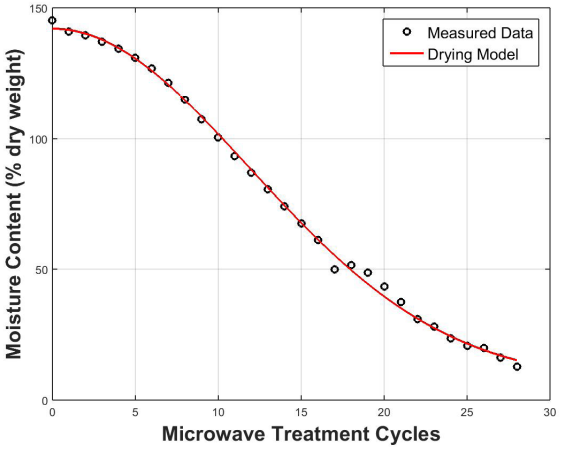

Figure 15.4: Wood moisture content as a function of the number of microwave energy cycles applied.

15.3 Effect of Microwave Drying on Milling Properties

Walde, et al. (2002) studied the effect of microwave drying on the grinding properties of wheat. The microwave dried samples were crisp and consumed less energy for grinding compared to the control samples. The Bond's work index for the bulk sample was 8.1 MJ kg^{-1} compared to 8.8 MJ kg^{-1} for the control samples of equal moisture content. These studies indicated that microwave drying of wheat before grinding helps reduce power consumption in wheat milling. The microwave drying did not change the total protein content, but there were some functional changes in the protein, which was evident from gluten measurements.

Studies have also been carried out on the dry milling characteristics of maize grains, which were dried previously from different initial moisture contents (MCi) in a domestic microwave oven (Velu, *et al.* 2006). The MCi ranged from 9.6% to 32.5% on a dry sample basis. Drying was also carried out in a convective dryer at temperatures of 65 – 90 °C. The drying rate curve for the conventionally dried samples showed a typical case of moisture loss by diffusion from grains. The dried samples were ground in a hammer mill and the Bond's work index was found to decrease with increasing duration of microwave drying. There was no difference in protein and starch content between the different treatments. Viscosity measurements were made with 10% suspensions of the flour in water which were heated to 80 – 90 °C and allowed to cool. Viscosity decreased with increasing microwave drying of the grains. The colour analysis showed that flour of the microwave-dried samples was brighter than the colour of the conventionally dried samples.

Based on these and other studies, microwave drying of organic materials appears to be a viable alternative to conventional methods, especially when rapid drying and high throughputs of moist material are desirable; however the energy needed to evaporate water is very high. Another application of microwave treatment in the drying process is to apply a short intense pre-treatment to the moist material to modify its moisture permeability, which can then speed up drying in conventional systems. This will be discussed in a future chapter.

References

Adu, B. and Otten, L. 1996. Microwave heating and mass transfer characteristics of white beans. *Journal of Agricultural Engineering Research*. 64(1): 71 -78.

Brodie, G. 2007. Simultaneous heat and moisture diffusion during microwave heating of moist wood. *Applied Engineering in Agriculture*. 23(2): 179-187.

Chen, Z., Afzal, M. T. and Salema, A. A. 2014. Microwave drying of wastewater sewage sludge. *Journal of Clean Energy Technologies*. 2(3): 282-286.

Chuah, H. T., Kam, S. W. and Chye, Y. H. 1997. Microwave dielectric properties of rubber and oil palm leaf samples: measurement and modelling. *International Journal of Remote Sensing*. 18(12): 2623 - 2639.

Crank, J. 1979, *The Mathematics of Diffusion*, Bristol: J. W. Arrowsmith Ltd.

El-Rayes, M. A. and Ulaby, F. T. 1987. Microwave Dielectric Spectrum of Vegetation-Part I: Experimental Observations. *Geoscience and Remote Sensing, IEEE Transactions on*. GE-25(5): 541-549.

Harris, G. A., Brodie, G. I., Ozarska, B. and Taube, A. 2011. Design of a Microwave Chamber for the Purpose of Drying of Wood Components for Furniture. *Transactions of the American Society of Agricultural and Biological Engineers*. 54(1): 363-368.

Henry, P. S. H. 1948. The diffusion of moisture and heat through textiles. *Discussions of the Faraday Society*. 3: 243-257.

Higgins, T. R. and Spooner, A. E. 1986. Microwave drying of alfalfa compared to field-and oven-drying: Effects on forage quality. *Animal Feed Science and Technology*. 16(1-2): 1-6.

Kiranoudis, C. T., Maroulis, Z. B., Tsami, E. and Marinos-Kouris, D. 1993. Equilibrium moisture content and heat of desorption of some vegetables. *Journal of Food Engineering*. 20(1): 55-74.

Manickavasagan, A., Jayas, D. S. and White, N. D. G. 2006. Non-Uniformity of Surface Temperatures of Grain after Microwave Treatment in an Industrial Microwave Dryer. *Drying Technology*. 24(12): 1559–1567.

Nelson, S. O. 1987. Frequency, moisture, and density dependence of the dielectric properties of small grains and soybeans. *Transactions of the American Society of Agricultural and Biological Engineers*. 30(5): 1538-1541.

Setiady, D., Tang, J., Younce, F., Swanson, B. A., Rasco, B. A. and Clary, C. D. 2009. Porosity, Color, Texture, and Microscopic Structure of Russet Potatoes Dried Using Microwave Vacuum, Heated Air, and Freeze Drying *Applied Engineering in Agriculture*. 25(5): 719-724.

Torgovnikov, G. and Vinden, P. 2003 Innovative microwave technology for the timber industry. In *Microwave and Radio Frequency Applications: Proceedings of the Third World Congress on Microwave and Radio Frequency Applications*, 349-356. Folz, D. C., et al. eds. The American Ceramic Society: Westerville, Ohio.

Ulaby, F. T. and El-Rayes, M. A. 1987. Microwave Dielectric Spectrum of Vegetation - Part II: Dual-Dispersion Model. *IEEE Transactions on Geoscience and Remote Sensing*. GE-25(5): 550-557.

Velu, V., Nagender, A., Prabhakara Rao, P. G. and Rao, D. G. 2006. Dry milling characteristics of microwave dried maize grains (Zea mays L.). *Journal of Food Engineering*. 74(1): 30-36.

Walde, S. G., Balaswamy, K., Velu, V. and Rao, D. G. 2002. Microwave drying and grinding characteristics of wheat (Triticum aestivum). *Journal of Food Engineering*. 55(3): 271-276.

Zielonka, P. and Dolowy, K. 1998. Microwave Drying of Spruce: Moisture Content, Temperature and Heat Energy Distribution. *Forest Products Journal*. 48(6): 77-80.

16 Radio Frequency and Microwave Processing of Food

Microwaves have been used as a heat source since the 1940s (Spencer 1949, 1952). Industrial applications of microwave heating include: polymer and ceramics industries (Ayappa, *et al.* 1991), medicine (Pchelnikov 2003) and food processing (Van Remmen, *et al.* 1996, Oliveira and Franca 2002, Shaheen, *et al.* 2012). The food industry is the single largest consumer of microwave energy, where it can be employed for cooking, thawing, tempering, drying, freeze-drying, pasteurization, sterilization, baking, heating and re-heating (Ayappa, *et al.* 1991). Most homes in western countries have microwave ovens for cooking and reheating food.

Water, which is the major constituent of most food products, is the main source for microwave interactions due to its dipolar nature. Heat is generated throughout the material, leading to faster heating rates and shorter processing times compared to conventional heating. Other advantages include space savings and energy efficiency, since most of the electromagnetic energy is converted into heat (Oliveira and Franca 2002).

Factors affecting microwave heating of food include: the dielectric, thermal and physical properties of the food stuff; the moisture content and moisture permeability of the food material; the geometry of the food stuff; and the geometry of the microwave applicator used to irradiate the food.

16.1 Dielectric Properties of Foods

The dielectric properties of food stuffs vary with frequency, temperature and moisture content. Foodstuffs are complex materials and they exhibit extremely complicated dielectric spectra (Daschner, *et al.* 2000). The complex dielectric properties of foods vary with frequency, temperature and possibly time, depending on the dipolar relaxation frequencies of the polar molecules involved (Daschner, *et al.* 2000). Most foodstuffs contain both bound and free water, which itself has a complex dielectric behaviour (Ellison, *et al.* 1996, Tikhonov 1997, Buchner, *et al.* 1999, Boyarskii, *et al.* 2002, Chaplin 2007). Table 16.1 lists the measured dielectric properties of several food stuffs at a frequency of 2.8 GHz.

Fat and water content of the food change the dielectric properties. Their heating behaviours are also quite different. Fat will be heated more quickly than water because of its relatively low heat capacity. Fat can be heated to greater than 200 °C whereas the temperature of water will be no greater than 100 °C until it is completely evaporated (Food and Environmental Hygiene Department 2005); therefore mixed foods tend to heat at different rates due to their different thermal and dielectric properties.

One of the common concerns of microwave heating is uneven heating. This is partly due to the geometry of the object being heated and partly due to the geometry of the microwave fields inside the applicator used to apply the energy to the material.

The influence of material geometry over microwave heating has been discussed in Chapter 13 and the influence of applicator geometry will be presented in the next chapter; however differences in dielectric properties are the other major contributor to uneven heating in foods. Most food products have several products in the same sample, with each material having different dielectric properties (Table 16.1), which leads to differential heating.

Table 16.1: Dielectric properties of common foods at 2.8 GHz (Source: Ohlsson and Bengtsson 1975.).

Material	Temperature (K)	κ'	κ''
Potato, freeze dried	298.16	7.5	2.5
Potato, Raw	298.16	57.3	15.7
Aqueous non-fat dry milk	308.16	63.3	16
Pizza stuffing	323.16	10.1	3.1
Pizza dough	323.16	4.6	0.6
Pizza dough	373.16	6.2	0.9
Pineapple syrup	323.16	67.8	11.6
Pineapple syrup	373.16	57.1	9.2
Fish, Cooked	313.16	45	11.9
Fish, Cooked	353.16	42.6	12.7
Fish, Cooked	413.16	39.9	16.8
Gravy	313.16	76.1	24.1
Gravy	353.16	73.6	26.2
Gravy	413.16	68.7	28.8
Water	313.16	72.8	6.5
Water	353.16	61.8	3.2
Water	413.16	48.1	1.5
Potato, mashed	313.16	60.6	17.4
Potato, mashed	353.16	54.2	16.5
Potato, mashed	413.16	44.7	15
0.1 M NaCl	313.16	71.1	13.7
0.1 M NaCl	353.16	63.5	14.8
0.1 M NaCl	413.16	51.9	17.4
Beef, raw	353.16	42.6	13.1
Beef, raw	413.16	40.5	16
Liver pate	313.16	41.4	16.5
Liver pate	353.16	38.9	18.4
Liver pate	413.16	38.7	20.7
Peas, cooked	313.16	60.8	12.6
Peas, cooked	353.16	50.5	9.7

Continued **Table 16.1:** Dielectric properties of common foods at 2.8 GHz (Source: Ohlsson and Bengtsson 1975.).

Material	Temperature (K)	κ'	κ''
Peas, cooked	413.16	41.2	8.9
Carrots, Cooked	313.16	70.1	11.8
Carrots, Cooked	353.16	61.8	12.5
Carrots, Cooked	413.16	41.5	11
Peanut Butter	327.16	3.1	4.1
Peanut Butter	373.16	3.5	5
Frankfurters	323.16	39	26.9
Ground beef patties	323.16	31.7	10.4
Ground beef patties	373.16	31.7	12.6
Concentrated orange juice	323.16	54.1	15.7
Beef steak, cooked	323.16	37	10.6
Beef steak, cooked	373.16	33.6	12.6
Ham	323.16	66.6	47
Pork chop	323.16	49.8	18.3
Pork chop	373.16	44.5	19.4
Fillet of turbot	323.16	53.6	14.1

One of the consequences of uneven heating is that some parts of the heated material will be over heated while other parts will remain under heated. Under heating can be a concern for food safety (Food and Environmental Hygiene Department 2005) because pathogenic organisms can survive and cause illness. Concerns have arisen regarding whether microwave cooking can kill food-borne pathogens as effective as conventional cooking methods since microwave cooking generally requires shorter times and may sometimes result in lower temperatures at the food surface; however many studies have concluded that microwave cooking kills microorganisms and spores provided that appropriate temperature and time are reached (Food and Environmental Hygiene Department 2005).

There are concerns that microwave heating of food is unhealthy because it could affect its chemical or physical properties, other than simple cooking. For chemical alteration to happen, the microwaves would need to create chemical radicals involving energies of the order of an electron-volt (eV) (Vollmer 2004). Microwave photons have energies of the order of 10^{-5} eV; therefore simple estimates easily show that the number of microwave photons within commercial microwave oven is orders of magnitude too small to establish multi-photon dissociation or ionization (Vollmer 2004); therefore microwave cooking cannot chemically alter food.

Cooking processes, especially the high temperature ones (e.g. grilling, baking, etc.) are known to induce the production of potential carcinogens. There have been concerns that microwave cooking may also increase the production of carcinogens or

mutagens in foods. Currently there is no scientific evidence that the production of any carcinogenic substances would increase upon the application of microwave heating. A study examined mutagen production in cooked lamb and beef found no evidence of mutagenicity in microwave-cooked lamb chops, sirloin steak, leg of lamb, or rolled beef loaf (Food and Environmental Hygiene Department 2005).

16.2 Comparative Efficiency of Convective and Microwave Heating

Thermal transfer in conventional systems depends on the temperature differential between the heated object and its surroundings. As this temperature differential reduces the heat transfer reduces also. Thermal conductivity of the material and the complex interactions between heat transfer and moisture transport also influence the thermal transfer in the system. The coupling between heat and moisture transport in a conventional system usually results in slower heating because the water vapour is moving out of the material opposing the transfer of heat into the material. This creates an evaporation surface inside the material (Shaeri, *et al.* 2013) that effectively cools the material until the water source is exhausted.

Microwave heating is a volumetric phenomenon. Although the interactions are complex, the combination of geometry, material properties, microwave field intensities and changes in these parameters induces very rapid heating. There is also a coupling between microwave heating and moisture transport that enhances both heat and moisture transport (Brodie 2007), rather than diminishing each other as happens in conventional heating systems. Consequently, microwave heating is many times faster than convective heating. As an easy to understand example of the differences in efficiency between microwave heating and other systems, Table 16.2 compares the energy required for cooking a casserole using different heating systems.

Table 16.2: Comparative energy requirements for cooking a casserole (Source: Jennifer Thorne, et al. 2012).

Appliance	Temperature	Time	Energy
Electric Oven	350	1 hour	2.0 kWh
Electric Convection Oven	325	45 minutes	1.39 kWh
Gas Oven	350	1 hour	3.3 kWh
Electric Frying Pan	420	1 hour	0.9 kWh
Toaster Oven	425	50 minutes	0.95 kWh
Electric Crockpot	200	7 hours	0.7 kWh
Domestic Microwave Oven	“High”	15 minutes	0.36 kWh

References

Ayappa, K. G., Davis, H. T., Crapiste, G., Davis, E. J. and Gordon, J. 1991. Microwave heating: An evaluation of power formulations. *Chemical Engineering Science*. 46(4): 1005-1016.

Boyarskii, D. A., Tikhonov, V. V. and Komarova, N. Y. 2002. Modeling of dielectric constant of bound water in soil for applications of microwave remote sensing. *Progress In Electromagnetics Research*. 35: 251–269.

Brodie, G. 2007. Simultaneous heat and moisture diffusion during microwave heating of moist wood. *Applied Engineering in Agriculture*. 23(2): 179-187.

Buchner, R., Barthel, J. and Stauber, J. 1999. The dielectric relaxation of water between 0° C and 35° C. *Chemical Physics Letters*. 306(1-2): 57-63.

Chaplin, M. 2007. *Water Structure and Science*. 7th June, 2007. http://www.lsbu.ac.uk/water/

Daschner, F., Knoechel, R. and Kent, M. 2000. Rapid monitoring of selected food properties using microwave dielectric spectra. *Proc. 2nd International Conference on Microwave and Millimeter Wave Technology*.

Ellison, W. J., Lamkaouchi, K. and Moreau, J. M. 1996. Water: a dielectric reference. *Journal of Molecular Liquids*. 68(2–3): 171-279.

Food and Environmental Hygiene Department. 2005 *Microwave Cooking and Food Safety* The Government of the Hong Kong Special Administrative Region

Jennifer Thorne, A., Katie, A. and Alex, W. 2012, *Consumer Guide to Home Energy Savings*, [N.p.]: New Society Publishers.

Ohlsson, T. and Bengtsson, N. E. 1975. Dielectric food data for microwave sterilization processing. *J Microw Power*. 10(1): 93-108.

Oliveira, M. E. C. and Franca, A. S. 2002. Microwave heating of foodstuffs. *Journal of Food Engineering*. 53(4): 347-359.

Pchelnikov, Y. N. 2003. Features of slow waves and potentials for their nontraditional application. *Applications of Radiotechnology and Electronics in Bioligy and Medicine*. 48(4): 450-462.

Shaeri, M. R., Beyhaghi, S. and Pillai, K. M. 2013. On applying an external-flow driven mass transfer boundary condition to simulate drying from a pore-network model. *International Journal of Heat and Mass Transfer*. 57(1): 331-344.

Shaheen, M. S., El-Massry, K. F., El-Ghorab, A. H. and Anjum, F. M. 2012 Microwave Applications in Thermal Food Processing. In *The Development and Application of Microwave Heating*. Shaheen ed.

Spencer, P. L. 1949. *Prepared food article and method of preparing*. Patent No. 2480679

Spencer, P. L. 1952. *Electronic cooking*. Patent No. 2582174

Tikhonov, V. V. 1997. Dielectric model of bound water in wet soils for microwave remote sensing. *Proc. IEEE International Geoscience and Remote Sensing Symposium, 1997*. 3: 1108 - 1110. Singapore International Convention and Exhibition Centre, Singapore

Van Remmen, H. H. J., Ponne, C. T., Nijhuis, H. H., Bartels, P. V. and Herkhof, P. J. A. M. 1996. Microwave Heating Distribution in Slabs, Spheres and Cylinders with Relation to Food Processing. *Journal of Food Science*. 61(6): 1105-1113.

Vollmer, M. 2004. Physics of the microwave oven. *Physics Education*. 39(1): 74-81.

17 Microwave Applicators

Radiofrequency and microwave energy can be transferred through space by simple propagation between a transmitter and a receiver or they can be guided through some form of channel. Common channels include transmission lines and wave-guides. Transmission lines will be discussed in more detail later in Chapter 26; however it is appropriate to explore the properties of wave guides here.

17.1 Wave-Guides

In general, a wave-guide consists of a tube of uniform cross section through which light may travel. Light is an electro-magnetic wave which can travel very long distances very fast (Metaxas and Meredith 1983, Meredith 1994, Cronin 1995). Radio waves, microwaves and visible light waves are commonly used for data communication.

The wave-guide, as the name suggests guides light waves. In practice it is even possible to guide light waves around corners. The specific type of wave-guide to be used depends on the wavelength of the light being guided. Radio waves, which have a wavelength that is several metres long, would need an impractically large wave-guide to channel them (Connor 1972); however microwaves and visible light are commonly channelled through wave-guides (Cronin 1995). Generally speaking, microwaves are channelled through wave-guides which are basically metallic tubes, while light of shorter wave length, including visible light is usually channelled through optic fibre wave guides.

Microwave frequencies begin at about 0.3 GHz and continue until about 40 GHz. The corresponding wavelengths are less than one metre long. Frequencies above 40 GHz are referred to as millimetre waves, because their wavelengths are only millimetres in length. The microwave frequencies are broken up into a number of bands for convenience of design and specification. Common microwave guides are rectangular, as shown in Figure 17.1, circular, or ridged. Commonly used rectangular wave-guides have an aspect ratio $\left(r = \frac{a}{b}\right)$ of approximately 0.5.

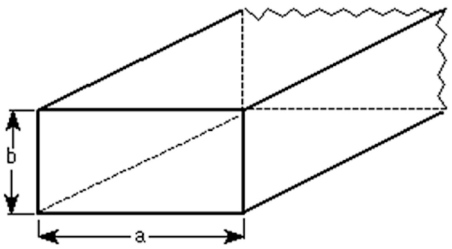

Figure 17.1: Rectangular wave guide.

Wave-guides are used principally at frequencies in the microwave range. Inconveniently large guides would be required to transmit radio-frequency power at longer wavelengths. For example, in the X-Band frequency range of 8.2 to 12.4 GHz, the standard rectangular wave-guide has an inner width of 2.286 cm and an inner height of 1.016 cm (Department of Defense 1999).

17.2 Waveguide Modes

A mathematical treatment is required to explore all the essential features of wave-guide propagation. With electromagnetic radiation it is expected that both electric and magnetic fields should satisfy Maxwell's equations. If a co-ordinate system, similar to that shown in Figure 17.1, is adopted and the electric field is assumed to be oriented in the y direction, then Maxwell's wave equation for the electric field is:

$$\frac{\partial^2 \vec{E}_y}{\partial x^2} + \frac{\partial^2 \vec{E}_y}{\partial y^2} + \frac{\partial^2 \vec{E}_y}{\partial z^2} = \mu\varepsilon \frac{\partial^2 \vec{E}_y}{\partial t^2} \tag{17.1}$$

If Ey is a monochromatic wave, then the solution of equations (17.1) will be of the form E = X(x)Y(y)Z(z)T(t). If the walls of the wave-guide are assumed to be perfect conductors, then the tangential components of the electrical field on all of the internal walls of the wave guide must be zero. Substituting the expected solution for E into equation (17.1) yields:

$$\frac{\partial^2 X}{\partial x^2} YZT + \frac{\partial^2 Y}{\partial y^2} XZT + \frac{\partial^2 Z}{\partial z^2} XYT = \mu\varepsilon \frac{\partial^2 T}{\partial t^2} XYZ \tag{17.2}$$

If the time dependency is assumed to be e^{jwt}, then equation (17.2) becomes:

$$\frac{\partial^2 X}{\partial x^2} YZe^{j\omega t} + \frac{\partial^2 Y}{\partial y^2} XZe^{j\omega t} + \frac{\partial^2 Z}{\partial z^2} XYe^{j\omega t} = -\omega^2 \mu\varepsilon XYZe^{j\omega t} \tag{17.3}$$

Dividing throughout by $XYZe^{jwt}$ yields:

$$\frac{1}{X}\frac{\partial^2 X}{\partial x^2} + \frac{1}{Y}\frac{\partial^2 Y}{\partial z^2} + \frac{1}{Z}\frac{\partial^2 Z}{\partial z^2} = -\omega^2 \mu\varepsilon \tag{17.4}$$

Because the right hand side of this equation is a constant, it follows that the left hand side must also be a constant and can be expressed as:

$$k_x{}^2 + k_y{}^2 + k_z{}^2 = \left(\frac{\omega}{c}\right)^2 \tag{17.5}$$

where $c = \frac{1}{\sqrt{\mu\varepsilon}}$

Therefore:

$$\frac{1}{X}\frac{\partial^2 X}{\partial x^2} = -k_x{}^2; \frac{1}{Y}\frac{\partial^2 Y}{\partial z^2} = -k_y{}^2; \frac{1}{Z}\frac{\partial^2 Z}{\partial z^2} = -k_z{}^2 \tag{17.6}$$

The solution for *X(x)* will be of the form:

$$X(x) = Ae^{jk_x x} + Be^{-jk_x x} \tag{17.7}$$

Applying the boundary condition that the fields must be zero at x = 0 yields:

$$\begin{aligned} &Ae^0 + Be^0 = A + B = 0 \\ &\therefore A = -B \end{aligned} \tag{17.8}$$

Substituting into equation (17.7) yields:

$$X(x) = A\left(e^{jk_x x} - e^{-jk_x x}\right) = 2jASin(k_x x) \tag{17.9}$$

Since A is an arbitrary complex number anyway, the *2j* can be absorbed into it to yield:

$$X(x) = ASin(k_x x) \tag{17.10}$$

For the tangential fields to be zero at x = a; $Sin(k_x a) = 0$. This is only possible when

$$k_x = 0, \frac{\pi}{a}, \frac{2\pi}{a}, \ldots, \frac{n\pi}{a}, \ldots$$

Therefore:

$$X(x) = ASin\left(\frac{n\pi}{a}x\right) \tag{17.11}$$

The solution for Z*(z)* will be of the form:

$$Z(z) = Ce^{jk_z z} + De^{-jk_z z} \tag{17.12}$$

When combined with the time dependency, this yields:

$$Z(z)e^{j\omega t} = Ce^{j(\omega t + k_z z)} + De^{j(\omega t - k_z z)} \tag{17.13}$$

This represents two waves traveling in opposite directions along the wave-guide. Focusing on the wave traveling in the positive z direction and combining all the components of the solution yields:

$$E_y = X(x)Y(y)Z(z) = ADSin\left(\frac{n\pi}{a}x\right)Y(y)e^{j(\omega t - k_z z)} \tag{17.14}$$

Combining A and D into a single constant yields:

$$E_y = E_{yo}Sin\left(\frac{n\pi}{a}x\right)Y(y)e^{j(\omega t - k_z z)} \tag{17.15}$$

17.3 Other Wave-guide Modes

The derivation presented above applies only to TE_{n0} modes. Other transverse electrical modes may have an Ex component to the electrical field, in which case the tangential components of the Ex component at the bottom and top of the wave-guide must also be zero. This implies that $E_x \propto Sin\left(\frac{m\pi}{b}y\right)$. Therefore:

$$E_x = E_{xo} X'(x) Sin\left(\frac{m\pi}{b} y\right) e^{j(\omega t - k_z z)} \tag{17.16}$$

The magnetic field components can be determined from Maxwell's equations:

$$\frac{\partial E_y}{\partial x} - \frac{\partial E_x}{\partial y} = \mu \frac{\partial H_z}{\partial t} = -j\omega\mu H_z \tag{17.17}$$

Therefore:

$$H_z = \frac{j}{\omega\mu}\left[E_{yo}\left(\frac{n\pi}{a}\right) Y(y) Cos\left(\frac{n\pi}{a} x\right) - E_{xo}\left(\frac{m\pi}{b}\right) X'(x) Cos\left(\frac{m\pi}{b} y\right)\right] e^{j(\omega t - k_z z)} \tag{17.18}$$

Now, Hz must also satisfy its own wave equation of the form:

$$\frac{\partial^2 \vec{H}_z}{\partial x^2} + \frac{\partial^2 \vec{H}_z}{\partial y^2} + \frac{\partial^2 \vec{H}_z}{\partial z^2} = \mu\varepsilon * \frac{\partial^2 \vec{H}_z}{\partial t^2} \tag{17.19}$$

This could only happen if $Y(y) = Cos\left(\frac{m\pi}{b} y\right)$ and $X'(x) = Cos\left(\frac{n\pi}{a} x\right)$. Therefore:

$$E_y = E_{yo} Sin\left(\frac{n\pi}{a} x\right) Cos\left(\frac{m\pi}{b} y\right) e^{j(\omega t - k_z z)} \tag{17.20}$$

and

$$E_x = E_{xo} Cos\left(\frac{n\pi}{a} x\right) Sin\left(\frac{m\pi}{b} y\right) e^{j(\omega t - k_z z)} \tag{17.21}$$

Therefore it is possible to define all transverse electrical modes in terms of two integers, m and n (ie. TE_{nm}), such that they designate the number of components of the electric field vector and the number of half wave "lobes" associated with their distribution across the wave-guide. Figure 17.2 shows the field distributions across the wave-guide's cross section for several lower order modes of a rectangular wave-guide.

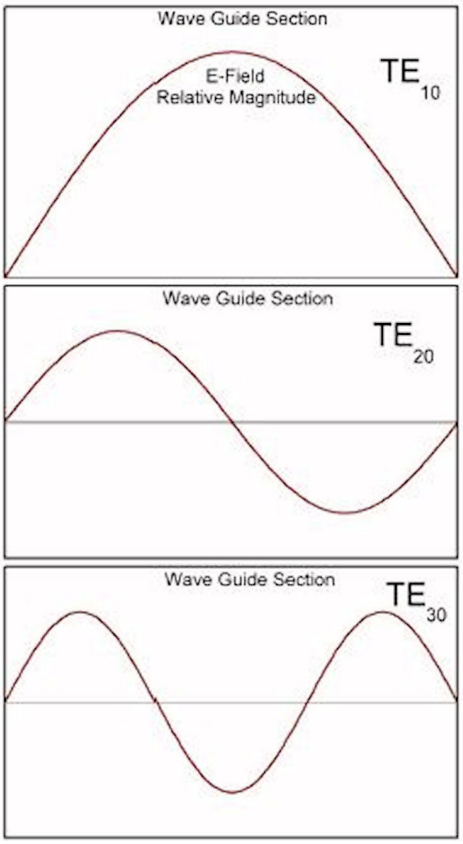

Figure 17.2: Field distributions for TE_{10}, TE_{20} and TE_{30} modes of a rectangular wave-guide without dielectric loads.

17.4 Transverse Magnetic Modes

The derivation presented so far has assumed that Ez = 0. It may be possible to generate modes in which Ez ≠ 0. In these cases, the magnetic fields become transverse such that:

$$H_x \propto Cos\left(\frac{m\pi}{b}y\right) \quad and \quad H_y \propto Cos\left(\frac{n\pi}{a}x\right) \tag{17.22}$$

These transverse magnetic modes are defined using the TM_{nm} nomenclature. Because the divergence of the magnetic field is always zero, it turns out that TM modes with either m or n being zero are not permissible.

17.5 Wave-guide Cut-off Conditions

The complete set of allowable propagation modes for a particular wave-guide design can be deduced from equation (17.5). After substituting for k_x^2 and k_y^2 and rearranging this becomes:

$$k_z = \sqrt{\left(\frac{\omega}{c}\right)^2 - \left(\frac{n\pi}{a}\right)^2 - \left(\frac{m\pi}{b}\right)^2} \tag{17.23}$$

If $\left(\frac{\omega}{c}\right)^2 < \left(\frac{n\pi}{a}\right)^2 + \left(\frac{m\pi}{b}\right)^2$ then k_z becomes an imaginary number that can be expressed as $k_z = -ja$ and equation (17.20) can be rewritten as:

$$E_y = E_{yo} Sin\left(\frac{n\pi}{a}x\right) Cos\left(\frac{m\pi}{b}y\right) e^{j(\omega t + j\alpha z)} = E_{yo} Sin\left(\frac{n\pi}{a}x\right) Cos\left(\frac{m\pi}{b}y\right) e^{j\omega t} \cdot e^{-\alpha z} \tag{17.24}$$

This describes an exponentially decaying wave that will not propagate very far through the wave-guide.

On the other hand, if $\left(\frac{\omega}{c}\right)^2 > \left(\frac{n\pi}{a}\right)^2 + \left(\frac{m\pi}{b}\right)^2$ then k_z is a real number and equation (17.20) describes a propagating wave traveling in the positive z direction along the length of the wave-guide. Therefore the critical case when this transition from non-propagating to propagating wave occurs is when:

$$\left(\frac{\omega_c}{c}\right)^2 = \left(\frac{n\pi}{a}\right)^2 + \left(\frac{m\pi}{b}\right)^2 \quad or \quad \omega_c = c\sqrt{\left(\frac{n\pi}{a}\right)^2 + \left(\frac{m\pi}{b}\right)^2} \tag{17.25}$$

The dominant mode in a particular wave-guide is the mode having the lowest cutoff frequency (w_c). For rectangular wave-guides this is the TE_{10} mode. Modes that have the same cutoff frequency but different field distributions are said to be *degenerate*. If operation is below the cut-off frequency the wave is said to be *evanescent*.

17.6 Wavelength in a Wave-guide

By definition, $k_z = \frac{2\pi}{\lambda_g}$ it is apparent that:

$$\lambda_g = \frac{2\pi}{k_z} = \frac{2\pi}{\sqrt{\left(\frac{\omega}{c}\right)^2 - \left(\frac{n\pi}{a}\right)^2 - \left(\frac{m\pi}{b}\right)^2}} \tag{17.26}$$

In free space, $\frac{\omega}{c}=\frac{2\pi}{\lambda_o}$ therefore:

$$\lambda_g=\frac{2\pi}{\sqrt{\left(\frac{2\pi}{\lambda_o}\right)^2-\left(\frac{n\pi}{a}\right)^2-\left(\frac{m\pi}{b}\right)^2}}=\frac{\lambda_o}{\sqrt{1-\left(\frac{n\lambda_o}{2a}\right)^2-\left(\frac{m\lambda_o}{2b}\right)^2}} \tag{17.27}$$

17.7 Wave Impedance in a Wave-guide

The wave impedance in the wave-guide is defined as:

$$\eta_g=\frac{|E_y|}{|H_x|} \tag{17.28}$$

Now H_x can be deduced from Maxwell's equations:

$$H_x=\frac{\frac{\partial E_y}{\partial z}-\frac{\partial E_z}{\partial y}}{j\mu\omega} \tag{17.29}$$

Therefore:

$$H_x=\frac{k_z}{\mu\omega}E_{yo}Sin\left(\frac{n\pi}{a}x\right)Cos\left(\frac{m\pi}{b}y\right)e^{j(\omega t-k_z z)} \tag{17.30}$$

Substituting into equation (17.28) yields:

$$\eta_g=\frac{E_{yo}Sin\left(\frac{n\pi}{a}x\right)Cos\left(\frac{m\pi}{b}y\right)e^{j(\omega t-k_z z)}}{\frac{k_z}{\mu\omega}E_{yo}Sin\left(\frac{n\pi}{a}x\right)Cos\left(\frac{m\pi}{b}y\right)e^{j(\omega t-k_z z)}}=\frac{\mu\omega}{k_z} \tag{17.31}$$

Substituting for k_z and rearranging the equation yields:

$$\eta_g=\frac{\omega\mu}{\sqrt{\left(\frac{\omega}{c}\right)^2-\left(\frac{n\pi}{a}\right)^2-\left(\frac{m\pi}{b}\right)^2}}=\frac{\mu c}{\sqrt{1-\left(\frac{n\pi c}{a\omega}\right)^2-\left(\frac{m\pi c}{b\omega}\right)^2}} \tag{17.32}$$

Remembering that in free space $\frac{\omega}{c}=\frac{2\pi}{\lambda_o}$ and $\eta_o = \mu c$ yields:

$$\eta_g = \frac{\eta_o}{\sqrt{1-\left(\frac{n\lambda_o}{2a}\right)^2-\left(\frac{m\lambda_o}{2b}\right)^2}} \tag{17.33}$$

It is important to note that because the denominator in equation (17.33) will be less that one for all propagating modes, the wave impedance for a TE mode in a wave-guide will always be greater than the wave impedance in free space.

17.8 Power Flow along a Wave-guide Propagating in TE_{10} Mode

Power flow along a wave-guide can be deduced from Poynting's Theorem. The total power per unit surface area of the cross-section of the wave guide is given by the Poynting Vector:

$$p = \vec{E}\times\vec{H} = -E_y H_x \tag{17.34}$$

Substituting from equations (17.20) and (17.30) and putting m = 0 yields:

$$p = \frac{k_z {E_o}^2}{\omega\mu} Sin^2\left(\frac{n\pi}{a}x\right) e^{2j(\omega t - k_z z)} \tag{17.35}$$

The total power propagating along the wave-guide is found by integrating the power density over the full cross-section of the guide. Therefore:

$$P = \int_0^a\int_0^b p\cdot dy\cdot dx = \int_0^a\int_0^b \frac{k_z {E_o}^2}{\omega\mu} Sin^2\left(\frac{n\pi}{a}x\right) e^{2j(\omega t - k_z z)}\cdot dy\cdot dx \tag{17.36}$$

Evaluating the integrals yields:

$$P = \frac{k_z abE_o^2}{2\omega\mu} e^{2j(\omega t - k_z z)} \tag{17.37}$$

This represents the instantaneous power at any given time. It is more useful to speak in terms of average power, which can be found using:

$$\overline{P} = \frac{k_z abE_o^{\,2}}{T2\omega\mu} \int_0^T e^{2j(\omega t - k_z z)} \cdot dt \tag{17.38}$$

Note: $\frac{1}{T}\int_0^T e^{2j(\omega t - k_z z)} \cdot dt = \frac{1}{2}$, therefore:

$$\overline{P} = \frac{k_z abE_o^{\,2}}{4\omega\mu} \tag{17.39}$$

Note: $\eta_g = \frac{\omega\mu}{k_z}$, therefore:

$$\overline{P} = \frac{abE_o^{\,2}}{4\eta_g} \tag{17.40}$$

The TE_{10} mode is usually chosen for microwave heating systems. If the dimensions of the guide are small enough, no other modes will propagate. In the S-Band frequency range of 2.0 to 4.0 GHz (See Figure 13.4) the standard rectangular wave-guide has an inner width of 8.6 cm and an inner height of 4.3 cm (US Naval Air Systems Command 1999). When a dielectric load is introduced into the wave-guide these field distributions are distorted by the reflections and internal attenuation associated with the material's dielectric properties.

In practical terms, wave-guide applicators allow conveyor belt processing techniques to be used, provided appropriately designed wave-guide chokes and feed tunnels are employed to prevent radiation from the system into open space (Metaxas and Meredith 1983). Another important consideration is that the microwave fields are not even across the waveguide, therefore the material to be heated must be positioned to coincide with the peak of the microwave field intensity.

17.9 Cylindrical Wave Guides

Occasionally it is appropriate to use a cylindrical wave guide applicator rather that a rectangular one. For cylindrical coordinates, the electric field associated with a TE mode wave propagating in the z direction in a resonant cavity (or oven) is:

$$E_\phi = \frac{j\omega\mu}{\left(\frac{p'_{\nu n}}{a}\right)} \left[ASin(\nu\phi) + BCos(\nu\phi)\right] J'_\nu \left(\frac{p'_{\nu n}}{a}\rho\right) Sin\left(\frac{l\pi}{d}z\right) e^{j\omega t} \tag{17.41}$$

Where: A and B are constants associated with the amplitude of the field; a is the radius of the cylindrical chamber and d is the length of the chamber; and ν , n, and l are the mode numbers for the corresponding field distributions, w is the angular velocity of the wave, $J'_{\nu}(x) = \frac{d}{dx} J_{\nu}(x)$, $J_n(x)$ is the nth Bessel function of x, and t is time.

The term p'_{vn} is the nth root of $J'_{vn}(x)$. The first few values for p'_{vn} are shown in Table 17.1:

Table 17.1: Values for p'_{vn}.

	n = 1	n = 2	n = 3
v = 0	0.00	3.8317	7.0156
v = 1	1.8412	5.3314	8.5363
v = 2	3.0542	6.7061	9.9695

The cut off frequency for cylindrical guides is given by:

$$f_c = \frac{c}{2\pi} \frac{p'_{\nu n}}{a} \tag{17.42}$$

In this case the lowest order mode is the TE_{11} mode and at 2.45 GHz, the minimum radius of the chamber will be 36 mm. it is important to only allow one mode to propagate in the chamber. The next mode is the TM_{01} mode, which has a minimum chamber radius of 49 mm at 2.45 GHz.

17.10 Microwave Ovens

To some extent, microwave ovens must be visualised as a section of over-sized wave guide with a short circuit at either end into which microwave energy is injected. Single and multi-mode resonators usually require batch-processing techniques. The electric field within multi-mode resonators, such as a microwave oven, is a very complex standing wave involving several modes. The electric field associated with the wave propagating in the z direction in a resonant cavity (or oven) is:

$$E_y = E_o Sin\left(\frac{n\pi}{a}x\right) Cos\left(\frac{m\pi}{b}y\right) Sin\left(\frac{l\pi}{d}z\right) e^{j(\omega t)} \tag{17.43}$$

The electric field within a microwave oven is a very complex standing wave involving several modes. The resulting wave must satisfy (Metaxas and Meredith 1983):

$$f_r = \frac{c}{2}\sqrt{\left(\frac{n}{a}\right)^2 + \left(\frac{m}{b}\right)^2 + \left(\frac{l}{d}\right)^2} \tag{17.44}$$

where d is the third dimension of the oven or cavity.

The field distribution inside the resonator depends on the mode, or combination of modes, which establish within the cavity. A multi-mode resonator will simultaneously support many transverse electrical and transverse magnetic modes. These are indicated as TEmnl and TMmnl (Meredith 1994). The final field distribution in the cavity will be the sum of all the fields associated with the modes excited at any given frequency (Metaxas and Meredith 1983). Table 17.2 lists the possible modes for a microwave oven operating at 2.45 GHz with internal dimensions of 29 cm × 29 cm × 19 cm, which lead to a wavelength in the interval 12.0 cm < $\lambda 0$ < 12.5 cm.

The result of these various modes is a non-uniform field distribution within the cavity. Microwave heating occurs where peaks in the microwave fields occur. Little heating occurs at the nodes of the electric field, except in the case of small particles of ferrite based materials where eddy currents, created by the microwave's magnetic field, induce resistive heating (Takayama, *et al.* 2005).

Because of this uneven field distribution, most domestic microwave ovens employ a turntable to move the heated load through the microwave field to more evenly irradiate the load. The average power in a microwave oven cavity can be determined using (Metaxas and Meredith 1983):

$$\overline{P} = \frac{\pi f abd \varepsilon E_o^{\,2}}{2Q} \tag{17.45}$$

Metaxas and Meredith (1983) have published charts that can be used to calculate the Q-factor based on the dielectric properties of the material and the volume fraction of the object compared with the volume of the oven cavity.

Table 17.2: Allowable modes (Source: Vollmer 2004).

$\lambda 0$ (cm)	l	m	n
12.103	1	1	3
12.274	2	4	1
12.274	4	2	1
12.277	2	3	2
12.277	3	2	2
12.375	0	1	3

Unfortunately, the electric field strength inside a microwave applicator is very difficult to determine theoretically as the inclusion of a dielectric material within a microwave oven effectively alters the field distribution (Metaxas and Meredith 1983). Many authors (Van Remmen, *et al.* 1996, Perre and Turner 1997, Zhao, *et al.* 1998) have adopted a variety of numerical techniques, such as the Finite-Difference Time-Domain technique, to predict the electric field strength within irradiated objects.

17.11 Finite-Difference Time-Domain (FDTD) Simulating Microwave Field Distributions in Applicators

Maxwell's equations can be formulated to allow numerical techniques such as the Finite-Difference Time-Domain (FDTD) method (Taflove 1998), the Finite Element method or the Method of Lines to be used to calculate the electromagnetic field strength (Walker 2001). The FDTD simulation method of determining field distributions is a popular electromagnetic modelling technique. It is easy to understand, and easy to implement.

The FDTD method, as first proposed by Yee (Yee 1966), is a simple and elegant way to transform the differential form of Maxwell's equations into difference equations. Yee used an electric field grid, which was offset both spatially and temporally from a magnetic field grid to obtain update equations that yield the present fields throughout the computational domain in terms of the past fields. This is illustrated in Figure 17.3.

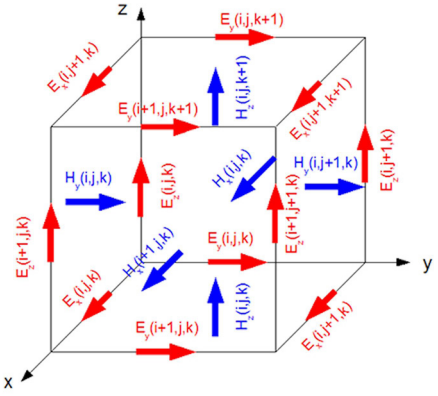

Figure 17.3: Single cell from the computational space used to compute Maxwell's equations using FDTD techniques.

The update equations are used in a leap-frog scheme to incrementally march the electric and magnetic fields forward in time; therefore this numerical technique is a simulation of the microwave field associated with some predetermined initial conditions for each time step rather than a direct solution of the field equations in space and time.

The basic form of the equations used in the FDTD algorithm is:

$$E_x^{n+1}(i,j,k) = E_x^{n}(i,j,k) + \frac{\Delta t}{\varepsilon}\left[\frac{H_z^{n+\frac{1}{2}}(i,j+1,k) - H_z^{n+\frac{1}{2}}(i,j,k)}{\Delta y} - \frac{H_y^{n+\frac{1}{2}}(i,j,k+1) - H_y^{n+\frac{1}{2}}(i,j,k)}{\Delta z}\right] \tag{17.46}$$

$$H_x^{n+\frac{1}{2}}(i,j,k) = H_x^{n-\frac{1}{2}}(i,j,k) + \frac{\Delta t}{\mu}\left[\frac{E_y^{n}(i,j,k+1) - H_y^{n}(i,j,k)}{\Delta z} - \frac{E_z^{n}(i,j+1,k) - H_z^{n}(i,j,k)}{\Delta y}\right] \tag{17.47}$$

In this case the equations calculate the electric and magnetic fields in the x direction. Similar equations are required to calculate Ey, Ez, Hy and Hz.

The FDTD method was originally developed to solve electromagnetic transmission problems associated with the communications industry (Kopyt, *et al.* 2003), but it is now commonly used to determine electromagnetic field distributions within microwave applicators (Kopyt, *et al.* 2003).

Every modelling technique has some strengths and some weaknesses. FDTD is a very versatile modelling technique. It is very intuitive, so users can easily understand how to use it and what to expect from a given model.

FDTD is a time domain technique, and when a time-domain pulse (such as a Gaussian pulse) is used as an input to the computational model, a wide frequency range can be explored in a single simulation. This is extremely useful in applications where resonant frequencies are not known or when broadband performance is desirable.

Since FDTD is a time-domain technique which finds the E/H fields everywhere in the computational domain, it lends itself to providing animation displays (movies) of the E/H field movement throughout the model. FDTD also allows the user to specify the material properties at all points within the computational domain, which provides useful insight into the field distributions inside dielectric materials as they are processed using microwave systems.

If aliasing of the final solution is to be avoided (Vandoren 1982), the grid size must be small enough so that the electromagnetic field does not change significantly from one grid cell to the next. Similarly the time steps for each computational cycle must satisfy the Courant stability criterion (Yee 1966, Taflove 1998, Walker 2001). This implies that the simulated time step for many problems may be no more than a few picoseconds. Therefore solving heating problems that may span many seconds or minutes of real time requires a significant number of computational iterations.

For computational stability to be satisfied (Yee 1966, Walker 2001), the time step used in the program must satisfy:

$$\Delta t = \frac{\sqrt{\Delta x^2 + \Delta y^2 + \Delta z^2}}{c} \tag{17.48}$$

When establishing an appropriate grid for analysis, it must be remembered that the wavelength of the microwaves inside a dielectric material is:

$$\lambda = \frac{\lambda_o}{\sqrt{\kappa'}} \tag{17.49}$$

The values of Δx, Δy and Δz must be small compared to λ to ensure accurate simulations.

Since FDTD requires that the entire computational domain be gridded, and these grids must be small compared to the smallest wavelength and smaller than the smallest feature in the model, very large computational domains can be developed, which result in very long calculation times.

To put this into some perspective, simulating the first 20 nanoseconds of electromagnetic activity inside a 335 mm by 335 mm by 205 mm microwave oven that has a cup (cylinder) of water in it, using a 4 mm grid, requires approximately 30 minutes of uninterrupted computational time on a Pentium 4 computer. Trying to simulate 10 minutes of real time would take 950 years on the same machine using the same code.

To place these comments into perspective, Pentium 4 processors were used in personal computers between 2000 and 2008. Pentium 4 processors that were produced after 2004 used a 64 bit instruction set and a clock speed of between 1.3 and 3.8 GHz, depending on the particular model of computer they were installed in. The calculations mentioned in the previous paragraph were performed on a personal computer with a 64 bit Pentium 4 processor operating at 2.4 GHz clock speed.

FDTD finds the E/H fields everywhere in the computational domain. If the field values at some distance (like 10 meters away) are required, the computational domain will be excessively large. Far field extensions, which apply a Fast Fourier Transformation to the field distribution in a fixed plane of the FDTD computational domain, are available, but this usually requires some post processing rather than direct calculations.

Most authors use FDTD and other numerical techniques to analyse "static systems". This implies that apart from the initial field excitation imposed onto the system, all other components are stationary. Commercial microwave applicators use mode stirrers (Metaxas and Meredith 1983) or movement of the heated product relative to the microwave fields to deliberately perturb the fields and more evenly irradiate the load. Consequently, any attempt to evaluate the electric field, including numerical techniques, only provides an approximation of the field strength (Kopyt, *et al.* 2003). Unfortunately, direct measurement of the field strength is virtually impossible also because the high intensity fields will damage any instruments inside the microwave applicator and a probe will perturb the field it is trying to measure anyway.

The main advantage of the FDTD analysis technique is its ability to provide insight into the field distribution inside complex microwave systems. For example, including various sized cylinders of water in a microwave oven has a profound effect on the microwave field strength and distribution inside the cavity. This can be clearly demonstrated when an FDTD simulation for an oven is performed. The results are shown in Figure 17.4.

Clearly the inclusion of the water in the microwave oven perturbs the fields and reduces the quality factor (Q) of the resonant cavity. In the empty oven there is little damping of the fields, so the intensity of the microwaves is much higher than when there is a substantial volume of material in the oven.

Because the wave patterns inside the microwave cavity are uneven, most systems employ mode stirrers or turn tables to better distribute the microwave fields through the heated material. This is quite effective in most cases, however many materials will

have higher internal temperatures than surface temperatures (Zielonka and Gierlik 1999); therefore care must be taken when handling microwave heated food.

17.12 Microwave Safety

There are very strict regulations governing how much radiation is allowed to be emitted from microwave ovens: they could be a health risk and they could interfere with other electronic apparatus. For example, according to the Radiation Protection Standard for Maximum Exposure Levels (Australian Radiation Protection and Nuclear Safety Agency 2002), the maximum time average operator exposure to electric fields at 2.45 GHz is 137 V m^{-1} (RMS), while the exposure for the general public must be below 61.4 V m^{-1} (RMS).

Because a microwave oven is a Faraday cage little radiation is expected to escape. The most crucial part is the door, which is equipped with additional so-called $\lambda/4$ radiation traps (Vollmer 2004).

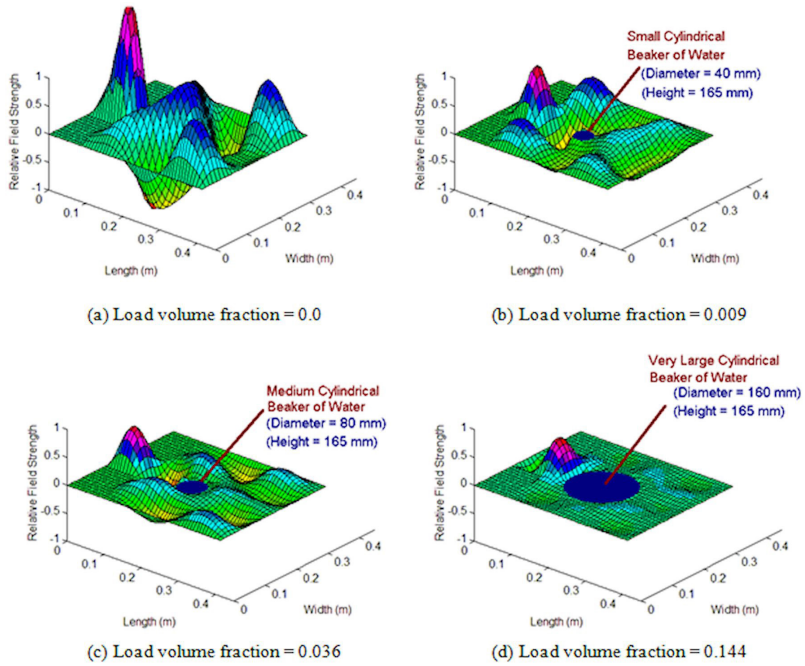

Figure 17.4: The effect of varying the load size inside a 335 mm by 335 mm by 205 mm microwave oven operating at 2.45 GHz.

17.13 Antenna Applicators

An antenna is a radiating structure that usually launches electromagnetic energy from some electrical circuit or waveguide structure into free space. Antennae are usually associated with communication systems however they can be used to apply electromagnetic energy to materials that are extensive and can not be enclosed in a normal applicator. Although any antenna could be used as an applicator, horn antennae are commonly used for this purpose. They are simple to fabricate and readily fit to the end of a waveguide. When used to apply electromagnetic energy for heating purposes, these antennae operate in the "Near Field".

17.13.1 Analysis of a Horn Antenna

In order to properly understand the energy requirements for microwave antenna applicator, an analysis of the microwave field intensity in the Near Field, immediately in front of a pyramidal horn antenna, is required. This problem is not trivial and developing a method that can provide an exact analysis of the field distribution is unlikely. Direct measurement of these fields is extremely hazardous, and should therefore be avoided. The following sections will outline three techniques that can yield estimates of the expected microwave field strength in front of the antenna.

17.13.2 A Uniformly Illuminated Aperture Approximation

According to Huygen's principle (Connor 1972), when the source of radiation is an EM field propagating through a waveguide structure into a horn antenna, the radiating sources can be regarded as an array of minute radiators distributed over the entire antenna aperture. The total field at some point in the space in front of the antenna is therefore determined by integrating the contributions from these spatially distributed sources. As a first approximation to this problem, the aperture of the horn antenna can be regarded as a uniformly illuminated rectangular source. In this case the field will be approximated by:

$$E_P \approx \frac{E_o}{4\pi} \int_{-B/2}^{B/2} \int_{-A/2}^{A/2} \frac{e^{-j\beta_o \sqrt{(x-x')^2+(y-y')^2+z^2}}}{\sqrt{(x-x')^2+(y-y')^2+z^2}} \cdot dx' \cdot dy' \tag{17.50}$$

An approximation of this integral (Appendix A) is:

$$E_P \approx \frac{j\pi E_o e^{-j\beta_o z}}{2\beta_o \lambda z}\left\{\begin{array}{l} S\left[-\sqrt{\frac{\beta_o}{\pi}}\left(\frac{A}{2}+x\right)\right]\left\{S\left[\sqrt{\frac{\beta_o}{\pi}}\left(\frac{B}{2}-y\right)\right]-S\left[-\sqrt{\frac{\beta_o}{\pi}}\left(\frac{B}{2}+y\right)\right]\right\}- \\ C\left[-\sqrt{\frac{\beta_o}{\pi}}\left(\frac{A}{2}+x\right)\right]\left\{C\left[\sqrt{\frac{\beta_o}{\pi}}\left(\frac{B}{2}-y\right)\right]-C\left[-\sqrt{\frac{\beta_o}{\pi}}\left(\frac{B}{2}+y\right)\right]\right\}+ \\ C\left[\sqrt{\frac{\beta_o}{\pi}}\left(\frac{A}{2}-x\right)\right]\left\{C\left[\sqrt{\frac{\beta_o}{\pi}}\left(\frac{B}{2}-y\right)\right]-C\left[-\sqrt{\frac{\beta_o}{\pi}}\left(\frac{B}{2}+y\right)\right]\right\}- \\ S\left[\sqrt{\frac{\beta_o}{\pi}}\left(\frac{A}{2}-x\right)\right]\left\{S\left[\sqrt{\frac{\beta_o}{\pi}}\left(\frac{B}{2}-y\right)\right]-S\left[-\sqrt{\frac{\beta_o}{\pi}}\left(\frac{B}{2}+y\right)\right]\right\} \end{array}\right\} \tag{17.51}$$

17.13.3 A Numerical Integration Approximation

Although closed solutions like equation (17.51) are very convenient for fast calculations, they do not account for the phase delay introduced as the microwave fields propagate along the flare of the horn antenna (Figure 17.5); nor do they account for the tapered field distribution in the aperture associated with the dominant TE_{10} mode propagating in the feeding wave guide.

Based on the geometry of the horn antenna, sown in Figure 17.5, a more accurate approximation of the problem can be described by:

$$E_P = \frac{E_a}{4\pi}\int_{-B/2}^{B/2}\int_{-A/2}^{A/2}\cos\left(\frac{\pi}{A}x'\right)\frac{e^{-j\beta_o\left\{\sqrt{(x-x')^2+(y-y')^2+z^2}+\sqrt{R_o{}^2+(x')^2}+\sqrt{R_o{}^2+(y')^2}\right\}}}{\sqrt{(x-x')^2+(y-y')^2+z^2}}\cdot dx'\cdot dy' \tag{17.52}$$

Unfortunately there is no simple solution for equation (17.52); however the integral can be evaluated numerically using Simpson's numerical approximation.

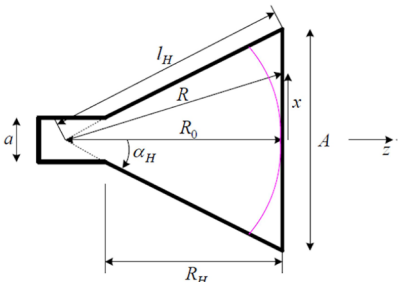

Figure 17.5: Geometry of a horn antenna showing a propagating wave front in the flare of the antenna (Source: Nikolova 2012).

17.13.4 Other Options

It is possible to simulate the propagation of microwave energy from a horn antenna using the Finite-Difference Time-Domain (FDTD) technique. It is also possible to assume a spherical wave emanates from the aperture of the horn antenna.

All four techniques for estimating the microwave field strength in the near field of the horn antenna suggest that the field intensity dissipates very rapidly with distance from the antenna (Figure 17.6). Although there is some discrepancy in the estimated field strength between the different techniques at very close range, the differences in estimated field strength at a range of 0.05 m and beyond is negligible. The average relative field strength, from all four techniques, at a range of 0.18 m from the antenna's aperture is -0.093.

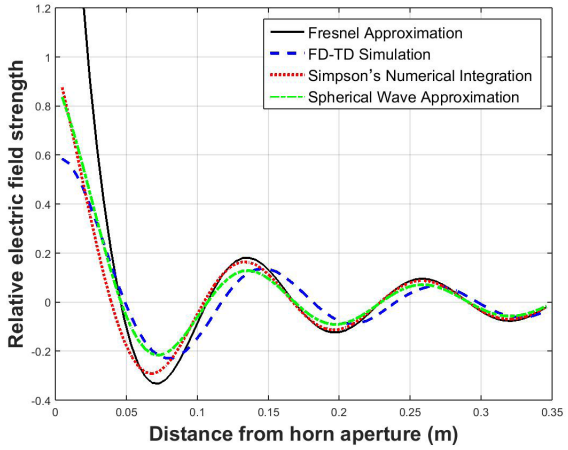

Figure 17.6: Comparison of estimated relative instantaneous field strength along the centre line in front of the horn antenna as a function of distance from the antenna's aperture plane.

The peak electric field strength of a microwave propagating through a waveguide in TE_{10} mode is calculated by:

$$E_o = \sqrt{\frac{4\eta_o \overline{P}}{ab\sqrt{1-\left(\frac{n\lambda_o}{2a}\right)^2-\left(\frac{m\lambda_o}{2b}\right)^2}}} \tag{17.53}$$

As an example, the peak field strength in the waveguide for 2 kW of microwave power is approximately 38,950 V m^{-1} and the Root Mean Square (RMS) field strength is

approximately 27,540 V m^{-1}. Allowing for expansion of the field in the horn antenna, the field strength at the aperture of the horn is approximately 19,350 V m^{-1} (RMS). Field reflections occur at the mouth of the antenna due to the sudden change in impedance as the wave transits from the horn's aperture into open space. The transmission coefficient of the horn's aperture is given by:

$$\tau = \frac{2\sqrt{1-\left(\frac{n\lambda_o}{2a}\right)^2-\left(\frac{m\lambda_o}{2b}\right)^2}}{1+\sqrt{1-\left(\frac{n\lambda_o}{2a}\right)^2-\left(\frac{m\lambda_o}{2b}\right)^2}} \tag{17.54}$$

Therefore, allowing for incomplete field transmission at the mouth of the antenna (t ~ 0.95), the field strength immediately in front of the antenna's aperture plane is 18,400 V m^{-1} (RMS) and the subsequent dissipation of the field strength with distance from the aperture (Figure 7), the RMS field strength at a range of 0.18 m from the antenna is approximately 1,710 V m^{-1} (RMS). The power density in a propagating field in front of the antenna is given by:

$$\overline{P} = \frac{E_p^2}{\eta_o} \tag{17.55}$$

Therefore the power density at 0.18 m from the antenna's aperture is approximately: 7,750 W m^{-2}, which is 7,750 J m^{-2} s^{-1} or 0.8 J cm^{-2} s^{-1}.

Nomenclature

$\overline{P}$	Microwave power (W)
w	Angular frequency of electromagnetic wave (Rad s^{-1})
h_o	Wave impedance of free space (W m^{-1})
A	Antenna aperture width (m)
a	Is the width of a waveguide (m)
B	Antenna aperture height (m)
b	Is the height of a waveguide (m)
C(x)	Is the Fresnel cosine integral equation of the parameter x. $C[x] = \int Cos\left(x^2\right) \cdot dx$
E_o	Electric field strength in the antenna's aperture (V m^{-1})
E_p	Electric field strength at any point in front of a horn antenna (V m^{-1})
E_x	Represents the electric field component of the electromagnetic wave in the x coordinate direction

H_x	Represents the magnetic field component of the electromagnetic wave in the x coordinate direction
i, j, and k	Are grid indices of the FDTD computational space in the x, y and z directions respectively
n and m	Are waveguide mode numbers
R_o	Length of the horn antenna (m)
S(x)	Is the Fresnel sine integral equation of the parameter x. $S[x] = \int Sin\left(x^2\right) \cdot dx$
x,y,z	Cartesian coordinates of a point in front of a horn antenna (m)
x', y'	Cartesian coordinates of a point in the horn antenna's aperture (m)
Δt	Is the incremental time step (s)
Δy and Δz	Are incremental spatial steps (m)
β_o	Wave number for free space (m^{-1})
ε	Is the electrical permittivity of the individual grid cell under consideration
λ_o	Is the free space wavelength of the microwave (m)
μ	Is the magnetic permeability of the individual grid cell under consideration
n	Is the current iteration in the FDTD simulation
τ	Is the transmission coefficient for the electromagnetic wave in the mouth of the horn antenna

Appendix A – Derivation of Near Field from a Uniformly Illuminated Rectangular Aperture

In this case the field along the centre line of the antenna will be approximated by:

$$E_P = \frac{zE_o}{j\lambda}\int_{-B/2}^{B/2}\int_{-A/2}^{A/2}\frac{e^{-j\beta_o\sqrt{(x-x')^2+(y-y')^2+z^2}}}{(x-x')^2+(y-y')^2+z^2}\cdot dx'\cdot dy' \tag{B1}$$

Let $\rho^2 = (x-x')^2+(y-y')^2$ and $r = \sqrt{z^2+\rho^2} = z\sqrt{1+\frac{\rho^2}{z^2}}$
If $\frac{\rho^2}{z^2} < 1.0$ then

Substituting into (B1) and ignoring the $(x-x')^2+(y-y')^2$ in the denominator of the integrand yields:

$$E_P \approx \frac{E_o}{j\lambda z}\int_{-B/2}^{B/2}\int_{-A/2}^{A/2} e^{-j\beta_o z\left(1+\frac{(x-x')^2+(y-y')^2}{2z}\right)}\cdot dx'\cdot dy' \tag{B2}$$

Now $e^{-j\theta} = Cos(-\theta)+jSin(-\theta)$ therefore:

$$E_P \approx \frac{E_o e^{-j\beta_o z}}{j\lambda z}\left\{\begin{array}{l}\int_{-B/2}^{B/2}\int_{-A/2}^{A/2} Cos\left(-\beta_o\frac{(x-x')^2+(y-y')^2}{2}\right)\cdot dx'\cdot dy'+\\ j\int_{-B/2}^{B/2}\int_{-A/2}^{A/2} Sin\left(-\beta_o\frac{(x-x')^2+(y-y')^2}{2}\right)\cdot dx'\cdot dy'\end{array}\right. \tag{B3}$$

Considering only the real part of this equation yields:

$$E_P \approx \frac{\pi E_o e^{-j\beta_o z}}{\beta_o\lambda z}\left\{C\left[\sqrt{\frac{\beta_o}{\pi}}(x-x')\right]S\left[-\sqrt{\frac{\beta_o}{\pi}}(y-y')\right]+S\left[\sqrt{\frac{\beta_o}{\pi}}(x-x')\right]C\left[-\sqrt{\frac{\beta_o}{\pi}}(y-y')\right]\right\}\Bigg|_{x'=-A/2}^{A/2}\Bigg|_{y'=-B/2}^{B/2} \tag{B4}$$

$$E_P \approx \frac{j\pi E_o e^{-j\beta_o z}}{2\beta_o\lambda z}\left\{\begin{array}{l}S\left[-\sqrt{\frac{\beta_o}{\pi}}\left(\frac{A}{2}+x\right)\right]\left\{S\left[\sqrt{\frac{\beta_o}{\pi}}\left(\frac{B}{2}-y\right)\right]-S\left[-\sqrt{\frac{\beta_o}{\pi}}\left(\frac{B}{2}+y\right)\right]\right\}-\\ C\left[-\sqrt{\frac{\beta_o}{\pi}}\left(\frac{A}{2}+x\right)\right]\left\{C\left[\sqrt{\frac{\beta_o}{\pi}}\left(\frac{B}{2}-y\right)\right]-C\left[-\sqrt{\frac{\beta_o}{\pi}}\left(\frac{B}{2}+y\right)\right]\right\}+\\ C\left[\sqrt{\frac{\beta_o}{\pi}}\left(\frac{A}{2}-x\right)\right]\left\{C\left[\sqrt{\frac{\beta_o}{\pi}}\left(\frac{B}{2}-y\right)\right]-C\left[-\sqrt{\frac{\beta_o}{\pi}}\left(\frac{B}{2}+y\right)\right]\right\}-\\ S\left[\sqrt{\frac{\beta_o}{\pi}}\left(\frac{A}{2}-x\right)\right]\left\{S\left[\sqrt{\frac{\beta_o}{\pi}}\left(\frac{B}{2}-y\right)\right]-S\left[-\sqrt{\frac{\beta_o}{\pi}}\left(\frac{B}{2}+y\right)\right]\right\}\end{array}\right. \tag{B5}$$

References

Australian Radiation Protection and Nuclear Safety Agency. 2002. RPS3 Radiation Protection Standard for Maximum Exposure Levels to Radiofrequency Fields—3 kHz to 300 GHz.

Connor, F. R. 1972, *Antennas*, London: Edward Arnold.

Cronin, N. J. 1995, *Microwave and Optical Waveguides*, Bristol: J W Arrowsmith Ltd.

Department of Defense 1999, *Electronic Warfare and Radar Systems Engineering Handbook*, Avionics Department, Naval Air Systems Command, US Navy.

Kopyt, P., Celuch-Marcysiak, M. and Gwarek, W. K. 2003 Microwave processing of temperature-dependent and rotating objects: Development and experimental verification of FDTD algorithms. In *Microwave and Radio Frequency Applications: Proceeding of the Third World Congress on Microwave and Radio Frequency Applications*, 7-16. Folz, D. C., et al. eds. The American Ceramic Society: Westerville, Ohio.

Meredith, R. J. 1994. A three axis model of the mode structure of multimode cavities. *The Journal of Microwave Power and Electromagnetic Energy*. 29(1): 31-44.

Metaxas, A. C. and Meredith, R. J. 1983, *Industrial Microwave Heating*, London: Peter Peregrinus.

Nikolova, N. K. 2012. *Modern Antennas in Wireless Telecommunications*. 5th of August, 2013. http://www.ece.mcmaster.ca/faculty/nikolova/antennas.htm

Perre, P. and Turner, I. W. 1997. Microwave drying of softwood in an oversized waveguide: Theory and experiment. *AIChE Journal*. 43(10): 2579-2595.

Taflove, A. 1998, *Computational Electrodynamics: The Finite-Difference Time-Domain Method*, Boston: Artech House.

Takayama, S., Link, G., Sato, M. and Thumm, M. 2005 Microwave sintering of metal powder compacts. In *Microwave and Radio Frequency Applications: Proceedings of the Fourth World Congress on Microwave and Radio Frequency Applications*, 311-318. Schulz, R. L. and Folz, D. C. eds. The Microwave Working Group: Arnold MD.

US Naval Air Systems Command 1999, *Electronic Warfare and Radar Systems Engineering Handbook*, Avionics Department, Naval Air Systems Command, US Navy.

Van Remmen, H. H. J., Ponne, C. T., Nijhuis, H. H., Bartels, P. V. and Herkhof, P. J. A. M. 1996. Microwave Heating Distribution in Slabs, Spheres and Cylinders with Relation to Food Processing. *Journal of Food Science*. 61(6): 1105-1113.

Vandoren, A. 1982, *Data Acquisition Systems*, Reston, Virginia: Reston Publishing.

Vollmer, M. 2004. Physics of the microwave oven. *Physics Education*. 39(1): 74-81.

Walker, S. J. 2001. Multi-mode cavity effects on the microwave heating of a ceramic slab. Unpublished PhD thesis. Newark: State University of New Jersey,

Yee, K. S. 1966. Numerical solution of initial boundary value problems involving Maxwell's equations in isotropic media. *IEEE Transactions on Antennas and Propagation*. 14(3): 302-307.

Zhao, H., Turner, I. and Torgovnikov, G. 1998. An experimental and numerical investigation of the microwave heating of wood. *The Journal of Microwave Power and Electromagnetic Energy*. 33(2): 121-133.

Zielonka, P. and Gierlik, E. 1999. Temperature distribution during conventional and microwave wood heating. *Holz als Roh- und Werkstoff*. 57(4): 247-249.

18 Quarantine and Biosecurity

Dried timber, nuts and fruits are commonly treated by chemical fumigation to control field and storage pests before being shipped to domestic and international markets. Because chemical fumigants such as methyl bromide are no longer available (Carter, *et al.* 2005), there is a heightened interest in developing non–chemical pest control. An important key to developing successful thermal treatments is to balance the need for complete insect mortality with minimal impact on the product quality. A common difficulty in using conventional hot–air disinfestation is the slow heating rate, non–uniform temperature distribution, and possible heat damage to heat–sensitive commodities (Wang, *et al.* 2003). A more promising approach is to heat the commodity rapidly using radiofrequency (RF) or microwave dielectric heating to control pest infestations (Nelson 2001, Wang, *et al.* 2003). This chapter will explore some of these applications.

18.1 Insect Control

Interest in controlling insects, using electromagnetic energy, dates back nearly 70 years. Headlee (Headlee and Burdette 1929, Headlee 1931), cites one earlier report of experiments determining lethal exposures for several insect species to 12 MHz electric fields and the body temperatures produced in honey bees due to dielectric heating. Nelson (1996) has shown that microwaves can kill insects in grain; however one of the challenges for microwave insect control is to differentially heat the insects in preference to their surrounds. Nelson (1996) also shows that differential heating depends on microwave frequency. It appears that using a 2.45 GHz microwave system, which is the frequency used in domestic microwave ovens, heats the bulk material, which then transfers heat to the insects; however lower frequencies heat the insects without raising the temperature of the surrounding material beyond 50°C (Nelson 1996).

Nzokou et al (2008) investigated the use of kiln and microwave heat treatments for the sanitisation of emerald ash borer (*Agrilus planipennis* Fairmaire) infested logs. Their microwave treatment method was conducted in a 2.8 GHz microwave oven (volume: 0.062 m^3, power: 1250 W) manufactured by Panasonic (Panasonic Co., Secaucus, New Jersey). Due to the limited volume of the microwave oven, two runs were necessary to treat logs assigned to each microwave treatment temperature. Their results showed that a temperature of 65°C was successful at sanitising the infested logs. Microwave treatment was not as effective as kiln treatment, probably because of the uneven distribution of the microwave fields and temperature inside the treated logs. This uneven temperature distribution is partly due to the nature of microwave heating, but may also be due to their choice of microwave chamber used during their experiments.

A specialized multiple-magnetron, microwave chamber was designed and built by the University of Melbourne (Harris, *et al.* 2011) to facilitate research into treatment of timber components. The microwave chamber provides three power levels (2 kW, 4 kW and 6 kW) by engaging appropriate numbers of standard 1 kW microwave magnetrons. The microwave chamber (Figure 18.1) consisted of two compartments, one to house the high voltage electrical components and the other was designed as the treatment compartment. The treatment compartment was a stainless steel enclosure, which was approximately 0.8 m^3 in volume. This kind of chamber would have been more appropriate for the experiments conducted by Nzokou et al (2008).

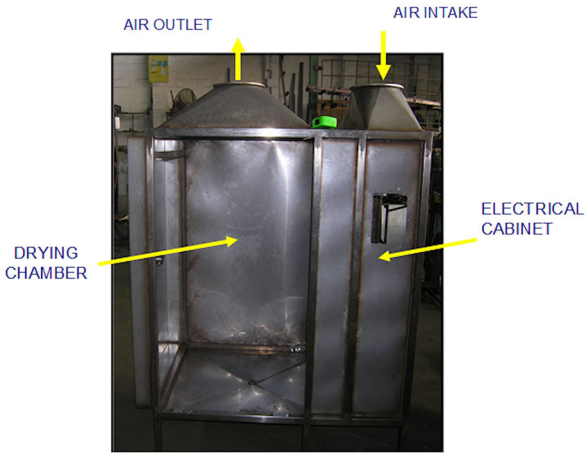

Figure 18.1: The microwave drying chamber showing the various components of the system (Source: Harris, et al. 2011).

In spite of the poor microwave heat distributions in the experiments conducted by Nzokou et al (2008), with the high costs and level of energy needed to thoroughly heat logs to the desired 65 °C using conventional heating, microwave heating is still a very attractive solution for rapid heat sterilisation of infested wood materials (Nzokou, *et al.* 2008).

The problem of ensuring appropriate temperature distribution inside treated materials can be easily overcome by using appropriate microwave applicators rather than a multi-mode cavity (Torgovnikov and Vinden 2009). Several options are available including conveyer belt feeds through a long choke tunnel into a purpose built applicator (Torgovnikov and Vinden 2009), or projecting a very intense but short duration microwave field pulse into the material, using an antenna.

Plaza *et al.* (2007) have developed a system which employs a circular wave-guide energized by two microwave sources oriented at 90 ° to one another. This orthogonal orientation of the microwave fields ensures that they do not interfere with each other, but provides a high power source from relatively cheap mass produced 1 kW magnetrons. Microwave magnetrons of greater power output than 1 kW are usually one or two orders of magnitude more expensive than the 1 kW versions.

It has been shown earlier that microwave heating in moist materials, such as the body of an insect, induces a very fast moving wave of heat and water vapour (Brodie 2007). The intensity of this wave is directly linked to the intensity of the microwave fields (Brodie 2008), therefore using very intense microwave fields may rupture the internal organs of insects, due to local steam explosions.

18.2 The Background to Microwave and Radiofrequency Quarantine

The interaction of electromagnetic energy with matter is determined by the dielectric properties of the material. The permittivity of a material can be expressed as a complex quantity, the real part (k') of which is associated with the capability of the material for storing energy in the electric field of the electromagnetic wave, and the imaginary part (k") is associated with the conversion of electromagnetic energy to heat inside the material (Nelson 1996). This is the phenomenon commonly referred to as dielectric heating. The dielectric properties also determine the reflectivity of a material.

The power dissipated per unit volume in a nonmagnetic, uniform material exposed to radio frequency (RF) or microwave fields can be expressed as:

$$P = (\tau E)^2 \sigma \; = \; 55.63 \text{ x } 10^{-12} \text{ f } (\tau E)^2 \kappa'' \tag{18.1}$$

Therefore in a system composed of two or more materials, there will be preferential heating in favour of the material with the least reflectivity and higher dielectric loss factor. The rate of temperature increase also depends on the density and thermal capacity of the heated material (Nelson 2001, Wang, *et al.* 2003):

$$\frac{dT}{dt} = \frac{P}{\rho C} \tag{18.2}$$

18.2.1 Termites as a Case Study

Termites are a good example of insects that infest economically important products. For example, in the United States, the annual cost of treating damage caused by the Formosan termite (*Coptotermes formosanus*) exceeds $US 1 billion (Pimentel, *et al.* 2002). The radar cross section of some insect species, including termites, has been modelled by treating them as drops of water of equivalent size and shape (Riley 1992). Liquid water exhibits dielectric relaxation at around 22 GHz (Meissner and Wentz 2004) (Figure 18.2). There are higher dielectric relaxations in water at about 280 GHz (Meissner and Wentz 2004), 4.5 THz and 15.4 THz (Ellison, *et al.* 1996). The dielectric properties of grains, soil and wood also depend on their moisture content (Torgovnikov 1993) (Figure 18.3).

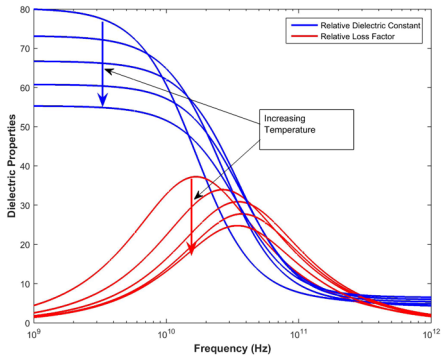

Figure 18.2: Dielectric properties of pure water as a function of frequency and temperature (calculated using equations and data from literature (Meissner and Wentz 2004)).

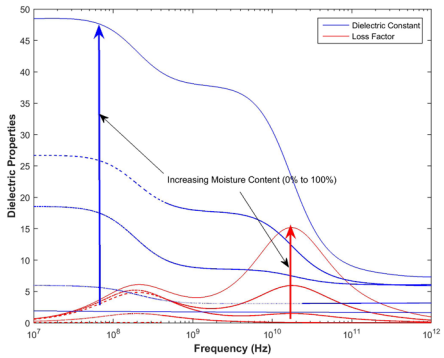

Figure 18.3: Dielectric properties of wood (density = 500 kg m^{-3}) as a function of frequency and moisture content varying between 0 % and 100 % on a dry wood basis (calculated using equations and data from literature (Torgovnikov 1993)).

Dry wood-in-service is in hydro-thermodynamic equilibrium with its surroundings. This condition is known as the equilibrium moisture content (Jackson and Day 1989). Depending on the atmospheric conditions, equilibrium moisture content is usually about 12% moisture on a dry wood weight for weight basis. When termites invade wood, they often import moisture into the structure to maintain a suitable microclimate for their foraging activities. The maximum moisture content that wood can attain before free water begins to form is known as fibre saturation. This occurs at about 25 - 30 % moisture content (Jackson and Day 1989), depending on the wood species. Fibre saturation refers to the state when all the cells are free of water and only bound water is found within the cell walls. Usually termites do not increase the moisture content beyond fibre saturation. The dielectric properties of termites (modelled as water) and wood at fibre saturation are significantly different from each other (Figure 18.4).

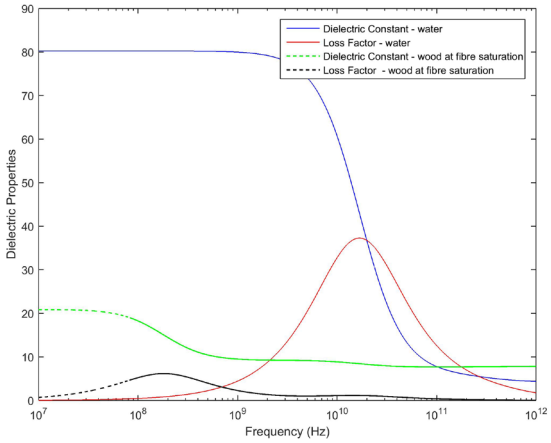

Figure 18.4: Comparison of the dielectric properties of wood (density = 500 kg m^{-3}) at fibre saturation with water.

Treatment of termite infestations using microwave energy, at 2.45 GHz, has been available for some time (Lewis and Haverty 1996, Lewis 2000). This technique does not directly heat the termites, but heats the surrounding wood to more than 55°C (Tirkel, *et al*. 2011), which then causes termite mortality. Unfortunately, the combination of high reflectivity and low dielectric losses for water in the lower microwave frequency band (2.45 GHz) means that there is virtually no differential heating between the termites and wood that is at fibre saturation; however significant differential heating should occur once the frequency increases above 20 GHz (Figure 18.5). Research in the field of ultra-high frequencies (>20 GHz) indicates that these frequencies may selectively

heat insect pests in favour of the materials they infest (Halverson, *et al.* 1996, Tirkel, *et al.* 2011).

Microwave heating for quarantine control of pests in dry materials, such as wood, has been accepted internationally. This technology is now recognised by the Food and Agriculture Organisation (FAO) and implemented in the "International Standards for Phytosanitary Measures" (ISPM 15) (Henin, *et al.* 2008, Bisceglia, *et al.* 2009, Secretariat of the International Plant Protection Convention 2009). At present, the heating and methyl bromide fumigation of wooden packaging materials are the only sanitary treatments approved under ISPM15 (Secretariat of the International Plant Protection Convention 2009). Since both methods present noticeable disadvantages, the use of microwaves for the disinfestation of wooden materials is a very attractive alternative (Bisceglia, *et al.* 2009).

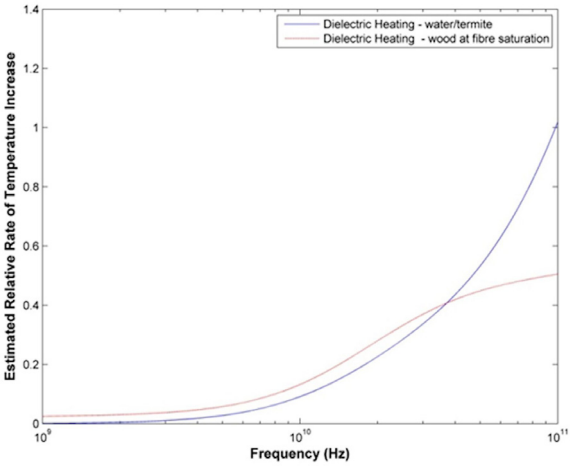

Figure 18.5: Relative dielectric heating and wood at fibre saturation moisture content, calculated using equation (18.2) and the dielectric properties of water and wood (Torgovnikov 1993).

18.3 Microbial Control

Park, *et al.* (2006) studied the survival of microorganisms after heating in a conventional microwave oven. Kitchen sponges, scrubbing pads, and syringes were deliberately contaminated with wastewater and subsequently exposed to microwave radiation. The heterotrophic plate count of the wastewater was reduced by more than 99 percent within 1 to 2 minutes of microwave heating. Coliform and E. coli in kitchen sponges were completely inactivated after 30 seconds of microwave heating. Bacterial phage MS2 was totally inactivated within 1 to 2 minutes, but spores of *Bacillus cereus*

were more resistant than the other microorganisms tested, requiring 4 minutes of irradiation for complete eradication. Similar inactivation rates were obtained in wastewater-contaminated scrubbing pads; however microorganisms attached to plastic syringes were more resistant to microwave irradiation than those associated with kitchen sponges or scrubbing pads. It took 10 minutes for total inactivation of the heterotrophic plate count and 4 minutes of treatment for total inactivation of total coliform and E. coli. A 4-log reduction of phage MS2 was obtained after 2 minutes of treatment with 97.4 percent reductions after 12 minutes of microwave treatment.

Devine et al. (2007) conducted a trial in which microwave radiation, coupled with steam heat, was used to treat organic waste (1,136 kg of culled turkey carcasses), designed to simulate a small-scale poultry mortality event. They inoculated the turkey carcasses with *Bacillus atrophaeus* spores and *Salmonella enterica* before inserting them into a purpose built portable microwave unit (Sanitec Industries), along with other organic waste. The units are designed to treat in excess of 250 kg/per hour of waste. The system has been designed so that the waste is transported through the microwave fields along a screw so that the final exposure time and temperature profile is a minimum of 30 minutes at 95 °C. The system generated a seven-log reduction in the microbial load of Salmonella and a five-log reduction in Bacillus spores. These results illustrate the potential of using microwave radiation for quarantine procedures. The following sections will illustrate more specifically how microwave energy can manage pests in agricultural and forestry systems.

18.4 Conclusions

This has been a brief overview of how radiofrequency and microwave energy can be used for biosecurity and quarantine applications. It is highlights the potential for quick treatment that can replace potentially dangerous chemicals. The use of appropriate microwave applicators is important. The next chapter will address another important issue where microwave treatment may supplement or replace chemical treatments, which is weed management.

References

Bisceglia, B., De Leo, R. and Diaferia, N. 2009. MW PALLETS DISINFESTATIONS. *Journal of Microwave Power & Electromagnetic Energy*. 43(4): 1-13.

Brodie, G. 2007. Simultaneous heat and moisture diffusion during microwave heating of moist wood. *Applied Engineering in Agriculture*. 23(2): 179-187.

Brodie, G. I. 2008, *Innovative wood drying: Applying microwave and solar technologies to wood drying*, Saarbruecken, Germany: VDM Verlag.

Carter, C. A., Chalfant, J. A., Goodhue, R. E., Han, F. M. and DeSantis, M. 2005. The Methyl Bromide Ban: Economic Impacts on the California Strawberry Industry. *Review of Agricultural Economics*. 27(2): 181-197.

Devine, A. A., Grunden, A. M., Krisiunas, E., Davis, D. K., Rosario, G., Scott, S., Faision, S. and Cosby, W. M. 2007. Testing the Efficacy of a Combination of Microwave and Steam Heat for Log Reduction of the Microbial Load Following a Simulated Poultry Mass Mortality Event. *Applied Biosafety*. 12(2): 79-84.

Ellison, W. J., Lamkaouchi, K. and Moreau, J. M. 1996. Water: a dielectric reference. *Journal of Molecular Liquids*. 68(2–3): 171-279.

Halverson, S. L., Burkholder, W. E., Bigelow, T. S., Nordheim, E. V. and Misenheimer, M. E. 1996. High-power microwave radiation as an alternative insect control method for store products. *Journal of Economic Entomology*. 89(6): 1638-1648.

Harris, G. A., Brodie, G. I., Ozarska, B. and Taube, A. 2011. Design of a Microwave Chamber for the Purpose of Drying of Wood Components for Furniture. *Transactions of the American Society of Agricultural and Biological Engineers*. 54(1): 363-368.

Headlee, T. J. 1931. The difference between the effect of radio waves on insects and on plants. *Journal of Economic Entomology*. 24(2): 427-437.

Headlee, T. J. and Burdette, R. C. 1929. Some Facts Relative to the Effect of High Frequency Radio Waves on Insect Activity. *Journal of the New York Entomological Society*. 37(1): 59-64.

Henin, J.-M., Charron, S., Luypaert, P. J., Jourez, B. and Hebert, J. 2008. Strategy to control the effectiveness of microwave treatment of wood in the framework of the implementation of ISPM 15. *Forest Products Journal*. 58(12): 75-81.

Jackson, A. and Day, D. 1989, *Wood Worker's Manual*, Sydney: William Collins Sons & Co. Ltd.

Lewis, V. R. and Haverty, M. I. 1996. Evaluation of six techniques for control of the western drywood termite (Isoptera: Kalotermitidae) in structures. *Journal of Economic Entomology*. 89(4): 922-934.

Lewis, V. R., Power, A. B., and Haverty, M. I. 2000. Laboratory evaluation of microwaves for control of the western drywood termite. *Forest Products Journal*. 50(5): 79-87.

Meissner, T. and Wentz, F. J. 2004. The Complex Dielectric Constant of Pure and Sea Water From Microwave Satellite Observations. *IEEE Transactions on Geoscience and Remote Sensing*. 42(9): 1836-1849.

Nelson, S. O. 1996. Review and assessment of radio-frequency and microwave energy for stored-grain insect control. *Transactions of the ASAE*. 39(4): 1475-1484.

Nelson, S. O. 2001. Radio-frequency and microwave dielectric properties of insects. *Journal of Microwave Power and Electromagnetic Energy*. 36(1): 47-56.

Nzokou, P., Tourtellot, S. and Kamdem, D. P. 2008. Kiln and microwave heat treatment of logs infested by the emerald ash borer (Agrilus planipennis Fairmaire) (Coleoptera: Buprestidae). *Forest Products Journal*. 58(7/8): 68.

Park, D., Bitton, G. and Melker, R. 2006. Microbial inactivation by microwave radiation in the home environment. *Journal of Environmental Health*. 69(5): 17-24.

Pimentel, D., Lach, L., Zuniga, R. and Morrison, D. 2002 Environmental and economic costs associated with non-indigenous species in the United States. In *Biological invasions: economic and environmental costs of alien plant, animal, and microbe species*, 285-303. Pimentel, D. ed. CRC Press Inc.: Boca Raton; USA.

Plaza, P. J., Zona, A. T., Sanshis, R., Balbastre, J. V., Martinez, A., Munoz, E. M., Gordillo, J. and Reyes, E. d. l. 2007. Microwave disinfestation of bulk timber. *Journal of Microwave Power and Electromagnetic Energy*. 41(3): 21-36.

Riley, J. R. 1992. A millimetric radar to study the flight of small insects. *Electronics & Communication Engineering Journal*. 4(1): 43-48.

Secretariat of the International Plant Protection Convention. 2009. International Standards for Phytosanitary Measures (ISPM 15) Regulation of Wood Packaging Material in International Trade.

Tirkel, A. Z., Lai, J. C. S., Evans, T. A. and Rankin, G. A. 2011. Heating and Provocation of Termites Using Millimeter Waves. *Progress in Electromagnetic Research Symposium (Online)*. 7(1): 27-30.

Torgovnikov, G. and Vinden, P. 2009. High-intensity microwave wood modification for increasing permeability. *Forest Products Journal*. 59(4): 84-92.

Torgovnikov, G. I. 1993, *Dielectric Properties of Wood and Wood-Based Materials*, Springer Series in Wood Science, Berlin: Springer-Verlag.

Wang, S., Tang, J., Cavalieri, R. P. and Davis, D. C. 2003. Differential heating of insects in dried nuts and fruits associated with radio frequency and microwave treatment. *Transactions of the ASAE*. 46(4): 1175–1182.

19 Weed Management

In 2006, the cost of weeds to Australian agricultural industries, due to management costs or loss of production, was estimated to be about $4 billion annually (DAFF 2006). Depletion of the weed seed bank is critically important to overcoming infestations of various weed species (Kremer 1993). Mechanical and chemical controls are the most common methods of weed control in cropping systems (Batlla and Benech-Arnold 2007, Bebawi, *et al.* 2007). The success of these methods usually depends on destroying the highest number of plants during their seedling stage (Batlla and Benech-Arnold 2007) before they interfere with crop production and subsequently set further seed. These strategies must be employed over several years to deplete the weed seed bank. Burnside *et al.* (1986) reported that viable weed seeds in the soil can be reduced by 95% after five years of consistent herbicide management; however, Kremer (1993) pointed out that in spite of achieving good weed control over several years, weed infestations will recur in succeeding years if intensive weed management is discontinued or interrupted. These efforts to deplete the soil seed bank are hindered by the growing list of herbicide resistant weed biotypes (Heap 1997).

Herbicide resistance in many weed species is becoming wide spread (Heap 1997) and multiple herbicide resistances in several economically important weed species has also been widely reported (Owen, *et al.* 2007). Some studies have demonstrated that competition from weeds can reduce the expected yield of some crops by between 35 % and 55 % (Cathcart and Swanton 2003, Mondani, *et al.* 2011). In time, herbicide resistant weeds may ultimately result in significant yield reductions and grain contamination.

It can be demonstrated (Appendix A) that equation (19.1) approximates the crop yield potential in response to weed infestation and herbicide application. This model also attempts to account for herbicide resistance within the weed population and the potential toxicity of the herbicide to the crop itself.

$$Y = Y_o \left[\begin{array}{l} 1 - \\ \dfrac{I \cdot \left[W\left(1 - N - D_o\right) - E_m + I_m \right] \left[\left(1 - p_o e^{sg}\right) e^{-\lambda H} + p_o e^{sg} \right]}{100 \left(e^{ct} \left[1 + e^{-\left[\frac{t - t_e}{d} \right]} \right] \left[1 + p_o \left(e^{sg} - 1 \right) \right] + \dfrac{I \cdot \left[W\left(1 - N - D_o\right) - E_m + I_m \right] \left[\left(1 - p_o e^{sg}\right) e^{-\lambda H} + p_o e^{sg} \right]}{A_w} \right)} \\ + aH^2 - bH \end{array} \right] \tag{19.1}$$

One of the reasons for developing a comprehensive model for any system is to perform sensitivity analyses on various parameters. This is achieved by differentiating the model equations with respect to the parameter of interest. For example, the sensitivity of crop yield to the application of herbicide can be determined by differentiating equation (19.1) with respect to H:

$$\frac{\partial Y}{\partial H} = Y_o \left[\begin{array}{l} \dfrac{\lambda I \cdot \left[W\left(1-N-D_o\right)-E_m+I_m\right]\left(1-p_o e^{sg}\right)e^{-\lambda H}}{100\left(e^{ct}\left[1+e^{-\left(\frac{t-t_o}{d}\right)}\right]\left[1+p_o\left(e^{sg}-1\right)\right]+\dfrac{I\cdot\left[W\left(1-N-D_o\right)-E_m+I_m\right]\left[\left(1-p_o e^{sg}\right)e^{-\lambda H}+p_o e^{sg}\right]}{A_w}\right)} \\ -\dfrac{\lambda I^2 \cdot \left[W\left(1-N-D_o\right)-E_m+I_m\right]^2\left[\left(1-p_o e^{sg}\right)e^{-\lambda H}+p_o e^{sg}\right]\left(1-p_o\right)}{100A_w\left(e^{ct}\left[1+e^{-\left(\frac{t-t_o}{d}\right)}\right]\left[1+p_o\left(e^{sg}-1\right)\right]+\dfrac{I\cdot\left[W\left(1-N-D_o\right)-E_m+I_m\right]\left[\left(1-p_o e^{sg}\right)e^{-\lambda H}+p_o e^{sg}\right]}{A_w}\right)^2} \\ +2aH-b \end{array} \right] \tag{19.2}$$

Weed competition in any season depends on the recruitment rate from the viable weed seed bank. The weed seed bank at the start of any cropping cycle, in simplified terms, can be understood as the sum of the dormant seed bank and the seed set from survivors of the previous season's weed management strategies; therefore an iterative approach to weed studies must be adopted (Pekrun, *et al.* 2005, Bagavathiannan, *et al.* 2012). This can be approximated by:

$$W_i = \frac{\left[W_{i-1}\left(1-N_{i-1}+D_b\right)-E_m+I_m\right]\left[\left(1-p_o e^{sg_{i-1}}\right)e^{-\lambda H}+p_o e^{sg_{i-1}}\right]\cdot S_s}{1+e^{-\left(\frac{t-t_o}{d}\right)}} + D_o W_{i-1} \tag{19.3}$$

Systemic studies of cropping systems (Mari and Changying 2007, Fore, *et al.* 2011) demonstrate that the embodied energy in manufacturing, delivering and applying herbicide is approximately 2.2 GJ ha^{-1} (or 22 J cm^{-2}); therefore the crop response to herbicide application can be expressed in terms of "applied energy". Using data published by Bosnić and Swanton (1997) for Rimsulfuron herbicide and an initial resistant portion of the population $p_o = 1 \times 10^{-5}$, Figure 19.1 shows the expected crop response as a function of the herbicide's applied energy, if weed infestation has the potential to reduce potential crop yield by 38 %.

Herbicide resistance in many weed species is becoming more prevalent (Heap 1997, 2008). Thornby and Walker (2009) simulated continuous summer fallows using glyphosate. Their modelling showed that barnyard grass (*Echinochloa colona*) could become resistant to glyphosate in about 15 years. Validation of their model against paddock history data for glyphosate-resistant population of barnyard grass showed that their model correctly predicted resistance development to within a few years of the real situation.

Selection pressure for genetic traits depends on the initial efficacy of the herbicide to remove susceptible individuals from the population, leaving only the resistant individuals to reproduce and the adoption of a single herbicide over a long period of time to sustain this selection pressure. Assuming an initially same small resistant population ($p_o = 1 \times 10^{-8}$), an average seed set of 700 seeds per weed plant, a slightly positive selection coefficient of 0.0001 for herbicide resistance (Baucom

and Mauricio 2004), and other key herbicide data published by Bosnić and Swanton (1997) and Yin et al. (2008), equations (19.1) and (19.3) predict the same 15 year period to develop herbicide resistance (Figure 19.2) as predicted by Thornby and Walker (2009). Herbicide rotations can forestall the development of a resistant population; however several weed species have developed resistance to several herbicide groups (Owen, *et al.* 2007).

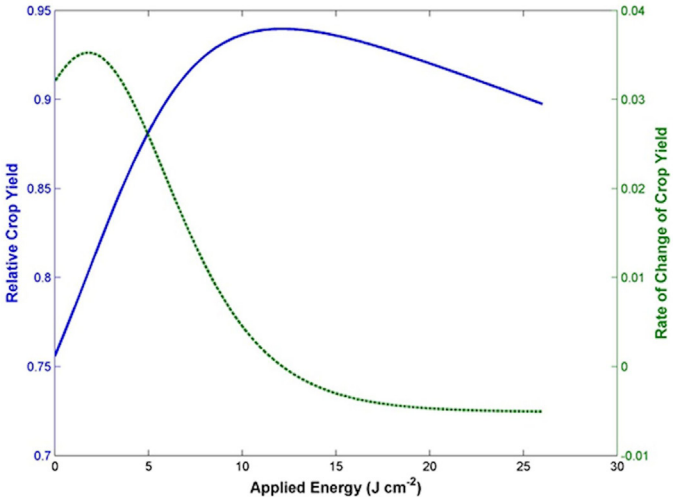

Figure 19.1: Relative crop yield and rate of change of crop yield response as a function of applied herbicide energy, based equations (19.1) and (19.2).

A growing herbicide resistance problems in most Australian cropping systems is already evident (Gill and Holmes 1997, Broster and Pratley 2006). There is evidence that glyphosate resistance has already developed in some weed populations (Broster and Pratley 2006) and multiple herbicide resistances in weed species has been widely reported (Kuk, *et al.* 2000, Walsh, *et al.* 2004, Owen, *et al.* 2007, Yu, *et al.* 2007); therefore significant crop yield (Figure 19.2) and farm income losses are to be expected. Alternative weed management strategies need to be considered if no-till cropping is to be maintained.

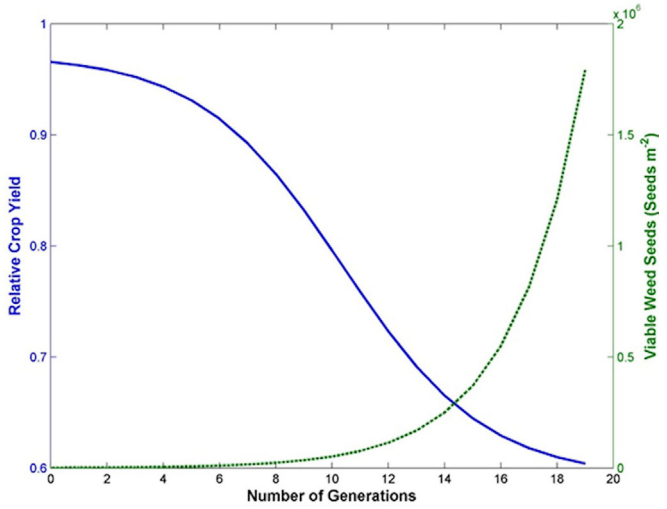

Figure 19.2: Modelling the generational impact of herbicide resistant weeds on potential crop yield under continuous herbicide weed management, based on equations (19.1) and (19.3).

Weed flaming and steam treatment have been considered (Gourd 2002, Vitelli and Madigan 2004, Bebawi, *et al.* 2007, Rask and Kristoffersen 2007) as no-till alternatives for weed management; however fire hazards and energy requirements for generating large volumes of steam are serious concerns. The high thermal capacity, poor thermal conductivity, and the cooling effect of water evaporation from the surface of plants may also limit the efficacy of flame and steam treatments for thermal weed control. Complete tillage has also been seriously considered for control of some weed infestations (Gallandt, *et al.* 2004, Chauhan, *et al.* 2006); however these practices are detrimental to soil structure and health. Microwave radiation volumetrically heats plant tissues and soil with minimal fire risk and without needing to heat large volumes of water. Microwave radiation is also compatible with no-till farming practices because it does not disturb the soil.

19.1 Radio Frequency and Microwave Treatments

Interest in the effects of high frequency electromagnetic waves on biological materials dates back to the late 19th century (Ark and Parry 1940), while interest in the effect of high frequency waves on plant material began in the 1920's (Ark and Parry 1940). Many of the earlier experiments on plant material focused on the effect of radio frequencies (RF) on seeds (Ark and Parry 1940). In many cases, short exposure resulted in increased germination and vigour of the emerging seedlings (Tran 1979,

Nelson and Stetson 1985); however long exposure usually resulted in seed death (Ark and Parry 1940, Bebawi, *et al.* 2007, Brodie, *et al.* 2009).

Davis *et al.* (Davis, *et al.* 1971, Davis 1973) were among the first to study the lethal effect of microwave heating on seeds. They treated seeds, with and without any soil, in a microwave oven and showed that seed damage was mostly influenced by a combination of seed moisture content and the energy absorbed per seed. Other findings suggested that both the specific mass and specific volume of the seeds were strongly related to a seed's susceptibility to damage by microwave fields (Davis 1973). The association between the seed's volume and its susceptibility to microwave treatment may be linked the "*radar cross-section*" (Wolf, *et al.* 1993) presented by seeds to propagating microwaves. Large radar cross-sections allow the seeds to intercept, and therefore absorb, more microwave energy.

Barker and Craker (1991) investigated the use of microwave heating in soils of varying moisture content (10-280 g water/kg of soil) to kill 'Ogle' Oats (*Avena sativa*) seeds and an undefined number of naturalised weed seeds present in their soil samples. Their results demonstrated that a seed's susceptibility to microwave treatment is entirely temperature dependent. When the soil temperature rose to 75°C there was a sharp decline in both oat seed and naturalised weed seed germination. When the soil temperature rose above 80°C, seed germination in all species was totally inhibited.

Several patents dealing with microwave treatment of weeds and their seeds have been registered (Haller 2002, Clark and Kissell 2003, Grigorov 2003); however none of these systems appear to have been commercially developed. This may be due to concerns about the energy requirements to manage weed seeds in the soil using microwave energy. In a theoretical argument based on the dielectric and density properties of seeds and soils, Nelson (1996) demonstrated that using microwaves to selectively heat seeds in the soil "*can not be expected*". He concluded that seed susceptibility to damage from microwave treatment is a purely thermal effect, resulting from soil heating and thermal conduction into the seeds. This has been confirmed experimentally by Brodie *et al.* (Brodie, *et al.* 2007a).

Experience to date confirms that microwaves can kill a range of weed seeds in the soil (Davis, *et al.* 1971, Davis 1973, Barker and Craker 1991, Brodie, *et al.* 2009), however far fewer studies have considered the efficacy of using microwave energy to manage weed plants.

19.2 Microwave Treatment of Plants

Experiments have shown that microwave treatment using a 2 kW, continuous wave, 2.45 GHz industrial microwave source and a pyramidal horn antenna with an aperture of 110 mm by 55 mm, at a range of 18 cm from the aperture, resulted in 100 % broad-leafed plant death after 4 to 5 seconds of treatment (Figure 19.3). Earlier experiments

using a modified domestic microwave oven (Figure 19.4) with a measured output power of 163 W (Brodie, *et al.* 2009) resulted in 100 % mortality of prickly paddy melon (*Cucumis myriocarpus*) (Brodie, *et al.* 2012a) and fleabane (*Conyza bonariensis*) (Brodie, *et al.* 2012b) within about 20 seconds of treatment; however, a recently completed pot trial (Hollins 2013) on annual ryegrass (*Lolium rigidum*) seedlings using the 2 kW trailer mounted system for microwave treatment only achieved 85 % to 90 % ryegrass plant mortality in 5 seconds of treatment. It is unclear at this stage why the mortality rate was not higher; however it is noted that the shoot apical meristem of grasses is located at the base of the plant as opposed to the tips of the plant as in broad-leafed species. This may influence the susceptibility of grasses to microwave treatment. This requires further experimental study.

Figure 19.3: Trailer mounted four by 2 kW microwave system to treat weeds and soil.

Figure 19.4: Modified microwave oven with a waveguide and horn antenna arrangement to treat weeds and soil (Source: Bebawi, et al. 2007).

Microwave treatment of ryegrass seeds in the top 2 cm of soil is also effective; however the amount of time (and therefore energy) required is much higher than for growing plants (Brodie, *et al.* 2007c, Brodie, *et al.* 2009). It is noted that seeds in moist soil are much more susceptible to microwave treatment (Brodie, *et al.* 2007c, Brodie, *et al.* 2009).

19.3 Reinterpretation of Earlier Microwave Weed Experiments

Data from earlier experiments (Brodie, *et al.* 2012a, b) with fleabane (*Conyza bonariensis*) and prickly paddy melon (*Cucumis myriocarpus*) reveals that a simple logistical model can describe the survival response (Figure 19.5):

$$Survival = \frac{1.0}{\left[1+\left(\frac{\psi}{4.7}\right)^{6}\right]} \tag{19.4}$$

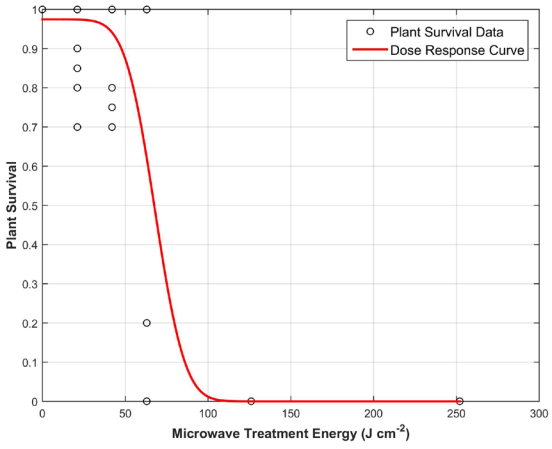

Figure 19.5: Combined fleabane and prickly paddy melon survival response as a function of applied microwave energy (Data from: Brodie, et al. 2012b, a).

Data from Hollins' recent experiment (Hollins 2013) in which she treated annual ryegrass plants using the 2 kW microwave system has been regressed against the estimated energy density (Figure 19.6) to reveal that a double logistic function can be used to model the response:

$$Survival = \frac{1.0-0.18}{\left[1+\left(\frac{\psi}{5.6}\right)^{1.0}\right]} + \frac{0.18}{\left[1+\left(\frac{\psi}{82.4}\right)^{22.5}\right]} \tag{19.5}$$

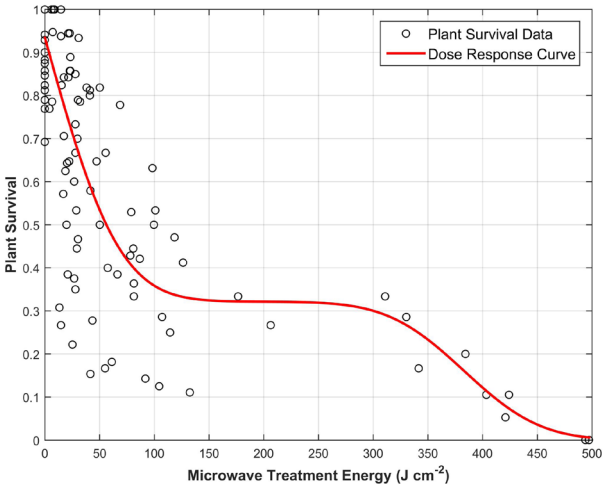

Figure 19.6: Ryegrass survival response as a function of applied microwave energy (Data from: Hollins 2013).

Other data for both perennial and annual ryegrass seeds in the top 2 cm of soil (Brodie, *et al.* 2009) reveal that for dry seeds in dry soil (Figure 19.7 a) can be described by:

$$Survival = 0.4 \times erfc\left[0.057\left(\Psi \cdot e^{-0.058d} - 66.7\right)\right] \tag{19.6}$$

Where erfc(x) is the Gaussian complementary error function of x, Y is the applied microwave energy and d is the depth of the seed in the soil.
For moist seeds in moist soil (Figure 19.7 b) the relationship is:

$$Survival = 0.43 \times erfc\left[0.31\left(\Psi \cdot e^{-0.13d} - 11.5\right)\right] \tag{19.7}$$

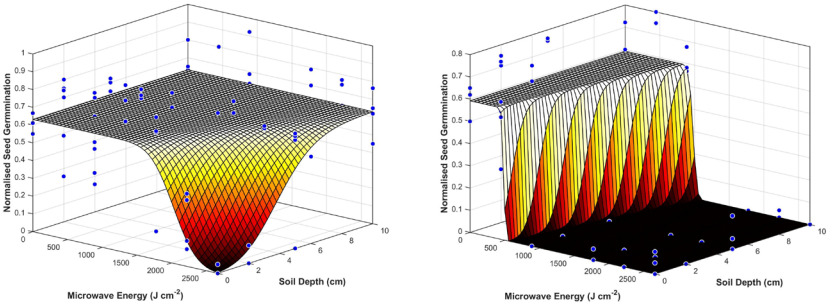

(a) (b)

Figure 19.7: Ryegrass survival response as a function of seed depth in soil and applied microwave energy for (a) dry soil and (b) wet soil (Data from: Brodie, et al. 2009).

19.4 Impact of Microwave Treatment on Soil

Based on the work by Ayappa et al. (1991) the heat generated in a very thick dielectric slab (such as soil) can be described by:

$$Q = \frac{\omega \varepsilon_o \kappa'' \tau^2 E^2 e^{-2\beta z'}}{2} \tag{19.8}$$

The microwave field strength (E) from a horn antenna was developed in Chapter 17. This can be substituted into the equation for the simultaneous diffusion of heat and moisture due to microwave heating presented in Chapters 13 to yield an estimate of the temperature profile in soil:

$$\Omega(t) = \frac{n\omega\varepsilon_o\kappa''\tau^2}{8k\beta^2}\left[e^{-2\beta z'} + \left(\frac{h}{k} + 2\beta\right) z' \cdot e^{\frac{-(z')^2}{4\gamma t}}\right]\left(e^{4\gamma\beta^2 t} - 1\right)\times$$
$$\left[\frac{E_a}{4\pi}\int_{-B/2}^{B/2}\int_{-A/2}^{A/2}\cos\left(\frac{\pi}{A}x'\right)\frac{e^{-j\beta_o\left(\sqrt{(x-x')^2+(y-y')^2+z^2}+\sqrt{R_o{}^2+(x')^2}+\sqrt{R_o{}^2+(y')^2}\right)}}{\sqrt{(x-x')^2+(y-y')^2+z^2}}\cdot dx'\cdot dy'\right]^2 \tag{19.9}$$

In an experiment using an Orthic, Basic Rudosol (Isbell 2002), Brodie, et al. (2007b) confirmed the temperature distribution that could be expected in the soil from microwave heating using a horn antenna. The soil was crushed, mixed thoroughly, and passed through a 2 mm sieve to ensure homogeneity and uniform response to the microwave fields. The soil was air-dried to constant weight. Samples of approximately

2.3 kg were placed into a 20 cm by 20 cm plastic dish to a depth of 5 cm. Temperatures were measured using sixteen 120 °C thermometers placed into the soil in the arrangement shown in Figure 19.8. Samples were heated using the experimental prototype microwave system for 150 seconds at full power. Thermometers were inserted into the soil immediately after heating was completed.

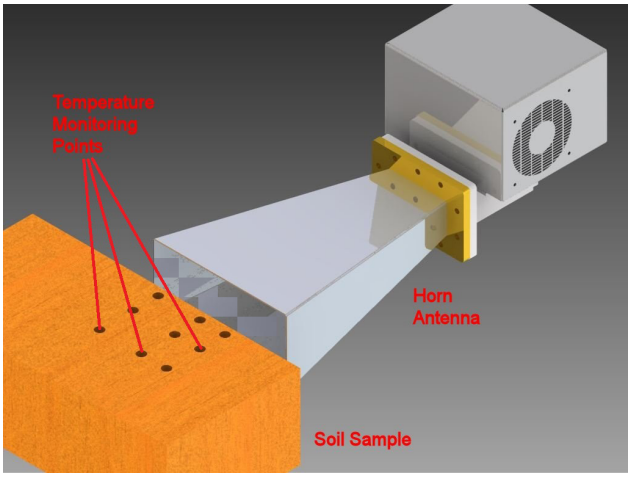

Figure 19.8: Schematic of thermometer placement during temperature measurement experiment.

The hottest place in the heating pattern was along the centre line of the antenna and between 2 cm and 5 cm below the surface. Figure 19.9 compares the expected temperature profile in the soil to the average soil temperature profile measured during these experiments. The temperature profiles are similar, although not quite the same.

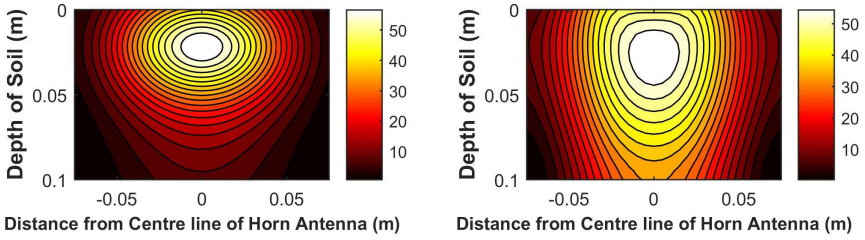

Figure 19.9: Comparison of expected soil temperature profile (a) with measured soil temperature profile (b) for the 750 W prototype microwave unit after 150 seconds of heating.

Having the antenna well above the soil surface provides a wider soil surface coverage but low intensity heating; however having the antenna close to the soil surface provides a smaller treatment footprint but more intense heating (Figure 19.10). Unlike conventional heating, the maximum temperature occurs just below the soil surface rather than at the surface. This is a common feature of microwave heating (Zielonka and Dolowy 1998, Brodie 2008).

As part of her study on microwave treatment of ryegrass and ryegrass seeds in soil, Hollins (2013) det mples of soil were inoculated with *E. coli*, incubated, placed into small paper envelopes and placed into pots of sterilised soil at 0, 2, 5, 10, and 20 cm depths. These pots were exposed to microwave treatment for 0, 10, 30, and 120 seconds using the 2 kW microwave system.

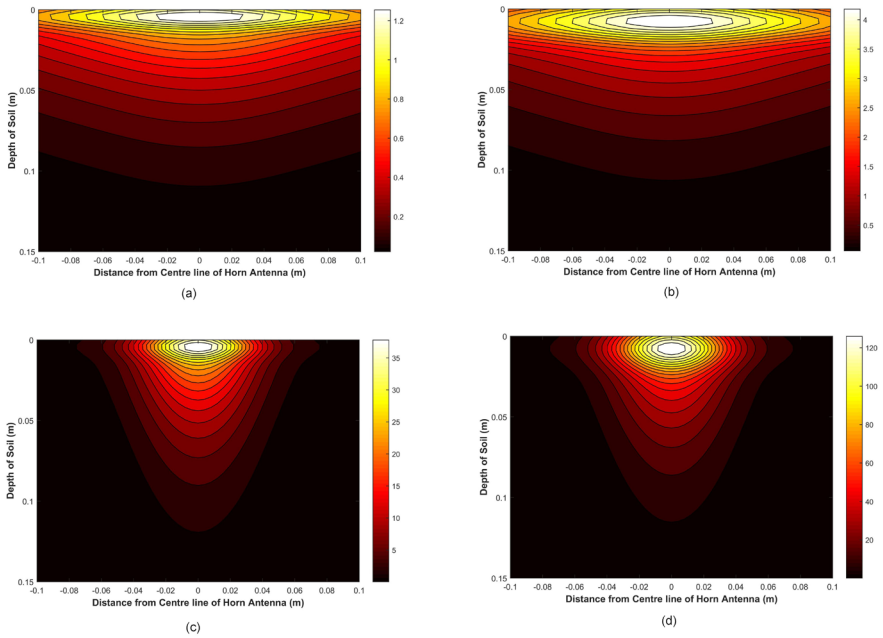

Figure 19.10: Estimated change in soil temperature from the 2 kW microwave system after (a) 10 seconds with antenna at 18 cm above the soil, (b) 30 seconds with antenna at 18 cm above the soil, (c) 10 seconds with antenna at 2 cm above the soil, and (d) 30 seconds with antenna at 2 cm above the soil.

Her results showed a sharp reduction in colony forming units after 10 seconds of microwave treatment at the soil surface. Complete sterilisation of the top 2 cm of soil occurred after 120 seconds of treatment; however there was no significant effect of microwave treatment beyond 5 cm of soil depth (Hollins 2013). This would be expected from the soil heating patterns shown in Figures 19.9 and 19.10. The bacterial survival response in the top 2 cm of soil could be described by logistic functions (Figure 19.11). Earlier experiments showed similar results (Cooper and Brodie 2009).

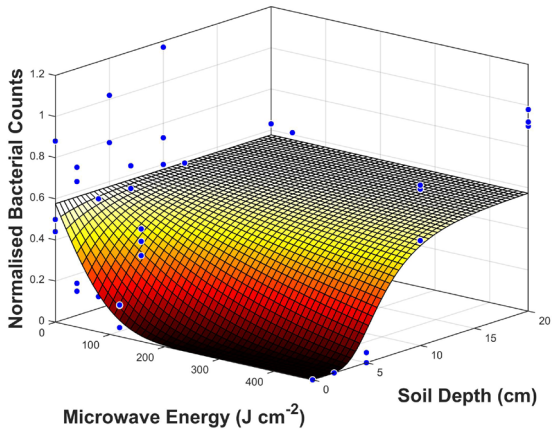

Figure19.11: Assessment of E. coli survival in top 2 cm of soil as a function of applied microwave energy (Data from Hollins 2013).

19.5 Crop Growth Response

An experiment is currently under way to determine the effect of microwave treatment of soil on the subsequent crop growth. The first crop species to be tried was wheat. This was followed by canola, subterranean clover, maize, and rice. Soil was removed from the top 2 cm of a cropping paddock at the Dookie campus of the University of Melbourne, thoroughly mixed and placed into pots. Twenty pots were exposed to microwave treatment for 0, 30, 70, and 120 seconds, with five replications in each treatment, using the 2 kW microwave system.

The pots were allowed to cool to ambient temperature. After cooling, ten wheat seeds were planted into each pot. The pots were incubated in growth chambers at the Dookie campus and the soil moisture was maintained at field capacity by regular watering. Plant height and development were assessed every 2 to 3 days. After 17 days, post planting, the wheat plants in the higher microwave treatments were significantly

taller and significantly more advanced than the control samples (Table 19.1). Data from this trial reveals that mean plant height in comparison to the mean control plant height can be described by:

$$\frac{\overline{H}-\overline{H_c}}{\overline{H_c}} = 0.4 - \frac{0.4}{\left[1+\left(\frac{30.0}{\psi}\right)^{10}\right]} \tag{19.10}$$

In terms of plant development, at 17 days post planting, the control specimens were mostly at the 4 to 5 leaf stage, while the specimens planted in the soil with higher microwave treatment had developed 3 to 4 tillers in most cases. Early crop vigour has been positively correlated with higher grain yields (Botwright, *et al.* 2002, Maydup, *et al.* 2012); therefore a significant increase in crop yield may be expected.

Table 19.1: Mean wheat plant height (mm) as a function of time from planting and microwave energy applied to the surface of the soil.

Microwave Treatment Energy (J/cm²)	Days from Planting					
	0.0	**3.0**	**5.0**	**10.0**	**13.0**	**17.0**
0.0	0.0	38.5[a]	70.9[a]	145.0[a]	192.6[a]	217.1[a]
23.9	0.0	36.1[a]	69.9[a]	146.8[a]	193.5[a]	219.2[a]
30.3	0.0	50.6[b]	82.9[b]	174.8[b]	245.2[b]	259.8[b]
36.7	0.0	64.9[c]	93.3[b]	206.2[c]	271.8[c]	293.0[c]
LSD (P = 0.05)	0.0	9.2	10.4	15.2	11.1	9.2

Note: Means with different superscripts in each column are significantly different from one another

19.6 Analysis of Potential Crop Yield Response to Microwave Weed Management

It can be shown (Appendix A) that the crop yield response to microwave management of ryegrass seedlings can be described by:

$$Y = Y_o - \frac{Y_o I \cdot \left[W\left(1-N-D_o\right)-E_m+I_m\right]}{100\left\{\left[\frac{e^{ct}\left[1+e^{-\left(\frac{t-t_o}{d}\right)}\right]\left[1+p_o\left(e^{sg}-1\right)\right]}{\left\{\left[1+\left(\frac{\psi}{LD_1}\right)^{q_1}\right]+\left[1+\left(\frac{\psi}{LD_2}\right)^{q_2}\right]\right\}}+\frac{I\cdot\left[W\left(1-N-D_o\right)-E_m+I_m\right]}{A_w}\right]\right\}} + Y_o\left[0.4-\frac{0.4}{\left[1+\left(\frac{\psi}{30.0}\right)^{10}\right]}\right] \tag{19.11}$$

Differentiating equation (19.17) with respect to Y to determine the sensitivity of crop yield to microwave weed treatments yields:

$$\frac{dY}{d\psi} = \frac{-100Y_o I\cdot\left[W\left(1-N-D_o\right)-E_m+I_m\right]\left\{\frac{0.85q_1\left(\frac{\psi}{LD_1}\right)^{q_1-1}}{LD_1\left[1+\left(\frac{\psi}{LD_1}\right)^{q_1}\right]^2}+\frac{0.15q_2\left(\frac{\psi}{LD_2}\right)^{q_2-1}}{LD_2\left[1+\left(\frac{\psi}{LD_2}\right)^{q_2}\right]^2}\right\}}{100\left\{\left[\frac{1.0-0.15}{\left[1+\left(\frac{\psi}{LD_1}\right)^{q_1}\right]}+\frac{0.15}{\left[1+\left(\frac{\psi}{LD_2}\right)^{q_2}\right]}\right]\right\}^2\left\{\left[\frac{e^{ct}\left[1+e^{-\left(\frac{t-t_o}{d}\right)}\right]\left[1+p_o\left(e^{sg}-1\right)\right]}{\left\{\left[1+\left(\frac{\psi}{LD_1}\right)^{q_1}\right]+\left[1+\left(\frac{\psi}{LD_2}\right)^{q_2}\right]\right\}}+\frac{I\cdot\left[W\left(1-N-D_o\right)-E_m+I_m\right]}{A_w}\right]\right\}^2} + Y_o\left[\frac{2.0\times\left(\frac{\psi}{30}\right)^9}{15\left[1+\left(\frac{\psi}{30}\right)^{10}\right]^2}\right] \tag{19.12}$$

Therefore, using similar parameters to the earlier analysis of herbicide responses (Bosnić and Swanton 1997), Figure 19.12 shows the potential crop yield response to microwave-based weed control as a function of applied microwave energy. This model implies that an improvement in crop yield may be possible, due to the enhanced development of a crop grown in microwave treated soil. These models are useful for assessing the potential for using microwave weed management strategies as a tool for managing herbicide resistant weed populations.

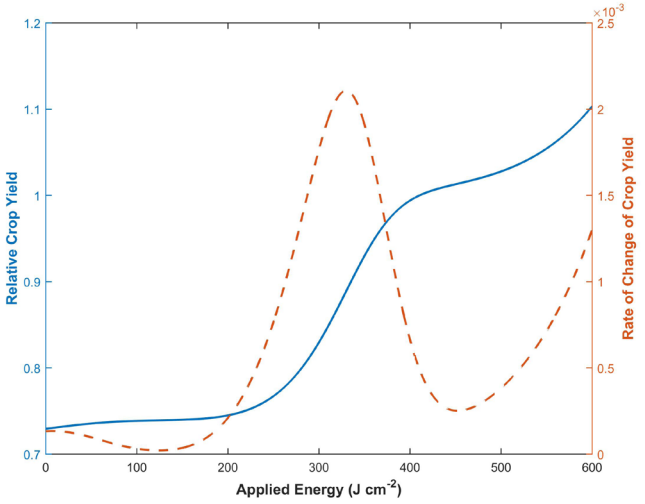

Figure 19.12: Relative crop yield as a function of applied microwave energy to control ryegrass infestations, based on the derived microwave response model in equation (20).

19.7 The Potential for Including Microwave Weed Control for Herbicide Resistance Management

If herbicide resistance becomes endemic in the weed populations, cumulative crop yield losses become significant (Figure 19.13). In this scenario, which is similar to the modelling performed by Thornby and Walker (2009) mentioned earlier, the cumulative crop yield loss over 20 years may approach the equivalent to the yield of four normal crops. It is always tempting to present the best possible scenario for a new technology; however it is unlikely that any new technology will actually be used to its full potential in the early stages of implementation. Therefore it is better to initially assess a new technology based on a sub-optimal treatment regime. As an example, if sub-optimal microwave weed treatments are used to managing herbicide resistant grass weeds, these models suggest that potential crop losses can be recovered, depending on how quickly the microwave treatment regime can be implemented (Figure 19.14). Note: in these assessments, microwave treatment is being used as the equivalent of a knock-down herbicide to kill already growing grass weeds.

Sub-optimal knock-down microwave treatment, if adopted early enough, may manage the growing weed seed bank and therefore recover lost production potential; however there appears to be a period in which weed suppression may not be as evident as herbicide and crop yield potential during this time may actually decline for a while (Figure 19.14). Late adoption of any sub-optimal weed management strategy may not provide any measureable benefits. If an optimal knock-down microwave

treatment is used, these models suggest that a net crop yield enhancement may be possible within the first year of implementation (Figure 19.15). In this case there is no long term cumulative yield loss and over a 20 year period, this scenario suggests a potential cumulative gain in crop yield that is equivalent to approximately six normal harvests. Therefore, in comparison to continued herbicide treatment of resistant weeds, incorporating optimal microwave weed management into an integrated weed management regime has a beneficial outcome (equivalent to approximately ten normal harvests over a 20 year period if herbicide resistance becomes endemic).

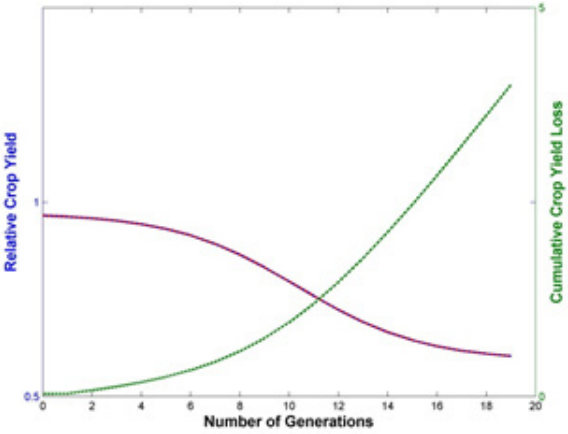

Figure 19.13: Relative crop yield and cumulative crop yield loss as a function of weed population generations (years)if herbicide resistance develops.

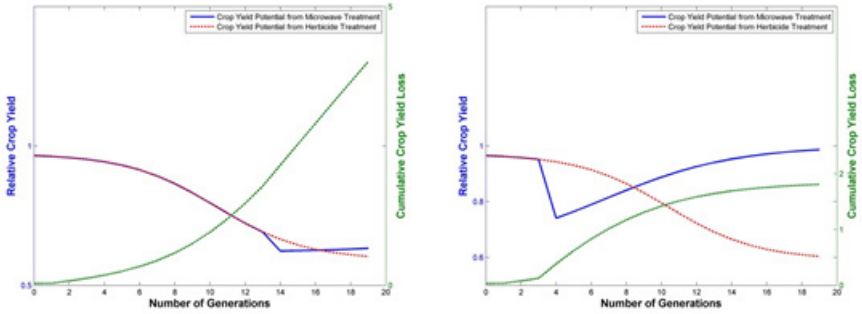

Figure 19.14: Comparison of crop yield potential and cumulative crop yield loss with sub-optimal microwave weed treatment included at various times (left = adoption of microwave technology after 15 years of herbicide resistance being evident and right = adoption of microwave technology after only 5 years of herbicide resistance being evident).

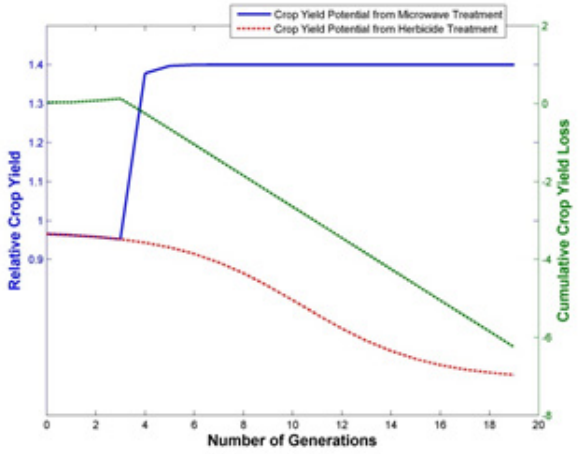

Figure 19.15: Comparison of crop yield potential and cumulative crop yield loss with optimal microwave weed treatment included.

19.8 Conclusion

This chapter has developed a comprehensive crop ecology model to investigate the potential long term benefits of developing and incorporating microwave weed management techniques into cropping systems where herbicide resistant weed populations are evident. Even at a sub-optimal level of microwave treatment, if microwave technologies are adopted early, there may be longer term benefits for the cropping system, in spite of an initial reduction in weed control compared to conventional herbicide use. At an optimal treatment level the modelling suggests that a significant improvement in crop yield may be expected.

Nomenclature

- ψ Is the applied microwave energy
- $\mathbf{A_w}$ Is the percentage yield loss as weed density approaches ∞ (= 38.0; Bosnić and Swanton 1997)
- **c** Is the speed of light (m/s) or the rate at which I approaches zero as t approaches ∞ (= 0.017; Bosnić and Swanton 1997)
- **d** Is the slope of the seed bank recruitment curve at t_o
- $\mathbf{D_o}$ Fraction of the seed population developing dormancy (Note: this is expressed as a fraction of the initial seed bank population W_o)

D_b Fraction of the seed population from previous seasons breaking dormancy (Note: this is expressed as a fraction of the initial seed bank population W_o)
E_m Seed emigration from the area of interest
g Is the generational number
H Is the herbicide dose
I Is the percentage yield loss as the weed density tends towards zero (= 0.38; Bosnić and Swanton 1997)
Im Seed immigration into the area of interest
N Is the natural death rate for the whole population (Note: this is expressed as a fraction of the initial seed bank population W_o)
p_o Is the initial frequency of herbicide resistant plants
q Is a constant
R_o Length of the horn antenna (m)
s Is the selection pressure for herbicide resistance
S_s Viable seed set per plant from surviving volunteers in the weed population
t Is the time difference between crop emergence and weed emergence
t_o Is the time for 50% germination of the viable seed bank
W Is the viable seed bank
Y_o Is the theoretical yield with no weed infestations
λ Is the efficacy of the herbicide killing action

Appendix A – Derivation of the Impact of Weed Infestation and Herbicide Control on Crop Yield Response

The effect of weed damage on crop yields can be described by (Schmidt and Pannell 1996):

$$Y = Y_o\left[1 - D(R)\right] \tag{A1}$$

where D(R) is the damage function caused by a weed density of R, and R represents the number of weeds that are recruited from the seed bank (plants m^{-1} of row).
The Damage function can be described by (Cousens, *et al.* 1987):

$$D(R) = \frac{I \cdot R}{100\left(e^{ct} + \frac{I \cdot R}{A_w}\right)} \tag{A2}$$

Substituting into equation (1) yields:

$$Y = Y_o\left[1 - \frac{I \cdot R}{100\left(e^{ct} + \frac{I \cdot R}{A_w}\right)}\right] \tag{A3}$$

Herbicide Weed Management

Now the weed infestations will be made up of some resistant weeds (R_R) and some weeds that can be easily controlled by herbicides (R_S). After some kind of herbicide treatment, the density of susceptible weeds will be (Schmidt and Pannell 1996):

$$R_s = R_{so}\left[1 - K(H)\right] \tag{A4}$$

where R_{So} is the initial susceptible weed density; K(H) is the kill function for the herbicide in this portion of the weed population for a herbicide treatment of H.

The resistant weed population will be (Schmidt and Pannell 1996):

$$R_{R} = R_{Ro} \tag{A5}$$

where R_{Ro} is the initial resistant weed density.

A typical kill function for a herbicide treatment is (Bosnić and Swanton 1997):

$$K(H) = 1 - e^{-\lambda H} \tag{A6}$$

Substituting all these components into equation (A3) yields:

$$Y = Y_o \left[1 - \frac{I\left(R_{so} e^{-\lambda H} + R_{Ro}\right)}{100\left(e^{ct} + \frac{I\left(R_{so} e^{-\lambda H} + R_{Ro}\right)}{A_w}\right)} \right] \tag{A7}$$

If p represents the portion of the population that is herbicide-resistant and R_o is the initial weed population density, then:

$$Y = Y_o \left[1 - \frac{I \cdot R_o\left[(1-p)e^{-\lambda H} + p\right]}{100\left(e^{ct} + \frac{I \cdot R_o\left[(1-p)e^{-\lambda H} + p\right]}{A_w}\right)} \right] \tag{A8}$$

The recruitment of seedlings from the seed bank can be described by (Neve, *et al.* 2011):

$$R_o = \frac{W}{1 + e^{-\left(\frac{t - t_o}{d}\right)}} \tag{A9}$$

Substituting into equation (A8) yields:

$$Y = Y_o\left[1-\frac{I\cdot W\left[(1-p)e^{-\lambda H}+p\right]}{100\left[1+e^{-\left(\frac{t-t_o}{d}\right)}\right]\left(e^{ct}+\frac{I\cdot W\left[(1-p)e^{-\lambda H}+p\right]}{A_w\left[1+e^{-\left(\frac{t-t_o}{d}\right)}\right]}\right)}\right] \tag{A10}$$

This can be simplified to:

$$Y = Y_o\left[1-\frac{I\cdot W\left[(1-p)e^{-\lambda H}+p\right]}{100\left(e^{ct}\left[1+e^{-\left(\frac{t-t_o}{d}\right)}\right]+\frac{I\cdot W\left[(1-p)e^{-\lambda H}+p\right]}{A_w}\right)}\right] \tag{A11}$$

The portion of the population that is resistant to herbicide will change from generation to generation depending on the selection pressure being applied by the herbicide treatments. Based on work by Gubbins and Gilligan (1999), if there is a relatively constant selection pressure (s) towards herbicide resistance from generation to generation, then:

$$\frac{\partial p}{\partial g} = sp(1-p) \tag{A12}$$

Therefore:

$$p = \frac{p_o e^{sg}}{1+p_o\left(e^{sg}-1\right)} \text{ and } 1-p = \frac{1-p_o e^{sg}}{1+p_o\left(e^{sg}-1\right)} \tag{A13}$$

Substituting into equation (A11) and simplifying yields:

$$Y = Y_o\left[1-\frac{I\cdot W\left[\left(1-p_o e^{sg}\right)e^{-\lambda H}+p_o e^{sg}\right]}{100\left(e^{ct}\left[1+e^{-\left(\frac{t-t_o}{d}\right)}\right]\left[1+p_o\left(e^{sg}-1\right)\right]+\frac{I\cdot W\left[\left(1-p_o e^{sg}\right)e^{-\lambda H}+p_o e^{sg}\right]}{A_w}\right)}\right] \tag{A14}$$

There is also evidence that herbicides have a toxic effect on the crop as well (Yin, *et al.* 2008). Using the study by Yin et al. (2008) as a guide, and assuming that the toxicity of the herbicide on a crop can be expressed as a polynomial of the form $Loss = aH^2 - BH$, equation (A14) can be modified to become:

$$Y = Y_o \left[\begin{array}{l} 1 - \dfrac{I \cdot W\left[\left(1 - p_o e^{sg}\right) e^{-\lambda H} + p_o e^{sg}\right]}{100\left(e^{ct}\left[1 + e^{-\left(\frac{t - t_o}{d}\right)}\right]\left[1 + p_o\left(e^{sg} - 1\right)\right] + \dfrac{I \cdot W\left[\left(1 - p_o e^{sg}\right) e^{-\lambda H} + p_o e^{sg}\right]}{A_w}\right)} \\ + aH^2 - bH \end{array} \right] \tag{A15}$$

The seed bank will be dynamic depending on factors such as natural seed mortality, immigration of seeds into the area from other locations via various vectors, emigration of seeds out of the area to other locations via various vectors, the onset of dormancy that prevents germination in the current season, and the breaking of dormancy from previous seasons in the seed bank. There is also replenishment of the seed bank due to seed set from survivors. Therefore equation (A15) is really only a static response model. Therefore it is apparent that any crop-weed ecological modelling exercise must be performed in an iterative way, with the previous state of the weed seed bank influencing the current state (Pekrun, *et al.* 2005).

$$Y = Y_o \left[\begin{array}{l} 1 - \\ \dfrac{I \cdot \left[W\left(1 - N - D_o\right) - E_m + I_m\right]\left[\left(1 - p_o e^{sg}\right) e^{-\lambda H} + p_o e^{sg}\right]}{100\left(e^{ct}\left[1 + e^{-\left(\frac{t - t_o}{d}\right)}\right]\left[1 + p_o\left(e^{sg} - 1\right)\right] + \dfrac{I \cdot \left[W\left(1 - N - D_o\right) - E_m + I_m\right]\left[\left(1 - p_o e^{sg}\right) e^{-\lambda H} + p_o e^{sg}\right]}{A_w}\right)} \\ + aH^2 - bH \end{array} \right] \tag{A16}$$

Differentiating equation (A16) with respect to any of the key parameters allows sensitivity analyses to be performed. For example, differentiating with respect to H determines the sensitivity of crop yield to herbicide weed treatments:

$$\frac{\partial Y}{\partial H} = Y_o \left[\begin{array}{l} \dfrac{\lambda I \cdot \left[W\left(1 - N - D_o\right) - E_m + I_m\right]\left(1 - p_o e^{sg}\right) e^{-\lambda H}}{100\left(e^{ct}\left[1 + e^{-\left(\frac{t - t_o}{d}\right)}\right]\left[1 + p_o\left(e^{sg} - 1\right)\right] + \dfrac{I \cdot \left[W\left(1 - N - D_o\right) - E_m + I_m\right]\left[\left(1 - p_o e^{sg}\right) e^{-\lambda H} + p_o e^{sg}\right]}{A_w}\right)} \\ - \dfrac{\lambda I^2 \cdot \left[W\left(1 - N - D_o\right) - E_m + I_m\right]^2 \left[\left(1 - p_o e^{sg}\right) e^{-\lambda H} + p_o e^{sg}\right]\left(1 - p_o\right)}{100 A_w\left(e^{ct}\left[1 + e^{-\left(\frac{t - t_o}{d}\right)}\right]\left[1 + p_o\left(e^{sg} - 1\right)\right] + \dfrac{I \cdot \left[W\left(1 - N - D_o\right) - E_m + I_m\right]\left[\left(1 - p_o e^{sg}\right) e^{-\lambda H} + p_o e^{sg}\right]}{A_w}\right)^2} \\ + 2aH - b \end{array} \right] \tag{A17}$$

Microwave Weed Management

In a recently conducted experiment, the survival of ryegrass seedlings during microwave treatment could be described by a double logistical function of the form (Hollins 2013):

$$W = \left[W_o\left(1-N-D_o\right)-E_m+I_m\right]\left\{\frac{0.85}{\left[1+\left(\frac{\psi}{LD_1}\right)^{q_1}\right]}+\frac{0.15}{\left[1+\left(\frac{\psi}{LD_2}\right)^{q_2}\right]}\right\} \tag{A18}$$

Apparent Response of Grass Weed

Substituting equation (A18) into equation (A16) yields:

$$Y = Y_o\left[\begin{array}{l} 1- \\ \dfrac{I\cdot\left[W\left(1-N-D_o\right)-E_m+I_m\right]\left[\left(1-p_o e^{sg}\right)e^{-\lambda H}+p_o e^{sg}\right]\left\{\dfrac{0.85}{\left[1+\left(\frac{\psi}{LD_1}\right)^{q_1}\right]}+\dfrac{0.15}{\left[1+\left(\frac{\psi}{LD_2}\right)^{q_2}\right]}\right\}}{100\left(\begin{array}{l} e^{ct}\left[1+e^{-\left(\frac{t-t_o}{d}\right)}\right]\left[1+p_o\left(e^{sg}-1\right)\right]+ \\ \dfrac{I\cdot\left[W\left(1-N-D_o\right)-E_m+I_m\right]\left[\left(1-p_o e^{sg}\right)e^{-\lambda H}+p_o e^{sg}\right]\left\{\dfrac{0.85}{\left[1+\left(\frac{\psi}{LD_1}\right)^{q_1}\right]}+\dfrac{0.15}{\left[1+\left(\frac{\psi}{LD_2}\right)^{q_2}\right]}\right\}}{A_w} \end{array}\right) \\ +aH^2-bH \end{array}\right] \tag{A19}$$

If no herbicide is used, then H = 0 and equation (A19) becomes:

$$Y = Y_o\left[1-\frac{I\cdot\left[W\left(1-N-D_o\right)-E_m+I_m\right]\left\{\frac{0.85}{\left[1+\left(\frac{\psi}{LD_1}\right)^{q_1}\right]}+\frac{0.15}{\left[1+\left(\frac{\psi}{LD_2}\right)^{q_2}\right]}\right\}}{100\left(\frac{e^{ct}\left[1+e^{-\left(\frac{t-t_o}{d}\right)}\right]\left[1+p_o\left(e^{sg}-1\right)\right]+I\cdot\left[W\left(1-N-D_o\right)-E_m+I_m\right]\left\{\frac{0.85}{\left[1+\left(\frac{\psi}{LD_1}\right)^{q_1}\right]}+\frac{0.15}{\left[1+\left(\frac{\psi}{LD_2}\right)^{q_2}\right]}\right\}}{A_w}\right)}\right] \tag{A20}$$

This can be rearranged to become:

$$Y = Y_o - \frac{Y_o I\cdot\left[W\left(1-N-D_o\right)-E_m+I_m\right]}{100\left(\frac{e^{ct}\left[1+e^{-\left(\frac{t-t_o}{d}\right)}\right]\left[1+p_o\left(e^{sg}-1\right)\right]}{\left\{\frac{0.85}{\left[1+\left(\frac{\psi}{LD_1}\right)^{q_1}\right]}+\frac{0.15}{\left[1+\left(\frac{\psi}{LD_2}\right)^{q_2}\right]}\right\}}+\frac{I\cdot\left[W\left(1-N-D_o\right)-E_m+I_m\right]}{A_w}\right)} \tag{A21}$$

Now taking into account the apparent improvement in crop development due to microwave treatment of the soil, this becomes:

$$Y = Y_o - \frac{Y_o I \cdot \left[W\left(1-N-D_o\right)-E_m+I_m\right]}{100\left\{\frac{e^{ct}\left[1+e^{-\left(\frac{t-t_o}{d}\right)}\right]\left[1+p_o\left(e^{sg}-1\right)\right]}{\left\{\left[1+\left(\frac{\psi}{LD_1}\right)^{q_1}\right]+\left[1+\left(\frac{\psi}{LD_2}\right)^{q_2}\right]\right\}}+\frac{I\cdot\left[W\left(1-N-D_o\right)-E_m+I_m\right]}{A_w}\right\}} + Y_o\left(0.4-\frac{0.4}{\left[1+\left(\frac{\psi}{30.0}\right)^{10}\right]}\right) \tag{A22}$$

Differentiating equation (A22) with respect to Y to determine the sensitivity of crop yield to microwave weed treatments yields:

$$\frac{dY}{d\psi} = \frac{-100Y_o I\cdot\left[W\left(1-N-D_o\right)-E_m+I_m\right]\left\{\frac{0.85q_1\left(\frac{\psi}{LD_1}\right)^{q_1-1}}{LD_1\left[1+\left(\frac{\psi}{LD_1}\right)^{q_1}\right]^2}+\frac{0.15q_2\left(\frac{\psi}{LD_2}\right)^{q_2-1}}{LD_2\left[1+\left(\frac{\psi}{LD_2}\right)^{q_2}\right]^2}\right\}}{100\left\{\left[1+\left(\frac{\psi}{LD_1}\right)^{q_1}\right]+\left[1+\left(\frac{\psi}{LD_2}\right)^{q_2}\right]\right\}^2\left\{\frac{e^{ct}\left[1+e^{-\left(\frac{t-t_o}{d}\right)}\right]\left[1+p_o\left(e^{sg}-1\right)\right]}{\left\{\left[1+\left(\frac{\psi}{LD_1}\right)^{q_1}\right]+\left[1+\left(\frac{\psi}{LD_2}\right)^{q_2}\right]\right\}}+\frac{I\cdot\left[W\left(1-N-D_o\right)-E_m+I_m\right]}{A_w}\right\}^2} + Y_o\left[\frac{2.0\times\left(\frac{\psi}{30}\right)^9}{15\left[1+\left(\frac{\psi}{30}\right)^{10}\right]^2}\right] \tag{A23}$$

Apparent Response of Broad-leafed Weeds and Weed Seeds

However earlier studies showed that the survival of broad-leafed weeds and seeds in the soil could be adequately described by a single logistical function of the form (Brodie, *et al*. 2012b):

$$W = \frac{\left[W\left(1-N-D_o\right)-E_m+I_m\right]}{\left[1+\left(\frac{\psi}{LD_1}\right)^q\right]} \tag{A24}$$

Substituting into equation (A16) and simplifying yields:

$$Y = Y_o\left[\frac{1-\dfrac{I\cdot\left[W\left(1-N-D_o\right)-E_m+I_m\right]\left[\left(1-p_o e^{sg}\right)e^{-\lambda H}+p_o e^{sg}\right]}{100\left(\begin{array}{l} e^{ct}\left[1+e^{-\left(\frac{t-t_o}{d}\right)}\right]\left[1+p_o\left(e^{sg}-1\right)\right]\left[1+\left(\frac{\psi}{LD_1}\right)^q\right]+ \\ \dfrac{I\cdot\left[W\left(1-N-D_o\right)-E_m+I_m\right]\left[\left(1-p_o e^{sg}\right)e^{-\lambda H}+p_o e^{sg}\right]}{A_w}\end{array}\right)}\right] \tag{A25}$$

Again, if no herbicide is used, then H = 0 and equation (A25) becomes:

$$Y = Y_o\left[\frac{1-\dfrac{I\cdot\left[W\left(1-N-D_o\right)-E_m+I_m\right]\left[1+p_o\left(e^{sg}-1\right)\right]}{100\left(\begin{array}{l} e^{ct}\left[1+e^{-\left(\frac{t-t_o}{d}\right)}\right]\left[1+p_o\left(e^{sg}-1\right)\right]\left[1+\left(\frac{\psi}{LD_1}\right)^q\right]+ \\ \dfrac{I\cdot\left[W\left(1-N-D_o\right)-E_m+I_m\right]\left[1+p_o\left(e^{sg}-1\right)\right]}{A_w}\end{array}\right)}\right] \tag{A26}$$

Equation (A27) can be rearranged to become:

$$Y = Y_o \left[1 - \frac{I \cdot \left[W\left(1 - N - D_o\right) - E_m + I_m \right] \left[1 + p_o\left(e^{sg} - 1\right) \right]}{100 \left[1 + p_o\left(e^{sg} - 1\right) \right] \left(e^{ct} \left[1 + e^{-\left(\frac{t - t_o}{d}\right)} \right] \left[1 + \left(\frac{\psi}{LD_1} \right)^q \right] + \frac{I \cdot \left[W\left(1 - N - D_o\right) - E_m + I_m \right] \left[1 + p_o\left(e^{sg} - 1\right) \right]}{A_w \left[1 + p_o\left(e^{sg} - 1\right) \right]} \right)} \right] \tag{A27}$$

This can now be simplified to become:

$$Y = Y_o \left[1 - \frac{I \cdot \left[W\left(1 - N - D_o\right) - E_m + I_m \right]}{100 \left(e^{ct} \left[1 + e^{-\left(\frac{t - t_o}{d}\right)} \right] \left[1 + \left(\frac{\psi}{LD_1} \right)^q \right] + \frac{I \cdot \left[W\left(1 - N - D_o\right) - E_m + I_m \right]}{A_w} \right)} \right] \tag{A28}$$

Now taking into account the apparent improvement in crop development due to microwave treatment of the soil, this becomes:

$$Y = Y_o \left[1 - \frac{I \cdot \left[W\left(1 - N - D_o\right) - E_m + I_m \right]}{100 \left(e^{ct} \left[1 + e^{-\left(\frac{t - t_o}{d}\right)} \right] \left[1 + \left(\frac{\psi}{LD_1} \right)^q \right] + \frac{I \cdot \left[W\left(1 - N - D_o\right) - E_m + I_m \right]}{A_w} \right)} + \left(0.4 - \frac{0.4}{\left[1 + \left(\frac{\psi}{30.0} \right)^{10} \right]} \right) \right] \tag{A29}$$

Differentiating equation (A29) with respect to Y to determine the sensitivity of crop yield to microwave weed treatments yields:

$$\frac{\partial Y}{\partial \psi} = Y_o \left[\frac{mI \cdot e^{ct}\left[1+e^{-\left(\frac{t-t_o}{d}\right)}\right]\left[W\left(1-N-D_o\right)-E_m+I_m\right]\left(\frac{\psi}{LD_1}\right)^{q-1}}{100LD_1\left(e^{ct}\left[1+e^{-\left(\frac{t-t_o}{d}\right)}\right]\left[1+\left(\frac{\psi}{LD_1}\right)^{q}\right]+\frac{I\cdot\left[W\left(1-N-D_o\right)-E_m+I_m\right]}{A_w}\right)^2} + \left[\frac{2.0\times\left(\frac{\psi}{30}\right)^{9}}{15\left[1+\left(\frac{\psi}{30}\right)^{10}\right]^2}\right] \right] \tag{A30}$$

References

Ark, P. A. and Parry, W. 1940. Application of High-Frequency Electrostatic Fields in Agriculture. *The Quarterly Review of Biology*. 15(2): 172-191.

Ayappa, K. G., Davis, H. T., Crapiste, G., Davis, E. J. and Gordon, J. 1991. Microwave heating: An evaluation of power formulations. *Chemical Engineering Science*. 46(4): 1005-1016.

Bagavathiannan, M. V., Begg, G. S., Gulden, R. H. and Van Acker, R. C. 2012. Modelling the Dynamics of Feral Alfalfa Populations and Its Management Implications. *PLoS ONE*. 7(6): 1-10.

Barker, A. V. and Craker, L. E. 1991. Inhibition of weed seed germination by microwaves. *Agronomy Journal*. 83(2): 302-305.

Batlla, D. and Benech-Arnold, R. L. 2007. Predicting changes in dormancy level in weed seed soil banks: Implications for weed management. *Crop Protection/Weed Science in Time of Transition*. 26(3): 189-197.

Baucom, R. S. and Mauricio, R. 2004. Fitness costs and benefits of novel herbicide tolerance in a noxious weed. *Proceedings of the National Academy of Sciences of the United States of America*. 101(36): 13386-13390.

Bebawi, F. F., Cooper, A. P., Brodie, G. I., Madigan, B. A., Vitelli, J. S., Worsley, K. J. and Davis, K. M. 2007. Effect of microwave radiation on seed mortality of rubber vine (*Cryptostegia grandiflora* R.Br.), parthenium (*Parthenium hysterophorous* L.) and bellyache bush (*Jatropha gossypiifolia* L.). *Plant Protection Quarterly*. 22(4): 136-142.

Bigu-Del-Blanco, J., Bristow, J. M. and Romero-Sierra, C. 1977. Effects of low-level microwave radiation on germination and growth rate in corn seeds. *Proceedings of the IEEE*. 65(7): 1086-1088.

Billari, F. C. 2001. A Log-Logistic Regression Model for a Transition Rate with a Starting Threshold. *Population Studies*. 55(1): 15-24.

Bosnić, A. Č. and Swanton, C. J. 1997. Economic Decision Rules for Postemergence Herbicide Control of Barnyardgrass (Echinochloa crus-galli) in Corn (Zea mays). *Weed Science*. 45(4): 557-563.

Botwright, T. L., Condon, A. G., Rebetzke, G. J. and Richards, R. A. 2002. Field evaluation of early vigour for genetic improvement of grain yield in wheat. *Australian Journal of Agricultural Research*. 53(10): 1137-1145.

Boyarskii, D. A., Tikhonov, V. V. and Komarova, N. Y. 2002. Modeling of dielectric constant of bound water in soil for applications of microwave remote sensing. *Progress In Electromagnetics Research*. 35: 251–269.

Brodie, G. 2007a. Microwave treatment accelerates solar timber drying. *Transactions of the American Society of Agricultural and Biological Engineers*. 50(2): 389-396.

Brodie, G. 2007b. Simultaneous heat and moisture diffusion during microwave heating of moist wood. *Applied Engineering in Agriculture*. 23(2): 179-187.

Brodie, G. 2008. The influence of load geometry on temperature distribution during microwave heating. *Transactions of the American Society of Agricultural and Biological Engineers*. 51(4): 1401-1413.

Brodie, G., Botta, C. and Woodworth, J. 2007a. Preliminary investigation into microwave soil pasteurization using wheat as a test species. *Plant Protection Quarterly*. 22(2): 72-75.

Brodie, G., Hamilton, S. and Woodworth, J. 2007b. An assessment of microwave soil pasteurization for killing seeds and weeds. *Plant Protection Quarterly*. 22(4): 143-149.

Brodie, G., Harris, G., Pasma, L., Travers, A., Leyson, D., Lancaster, C. and Woodworth, J. 2009. Microwave soil heating for controlling ryegrass seed germination. *Transactions of the American Society of Agricultural and Biological Engineers*. 52(1): 295-302.

Brodie, G., Pasma, L., Bennett, H., Harris, G. and Woodworth, J. 2007c. Evaluation of microwave soil pasteurization for controlling germination of perennial ryegrass (*Lolium perenne*) seeds. *Plant Protection Quarterly*. 22(4): 150-154.

Brodie, G., Ryan, C. and Lancaster, C. 2012a. The effect of microwave radiation on Paddy Melon (Cucumis myriocarpus). *International Journal of Agronomy*. 2012: 1-10.

Brodie, G., Ryan, C. and Lancaster, C. 2012b. Microwave technologies as part of an integrated weed management strategy: A Review. *International Journal of Agronomy*. 2012: 1-14.

Broster, J. C. and Pratley, J. E. 2006. A decade of monitoring herbicide resistance in Lolium rigidum in Australia. *Australian Journal of Experimental Agriculture*. 46(9): 1151-1160.

Burnside, O. C., Moomaw, R. S., Roeth, F. W., Wicks, G. A. and Wilson, R. G. 1986. Weed seed demise in soil in weed-free corn (Zea mays) production across Nabraska. *Weed Science*. 34(2): 248-251.

Cathcart, R. J. and Swanton, C. J. 2003. Nitrogen management will influence threshold values of green foxtail (Setaria viridis) in corn. *Weed Science*. 51(6): 975-986.

Chauhan, B. S., Gill, G. and Preston, C. 2006. Influence of tillage systems on vertical distribution, seedling recruitment and persistence of rigid ryegrass (Lolium rigidum) seed bank *Weed Science*. 54(4): 669-676.

Clark, W. J. and Kissell, C. W. 2003. *System and Method for In Situ Soil Sterilization, Insect Extermination and Weed Killing*. Patent No. 20030215354A1

Connor, F. R. 1972, *Antennas*, London: Edward Arnold.

Cooper, A. P. and Brodie, G. 2009. The effect of microwave radiation and soil depth on soil pH, N, P, K, SO4 and bacterial colonies. *Plant Protection Quarterly*. 24(2): 67-70.

Cousens, R., Brain, P., O'Donovan, J. T. and O'Sullivan, P. A. 1987. The use of biologically realistic equations to describe the effects of weed density and relative time of emergence on crop yield. *Weed science (USA)*.

DAFF. 2006. *Weeds*. Australian Department of Agriculture, Fisheries and Forestry

Dahlquist, R. M., Prather, T. S. and Stapleton, J. J. 2007. Time and Temperature Requirements for Weed Seed Thermal Death. *Weed Science*. 55(6): 619-625.

Davis, F. S., Wayland, J. R. and Merkle, M. G. 1971. Ultrahigh-Frequency Electromagnetic Fields for Weed Control: Phytotoxicity and Selectivity. *Science*. 173(3996): 535-537.

Davis, F. S., Wayland, J. R. and Merkle, M. G. 1973. Phytotoxicity of a UHF Electromagnetic Field. *Nature*. 241(5387): 291-292.

Diprose, M. F., Benson, F. A. and Willis, A. J. 1984. The Effect of Externally Applied Electrostatic Fields, Microwave Radiation and Electric Currents on Plants and Other Organisms, with Special Reference to Weed Control. *Botanical Review*. 50(2): 171-223.

Ferriss, R. S. 1984. Effects of microwave oven treatment on microorganisms in soil. *Phytopathology*. 74(1): 121-126.

Fore, S. R., Porter, P. and Lazarus, W. 2011. Net energy balance of small-scale on-farm biodiesel production from canola and soybean. *Biomass and Bioenergy*. 35(5): 2234-2244.

Gallandt, E. R., Fuerst, E. P. and Kennedy, A. C. 2004. Effect of tillage, fungicide seed treatment, and soil fumigation on seed bank dynamics of wild oat (Avena fatua). *Weed Science,*. 52(4): 597-604.

Gill, G. S. and Holmes, J. E. 1997. Efficacy of cultural control methods for combating herbicide-resistant Lolium rigidum. *Pesticide Science*. 51(3): 352-358.

Gourd, T. 2002. *Controlling weeds using propane generated flame and steam treatments in crop and non croplands*. Organic Farming Research Foundation

Grigorov, G. R. 2003. *Method and System for Exterminating Pests, Weeds and Pathogens*. Patent No. 20030037482A1

Gubbins, S. and Gilligan, C. A. 1999. Invasion Thresholds for Fungicide Resistance: Deterministic and Stochastic Analyses. *Proceedings: Biological Sciences*. 266(1437): 2539-2549.

Haller, H. E. 2002. *Microwave Energy Applicator*. Patent No. 20020090268A1

Harris, G. A., Brodie, G. I., Ozarska, B. and Taube, A. 2011. Design of a Microwave Chamber for the Purpose of Drying of Wood Components for Furniture. *Transactions of the American Society of Agricultural and Biological Engineers*. 54(1): 363-368.

Heap, I. M. 1997. The occurrence of herbicide-resistant weeds worldwide. *Pesticide Science*. 51(3): 235-243.

Heap, I. M. 2008. *International Survey of Herbicide Resistant Weeds*. 25th September, 2008. http://www.weedscience.org/in.asp

Helsel, Z. R. 1992 Energy and alternatives for fertilizer and pesticide use. In *Energy in Farm Production*, 177-201. Fluck, R. C. ed. Elsevier: New York.

Hill, J. M. and Marchant, T. R. 1996. Modelling Microwave Heating. *Applied Mathematical Modeling*. 20(1): 3-15.

Hollins, E. 2013. Microwave Weed Control and the Soil Biota. Unpublished thesis. Melbourne: University of Melbourne, Melbourne School of Land and Environment

Hülsbergen, K. J., Feil, B., Biermann, S., Rathke, G. W., Kalk, W. D. and Diepenbrock, W. 2001. A method of energy balancing in crop production and its application in a long-term fertilizer trial. *Agriculture, Ecosystems & Environment*. 86(3): 303-321.

Isbell, R. F. 2002, *The Australian soil classification*, Melbourne: CSIRO.

Kremer, R. J. 1993. Management of Weed Seed Banks with Microorganisms. *Ecological Applications,*. 3(1): 42-52.

Kuk, Y. I., Burgos, N. R. and Talbert, R. E. 2000. Cross- and multiple resistance of diclofop-resistant Lolium spp. *Weed Science*. 48(4): 412-419.

Langner, H.-R., Böttger, H. and Schmidt, H. 2006. A Special Vegetation Index for the Weed Detection in Sensor Based Precision Agriculture. *Environmental Monitoring and Assessment*. 117(1): 505-518.

Mari, G. R. and Changying, J. 2007. Energy analysis of various tillage and fertilizer treatments on corn production. *American-Eurasian Journal of Agricultural and Environmental Science*. 2(5): 486-497.

Mari, G. R. and Chengying, J. 2007. Energy Analysis of various tillage and fertilizer treatments on corn production. *American-Eurasian Journal of Agricultural and Environmental Science*. 2(5): 486-497.

Maydup, M. L., Graciano, C., Guiamet, J. J. and Tambussi, E. A. 2012. Analysis of early vigour in twenty modern cultivars of bread wheat (Triticum aestivum L.). *Crop and Pasture Science*. 63(10): 987-996.

Metaxas, A. C. and Meredith, R. J. 1983, *Industrial Microwave Heating*, London: Peter Peregrinus.

Mondani, F., Golzardi, F., Ahmadvand, G., Ghorbani, R. and Moradi, R. 2011. Influence of Weed Competition on Potato Growth, Production and Radiation Use Efficiency. *Notulae Scientia Biologicae*. 3(3): 42-52.

Nelson, M. I., Wake, G. C., Chen, X. D. and Balakrishnan, E. 2001. The multiplicity of steady-state solutions arising from microwave heating. I. Infinite Biot number and small penetration depth. *The ANZIAM Journal*. 43(1): 87-103.

Nelson, S. O. 1996. A review and assessment of microwave energy for soil treatment to control pests. *Transactions of the ASAE*. 39(1): 281-289.

Nelson, S. O. and Stetson, L. E. 1985. Germination responses of selected plant species to RF electrical seed treatment. *Transactions of the ASAE*. 28(6): 2051-2058.

Neve, P., Norsworthy, J. K., Smith, K. L. and Zelaya, I. A. 2011. Modelling evolution and management of glyphosate resistance in Amaranthus palmeri. *Weed Research*. 51(2): 99-112.

Nikolova, N. K. 2012. *Modern Antennas in Wireless Telecommunications*. 5th of August, 2013. http://www.ece.mcmaster.ca/faculty/nikolova/antennas.htm

Owen, M., Walsh, M., Llewellyn, R. and Powles, S. 2007. Widespread occurrence of multiple herbicide resistance in Western Australian annual ryegrass (Lolium rigidum) populations. *Australian Journal of Agricultural Research*. 58(7): 711-718.

Pekrun, C., Lane, P. W. and Lutman, P. J. W. 2005. Modelling seedbank dynamics of volunteer oilseed rape (Brassica napus). *Agricultural Systems*. 84(1): 1-20.

Rask, A. M. and Kristoffersen, P. 2007. A review of non-chemical weed control on hard surfaces. *Weed Research*. 47(5): 370-380.

Salisbury, F. B. and Ross, C. W. 1992, *Plant physiology*, 4th edn, Belmont, California: Wadsworth Publishing Company.

Schmidt, C. P. and Pannell, D. J. 1996. Economic Issues in Management of Herbicide-Resistant Weeds. *Research in Agricultural and Applied Economics*. 64(3): 301-308.

Thornby, D. F. and Walker, S. R. 2009. Simulating the evolution of glyphosate resistance in grains farming in northern Australia. *Annals Of Botany*. 104(4): 747-756.

Tikhonov, V. V. 1997. Dielectric model of bound water in wet soils for microwave remote sensing. *Proc. IEEE International Geoscience and Remote Sensing Symposium, 1997*. 3: 1108 - 1110. Singapore International Convention and Exhibition Centre, Singapore

Tran, V. N. 1979. Effects of Microwave Energy on the Strophiole, Seed Coat and Germination of Acacia Seeds. *Australian Journal of Plant Physiology*. 6(3): 277-287.

Tran, V. N. and Cavanagh, A. K. 1979. Effects of microwave energy on Acacia longifolia. *Journal of Microwave Power*. 14(1): 21-27.

Ulaby, F. T. and El-Rayes, M. A. 1987. Microwave Dielectric Spectrum of Vegetation - Part II: Dual-Dispersion Model. *IEEE Transactions on Geoscience and Remote Sensing*. GE-25(5): 550-557.

Vitelli, J. S. and Madigan, B. A. 2004. Evaluation of a hand-held burner for the control of woody weeds by flaming. *Australian Journal of Experimental Agriculture*. 44(1): 75-81.

Von Hippel, A. R. 1954, *Dielectric Materials and Applications*, Cambridge: M.I.T. Press.

Vriezinga, C. A. 1996. Thermal runaway and bistability in microwave heated isothermal slabs. *Journal of Applied Physics*. 79(3): 1779 -1783.

Vriezinga, C. A. 1998. Thermal runaway in microwave heated isothermal slabs, cylinders, and spheres. *Journal of Applied Physics*. 83(1): 438 -442.

Vriezinga, C. A. 1999. Thermal profiles and thermal runaway in microwave heated slabs. *Journal of Applied Physics*. 85(7): 3774 -3779.

Vriezinga, C. A., Sanchez-Pedreno, S. and Grasman, J. 2002. Thermal runaway in microwave heating: a mathematical analysis. *Applied Mathematical Modelling*. 26(11): 1029 -1038.

Walsh, M. J., Powles, S. B., Beard, B. R., Parkin, B. T. and Porter, S. A. 2004. Multiple-Herbicide Resistance across Four Modes of Action in Wild Radish (Raphanus raphanistrum). *Weed Science*. 52(1): 8-13.

Wolf, W. W., Vaughn, C. R., Harris, R. and Loper, G. M. 1993. Insect radar cross-section for aerial density measurement and target classification. *Transactions of the American Society of Agricultural and Biological Engineers*. 36(3): 949-954.

Yin, X. L., Jiang, L., Song, N. H. and Yang, H. 2008. Toxic Reactivity of Wheat (Triticum aestivum) Plants to Herbicide Isoproturon. *Journal of Agricultural and Food Chemistry*. 56(12): 4825-4831.

Yu, Q., Cairns, A. and Powles, S. 2007. Glyphosate, paraquat and ACCase multiple herbicide resistance evolved in a Lolium rigidum biotype. *Planta*. 225(2): 499-513.

Zielonka, P. and Dolowy, K. 1998. Microwave Drying of Spruce: Moisture Content, Temperature and Heat Energy Distribution. *Forest Products Journal*. 48(6): 77-80.

20 Treatment of Animal Fodder

Various methods of improving the digestibility of hay and straw have been considered. Commonly used methods include urea and alkali treatments. Urea treatment increases cellulose and hemicellulose availability during rumen digestion. In a study by Kutlu et al. (2000), wheat straw samples were analysed for dry matter digestibility in the rumen of sheep, using nylon bags (*in situ*). They found that supplementing the straw with 2% urea, increased digestibility by about 19 % compared with untreated straw. Alkali treatment with NaOH or alkaline H_2O_2 can also significantly improve the digestibility of straw (Chaudhry 2000); however these methods can be expensive, hazardous, can lead to unwanted environmental effects such as sodium contamination of soil and water (Liu, *et al.* 1999), and can result in reduced feed intake because of palatability issues associated with chemically treated feed (Chaudhry 2000). This reduction in feed intake may offset any potential benefits in feed digestibility.

Steam treatments have successfully improved the digestibility of crop residues (Liu, *et al.* 1999); however steam treatment requires considerable energy and the use of high pressure vessels for the treatment process. Steam treatment in the timber industry (Kanagawa, *et al.* 1992) has been successfully replaced by atmospheric pressure microwave treatment (Harris, *et al.* 2008, Brodie 2010, Torgovnikov and Vinden 2010, Vinden, *et al.* 2011), therefore microwave treatment may also replace steam treatment of animal fodder and become a useful technique for improving digestibility.

20.1 Effect of Microwave Treatment on Digestibility

Dong *et al.* (2005) conducted an experiment in which 100 g samples of wheat straw were treated for 0 (Control), 4, or 8 minutes in a 750 W microwave oven, operating at 2.45 GHz. The chemical composition of untreated and treated samples was investigated. They also assessed the *in sacco* degradability of all straw samples in yak rumens, using suspended nylon bags containing the samples. They discovered that microwave treatment did not affect the chemical composition of wheat straw. They also found that the *in sacco* dry matter digestibility of straw was significantly improved by microwave treatment; however the crude protein degradability was not affected by microwave treatments. The *in sacco* organic matter degradability of the microwave treated straw was increased by about 20 % and the acid detergent fibre of microwave treated straw was increased by about 62 %.

Small scale *in vitro* pepsin-cellulase digestion experiments (Brodie, *et al.* 2010), using the technique developed by McLeod and Minson (1978, 1980), demonstrated that microwave treatment of lucerne hay: increased dry matter percentage with increasing microwave treatment time; increased *in vitro* dry matter digestion with increasing microwave treatment time; but had no significant effect on post-digestion

crude protein content. When 25 kg bags of lucerne fodder, which were treated in an experimental 6 kW, 2.45 GHz, microwave heating chamber (Harris, *et al.* 2011), were subjected to a similar *in vitro* pepsin-cellulase digestion study, dry matter digestion significantly increased compared with the untreated samples; however there was no significant difference attributable to the duration of microwave treatment (Brodie, *et al.* 2010). Feeding 12-14 month old Merino sheep on a maintenance ration of 1 kg of microwave treated lucerne per day resulted in a 3.65 kg gain in mean body weight over the five week feeding trial compared with the 0.2 kg increase in mean body weight for the sheep receiving 1 kg per day of untreated lucerne fodder (Brodie, *et al.* 2010).

The 25 kg bags of lucerne fodder were treated for 15 minutes using 6 kW of applied microwave power in the experimental chamber (Brodie, *et al.* 2010). This equates to 216 kJ/kg of applied microwave energy. The metabolizable energy available from lucerne is approximately 9.16 MJ/kg (El-Meccawi, *et al.* 2008). The average *in vitro* pepsin-cellulase digestibility of the microwave treated lucerne increased by 5.9 % compared with the control samples (Brodie, *et al.* 2010), therefore an additional 540 kJ/kg of metabolizable energy may have been available to these sheep during the feeding trial. Therefore an additional 2.5 Joules of metabolizable energy was made available in the fodder for every Joule of applied microwave energy.

In terms of a simplified economic consideration, each sheep consumed approximately 35 kg of fodder over the 5 week feeding trial. The applied microwave energy needed to treat the fodder was 0.06 kWh/kg of fodder. Assuming an electricity to microwave conversion efficiency of about 0.6, the electrical energy needed to treat the fodder was 0.1 kWh/kg. Electricity tariffs vary considerably; however in Australia at the time of the trial, domestic electrical tariffs were about $0.254 per kWh, peak industrial tariffs were about $0.12 per kWh and off-peak industrial tariffs were about $0.09 per kWh. The particular tariff that was applied during these experiments was the domestic supply tariff, therefore the additional cost of microwave treatment per sheep over the duration of the 5 week trial was (35 kg X 0.1 kWh X $0.254=) $0.89. Applying the same calculations for peak and off peak industrial tariffs yields a treatment cost of $0.42 and $0.32, respectively.

The average weight gain of the sheep that were eating the microwave treated lucerne during the trial was 3.65 kg. The average dressing percentage, which is the ratio of the usable carcass weight to the live weight of sheep, is about 52 % (Ekiz, *et al.* 2012). Therefore these sheep may have gained an average additional carcass weight of 1.9 kg during the five weeks of the trial. Sheep prices in Australia have been fluctuated around $3.42/kg carcass weight at the time of the trial (Meat and Livestock Australia Limited 2005), which means that the sheep receiving the microwave treated lucerne may have been worth an additional $6.50 per head after being feed microwave treated lucerne fodder for five weeks.

The efficiency of chaff and fodder treatment using microwave energy depends on the applied microwave energy and the frequency at which the microwave system operates. Absorbed energy, calculated by measuring the combination of sensible

(temperature rise) and latent heat (moisture loss) in treated samples, is much higher at 2.45 GHz than at 922 MHz (Figure 20.1). It is also evident that efficiency (i.e. the ratio of absorbed energy to applied microwave energy) decreases as the applied microwave energy increases (Figure 20.1). This is attributable to the increasing transparency of the fodder material at microwave frequencies as it dries out during treatment. The dielectric properties, and therefore the microwave heating effect, reduce as the moisture content of plant materials decrease (see Chapter 7). Some of these problems of material transparency during microwave treatment can be overcome by compressing the fodder, which increases its ability to absorb microwave energy (Figure 20.2).

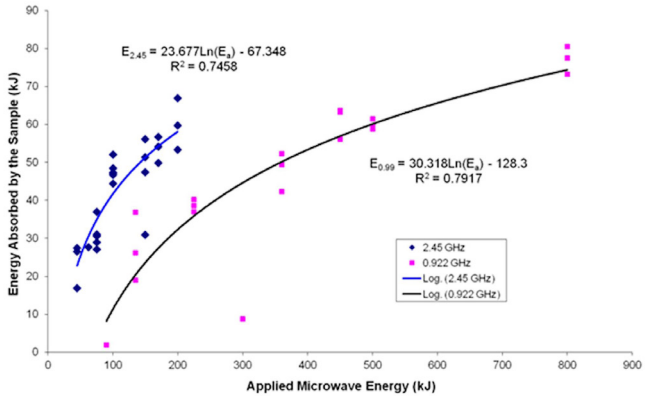

Figure 20.1: Absorbed energy in crop chaff (fodder) as a function of applied microwave energy for 922 MHz and 2.45 GHz.

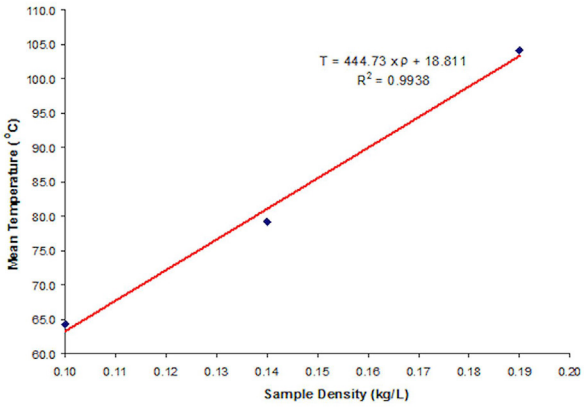

Figure 20.2: Mean temperature of 500 g samples of microwave treated fodder chaff as a function of material density (r) when heated by a 2.5 kW microwave source operating at 2.45 GHz for 30 seconds

.

During treatment of the 25 kg bags of lucerne, temperature was monitored using optic fibre temperature probes that are unaffected by microwave fields. The temperature in the air space at the top of the bags rose to 100 °C in ~12 min and fluctuated above 100 °C for the remainder of the treatment time (Figure 20.3). The maximum temperature in the air space was 115 °C. The maximum temperature in the lucerne (99.5 °C) was measured by the probe facing the microwave magnetrons whereas the maximum temperature measured by the probe in the front of the bag, facing the door of the microwave chamber, was only 94 °C.

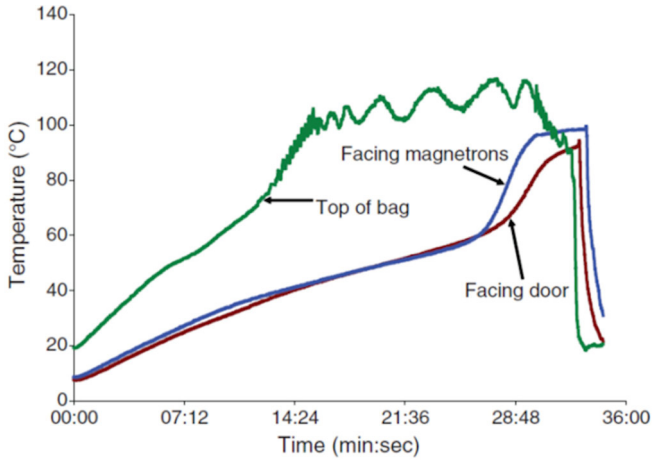

Figure 20.3: Temperature data from three locations within one 25-kg bag of lucerne being treated for 30 minutes.

The temperature in the lucerne increased steadily at a rate of ~2 °C/min of microwave heating time for the first 20–25 min of heating. At this stage there was a sudden increase in heating rate (~ 6 °C/min) until the temperature stabilised at approximately 98 °C (Figure 20.3). The sudden jump in the heating rate after some time of steady heating may be evidence of thermal runaway (Figure 15.1). Observation of the treated chaff showed no signs of charring; however the chaff was dry and crisp (Brodie, et al. 2010). The onset of thermal runaway dramatically increases the heating efficiency. In this example, the heating rate during thermal runaway is three times higher than during the normal heating phase. Provided charring can be avoided, inducing thermal runaway in the treated chaff may drastically improve treatment efficiency.

20.2 Microstructure Changes

The fast heat and moisture diffusion wave created during microwave heating (See chapter 14) has a profound effect on biological materials. In particular, very rapid heat and moisture diffusion during microwave heating can cause localized steam explosions which rupture plant cells (Torgovnikov and Vinden 2003, Brodie 2010). It has been demonstrated that microwave pre-treatment of timber creates micro-fractures throughout the material (Vinden and Torgovnikov 1996, 2000). Therefore microwave pre-treatment increases the porosity of biomass, which will enhance the moisture permeability (Vinden and Torgovnikov 1996) and enzymatic digestibility of treated fodder (Chen, *et al.* 2010).

Microwave pre-treatment of fibrous biomass also significantly reduces its mechanical strength of the material (Brodie, *et al.* 2011). In a separate trail, microwave treatment reduced the compressive strength of sugar cane to about 18 % of its original strength (Brodie, *et al.* 2011, Yin, *et al.* 2012). The implication for fodder digestion is that much less energy would be required to crush and break down fibrous biomass materials during mastication and rumination.

20.3 Potential Mitigation of Methane Production

Methane is regarded as a significant greenhouse gas, not because of its high concentrations in the atmosphere, but because its climate warming potential is 21 times higher than that of carbon dioxide (DeAngelo, *et al.* 2006). Methane production during enteric fermentation by microbial activity in the digestive tracts of animals also represents an energy loss from the digestive process. Methane emissions from enteric fermentation are the second largest global agricultural greenhouse gas source (DeAngelo, *et al.* 2006).

Forage quality has a significant impact on enteric CH_4 emissions (Mirzaei-Aghsaghali and Maheri-Sis 2011). The methane conversion rate is of critical importance for inventories of CH_4 emissions of ruminant livestock (Kurihara, *et al.* 1999). High methane conversion rates are associated with relatively high levels of fibre and lignin (Van Soest 1994), low levels of non-fibre carbohydrate (Van Soest 1994) and low digestibility (Minson and McDonald 1987). Therefore increasing the digestibility of animal foods should reduce their methane conversion rate and reduce energy losses from the digestive processes; however the effect of microwave treatment on the methane conversion rate has not yet been studied.

20.4 Microwave Treatment of Grains

Grain sorghum (*Sorghum bicolor* L. Moench) is the world's fifth cereal crop with an annual production in the order of 56 million tonnes (Taylor and Shewry 2006). Sorghum is used for both human consumption, particularly in Africa and India, and animal production (Selle, *et al.* 2010). However, one limitation of sorghum is that it has the lowest starch digestibility amongst cereal grains. This has been attributed to the resistant, peripheral endosperm layer encasing the starch granules (Rooney and Pflugfelder 1986). Heating grain using microwave energy offers a means of improving rumen fermentation of sorghum by disrupting the protein-starch complexes through the conductive migration and liberation of hydroscopically bound water within the material.

When samples of wheat, maize and sorghum (Mr Striker and Buster varieties) were ground and heated in a 900W microwave oven, operating at 2.45 GHz, for 3 and 5 minutes, significant improvements for *in vitro* rumen fermentation were observed compared with untreated samples (Bootes, *et al.* 2012). Samples (1.0 g) were incubated anaerobically at 39 °C for 48 hours in 100 mL of buffered rumen fluid and fermentation gas production was monitored automatically. Microwave treatment increased the maximum rate of rumen fermentation in Buster (+11%) and Mr Striker (+24%) sorghums, and also in the maize (+11%) but not in the wheat. No further improvements in rumen fermentation were observed by microwaving sorghum beyond 3 minutes. The extent of gas production during microbial fermentation of the substrate is directly related to the availability of nutrients to ruminant animals. It appears that microwave heating disrupts molecular cross-linking causing sudden granular rupture and disintegration of starch-protein complexes in the sorghum. This liberates a greater proportion of the sorghum starch and as a result of the higher available energy content, higher rates of *in vitro* rumen fermentation were observed (Bootes, *et al.* 2012).

Grains are also fed to mono-gastric animals such as horses and pigs. The major concern when feeding cereal grains to horses is the risk of incomplete starch digestion in the small intestine, which enables significant amounts of starch to pass through to the caecum and colon. When starch is able to reach these organs it rapidly ferments producing an accumulation of acidic products. This places the horse at risk of developing serious and potentially fatal illnesses such as laminitis, colic and ulcers (Bird, *et al.* 2001).

In vitro assessment of microwave treated oats, using the Megazyme Total Starch Assay Procedure (McCleary, *et al.* 1997) to assess starch digestion, significantly increased starch digestion as microwave treatment increased. This implies that microwave treatment of oats should increase the rate of intestinal digestion in horses and reduce the risk of undigested starch passing into the caecum and colon.

Microwave treatment profoundly affects the germination of grains, with any reasonable application of microwave power totally inhibiting grain germination

(Brodie, *et al.* 2012). Similarly, grain seeds that may be incorporated in fodder chaff will also be affected after microwave treatment. Significant reductions in grain germination occurred when 150 g (120 g of crop material + 20 g of wheat seeds and 10 g of annual ryegrass seed) samples of air-dry fodder chaff were treated with more than 100 kJ of microwave energy (Figure 20.4), using a 2.45 GHz conveyer feed wave-guide applicator system.

In addition to enhancing digestibility of the fodder chaff as shown earlier, inhibition of seed germination may also have useful applications for weed control. Importation of weed seeds in purchased fodder and hay is an important issue on many farms during times of drought. Microwave treatment of various materials has also been shown to kill pest insects and other pathogens (Nelson 1996, Park, *et al.* 2006).

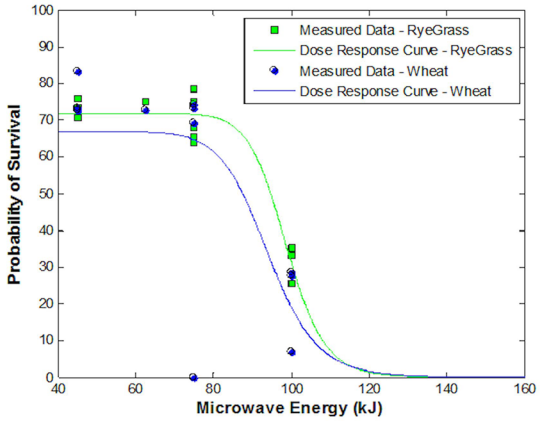

Figure 20.4: Seed germination as a function of applied microwave energy using a 2.45 GHz microwave system.

20.5 Effect of Microwave Heating on Crude Protein

Sadeghi et al. (2005) studied ruminal dry matter and crude protein degradation of 500 g untreated, 2-, 4- and 6-min microwave-treated samples of soya-bean meal. Nylon bags of untreated or treated soya-bean meal were suspended into the rumen of three Holstein steers from 0 to 48 h, and the data was fitted to non-linear degradation characteristics to calculate effective rumen degradation. There were significant differences in dry matter and crude protein degradation between the untreated and microwave-treated soya-bean meal. Microwave treatment decreased effective rumen degradation of crude protein.

In follow up studies (Sadeghi and Shawrang 2007), they tested both the ruminal and intestinal degradation of microwave treated cottonseed meal in non-lactating Holstein cows. They found that the effective ruminal degradability of crude protein significantly decreased as microwave processing time increased. Conversely, short duration microwave irradiation of the 500 g samples of cottonseed meal significantly increased intestinal digestibility of ruminally undegraded crude protein; however extending the microwave treatment to 6 min lowered the beneficial effect that the 4 min treatment had on intestinal crude protein digestibility. Non-rumen degradable crude protein, or "bypass protein", which is subsequently digested in the intestine, significantly increases animal production efficiency (Sklan and Tinsky 1993).

20.6 Conclusion

Microwave treatment of animal fodder and grains achieves many beneficial outcomes. It can be used for efficient drying and moisture levelling prior to long term fodder storage. Localised steam explosions within the cell structures during microwave treatment also significantly: increase the moisture permeability of biomass; decrease its mechanical strength; and increase its digestibility. Microwave treatment also modifies protein complexes making some grain starches more accessible to digestion and creating "bypass proteins", which are digested in the intestines rather than in the rumen. Creation of these proteins significantly improves animal production efficiency. As a secondary benefit, microwave treatment of hay and fodder can also kill weed seeds and provide some level of bio-security for farmers.

References

Bird, S., Brown, W. and Rowe, J. 2001. *Safe and Effective Grain Feeding for Horses*. Rural Industries Research and Development Corporation

Bootes, N. G., Brodie, G. I., Leury, B. J., Russo, V. M. and Dunshea, F. R. 2012. Microwaving improves in vitro rumen fermentation of sorghum. *Proc. 8th Joint INRA-Rowett Symposium on Gut Microbiology*. Clermont-Ferrand (FRANCE)

Brodie, G. 2007. Simultaneous heat and moisture diffusion during microwave heating of moist wood. *Applied Engineering in Agriculture*. 23(2): 179-187.

Brodie, G. 2010 Wood: Microwave Modification of Properties. In *Encyclopedia of Agricultural, Food and Biological Engineering*, 1878 - 1881. Heldman, D. R. ed. Taylor & Francis: London.

Brodie, G., Jacob, M. V., Sheehan, M., Yin, L., Cushion, M. and Harris, G. 2011. Microwave modification of sugar cane to enhance juice extraction during milling. *Journal of Microwave Power and Electromagnetic Energy*. 45(4): 178-187.

Brodie, G., Rath, C., Devanny, M., Reeve, J., Lancaster, C., Harris, G., Chaplin, S. and Laird, C. 2010. Effect of microwave treatment on lucerne fodder. *Animal Production Science*. 50(2): 124–129.

Brodie, G., Ryan, C. and Lancaster, C. 2012. Microwave technologies as part of an integrated weed management strategy: A Review. *International Journal of Agronomy*. 2012: 1-14.

Chaudhry, A. S. 2000. Rumen degradation in sacco in sheep of wheat straw treated with calcium oxide, sodium hydroxide and sodium hydroxide plus hydrogen peroxide. *Animal Feed Science and Technology*. 83(3–4): 313-323.

Chen, C., Aita, G. and Boldor, D. 2010. Enhancing Enzymatic Digestibility of Sweet Sorghum by Microwave-assisted Dilute Ammonia Pretreatment. *ASABE*. (1009192):

DeAngelo, B. J., De la Chesnaye, F. C., Beach, R. H., Sommer, A. and Murray, B. C. 2006. Methane and Nitrous Oxide Mitigation in Agriculture. *Energy Journal*. 27: 89.

Dong, S., Long, R., Zhang, D., Hu, Z. and Pu, X. 2005. Effect of microwave treatment on chemical composition and in sacco digestibility of wheat straw in yak cow *Asian-Australasian Journal of Animal Sciences*. 18(1): 27-31.

Ekiz, B., Yilmaz, A., Ozcan, M. and Kocak, O. 2012. Effect of production system on carcass measurements and meat quality of Kivircik lambs. *Meat Science*. 90(2): 465-471.

El-Meccawi, S., Kam, M., Brosh, A. and Degen, A. A. 2008. Heat production and energy balance of sheep and goats fed sole diets of Acacia saligna and Medicago sativa. *Small Ruminant Research*. 75(2–3): 199-203.

Harris, G. A., Brodie, G. I., Ozarska, B. and Taube, A. 2011. Design of a Microwave Chamber for the Purpose of Drying of Wood Components for Furniture. *Transactions of the American Society of Agricultural and Biological Engineers*. 54(1): 363-368.

Harris, G. A., Torgovnikov, G., Vinden, P., Brodie, G. I. and Shaginov, A. 2008. Microwave pretreatment of backsawn messmate boards to improve drying quality: Part 1. *Drying Technology*. 26(5): 579 - 584.

Kanagawa, Y., Hayashi, K. and Yasiizitna, M. 1992. Improvement of dryability by local steam explosion for Japanese cedar. *Proc. 3rd IUFRO Wood Drying Conference*. 269-276.Vienna, Austria

Kurihara, M., Magnera, T., Huntera, R. A. and McCrabba, G. J. 1999. Methane production and energy partition of cattle in the tropics. *British Journal of Nutrition*. 81(3): 227-234.

Kutlu, H., Gorgulu, M., Baykal, L., Ozcan, N. and Buyukalaca, S. 2000. Effects of Pleurotus florida inoculation or urea treatment on feeding value of wheat straw. *Turkish Journal of Veterinary and Animal Sciences*. 24(2): 169-175.

Liu, J.-X., Orskov, E. R. and Chen, X. B. 1999. Optimization of steam treatment as a method for upgrading rice straw as feeds. *Animal Feed Science and Technology*. 76(3–4): 345-357.

McCleary, B. V., Gibson, T. S. and Mugford, D. C. 1997. Measurement of total starch in cereal products by amyloglucosidase-alpha-amylase method: Collaborative study. *Journal of Aoac International*. 80(3): 571-579.

McLeod, M. N. and Minson, D. J. 1978. The accuracy of the pepsin-cellulase technique for estimating the dry matter digestibility in vivo of grasses and legumes. *Animal Feed Science and Technology*. 3(4): 277-287.

McLeod, M. N. and Minson, D. J. 1980. A note on Onozuka 3S cellulase as a replacement for Onozuka SS (P1500) cellulase when estimating forage digestibility in vitro. *Animal Feed Science and Technology*. 5(4): 347-350.

Meat and Livestock Australia Limited. 2005. *The National Livestock Reporting Service Sheep Assessment*. Meat and Livestock Australia Limited

Minson, D. J. and McDonald, C. K. 1987. Estimating forage intake from the growth of beef cattle. 21: 116-122.

Mirzaei-Aghsaghali, A. and Maheri-Sis, N. 2011. Factors Affecting Mitigation of Methane Emission from Ruminants I: Feeding Strategies. *Asian Journal of Animal & Veterinary Advances*. 6(9): 888-908.

Nelson, S. O. 1996. Review and assessment of radio-frequency and microwave energy for stored-grain insect control. *Transactions of the ASAE*. 39(4): 1475-1484.

Park, D., Bitton, G. and Melker, R. 2006. Microbial inactivation by microwave radiation in the home environment. *Journal of Environmental Health*. 69(5): 17-24.

Rooney, L. W. and Pflugfelder, R. L. 1986. Factors Affecting Starch Digestibility with Special Emphasis on Sorghum and Corn. 63(5): 1607-1623.

Sadeghi, A. A., Nikkhaha, A. and Shawrang, P. 2005. Effects of microwave irradiation on ruminal degradation and in vitro digestibility of soya-bean meal. *Animal Science*. 80(3): 369-375.

Sadeghi, A. A. and Shawrang, P. 2007. Effects of microwave irradiation on ruminal protein degradation and intestinal digestibility of cottonseed meal. *Livestock Science*. 106(2-3): 176-181.

Selle, P. H., Cadogan, D. J., Li, X. and Bryden, W. L. 2010. Implications of sorghum in broiler chicken nutrition. *Animal Feed Science and Technology*. 156(3–4): 57-74.

Sklan, D. and Tinsky, M. 1993. Production and reproduction responses by dairy cows fed varying undegradable protein coated with rumen bypass fat. *Journal of Dairy Science*. 76(1): 216-223.

Taylor, J. and Shewry, P. 2006. Preface to sorghum and millets reviews. *Journal of Cereal Science*. 44(3): 223.

Torgovnikov, G. and Vinden, P. 2003 Innovative microwave technology for the timber industry. In *Microwave and Radio Frequency Applications: Proceedings of the Third World Congress on Microwave and Radio Frequency Applications*, 349-356. Folz, D. C., et al. eds. The American Ceramic Society: Westerville, Ohio.

Torgovnikov, G. and Vinden, P. 2010. Microwave Wood Modification Technology and Its Applications. *Forest Products Journal*. 60(2): 173–182.

Van Soest, P. J. 1994, *Nutritional Ecology of the Ruminant*, 2nd edn, Ithaca, NY: Cornell University Press.

Vinden, P. and Torgovnikov, G. 1996. *A method for increasing the permeability of wood*. Patent No. PO 0850/96

Vinden, P. and Torgovnikov, G. 2000. The physical manipulation of wood properties using microwave. *Proc. International Conference of IUFRO*. 240-247.Tasmania, Australia

Vinden, P., Torgovnikov, G. and Hann, J. 2011. Microwave modification of Radiata pine railway sleepers for preservative treatment. *Holz als Roh- und Werkstoff: European journal of wood and wood industries*. 69(2): 271-279.

Yin, L., Singh, P., Brodie, G., Sheehan, M. and Jacob, M. V. 2012. Influence of microwave energy on mechanical strength in sugarcane. *Proc. 7th Australasian Congress on Applied Mechanics*. Adelaide, Australia

21 Wood Modification

Throughout history, wood has been used for the construction of homes and other structures, furniture, tools, vehicles, and decorative objects. Wood is used to produce a variety of products, including cut and dressed poles, sawn and dressed planks, veneers, laminated products, particleboard, fiberboard, paper and cardboard.
The anatomy and growth behaviour of trees clearly influences the properties and behaviour of wood. A cross section of a tree trunk (Figure 21.1) shows the well defined features of most trees (Forest Products Laboratory 1999):

1. ***bark***, which may be divided into an outer corky dead part, whose thickness varies greatly with species and age of trees, and an inner thin living part, which carries food from the leaves to growing parts of the tree;
2. ***wood***, which in merchantable trees of most species is clearly differentiated into sapwood and heartwood; and
3. ***pith***, a small core of tissue located at the center of tree stems, branches, and twigs about which initial wood growth takes place.

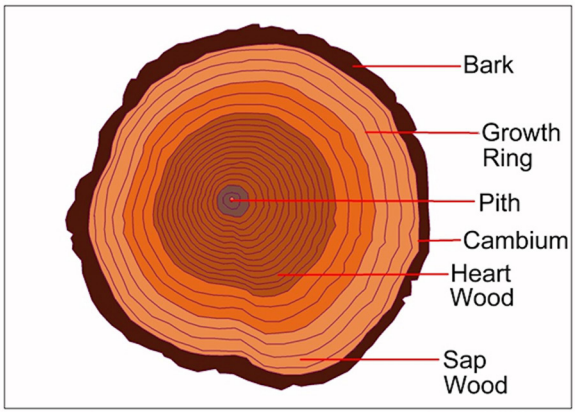

Figure 21.1: Cross section of tree trunk (Source: Brodie 2008).

Sapwood contains both living and dead tissue and carries sap from the roots to the leaves (Jackson and Day 1989, Forest Products Laboratory 1999). Heartwood is formed by a gradual change in the sapwood and is inactive (Jackson and Day 1989, Forest Products Laboratory 1999). Rays, which are horizontally oriented tissue running from the pith to the cambium, vary in size from one cell wide and a few cells high to more than 15 cells wide and several centimetres high (Jackson and Day 1989, Forest Products Laboratory 1999). The cambium layer is inside the inner bark and forms both wood and bark cells. The cambium layer can only be seen with a microscope (Jackson and Day 1989, Forest Products Laboratory 1999).

The macroscopic structure of wood can be described in terms of early wood and later wood, longitudinal tracheids, rays, resin channels in softwoods and vessels in hardwoods (Meyland and Butterfield 1972, Jackson and Day 1989, Torgovnikov 1993). Some of these elements are illustrated in Figure 21.2.

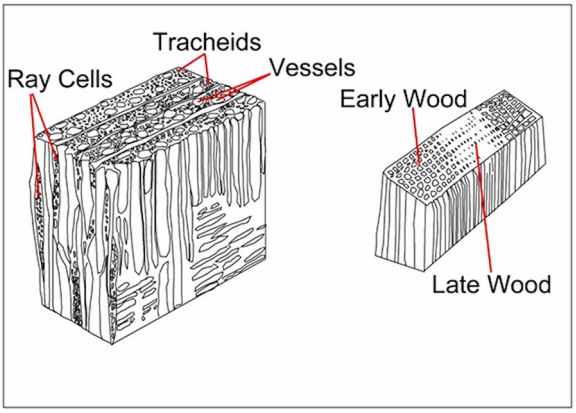

Figure 21.2: Macro-structural elements of wood (Source: Brodie 2008).

The appearance of growth rings, associated with the deposition of early and late wood, is due to structural changes in the wood cells produced by the cambium through the growing season (Jackson and Day 1989). Cells produced at the beginning of the growing season are usually larger, and so this early wood appears less dense than the late wood produced towards the end of the season.

Although all trees produce concentric layers of wood, not all trees produce visible growth rings, neither are all growth rings necessarily annual (Jackson and Day 1989). In some trees seasonal changes in wood structure may be so slight that growth rings are not evident. Under conditions of severe drought a visible growth ring may not be produced at all. On the other hand, under continuously favourable conditions, such as in the tropics, several growth rings may be produced in a single year (Society of Wood Science and Technology 2001).

Moist wood is essentially a heterogeneous mixture of solid, liquid and gaseous materials. Wood cells are built up as a honeycomb like structure oriented along the stem, except in the case of ray cells. The cell wall is a composite material consisting of partly crystalline cellulose micro-fibrils embedded in an amorphous matrix made up of hemicelluloses and lignin (Torgovnikov 1993, Forest Products Laboratory 1999).

At the micro-structural level, wood can be described in terms of longitudinal tracheids, pit pairs, which connect between tracheids, the primary cell walls and the secondary cell walls (Meyland and Butterfield 1972, Hofstetter, *et al.* 2007). Hardwoods

contain vessel elements (Forest Products Laboratory 1999) while softwoods often contain resin channels (Jackson and Day 1989). The orientation of wood cells profoundly affect all the measurable properties of wood (Torgovnikov 1993).

A vessel is a wood cell with open ends. When vessel elements are set one above another, they form a continuous tube (vessel), which serves as a conduit for transporting water or sap in the tree. Vessels may extend to the full height of the tree; however they more commonly only extend over short distances (< 200 mm) in most species (Forest Products Laboratory 1999). Tyloses are balloon-shaped intrusions (Meyland and Butterfield 1972) that appear in hardwood vessels at the time of heartwood formation. They extend from the parenchyma cells into the vessels and have the effect of blocking or clogging vessels that have been damaged by cavitation in the water column inside the vessel (Forest Products Laboratory 1999, Jackson and Day 1989).

At the molecular level, wood must be described in terms of polymers, free and bound water, extractives, minor amounts (5% to 10%) of extraneous materials contained in a cellular structure and air (Meyland and Butterfield 1972, Hofstetter, *et al.* 2007). The polymers of wood can be classified into three major types: cellulose, hemi-cellulose, and lignin. The proportion of these three polymers varies between species (Society of Wood Science and Technology 2001). Variations in the characteristics and volume of these components and differences in cellular structure make woods heavy or light, stiff or flexible, and hard or soft (Forest Products Laboratory 1999).

Cellulose is the most important single compound in wood. It provides wood's strength. Cellulose is a product of photosynthesis (Knox, *et al.* 2001). In photosynthesis, glucose and other sugars are manufactured from water and carbon dioxide. The glucose is chemically changed to glucose anhydride by the removal of one molecule of water from each glucose unit. These glucose anhydride units then polymerize into long chain cellulose molecules that contain from 5,000-10,000 glucose units (Society of Wood Science and Technology 2001).

Hemi-celluloses are a group of compounds similar to cellulose, but with a lower molecular weight. The number of repeating end-to-end molecules in hemi-cellulose is only about 150 compared to the 5,000-10,000 of cellulose (Society of Wood Science and Technology 2001). Lignin is a complex, high molecular weight polymer whose exact structure varies. It is an amorphous polymer that acts as a binding agent to hold cells together. Lignin also occurs within cell walls to impart rigidity (Society of Wood Science and Technology 2001).

When timber is harvested, it is usually sawn before further processing takes place. There are several methods of sawing timber (Figure 21.3). in most cases, freshly sawn timber needs to dry before it can be used.

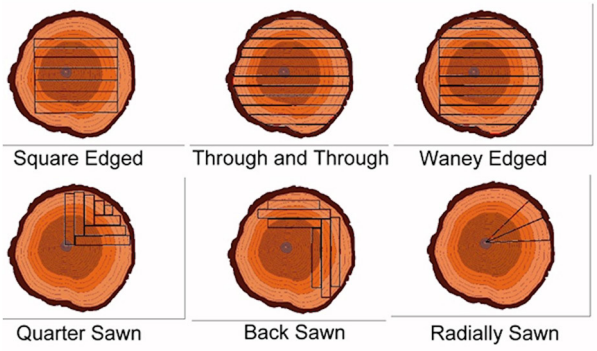

Figure 21.3: Various methods of sawing timber (Source: Brodie 2008).

21.1 Applications of Microwave Modification in Wood Drying

Emphasis in the Australian hardwood industry is shifting away from structural-grade timber toward the production of high-value products (Vermaas 2000). This is also true in China, Chile, Brazil, and South Africa, all of which have substantial eucalyptus-based hardwood industries (Vermaas 2000). The high shrinkage, low diffusivity, and highly refractory properties of many hardwoods and some softwoods make them extremely difficult to dry without drying defects, especially in back-sawn boards (Rozsa 1998). Drying defects include: splitting (often referred to as checking), warping, twisting, and collapse. To facilitate this shift in industry emphasis toward high-quality products, drying technology is once again becoming an important focus of research and development.

The first stage in the drying of timber from eucalypt species is usually a slow process involving a long period of air drying or pre-drying under mild conditions until the moisture content of the board approaches the fibre saturation point (FSP). However, even under the best controlled conditions surface checks, collapse of the cross section and internal collapse checks degrade a significant proportion of timber that would otherwise be used for appearance grade products (Rozsa 1995).

As wood dries below fibre saturation, the various polymers loose bound water and shrink. The drying rate varies across a sawn board's cross section; therefore the rate of shrinkage also varies. This induces drying stresses in the timber. When the local drying stress exceeds the tensile strength of wood perpendicular to the grain, the timber fibres separate. This is commonly referred to as checking. There are two types of checks that can develop: surface checks, which develop on the surface of a board and internal checks (or honeycombing), which develop within the board. Both types of defects can occur concurrently.

Surface checking usually develops during the early stages of drying when wood in the outer part, or case, of a section is low in moisture relative to the inner part, or core.

Under these circumstances, shrinkage in the case leads to tension stress, which in turn may lead to surface checking. In some circumstances, readily observable surface checks may be removed by planning (Standards Australia/New Zealand 2001).

Refractory species are difficult to dry and are prone to surface checking, particularly when back-sawing techniques are used to produce usable boards. For example, checks in mature messmate (*Eucalyptus oliqua*) begin to appear on the surface after the loss of only a small proportion of moisture (Mackay 1972). The rate of moisture movement out of wood during drying is influenced by the permeability of the wood, which in turn is affected by the availability of unobstructed pathways from the core of the sawn timber to the surface. The presence of vessels in hardwood provides longitudinal pathways for moisture movement, chemical impregnation, drying, gluing, painting, cutting and other processes (Hillis and Brown 1984); however the presence of tyloses and incrustations in the vessels inhibits moisture and solvent movement through the material. The extent of direct contact between vessels and other elements is also important and is influenced by the nature of pits, which varies according to the contiguous elements.

Kanagawa, et al. (1992) developed an effective method to improve the permeability of Japanese cedar wood (*Cryptomeria japonica*) by generating steam inside the wood cells. The method, which is called Local Steam Explosion, heats and softens wood in a chamber using high-pressure super-heated steam and then instantaneously exhausts the steam from the chamber. The sudden release of pressure instantaneously boils free water in the wood cells. Permeability of the woody material is significantly increased due to the creation of local fractures in the wood cells. Steam pre-conditioning has also been used for some time to increase the permeability of *Pinus radiata* (D. Don); however, a substantial strength loss is often incurred (Vinden and Torgovnikov 2000).

Research into the application of microwave pre-treatment to green wood, as an alternative to steam pressure treatment (Vinden and Torgovnikov 2000, Vinden, *et al*. 2010, 2011), found that intensive short duration microwave irradiation can be used to modify the structure of refractory hardwoods by bursting the tyloses (increasing longitudinal permeability), rupturing ray cells (increasing radial permeability) and creating micro-voids at the fibre/ray intersection (also improving the radial permeability of timber). This modification results from a build-up of steam pressure in the moist green wood. The improvement in wood permeability facilitates faster drying, with potentially fewer drying defects.

Vinden et al. (2003) were granted a patent for this process, which describes a method for increasing the permeability of timber by applying microwave energy with power densities between 10 W cm^{-2} and 100 kW cm^{-2} for durations of between 0.05 and 600 seconds resulting in a permeability increases of at least 500% compared to that of untreated wood. The preferential Electric field orientation is perpendicular to the grain and aligned with the radial direction of the timber. Preheating the timber to a temperature of between 80 and 110°C before final microwave treatment also seems to be beneficial. A study carried out by Manríquez and Moraes (2010) showed

that the molecular structure of moist lignin is modified and moist hemi-cellulous begins to soften when the temperature rises above 55 °C; therefore pre-heating of the green timber softens and weakens the cells that are targeted by the microwave preconditioning technique.

Vinden et al. (2007) described seven changes that occur in timber during microwave modification. Some of these included microscopic rupturing of pit membranes, tyloses, inter ray tissue and fibres, as well as macroscopic expansion of voids, resulting in an expansion of the cross section and a spongy wood product. Where these types of modification are not present after microwave treatment, the wood has simply been heated, but not modified, which still has applications for wood bending, sterilisation, drying, etc.

They later defined three levels of modification (Torgovnikov and Vinden 2008). Low level modification increases the permeability by 1.1 to 1.5 times; moderate modification increases the permeability by about a thousand times; and high modification converts wood to a highly permeable material with permeability increased by millions of times that of normal wood. Using a frequency of 2.45 GHz requires a power density of between 13,000 and 89,000 kW m^{-3} and energy densities between 270 and 1080 MJ m^{-3} to obtain the varying degrees of modification.

Any improvement in wood permeability has an impact on capillary flow of moisture (Hillis and Brown 1984). By increasing the permeability of wood, moisture is able to move more freely, ensuring the evaporative front is maintained close to the case of the board for a longer period during drying; therefore reducing tension stress in the wood and in turn preventing surface checking.

Harris et al. (2008) found that there was a significant reduction in surface checking, both in number and depth, in microwave modified messmate boards compared to the controls. Check assessment was carried out by comparing the total number of checks (including both internal/honeycombing and surface checks) per specimen. In addition a check area ratio (CAR) was calculated for each sample by dividing the total area of checks by the total sample cross sectional area (including the area occupied by the checks). The results indicate that microwave pre-treatment, prior to conventional drying, significantly reduced the total number of checks per specimen as well as reduced the CAR.

Brodie (2007) demonstrated that microwave treatment of *Populus alba* and *Eucalyptus regnans* prior to solar drying reduced drying time, compared with solar drying without microwave treatment, by 17% and 33%, respectively. This acceleration in drying may be attributed to a combination of the 8% to 9% reduction in wood density and a substantial improvement in moisture permeability associated with the internal fractures created in the wood structure.

21.2 Improving Wood Impregnation

Vinden and Torgovnikov (2000) also developed a product formed under intense microwave irradiation which they named Torgvin. In this process, larger cavities are formed in the longitudinal-radial plane, expanding the cross section of the timber, resulting in a reduced oven dry density of up to 15% and increasing the radial permeability by 170 to 1200 times. The main application of this material is a composite product where resin is introduced and the wood is compressed back to its original dimensions (Torgovnikov and Vinden 2002).

Microwave energy between 1 MJ m^{-3} and 4,000 MJ m^{-3} was applied to moist wood, increasing the permeability and creating cavities. This was followed by drying, impregnation of the cavities with resin and compression of the wood to close the voids left by the microwave treatment and bond the resin to the fibres (Torgovnikov and Vinden 2002). The resulting composite material has a high strength and dimensional stability while in most cases looking like normal wood.

Vinden and Torgovnikov (2000) also found that moderate modification could improve preservative uptake. A 60kW, 922 MHz microwave source was used to treat softwood as it was fed through on a conveyor. While modification of 90mm x 90mm heartwood was achieved using 7.5 kW, they demonstrated that using between 54 and 57 kW gave the best results. Energy densities of 421 MJ m^{-3} were required to make Douglas fir heartwood permeable, increasing preservative uptake by a factor of 5 to 6.

Similar results were reported in hardwoods, where intensive microwave treatment resulted in rupture of tracheids and libriform fibres in the ray tissue, formation of micro-checks at the interface of the ray tissue and longitudinal fibres and formation of voids in the longitudinal-radial plane. They found the resultant increase in permeability accelerated the drying process, relieved stresses, reduced check formation and improved impregnability.

21.3 Stress Relief

Carter et al. (2003) investigated the effect of a microwave treatment on growth stress in large rounds of *Eucalyptus globulus*. Microwave treated logs displayed considerably less crack formation than the control samples after air drying. They also showed negligible deformation in a prong test, indicating that internal stresses were relieved by microwave treatment. While the actual mechanism leading to the stress relief was not detailed, it could be due to a more even moisture gradient, or increased permeability, or heat softening of the timber to relieve the stresses.

21.4 Industrial Scale Pilot Plant

Vinden et al. (2006) used a 300 kW microwave system consisting of three 100 kW applicators arranged radially around a conveyor for continuous processing of logs and sleepers. They found that power densities up to 30 kW cm^{-2} produced more consistent modification. They also found that energy requirements for commercial scale applications were lower than expected from laboratory experiments. This may have been due to the larger cross sections facilitating the build-up of higher pressures and temperatures within the wood structure, leading to a higher degree of modification, with a lower portion of the energy lost to vaporisation of the surface moisture. Energy densities of between 273 and 1,080 MJ m^{-3} were required depending on species, moisture content and degree of modification.

Further details were provided on the 300kW, 0.922 GHz, microwave plant for modification of sawn and round timber (Torgovnikov and Vinden 2006b). Power densities of between 0.05 and 30 kW cm^{-2} were reported to produce modification, with higher power intensity providing better control. Energy densities ranged between 300 and 2000 MJ m^{-3}. High velocity heated air flow and a cyclonic separator were used to remove moisture and wood particles from the applicator and prevent condensation. The costs of microwave modification were assessed and found to be acceptable to industry.

Torgovnikov and Vinden (2006a) reported further on their research into the microwave modification of timber. A conveyor style 57 kW microwave treatment plant was used to treat timber to create Torgvin from a number of species, with electrical energy consumption ranging between 432 and 1,080 MJ m^{-3}. Volumetric expansions of up to 15% and preservative uptakes of 10 times greater than control samples were achieved.

The strength of the timber in the tangential and radial direction was reduced as a function of the treatment energy density, with losses of up to 80% and 70% respectively in the modulus of rupture (MOR). A reduction in the tangential MOR of between 15% and 23% was required to achieve significant increases in permeability. Microwave treatment energy densities of between 288 and 576 MJ m^{-3} were suitable for a pre-drying treatment of Messmate (*Eucalyptus obliqua*). These treatments reduced the drying time for Messmate, using conventional drying systems, by up to 90%. All microwave treatments were performed at atmospheric pressure.

Vinden et al. (2010) utilised a 300 kW, 0.922 GHz conveyor fed microwave plant, to treat *Pinus radiata* railway sleepers up to 130mm x 260mm in cross section. Permeability was increased (measured by preservative uptake) allowing for subsequent impregnation of both the sapwood and heartwood with preservative. Microwave treatment power densities were in the range of 5000 to 8800 kW m^{-3} and energy densities were in the range of 250 to 550 MJ m^{-3}, with the wood starting at a moisture content of 31 to 35%. They found proper treatment required an energy density of 270 to 395 MJ m^{-3}, with higher energy densities leading to significant strength

loss and deformation. Preservative uptakes, relative to control samples, increased by 1.7 to 4.5 fold, depending on preservative type.

21.5 Pre-treatment for Wood Pulping

Akhtar et al. (2004) were granted a patent on their invention of microwave treating logs prior to mechanical pulping, resulting in a decrease in pulping energy and increase in paper strength. They found that the microwave treatment of logs at 50 kW for five minutes resulted in increased porosity, with jets of steam escaping from the wood during treatment, suggesting a concurrent increase in permeability.

Lawrence (2006) demonstrated that application of intense microwave energy can reduce the density of *Eucalyptus obliqua* wood by up to 12 %, depending on microwave energy absorbed by the samples. Softwoods such as *Pinus radiata* can experience a more substantial change in density when exposed to the same energy levels (Lawrence 2005). This change in density associated with microwave treatment can reduce wood hardness by up to 54 % (Awoyemi 2003) compared to untreated wood. Brodie et al. (2011) found that microwave pre-treatment of sugar cane reduced the compressive strength of the cane to about 18 % of its original strength (the control samples). Scott and Klungness (2005) showed that using microwave preconditioning on logs, before reducing them to paper pulp, reduced total energy consumption in the wood pulping process by 15%.

Compere et al. (2004) also investigated the application of microwave pre-treatment to pulping logs and chips. They found that pulping energy and chemical consumption was reduced and up to 30% oversized chips could be processed, suggesting greater chemical penetration due to increased permeability from the microwave treatment.

This chapter has explored how microwave pre-treatment can rupture plant cells to facilitate faster movement of water, resins or solvents into or out of woody material. It has also shown how microwave pre-treatment can be used to soften woody material to reduce the energy required for down-stream processing. These same features can also be used to enhance extraction of other valuable products from plant materials. This will be briefly explored in the next chapter.

References

Akhtar, M., Lentz, M., Horn, E., Klungness, J. and Scott, C. 2004. *Microwave pre-treatment of logs for use in making paper and other wood products*. Patent No. US2004238134

Awoyemi, L. 2003. Effects of microwave modification on the hardness of *Eucalyptus obliqua* wood. *Journal of the Institute of Wood Science*. 16(3): 186-188.

Brodie, G. 2007. Microwave treatment accelerates solar timber drying. *Transactions of the American Society of Agricultural and Biological Engineers*. 50(2): 389-396.

Brodie, G., Jacob, M. V., Sheehan, M., Yin, L., Cushion, M. and Harris, G. 2011. Microwave modification of sugar cane to enhance juice extraction during milling. *Journal of Microwave Power and Electromagnetic Energy*. 45(4): 178-187.

Brodie, G. I. 2008, *Innovative wood drying: Applying microwave and solar technologies to wood drying*, Saarbruecken, Germany: VDM Verlag.

Carter, P., Hutchings, P. and Tran, V. 2003. Microwave technology for heating large diameter logs for sapstain treatment and stress relief. *Proc. Third World Conference on Microwave and Radio Frequency Applications*. 341-348.Sydney, Australia

Compere, A., Gardner, W., Griffith, W., White, T., Jameel, H., Argyropoulos, D. and Fricke, A. 2004. Microwave pre-treatment to decrease pulping energy and chemicals. *Proc. TAPPI Paper Summit - Spring Technical and International Environmental Conference*.

Forest Products Laboratory 1999, *Wood Handbook—Wood as an engineering material*, Madison, Wisconsin: U.S. Department of Agriculture, Forest Service, Forest Products Laboratory.

Harris, G. A., Torgovnikov, G., Vinden, P., Brodie, G. I. and Shaginov, A. 2008. Microwave pretreatment of backsawn messmate boards to improve drying quality: Part 1. *Drying Technology*. 26(5): 579 - 584.

Hillis, W. E. and Brown, A. G. 1984, *Eucalypts for Wood Production*, Australia: CSIRO Publications and Academic Press.

Hofstetter, K., Hellmich, C. and Eberhardsteiner, J. 2007. Micromechanical modeling of solid-type and plate-type deformation patterns within softwood materials. A review and an improved approach. *Holzforschung*. 61(4): 343-351.

Jackson, A. and Day, D. 1989, *Wood Worker's Manual*, Sydney: William Collins Sons & Co. Ltd.

Kanagawa, Y., Hayashi, K. and Yasiizitna, M. 1992. Improvement of dryability by local steam explosion for Japanese cedar. *Proc. 3rd IUFRO Wood Drying Conference*. 269-276.Vienna, Austria

Knox, B., Ladiges, P., Evans, B. and Saint, R. 2001, *Biology*, 2nd edn, Roseville, Australia: McGraw-Hill.

Lawrence, A. 2005. Differential response of hardwood and softwood to microwave modification. *Journal of the Timber Development Association of India*. 51(3/4): 49-53.

Lawrence, A. 2006. Effect of microwave modification on the density of *Eucalyptus obliqua* wood. *Journal of the Timber Development Association of India*. 52(1/2): 26-31.

Mackay, J. F. G. 1972. The occurrence, development and control of checking in Tasmanian Eucalyptus oliqua. *Holzforschung*. 26: 121-124.

Manríquez, M. J. and Moraes, P. D. 2010. Influence of the temperature on the compression strength parallel to grain of paricá. *Construction and Building Materials*. 24(1): 99-104.

Meyland, B. A. and Butterfield, B. G. 1972, *Three-dimensional Structure of Wood: A Scanning Electron Microscope Study*, Reed Education.

Rozsa, A. 1995. Moisture movement in eucalypt timbers during microwave vacuum drying. *Proc. International Conference on Wood Drying*. 289-294.Slovak Republic

Rozsa, A. 1998. *Processing Green Timber from South-East Australian Ash-Type Hardwoods*. CSIRO Forestry and Forest Products

Scott, C. T. and Klungness, J. 2005 Microwaving logs for energy savings and improved paper properties for mechanical pulps. In *Microwave and Radio Frequency Applications: Proceedings of the Fourth World Congress on Microwave and Radio Frequency Applications*, 75-82. Schulz, R. L. and Folz, D. C. eds. The Microwave Working Group: Arnold MD.

Society of Wood Science and Technology. 2001. *Structure of Wood*. Society of Wood Science and Technology

Standards Australia/New Zealand. 2001. Assessment of drying quality. AS/NZ 4787:2001:

Torgovnikov, G. and Vinden, P. 2002. *Modified wood product and the process for the preparation thereof*. Patent No.

Torgovnikov, G. and Vinden, P. 2006a Microwave Method for Increasing the Permeability of Wood and its Applications. In *Advances in Microwave and Radio Frequency Processing*, 303-311. Springer Berlin Heidelberg.

Torgovnikov, G. and Vinden, P. 2006b. New 300KW plant for microwave wood modification. *Proc. IMPI 40th annual international microwave symposium*. Boston, USA

Torgovnikov, G. and Vinden, P. 2008. Main aspect of microwave wood modification applicable to the timber industry. *Proc. Global congress on microwave energy applications*. 407-410.

Torgovnikov, G. I. 1993, *Dielectric Properties of Wood and Wood-Based Materials*, Springer Series in Wood Science, Berlin: Springer-Verlag.

Vermaas, H. F. 2000. A review of drying technologies for young fast-grown eucalypts. *Proc. International Conference of IUFRO*. 193-203.Tasmania, Australia

Vinden, P., Romero, F. J. and Torgovnikov, G. 2003. *Method for increasing the permeability of wood*. Patent No. 6,596,975

Vinden, P. and Torgovnikov, G. 2000. The physical manipulation of wood properties using microwave. *Proc. International Conference of IUFRO*. 240-247.Tasmania, Australia

Vinden, P., Torgovnikov, G., Blackwell, P., Hann, J. and Shaginov, A. 2006. Microwave processing of wood: the design of commercial plant. *Proc. European Panel Products Symposium*. Llandudno, Wales, UK

Vinden, P., Torgovnikov, G. and Hann, J. 2010. Microwave modification of Radiata pine railway sleepers for preservative treatment. *European Journal of Wood and Wood Products*. 1-9.

Vinden, P., Torgovnikov, G. and Hann, J. 2011. Microwave modification of Radiata pine railway sleepers for preservative treatment. *Holz als Roh- und Werkstoff: European journal of wood and wood industries*. 69(2): 271-279.

Vinden, P., Torgovnikov, G., Przewloka, S., Hann, J. and Shaginov, A. 2007. The Manufacture of Solid Wood Composites from Microwave Modified Wood. *Proc. International Panel Products Symposium*. Cardiff, Wales, UK

22 Microwave Assisted Extraction

The most widely described application of microwave treatment in organic materials processing has been microwave assisted extraction. In this method, plant materials such as wood, seeds and leaves are suspended in solvents and the mixture is exposed to microwaves instead of conventional heating. Enhanced rates of extraction for plant based oils have been observed for a range of plant materials.

All microwave-assisted extraction techniques can be considered an alternative to conventional techniques because they reduce: extraction times; costs; energy; solvent consumption; and CO_2 emissions (Chemat and Cravotto 2013). In addition, some techniques have been successfully applied at an industrial scale in the cosmetic, perfume, and nutraceutical industries (Chemat and Cravotto 2013).

This chapter outlines some examples of microwave assisted extraction.

22.1 Solvent based Extraction of Essential Oils

Microwaves assisted extraction maintains mild conditions and usually provides superior extraction; however, apart from laboratory trials, essential oil extraction using microwave energy has had limited commercial development. There are two problems to overcome in the extraction from solid plant materials: that of releasing the essential oil from solid matrix and letting it diffuse out successfully in a manner that can be scaled-up to industrial volumes (Ramanadhan 2005).

Chen and Spiro (1994) examined the extraction of the essential oils of peppermint and rosemary from hexane and ethanol mixtures using pulsed microwave energy and found that yields were more than one third greater than from conventional steam distillation techniques. They found that 10 s pulses and 5 minute cooling intervals using 90 % ethanol provided the greatest overall oil yield of a-pinene, with 30 s pulses and 5 minute cooling intervals in hexane providing the second highest yield.

The dielectric properties of ethanol are 7.9 + j 7.1 while the dielectric properties of hexane are 1.9 + j 0.0005 (Chen and Spiro 1994). The dielectric properties of rosemary and peppermint leaves are 19.0 + j 4.3 and 4.1 + j 1.3 respectively (Chen and Spiro 1994). Therefore it is expected that ethanol will heat faster than the leaf material wile hexane will heat slower than the leaf material when exposed to microwave fields. Based on temperature data acquired using an IR pyrometer, Chen and Spiro (1994) found that the temperature of peppermint and rosemary leaves was lower than that of the solution by 4 to 12 °C when hexane was used for the solvent. Saoud *et al.* (2006) studied microwave enhanced extraction of essential oils from tea leaves and achieved higher yields (26.8 mg g^{-1}) than steam distillation (24 mg g^{-1}).

Chemat et al. (2005) studied the extraction of oils from limonene and caraway seeds and found that microwave assisted extraction led to more rapid extraction as well as increased yields. Microwave assisted extraction yielded 32 compounds

in the caraway seed oil, while steam distillation yielded only 18 compounds. Scanning electron microscopy of the microwave treated and untreated seeds revealed significantly increased rupture of the cell walls in the treated seeds. Microwave assisted extraction also led to a more chemically complex extract, which was thought to be a better representation of the true composition of the available oils in caraway seed.

Cardoso-Ugarte, et al. (2013) demonstrated that the amount of solvent and heating time significantly affected the yield of essential oils from basil (*Ocimum basilicum*) and epazote (*Chenopodium ambrosioides*). They found that basil essential oil yield was not significantly different from steam distillation yields; however epazote essential oil yield was significantly higher than the oil yield obtained by steam distillation. In both cases, microwave assisted extraction required much less time and yielded a richer chemical mixture than steam distillation methods.

22.2 Solvent Free Extraction of Essential Oils

Solvent-free microwave extraction is a combination of microwave heating and dry distillation, performed at atmospheric pressure without added any solvent or water. Isolation and concentration of volatile compounds are performed by a single stage. Lucchesi, *et al.* (2004) compared this technique with conventional steam distillation, for the extraction of essential oil from three aromatic herbs: basil (*Ocimum basilicum* L.), garden mint (*Mentha crispa* L.), and thyme (*Thymus vulgaris* L.). The solvent free method yields an essential oil with higher amounts of more valuable oxygenated compounds, and allows substantial savings of costs, in terms of time, energy and plant material.

The energy required to perform the two extraction methods are respectively 4.5 kWh for steam distillation and 0.25 kWh for solvent free microwave extraction. Steam distillation required an extraction time of 270 min for heating 6 kg of water and 500 g of plant material to the extraction temperature, followed by evaporation of water and the essential oil. The solvent free microwave extraction required only 30 min of heating the plant matter and evaporation of the *in situ* water and essential oil of the plant material.

Singh, *et al.* (2014) compared extraction of essential oil from lemongrass using microwave-assisted hydrodistilation (using water as a solvent) and solvent free microwave extraction. Their results showed that oil yield increases with increasing microwave power, irradiation time and decreasing particle size. The maximum oil yield in microwave-assisted hydrodistilation was 1.72% after 90 minutes of heating and 1.61% in solvent free microwave extraction after 20 minutes of irradiation time. Longer irradiation time resulted in inferior quality of essential oil. Extraction using the solvent free technique was much faster than microwave-assisted hydrodistilation.

22.3 Microwave Pre-treatment Followed by Conventional Extraction Techniques

Although less well described in the literature, an alternative approach for utilising microwave heating of plant based materials has been to treat the materials prior to extraction. In a study by Miletic *et al.* (2009), greenery and fruits of conifers were treated in a conventional microwave prior to hydro distillation to extract essential oils. Both the kinetics of hydro distillation and oil yield were significantly increased for plant materials treated with microwaves.

22.4 Application to Sugar Juice Extraction

In a recent scoping study (Roberts 2010), sugar cane segments (without nodes) were exposed to varying levels of microwave treatment, in a conventional microwave oven, prior to sucrose diffusion in water at 65 °C for 60 minutes, which demonstrated that microwave treatment of cane prior to diffusion led to significant decreases in colour and significant increases in purity and pol. Qualitative observations indicated faster rates of extraction in the microwave treated cane; however decreases in juice quality was observed for long microwave treatment times, indicated that an optimum treatment time existed.

In another simple scoping experiment, sugar cane billets were randomly allocated to one of four microwave pre-treatments (0, 90, 120, or 150 seconds) in a low powered domestic microwave oven before being crushed in a small press made from a manual screw type car jack. There was a significant increase in cane juice yield as a result of microwave treatment (Table 22.1). The 120 seconds treatment yielded the greatest amount of sugar juice; however there was a significant decline in yield as microwave treatment increased to 150 seconds. This is probably due to excessive drying of the cane billets.

The samples that were treated for 120 seconds yielded approximately 3.2 times more cane juice than the untreated control samples. This additional yield from the microwave pre-treatment of sugar cane samples is probably due to several factors:

1. a significant softening of the woody polymers (cellulose, hemi-cellulous and lignin) as the internal temperature of the cane billets rose above their respective glass transition temperatures (Manríquez and Moraes 2010). Brodie et al. (2011) found that microwave pre-treatment of sugar cane reduced the compressive strength of the cane to about 18 % of its original strength (the control samples);
2. rupture of the internal cellular structures in the cane due to localized steam explosions induced by microwave heating (Vinden and Torgovnikov 2000); and
3. a reduction in viscosity of the sugar juice.

Table 22.1: Mean sugar juice yield as a percentage of initial cane billet mass.

Treatment	Yield (%)
Control	8.4a
90 s	26.5b
120 s	26.8b
150 s	18.1c
LSD (P = 0.05)	8.2

Note: Means with different superscripts are significantly different from one another.

22.5 Microwave Accelerated Steam Distillation

Chemat et al. (2006) developed a new process design and operation for microwave accelerated steam distillation of essential oils from lavender flowers (*Lavandula angustifolia*). In this system, the lavender flowers sit above the steam source generated by microwave heating. Only steam passes through the flowers without the boiling water mixing with vegetable raw material, as is the case in conventional hydro-distillation. Microwave accelerated steam distillation was compared with a conventional technique, steam distillation, for the extraction of essential oil from lavender flowers. Extraction of essential oils from lavender with microwave accelerated steam distillation was better than conventional steam distillation in terms of energy saving, rapidity (10 min versus 90 min), product yield, cleanliness and product quality.

Chemat et al. (2006) treated 50 g samples of lavender flowers, which required 5.4 MJ of energy for conventional steam distillation (or 180,000 MJ tonne^{-1}). Microwave accelerated steam distillation required 0.47 MJ of energy to achieve full distillation of the 50 g samples (or 9,400 MJ tonne^{-1}). The composition of the final oil from each treatment regime was very similar; therefore the faster extraction using microwave energy did not affect the product quality.

In a small trail, a 10 kW, 922 MHz, microwave system was used to treat 10 kg samples of tea tree (*Melaleuca alternifolia*) leaf material to distil tea tree oil. These experiments were conducted in a rotating microwave chamber, which tumbled the leaf material during microwave processing. Water was added to the leaf material at a rate of 20 % by mass to facilitate good steam generation to transport the oil vapour to the condenser. Estimated energy requirements for this process were 3,850 MJ tonne^{-1}.

References

Brodie, G., Jacob, M. V., Sheehan, M., Yin, L., Cushion, M. and Harris, G. 2011. Microwave modification of sugar cane to enhance juice extraction during milling. *Journal of Microwave Power and Electromagnetic Energy*. 45(4): 178-187.

Cardoso-Ugarte, G. A., Juarez-Becerra, G. P., Sosa-Morales, M. E. and Lopez-Malo, A. 2013. Microwave-assisted extraction of essential oils from herbs. *Journal of Microwave Power & Electromagnetic Energy*. 47(1): 63-72.

Chemat, F. and Cravotto, G. 2013. Microwave-assisted extraction for bioactive compounds. Theory and practice. *Food Engineering Series*. 238.

Chemat, F., Lucchesi, M. E., Smadja, J., Favretto, L., Colnaghi, G. and Visinoni, F. 2006. Microwave accelerated steam distillation of essential oil from lavender: A rapid, clean and environmentally friendly approach. *Analytica Chimica Acta*. 555(1): 157-160.

Chemat, S., Aït-Amar, H., Lagha, A. and Esveld, D. C. 2005. Microwave-assisted extraction kinetics of terpenes from caraway seeds. *Chemical Engineering and Processing*. 44(12): 1320-1326.

Chen, S. S. and Spiro, M. 1994. Study of microwave extraction of essential oil constituents from plant materials. *Journal of Microwave Power and Electromagnetic Energy*. 29(4): 231-241.

Lucchesi, M. E., Chemat, F. and Smadja, J. 2004. Solvent-free microwave extraction of essential oil from aromatic herbs: comparison with conventional hydro-distillation. *Journal of Chromatography A*. 1043(2): 323-327.

Manríquez, M. J. and Moraes, P. D. 2010. Influence of the temperature on the compression strength parallel to grain of paricá. *Construction and Building Materials*. 24(1): 99-104.

Miletic, P., Grujic, R. and Marjanovic-Balaban, Z. 2009. The application of microwaves in essential oil hydro-distillation processes. *Chemical Industry and Chemical Engineering Quarterly*. 15(1): 37-39.

Ramanadhan, B. 2005. Microwave Extraction of Essential Oils (from Black Pepper and Coriander) at 2.46 GHz. Unpublished thesis. Canada: University of Saskatoon, Saskatchewan, Department of Agricultural and Bioresource Engineering

Roberts, I. 2010. Analysis of the effects of micrwave treatment on sugarcane diffusion products. Unpublished Undergraduate thesis. Townsville: James Cook University, Engineering Department

Saoud, A. A., Yunus, R. M. and Aziz, R. A. 2006. Yield study for extracted tea leaves essential oil using microwave-assisted process. *American Journal of Chemical Engineering*. 6(1): 22-27.

Singh, N., Shrivastava, P. and Shah, M. 2014. Microwave-assisted extraction of lemongrass essential oil: Study of the influence of extraction method and process parameters on extraction process. *Journal of Chemical & Pharmaceutical Research*. 6(11): 385-389.

Vinden, P. and Torgovnikov, G. 2000. The physical manipulation of wood properties using microwave. *Proc. International Conference of IUFRO*. 240-247.Tasmania, Australia.

23 Thermal Processing of Biomass

There are several organic waste streams that are of interest to agriculture; however the use of manures (both animal and human) has been a part of agricultural activity for centuries (Sayre 2010). Semi-processed manures are collectively called biosolids. An important goal of waste management is to recover as much value as possible from the material. This value could be realised in terms of recovery of nutrients, energy or chemicals. These can be recovered from biomass through various biological, chemical or thermal processing techniques. Processes such as combustion, gasification, torrefaction, pyrolysis, pelletizing and biogas production through microbial digestion have been considered. Palletisation and microbial digestion for biogas production are not strictly thermal processes and fall beyond the scope of this discussion. This chapter will explore how microwave energy can be used to thermally process biosolids, with a particular focus on biosolids produced from human sewage.

23.1 BioSolids

Biosolids refers to dried sludge from wastewater treatment lagoons that typically contain 50 – 70% by weight of oven dried solids (Arulrajah, *et al.* 2011). Biosolids can be composted (Belyaeva, *et al.* 2012) before use elsewhere; however according to surveys of Victoria's 175 wastewater treatment plants in 1997 and again in 2001, 82 % of the biosolid material resides in stockpiles around the state (Department of Natural Resources and Environment 2002). Biosolids can be used as a soil ameliorant or a potential nutrient source for crop production; however material in some large stockpiles is unsuitable for land application because of its low nutrient content, contamination issues, especially from heavy metals such as zinc, mercury, cadmium and copper and associated risks (Department of Natural Resources and Environment 2002).

Composting usually involves a four stage process: an initial decomposition phase; a thermophilic phase of intense microbial decomposition; a second thermophilic phase; and a maturation phase (Arulrajah, *et al.* 2011). Other technologies for sewage sludge treatment have been suggested. These include: Anaerobic Digestion, Aerobic Digestion, Aerobic Thermophilic Pre-treatment (or Dual Digestion), Autothermal Thermophilic Aerobic Digestion (ATAD), Lime Stabilisation, Vermiculture, Oil from Sludge (OFS), Heat Drying, Active Sludge Pasteurisation (ASP) Processes, Sludge Lagoons (also Liquid Sludge Storage), and Storage of Dewatered Sludge (Department of Natural Resources and Environment 2002). This section of the report will highlight some of the important physical and nutrient characteristics of biosolids, which indicate potential applications for the material.

23.2 Biosolids' Composition and Characteristics

Several studies have been performed on the geotechnical and nutrient value of biosolids. The specific gravity of biosolids is substantially lower than that of natural inorganic soils (Arulrajah, *et al.* 2011). The consolidation characteristics of biosolids indicate that biosolids have similar behaviour to organic clays (Arulrajah, *et al.* 2011). Table 23.1 provides typical data for some physical attributes of biosolids.

Table 23.1: Summary of geotechnical test results (Source: Arulrajah, et al. 2011).

Test/properties	Result
Moisture content (%)	48–57
Specific gravity	1.86–1.88
Particle sizes >2.36 mm (%)	4–16
Particle sizes between 2.36 and 0.075 mm (%)	40–44
Particle sizes between 0.075 and 0.002 mm (%)	22–33
Particle sizes <0.002 mm (%)	18–23
Liquid limit (%)	100–110
Plastic limit (%)	79–83
Plasticity index (%)	21–27
Loss on ignition (%)	35.4–38.5
Standard Compaction Test	
Maximum dry unit weight (kN/m^3)	7.8–8.0
Optimum water content (%)	51–53
Hydraulic conductivity (10^{-7} m/s)	1.24–1.60
1-D consolidation test (oedometer and creep)	
Initial void ratio	1.49–1.63
Pre-consolidation pressure (kN/m^2)	190–210
Coefficient of consolidation (m^2/year)	0.04–1.0
Compression index	0.38–0.45
Recompression index	0.045–0.055
Coefficient of secondary consolidation	0.003–0.02
California Bearing Ratio (CBR)	0.9–1.0
Swell index (obtained in CBR test)	0.41–0.52
Vane shear test, undrained shear strength (kPa)	136–152

23.3 Nutrient Value of Biosolids

The chemical constituents of Biosolids vary depending on their source; however Arulrajah et al (2011) acquired some useful data during their study. They found that heavy metals and other prime contaminants were within their specified limit (Arulrajah, *et al.* 2011), based on guidelines prescribed by EPA Victoria (Environmental Protection Agency of Victoria 2004). Table 23.2 presents some useful insights into the chemical properties of biosolids.

Table 23.2: Summary of chemical analysis (Source: Arulrajah, et al. 2011).

Properties	Average Result
Nitrite as N (solid) (mg/kg)	0.24
Nitrate as N (solid) (mg/kg)	1049.8
Total phosphorous as P (mg/kg)	13350
Organic carbon (%)	17.4
Arsenic (mg/kg)	19.0
Chromium (mg/kg)	732.7
Copper (mg/kg)	847.8
Mercury (mg/kg)	4.4
Nickel (mg/kg)	115.7
Selenium (mg/kg)	5.8
Zinc (mg/kg)	1780.0

23.4 Current Applications of Biosolids

Biosolids have a number of applications; however these permissible end uses depend on the classification of the biosolid material after treatment. Table 23.3 indicates some acceptable end uses for biosolids. The various treatment grades (T1, T2, and T3) and chemical grades (C1 and C2) are defined in the '*Guidelines for environmental management: biosolids land application*' (Environmental Protection Agency of Victoria 2004).

Table 23.3: Summary of acceptable end uses for biosolids, based on their classification (Source: Environmental Protection Agency of Victoria 2004).

Treatment Grade	Chemical Grade	Unrestricted	Restricted Uses					
			Agricultural Uses			Non-agricultural Uses		
			Human food crops consumed raw in direct contact with biosolids	Dairy and cattle grazing /fodder (also poultry), human food crops consumed raw but not in direct contact	Processed food crops	Sheep grazing and fodder (also horses, goats), on food crops, woodlots	Landscaping (unrestricted public access)	Landscaping (restricted public access), forestry, land rehabilitation
T1	C1	v	v	v	v	v	v	v
T2	C1	×	×	v	v	v	v	v
T3	C1	×	×	×	v	v	×	v
T1	C2	×	v	v	v	v	v	v
T2	C2	×	×	v	v	v	v	v
T3	C2	×	×	×	v	v	×	v

The three treatment grades are based on satisfying three main criteria: the adoption of treatment processes with minimal performance criteria (e.g. temperature and time); microbial limits that demonstrate effective treatment; and implementing measures for controlling microbial regrowth, vector attraction and generation of nuisance odours (Environmental Protection Agency of Victoria 2004). The chemical grades are determined by levels of chemicals (especially heavy metals) (Environmental Protection Agency of Victoria 2004).

The most common methods for managing wastewater sludge disposal are: stockpiling; landfilling; farmland applications; use as a geotechnical material in road construction and landfill liners; and incineration; however none of these methods are exempt from drawbacks. Biosolids can be applied to agricultural, forests or disturbed landscapes as fertiliser; however the presence of heavy metals and trace elements in the material limits its use in agricultural application (Hossain, *et al.* 2009).

Unstabilised biosolids are generally associated with high organic matter, high compressibility, high rates of creep, and unsatisfactory strength characteristics (Arulrajah, *et al.* 2011). These properties limit their geotechnical application and increase the risk of excessive settlement in cases where they are used as load bearing media (Arulrajah, *et al.* 2011); however some material may be used for Type B fill. Disposal of biosolids in landfill should be avoided where possible, because it does not realise the value of the resource and in some cases it restricts the usage options for the landfill site (Hossain, *et al.* 2009). Incineration reduces the volume of the sludge but it is costly and generates emissions to air, soil and water (Karayildirim, *et al.* 2006). It

is clear that biosolids are a good nutrient source (Table 2); therefore nutrient recovery should be an important consideration wherever possible. This will be explored in the next section.

23.5 Thermal Processing of Materials

Combustion, gasification, torrefaction, and pyrolysis all involve thermal reactions in varying concentrations of oxygen. Combustion involves complete exothermic oxidation of the material; gasification is partial exothermic oxidation of the material to drive off volatile gasses which can be burned elsewhere. Torrefaction (a low temperature pyrolysis process) (Sarvaramini, *et al.* 2013) and pyrolysis are endothermic reactions in an oxygen depleted atmosphere where applied heat drives off volatile gasses and condensable liquids that are usually energy and chemically rich.

The main products of thermal processing include: heat, either from direct combustion or combustion of the volatile products of the process; syngas, which can be used as a fuel in industry or transport; bio-oil which can be used as a fuel or as precursor chemicals for polymer or pharmaceutical manufacture; and biochar, which can also be used as a fuel, as a potential nutrient source, or as a soil ameliorant for improving agricultural production and sequestering carbon. This section of the report provides an overview of the main thermal treatment processes.

23.5.1 Combustion

Combustion occurs when fuels react with oxygen in the air to produce heat. Carbon monoxide (CO) is formed when too little oxygen is supplied to completely form carbon dioxide (CO2) from all the carbon in the fuel. As with all other properties of biosolids, its calorific value depends on the source and moisture content of the material. Dry biosolids have a similar calorific value to that of low-grade coal (Fonts, *et al.* 2012); however studies have shown that the efficiency of using biomass for energy production is around 30% (Beenackers 1999).

One study reported that biosolids with a dry basis moisture content of 73 % had a calorific value of 5.65 MJ kg^{-1} while oven dried biosolids had a calorific value of 18.75 MJ kg^{-1} (Chen, *et al.* 2014). It is important to note that considerable energy must be expended in drying organic materials like biosolids, especially when the material reaches fibre saturation, where all free water has been removed from the material and only bound water remains. For example, the energy needed to dry wood based materials to equilibrium moisture content equates to between 3.6 and 6 MJ kg^{-1}, depending on the porosity, thickness and initial moisture content of the wood (Awadall, *et al.* 2004). Drying biosolids would require similar energy input.

Biosolids contain various nitrogen containing substances, including proteins. Combustion that involves nitrogen containing compounds will produce nitrogen oxides, principally nitric oxide (NO) and nitrogen dioxide (NO_2) (Anonomous 2004), which are pollutant gases that contribute to the formation of acid rain and smog. NO is generated first at high flame temperatures (Anonomous 2004). NO oxidizes to form NO_2 at cooler temperatures after being exhausted from the system (Anonomous 2004).

Sulphur dioxide can also be produced during combustion of biomass materials. Sulphur dioxide combines with water vapour in the exhaust to form a sulphuric acid mist (Anonomous 2004). Airborne sulphuric acid is a pollutant in fog, smog, acid rain and snow, ending up in the soil and ground water (Anonomous 2004). Therefore, although biosolids could be directly used as a fuel source, energy conversion efficiencies are very low and the pollution potential appears to be quite high.

Direct combustion also produces CO_2, which has become a great environmental and political concern in recent years. Although the energy value of dry biosolids is valuable, in a growing carbon economy like Australia, it is sensible to consider better value options. Gasification provides two product streams: syngas and biochar.

23.5.2 Gasification

Gasification is a process that converts organic materials, including biosolids, into carbon monoxide, hydrogen, methane, carbon dioxide, and biochar by reacting the material at high temperatures (>700 °C), without combustion, in a controlled amount of oxygen and/or steam. The resulting gas mixture is called *synthesis gas* or *syngas*, which can be used as a fuel (Pless and Jenkins 1996). The power derived from gasification and combustion of the resultant gas is considered to be a source of renewable energy if the gasified compounds were obtained from biomass.

Gasification is a three-phase process: the biomass dries until the temperature reaches approximately 120 °C; volatile matter is driven off between 120 °C and 350 °C; and some gasification of the remaining char occurs above 350 °C (Kirubakaran, *et al.* 2009); therefore, it is customary to classify the entire process as drying, volatilization and gasification (Kirubakaran, *et al.* 2009).

Syngas can be used directly in internal combustion engines, or it can be used to produce methanol and hydrogen through secondary reactions after the original gasification process (Albertazzi, *et al.* 2005). Studies have demonstrated that optimum H_2 yields, with negligible CH_4 and coke formation, can be achieved at a temperature range of 900 – 1100 K (Haryanto, *et al.* 2009); however these temperatures volatilize most of the condensable liquid phase of the initial gasification products.

While fuel production is important, its monetary value is quite low. Reported calorific values of syngas vary between 3.3 and 7.0 MJ m^{-3} (Zhao, *et al.* 2011, del Alamo, *et al.* 2012); however the final value depends on the source material and the conditions

under which it was generated (del Alamo, *et al.* 2012). This does not compare very favourably with the calorific value of natural gas (approximately 35 to 39 MJ m^{-3}). Current natural gas prices on the east coast of Australia are about \$3 to \$4 GJ^{-1} (Wood, *et al.* 2013). Syngas would need to compete with these prices, suggesting that its value in the market would be between \$0.01 and \$0.03 m^{-3}, based on its calorific value. Complex chemicals in the condensable liquid phase (bio-oil) can be much more valuable.

Combustion and gasification are exothermic reactions where all or part of the biomass react with oxygen to generate heat. Torrefaction and pyrolysis are endothermic reactions in which external heat is added to the material while it is in an inert atmosphere to thermally decompose organic polymers into smaller more useful chemicals.

23.5.3 Anaerobic Decomposition (Torrefaction and Pyrolysis)

Torrefaction involves heating biomass, without oxygen, to temperatures between 200 °C and 300 °C; while pyrolysis involves heating biomass, without oxygen, to temperatures ranging from 400 °C – 1200 °C. Pyrolysis dates back to at least ancient Egyptian times, when tar for caulking boats and certain embalming agents were made by pyrolysis (Farag, *et al.* 2002).

Pyrolysis is difficult to precisely define, especially when applied to biomass. The older literature generally equates pyrolysis to carbonization, in which the principal product was a solid char. Now, the term describes processes in which oils and gasses are the preferred products (Mohan, *et al.* 2006). The time frame for pyrolysis is much faster for the latter process.

It is important to differentiate pyrolysis from gasification. Gasification decomposes biomass to syngas by carefully controlling the amount of oxygen present. The products of pyrolysis are char, liquids and gases. The char can be extracted as a sold or combusted to contribute heat to the process. The calorific value of biochar is about 28 MJ kg^{-1} (Goodall 2007); however there are other uses for biochar, including soil amelioration.

Some of the gases from the pyrolysis process can be condensed into bio-oil, and the remaining, non-condensable gases, can be regarded as syngas. The major gas species from biosolid pyrolysis are: CO, CO_2, CH_4, C_2H_4, C_2H_6 and H_2 (Hossain, *et al.* 2009). The longer chain molecules in the syngas from pyrolysis improve the calorific value of the gas.

The properties of bio-oil depend on the feedstock material used to produce it. For example, bio-oil sourced from wood waste is an acidic, viscous, water-soluble liquid that has a dark brown colour and a pungent smoky odour (Mohan, *et al.* 2006). A common application for bio-oil is as a fuel, although some studies have shown that bio-oil is not commercially competitive with fossil fuels (Farag, *et al.* 2002). Another

use for bio-oil is as a source of pharmaceuticals (Dominguez, *et al.* 2005) and food flavouring (Farag, *et al.* 2002).

Studies by Hossain et al. (2009), which employed conventional furnaces to process sewage sludges and biosolids, determined that the energy required to pyrolyse samples ranged from 1180 kJ kg^{-1} for material sourced from domestic waste streams while 730 kJ kg^{-1} and 708 kJ kg^{-1} of energy was required to pyralyse material sourced from commercial and industrial waste (Hossain, *et al.* 2009). They concluded that only the material from the industrial waste streams provided sufficient thermal energy from the resulting bio-gas to sustain the heat required to pyralyse the material (Hossain, *et al.* 2009). The main reason for the high energy demand to heat commercial and domestic waste materials was because of a very high endothermic reaction these samples exhibit at the temperature between 110 °C and 290 °C. This means that the pyrolysis process for these samples required additional energy beyond what could be supplied from the syngas produced to sustain the thermal decomposition. This may require the combustion of the bio-oil fraction as well as the gas fraction to achieve an energy balance for the reaction (Hossain, *et al.* 2009). These endothermic reactions are believed to correspond to decomposition of strongly bonded hydrated compounds that release water upon heating (Hossain, *et al.* 2009).

The pyrolytic bio-oils are one of the important products of pyrolysis. Generally, bio-oils are mixed with the condensed water (Hossain, *et al.* 2009). Their composition is important for utilising the oils or for further processing to bio-diesel or petrochemicals (Hossain, *et al.* 2009).

23.6 Microwave-assisted Pyrolysis

Research into microwave-assisted pyrolysis of biosolids is currently lacking, therefore identifying a return on investment is difficult. Most pyrolytic processes yield between 20 % and 30 % by weight of combustible syngas. Conventional pyrolysis yields a very small liquid fraction (< 1 % by weight); however the main non-gaseous products are usually water (after condensing the water vapour) and bio-char.

One of the very few laboratory scale studies (Dominguez, *et al.* 2005) of microwave-assisted pyrolysis of wet sewage sludge (71 % water by wet weight), yielded similar quantities of combustible gaseous products to conventional pyrolysis; however the liquid fraction (mostly oil) from microwave processing was significantly higher (between 5 % and 7 % by weight) than for the conventional system (Dominguez 2006). Although the calorific value of bio-oil was approximately 36 MJ kg^{-1} (Menendez 2005) and can be used as fuel, over 70 different chemicals (Figure 28) were identified in this liquid phase. Traditional high temperature furnace-based pyrolysis of the same material yielded negligible amounts of oil from which only 35 - 40 chemicals (Dominguez, *et al.* 2005) could be identified. Some of the liquid phase chemicals released by microwave-assisted pyrolysis (Figure 23.1) included:

1. Peak 1 – Benzene, which has a value of approximately $1,200 per tonne;
2. Peak 3 - Toluene, which has a value of approximately $1,060 per tonne;
3. Peak 5 – Ethylbenzene, which is worth approximately $7,700 per tonne;
4. Peak 7 - Styrene, which has a value of approximately $1,765 per tonne;
5. Peak 51 - Palmitic acid, which is used in soap production and has a value of approximately $1,400 per tonne;
6. Peak 55 – Hexadecanamide, which is used as a pharmaceutical that induces programmed cell death with potential applications as a cancer treatment; its value is unclear but a few grams can cost about $30 in the final product;
7. Peak 60 – Cholestene, which is used as a pharmaceutical that controls cholesterol; its value is also unclear but a few grams can cost about $30- $40 in the final product.

Current processing and end use of biosolids in Australia include: stock piling; composting with subsequent application to agricultural land; entombment as land fill; and incineration or occasional pyrolysis in conventional furnaces. None of these existing uses for biosolids recover any of this potential value from the resource.

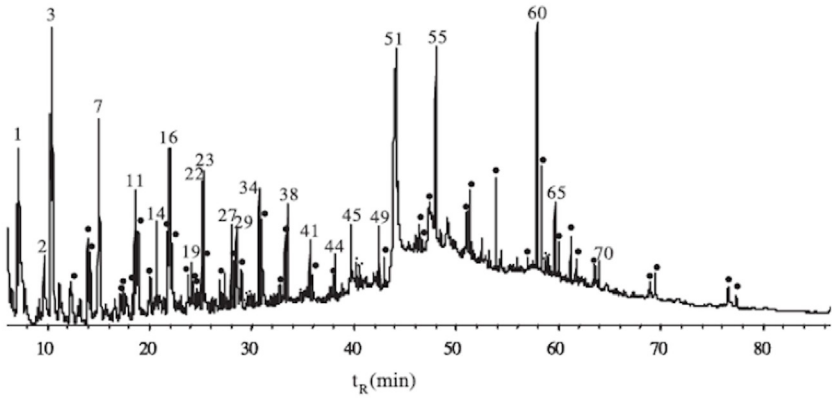

Figure 23.1: GC–MS chromatogram of the pyrolysis oil obtained from wet sewage sludge using a single-mode microwave oven and graphite as a microwave absorber (Source: Dominguez, et al. 2005).

Assuming that this technology can ultimately be commercialised throughout the Australian waste water industries and that about 5 % of the biosolid material can be recovered as oil with an average value of only $1,500 per tonne before further chemical separation, the value of the annual production of 360,000 tonnes of biosolids could be approximately $27 million. This simple analysis neglects the fuel value of the recovered gaseous fraction, which could potentially offset most of the running costs

of microwave processing systems. It also neglects the existing stockpiles at various waste water facilities and the resale value of recovered fertilisers and bio-char. At this stage the market value of biochar in Australia is unclear, but a 2011 study suggested that a market price of \$300 tonne^{-1}, could be economically sustainable, depending on the cost of the feed stock (original biomass) used to produce it (Tsaktsiras, *et al.* 2001).

23.7 Biochar

Biochar is a carbon-rich product obtained by pyrolisis, i.e. the thermal decomposition of organic material (e.g. wood, foliage, manure) under the partial or total absence of oxygen (Sohi, *et al.* 2010). Biochar is somehow similar to charcoal, since they are produced by a similar process and are comprised mainly by stable aromatic forms of organic carbon. However, it differs from charcoal in that its production is intended specifically for application to soil as a means of improving soil productivity, carbon storage, or filtration of percolating soil water among others (Lehmann and Joseph 2009).

The proportion of biochar produced during the pyrolisis process is balanced with that of liquid (oil) and gas products and depends upon the pyrolysis conditions used (Table 23.4).

Table 23.4: Mean pyrolised feedstock products by temperatures and residence times (Modified from: IEA 2007).

Process	Liquid (bio-oil)	Solid (biochar)	Gas (syngas)
FAST PYROLYSIS			
Moderate temperature (~500°C)	75%	12%	13%
Short hot vapour residence time (<2s)	(25% water)		
INTERMEDIATE PYROLYSIS			
Low-moderate temperature	50%	25%	25%
Moderate hot vapour residence time	(50% water)		
SLOW PYROLYSIS			
Low-moderate temperature	30%		
Long residence time	(70% water)	35%	35%

Interest in biochar has grown exponentially since Glaser et al (2001) first discovered that biochar-type substances are the explanation for high amounts of organic carbon and sustained soil fertility in Amazonian Dark Earths ('Terra Preta') (Lehmann and Joseph 2009). Initially biochar was praised because of it stability and capacity to

increase soil nutrients (Chan and Xu 2009, Lehmann, *et al.* 2009); however recent studies have demonstrated that biochar is much more effective at enhancing soil quality than any other organic soil amendment (Lehmann and Joseph 2009). This has been attributed to its particular physical and chemical properties (Liang, *et al.* 2006, Downie, *et al.* 2009).

Biochar contains both stable and labile components (carbon, volatile matter, mineral matter (ash) and moisture) (Antal and Grønli 2003), and the relative proportion of these components determines the chemical and physical behaviour and function of biochar (Brown 2009). For instance, biochar produced from manures are generally finer and less robust but with a higher nutrient content than those generated from wood-based feedstock (Sohi, *et al.* 2009). Biochar produced from sludges may have a high moisture content, and thus may require a pre- drying treatment to achieve a desirable 10% (weight) moisture content (Collison, *et al.* 2009).

A pervasive characteristic of biochar are its high carbon content and strongly aromatic structure, which account for its chemical stability. In general, carbon content of biochar is inversely related to biochar yield and it increases with pyrolsis temperature. For instance, increasing temperature from 300°C to 800°C decreased the yield of biochar from 67 to 26% and increased carbon content from 56 to 93% (Tanaka 1963) in (Sohi, *et al.* 2009).

Clearly, torrefaction or pyrolysis of biosolids (or any other organic waste) has potential. Many high value products can be recovered in the process and as with most situations which require a heat source, radio frequency and microwave energy is usually more efficient and produces a better product.

This section of the book has considered applications of high radio frequency and microwave power. The next section will consider how radio frequencies and microwave technology can be used to acquire and transmit data.

References

Albertazzi, S., Basile, F., Brandin, J., Einvall, J., Hulteberg, C., Fornasari, G., Rosetti, V., Sanati, M., Trifirò, F. and Vaccari, A. 2005. The technical feasibility of biomass gasification for hydrogen production. *Catalysis Today*. 106(1–4): 297-300.

Anonomous. 2004. *Combustion Analysis Basics: An Overview of Measurements, Methods and Calculations used in Combustion Analysis*. TSI Incorporated

Antal, M. J. and Grønli, M. 2003. The art, science, and technology of charcoal production. *Industrial & Engineering Chemistry Research*. 42(8): 1619-1640.

Arulrajah, A., Disfani, M. M., Suthagaran, V. and Imteaz, M. 2011. Select chemical and engineering properties of wastewater biosolids. *Waste Management*. 31(12): 2522-2526.

Awadall, H. S. F., El-Dib, A. F., Mohamad, M. A., Reuss, M. and Hussein, H. M. S. 2004. Mathematical modelling and experimental verification of wood drying process. *Energy Conversion and Management*. 45: 197–207.

Beenackers, A. A. C. M. 1999. Biomass gasification in moving beds, a review of European technologies. *Renewable Energy*. 16(1–4): 1180-1186.

Belyaeva, O. N., Haynes, R. J. and Sturm, E. C. 2012. Chemical, physical and microbial properties and microbial diversity in manufactured soils produced from co-composting green waste and biosolids. *Waste Management*. 32(12): 2248-2257.

Brown, R. 2009. Biochar production technology. *Biochar for environmental management: Science and technology*. 127-146.

Chan, K. Y. and Xu, Z. 2009. Biochar: nutrient properties and their enhancement. *Biochar for environmental management: science and technology. Earthscan, London*. 67-84.

Chen, Z., Afzal, M. T. and Salema, A. A. 2014. Microwave drying of wastewater sewage sludge. *Journal of Clean Energy Technologies*. 2(3): 282-286.

Collison, M., Collison, L., Sakrabani, R., Tofield, B. and Wallage, Z. 2009. Biochar and carbon sequestration: a regional perspective. *Low Carbon Innovation Centre, UEA, Norwich*.

del Alamo, G., Hart, A., Grimshaw, A. and Lundstrøm, P. 2012. Characterization of syngas produced from MSW gasification at commercial-scale ENERGOS Plants. *Waste Management*. 32(10): 1835-1842.

Department of Natural Resources and Environment. 2002. *Moving Towards Sustainable Biosolids Management*. Department of Natural Resources and Environment

Dominguez, A., Menendez , J. A., Inguanzo, M., and Pis, J. J. 2006. Production of bio-fuels by high temperature pyrolysis of sewage sludge using conventional and microwave heating. *Bioresource Technology*. 97(10): 1185 -1193.

Dominguez, A., Menendez , J. A., Inguanzo, M. and Pis, J. J. 2005. Investigations into the characteristics of oils produced from microwave pyrolysis of sewage sludge. *Fuel Processing Technology*. 86(9): 1007 -1020.

Downie, A., Crosky, A. and Munroe, P. 2009. Physical properties of biochar. *Biochar for environmental management: Science and technology*. 13-32.

Environmental Protection Agency of Victoria 2004, *Guidelines for environmental management: biosolids land application, Publication No. 943*, Melbourne: EPA Victoria.

Farag, I. H., LaClair, C. E. and Barrett, C. J. 2002. *Technical, Environmental and Economic Feasibility of Bio-Oil in New Hampshire's North Country*. New Hampshire Industrial Research Center

Fonts, I., Gea, G., Azuara, M., Ábrego, J. and Arauzo, J. 2012. Sewage sludge pyrolysis for liquid production: A review. *Renewable and Sustainable Energy Reviews*. 16(5): 2781-2805.

Glaser, B., Haumaier, L., Guggenberger, G. and Zech, W. 2001. The 'Terra Preta' phenomenon: a model for sustainable agriculture in the humid tropics. *Naturwissenschaften*. 88(1): 37-41.

Goodall, C. 2007. Biochar can sequester carbon cheaply.

Haryanto, A., Fernando, S. D., Pordesimo, L. O. and Adhikari, S. 2009. Upgrading of syngas derived from biomass gasification: A thermodynamic analysis. *Biomass and Bioenergy*. 33(5): 882-889.

Hossain, M. K., Strezov, V. and Nelson, P. F. 2009. Thermal characterisation of the products of wastewater sludge pyrolysis. *Journal of Analytical and Applied Pyrolysis*. 85(1–2): 442-446.

IEA. 2007. *IEA Bioenergy Annual Report 2006*.

Karayildirim, T., Yanik, J., Yuksel, M. and Bockhorn, H. 2006. Characterisation of products from pyrolysis of waste sludges. *Fuel*. 85: 1498–1508.

Kirubakaran, V., Sivaramakrishnan, V., Nalini, R., Sekar, T., Premalatha, M. and Subramanian, P. 2009. A review on gasification of biomass. *Renewable and Sustainable Energy Reviews*. 13(1): 179-186.

Lehmann, J., Czimczik, C., Laird, D. and Sohi, S. 2009. Stability of biochar in soil. *Biochar for Environmental Management: Science and Technology. Earthscan Publ., London*. 183-205.

Lehmann, J. and Joseph, S. 2009, *Biochar for environmental management: science and technology*, Earthscan.

Liang, B., Lehmann, J., Solomon, D., Kinyangi, J., Grossman, J., O'Neill, B., Skjemstad, J., Thies, J., Luizao, F. and Petersen, J. 2006. Black carbon increases cation exchange capacity in soils. *Soil Science Society of America Journal*. 70(5): 1719-1730.

Menendez , J. A., Dominguez, A., Inguanzo, M., and Pis, J.J. 2005. Microwave-induced drying, pyrolysis and gasification (MWDPG) of sewage sludge: Vitrification of the solid residue. *Journal of Analytical and Applied Pyrolysis*. 74(1-2): 406-412.

Mohan, D., Charles U. Pittman, J. and Steele, P. H. 2006. Pyrolysis of Wood/Biomass for Bio-oil: A Critical Review. *Energy & Fuels*. 20(3): 848-889.

Pless, D. E. and Jenkins, S. D. 1996. Coal's clean comeback. *Civil Engineering*. 66(9): 46-48.

Sarvaramini, A., Assima, G. P. and Larachi, F. 2013. Dry torrefaction of biomass – Torrefied products and torrefaction kinetics using the distributed activation energy model. *Chemical Engineering Journal*. 229(0): 498-507.

Sayre, L. B. 2010. The pre-history of soil science: Jethro Tull, the invention of the seed drill, and the foundations of modern agriculture. *Physics and Chemistry of the Earth, Parts A/B/C*. 35(15-18): 851–859.

Sohi, S., Lopez-Capel, E., Krull, E. and Bol, R. 2009. Biochar, climate change and soil: A review to guide future research. *CSIRO Land and Water Science Report*. 5(09): 17-31.

Sohi, S. P., Krull, E., Lopez-Capel, E. and Bol, R. 2010 Chapter 2 - A Review of Biochar and Its Use and Function in Soil. In *Advances in Agronomy*, 47-82. Donald, L. S. ed. Academic Press.

Tanaka, S. 1963. Fundamental study on wood carbonization. *Bulletin of Experimental Forest of Hokkaido University*.

Tsaktsiras, N., Crosthwaite, J., Stott, K., Opie, C., Dwyer, S. and Schmidt, J. 2001. How can biochar production have a future in Australia? :

Wood, T., Carter, L. and Mullerworth, D. 2013. *Getting gas right: Australia's energy challenge*. Grattan Institute

Zhao, X., Zhang, J., Song, Z., Liu, H., Li, L. and Ma, C. 2011. Microwave pyrolysis of straw bale and energy balance analysis. *Journal of Analytical and Applied Pyrolysis*. 92(1): 43-49.

Section 4: **Automatic Data Acquisition and Wireless Sensor Networks**

24 Section Introduction

Agriculture faces many challenges, such as climate variability, water shortages, labour shortages due to an aging urbanized population, and increased concern about issues such as animal welfare, food safety, and environmental impact (Wark, *et al.* 2007). The modern dilemma in most agricultural systems is to achieve high process efficiency, low costs, and good planning confidence in spite of a turbulent environment with limited manpower and resources. One approach to balancing these conflicting demands has been greater mechanisation and automation. Initially automation has involved better data acquisition and distribution within the industry, ultimately this will lead to autonomous machines working alongside human farm managers to achieve greater, and potentially cheaper, agricultural production (Graves 2013).

Wireless sensor networks that can interact over the InterNet and provide remote control of agricultural activates such as irrigation and animal drafting as they move through various handling yards to reach water have been in use for some time now. Radiofrequency identification (RFID) has also been common practice to provide paddock to plate tractability of production animals such as cattle and sheep have also been in place for several years.

Early agricultural practices were focused on individual plants and animals. During the industrial and green revolutions, the focus of agriculture shifted from the individual production unit to the flock, herd, or paddock. Modern data acquisition systems are refocusing agricultural production back to the individual plant or animal. This section will briefly explore how radiofrequency and microwave systems are being used to achieve some of these outcomes.

References

Graves, B. 2013. Growing reliance on technology: agriculture has high-tech helpers. (43): 1.

Wark, T., Corke, P., Sikka, P., Klingbeil, L., Ying, G., Crossman, C., Valencia, P., Swain, D. and Bishop-Hurley, G. 2007. Transforming Agriculture through Pervasive Wireless Sensor Networks. *Pervasive Computing, IEEE*. 6(2): 50-57.

25 Data Acquisition

Data Acquisition is simply the gathering of information about a system or process. It is a core tool to the understanding, control and management of systems or processes. Information such as temperature, pressure or flow is gathered by sensors that convert measurements into electrical signals. Sometimes only one sensor is needed, such as when recording local rainfall. Sometimes hundreds or even thousands of sensors are needed, such as when monitoring a complex industrial process. The signals from sensors are transferred by wire, optical fibre or wireless links to an instrument which conditions, amplifies, scales, processes, displays and stores the sensor signals. This is the Data Acquisition instrument.

In the past Data Acquisition equipment was largely mechanical, using clock work and chart recorders. Later, electrically powered chart recorders and magnetic tape recorders were used. Today, powerful microprocessors and computers perform Data Acquisition faster, more accurately, more flexibly, with more sensors, more complex data processing, and elaborate presentation of the final information.

Data Acquisition can be divided into two broad classifications – real time data acquisition and data logging. Real time data acquisition is when data acquired from sensors is used either immediately or within a short period of time, such as when controlling a process (Frey and Williams 1994). Data logging on the other hand is when data acquired from sensors is stored for later use (Frey and Williams 1994). In reality, there is a continuum of devices between real time data acquisition and data logging that share the attributes of both of these classifications.

Data logger can be pictured as a black box recorder in airplanes. These black box data loggers mainly record voices in the control deck and the plane's state variables. Data loggers can be used for all types of data acquisition purposes and some of the sensing devices that can be connected to them include:

- Temperature sensors
- Pressure sensors & strain gauges
- Flow and speed sensors
- Current loop transmitters
- Weather & hydrological sensors
- Laboratory analytical instruments
- And much more…

Successfully collecting physical data with a data logger or computer-based system involves several components. Beginning with the physical parameters being measured and working toward the computer, a data acquisition system will be comprised of four fundamental components (Frey and Williams 1994).

1. Sensors / Transducers
2. Signal Conditioning
3. Analogue-to-Digital Conversion (A/D)
4. Software

25.1 Sensors / Transducers

When taking measurements, the first consideration is the physical parameter to be measured and recorded. It could be temperature, pressure, acceleration, sound intensity, wavelength of light, or almost anything. The first component in a computer-based data acquisition system is used to convert these physical parameters to some type of electrical signal (Frey and Williams 1994). Sensor is the generic term for any device that can sense physical phenomena. A transducer is a sensor that responds to these phenomena by producing appropriately scaled electrical signals (Frey and Williams 1994).

Some common examples of environmental transducers include:

1. Submersible water level sensors, which uses a piezo-resistor whose electrical resistance changes when pressure is applied. Because water pressure is directly related to the depth of water above the point of measurement, this device can be used to measure the pressure exerted by water.
2. Electrical conductivity meters, which use magnetic coils to measure the electrical conductivity of the water. The ability of water to carry an electrical current is directly related to the amount of dissolved salt in the water. Therefore the output of this transducer can be either electrical conductivity or salt concentration.
3. Water turbidity meters, which use a miniature optical radar system to measure the amount of back scatter produced by suspended particles in the water. This system works on the same principle as car headlights reflecting off fog. When the water is clear very little light produced by the device's special light source is reflected back to the sensor; however when the water is very dirty, most of the light from the device is reflected back to the sensor.

A thermocouple is a good example of a simple transducer. A thermocouple is simply the junction of two different metals. The junction of these two metals produces a very small electric voltage. The strength of this voltage depends on the temperature of the junction between the two metals. Any two dissimilar metal wires will produce this voltage; however, certain types of thermocouples are used because of their output voltage strength. The voltage must be big enough so other instrumentation can utilise it for display and control purposes. In addition to being a strong enough signal it should also have a linear relationship to the temperature.

25.2 Power Supply

Many transducers require electrical power. One of the most common methods of powering a transducer is to provide a stable DC voltage to the sensing element. This is called the excitation voltage, and is typically in the range of a few volts up to about 30 volts DC. Usually this power can be supplied from a connection to mains power, but

in a remote situation power must be provided from other sources. The most common system used to provide power to remote data acquisition systems is a solar panel and battery.

25.3 Accuracy and Its Components

One of the most important principles of measurement to remember, especially when using transducers, is that it is rare to directly measure the parameter of interest. Some common examples of daily measurement will hopefully illustrate this point.

1. When measuring the mass of an object it is common to use a set of scales. The scales, if they are mechanical, are actually measuring the compression of a spring. The compression of the spring is directly related to the gravitational force exerted by the mass on the scales. If the scales are electronic, then the scales are replaced by a crystal that creates electrical charges when it is compressed.
2. The elapsed time of an event or process is measured by counting the number of regular intervals generated by some mechanical or electronic device (a clock) between when the event or process begins and when it ends.

Measurements made by a device are related to the parameter of interest. The exact relationship must be well understood by the manufacturers of the transducer and it must be correctly calibrated to make sure the output from the transducer is a true representation of the parameter being measured. If the output from the transducer and the true value of the measured parameter were plotted on a graph, the most desirable relationship between the two would be a straight line or linear relationship. Manufacturers go to great lengths to ensure the linearity of their instruments. In spite of this, the instrument should be regularly tested and calibrated to make sure it is providing accurate data.

Accuracy is a somewhat misleading and ill-defined term. Accuracy is a descriptive term concerning the closeness of a measured value to what is regarded as a true measurement of the quantity of interest. To fully define the accuracy of an instrument or transducer, the reading presented by the device must be compared to the measurement presented by a procedure which is considered to produce the standard value for this parameter. This process is called calibration. The error between the instrument's output and that of the standard is a measure of the instrument's accuracy.

As an example of a standard, the definition of a second is, '*The interval of time taken to complete 9,192,631,770 oscillations of the caesium 133 atom exposed to a suitable excitation*' (Brain 1998-2004).

Atomic clocks provide the international standard for time keeping. The standard is based on the oscillation frequency of the caesium atom. To turn the caesium atomic resonance into an atomic clock, it is necessary to measure one of its transition or

resonant frequencies accurately. This is normally done by locking a crystal oscillator to the principal microwave resonance of the caesium atom (Brain 1998-2004).

To create a clock, caesium is heated so that atoms boil off and pass down a vacuum tube. These pass through a magnetic field that selects atoms of the right energy state; then they pass through an intense microwave field. The frequency of the microwave energy sweeps backward and forward within a narrow range, so that at some point in each cycle it crosses the frequency of exactly 9,192,631,770 Hertz. When a caesium atom receives microwave energy at exactly this frequency, it changes its energy state.

At the far end of the tube, another magnetic field selects the atoms that have changed their energy state. A detector gives an output proportional to the number of caesium atoms having this altered energy state, and therefore peaks in output when the microwave frequency is exactly 9,192,631,770 Hertz. This peak is used to make the slight correction necessary to bring the crystal oscillator to the correct frequency. This locked frequency is then divided by 9,192,631,770 to give the familiar one pulse per second required by the real world (Brain 1998-2004).

The key components of accuracy are resolution, hysteresis, precision and linearity:

1. Resolution is the fineness with which a measurement can be made. For example, if a ruler is marked with millimetre graduations, it is possible by interpolation to measure objects to the nearest 0.5 mm. Thus the resolution is 0.5 mm.
2. Precision is the closeness of agreement between readings in a series of consecutive measurements made on the same parameter under the same conditions. Precision does not necessarily imply that the measurement is a true indication of the parameter's value. It does imply that the same reading is presented for the same conditions of the system when a measurement is made. Proper and regular calibration of the instrument should ensure that the measurement is a true representation of the system's state.
3. Linearity is a measure of how well the instrument behaves over its full range of measurement. Generally a transducer's output is converted to the real value of the parameter by applying appropriate (usually linear) mathematical manipulation to the signals from the circuitry. If the response of the circuitry deviates in some way from these basic relationships because of non-linear behaviour the output will have different calibration at different points along the range of the instrument's output. In some cases non-linearity may be overcome by appropriate signal conditioning.
4. Hysteresis is an interesting property of many transducers which results in the output being dependent on whether the parameter being measured was increasing or decreasing in value at the time of measurement.

An example of hysteresis is friction in the mechanism of a set of scales. This causes a slight lag in the response of the instrument to changes in mass. Therefore if the mass on the scales was increasing at the time of weighing, the measurement indicated by the scales may be slightly less than the true value. However, if the mass was decreasing at the time of measurement due to evaporation of water, the measurement indicated

by the scales may be slightly more than the true value, in spite of the fact that the same set of scales was used in each measurement.

25.4 Transducer Output

The output signals from most transducers are relatively weak. Some transducers produce a proportionally scaled voltage as their output, while others produce a proportionally scaled current. For example, many environmental monitoring systems employ transducers that produce a current based output which ranges between 4 mA and 20 mA. The exact value of the current is related to the parameter being measured. It is important to note that the 4 mA output represents a zero reading in the parameter being measured. This is actually a clever way of testing whether the transducer is still working and connected properly. If 0 mA were used to represent zero output then it could be a true reading or it could actually be that the transducer has failed or the connecting cable has been broken. With this industry standard system, if there is a 0 mA output from the transducer it is immediately obvious that there is a fault in the system and the operator can be notified or the data flagged as being in error.

Clearly there needs to be some interpretation of the output signals to convert a current in the range between 4 mA and 20 mA into a meaningful measurement. Therefore the output from the transducer requires signal conditioning.

25.5 Signal Conditioning

In most cases, it is necessary to condition the signal before the rest of the data acquisition system can make proper use of it. Signal conditioning refers to the electronic hardware that prepares the signal from the transducer for the next piece in the system. This might be amplification, linearization, filtering or conversion from current-based to voltage-based signals (Frey and Williams 1994). Often, the signal conditioning hardware includes two or more types of conditioning. One of the most important reasons for signal conditioning is the reduction of noise.

25.5.1 Noise

Noise may be generated within the electrical components as internal noise or it may be added to the signal as it travels down the input wires to the data acquisition system as external noise.

Internal noise arises from heat in the circuitry and although it can be minimized it cannot be completely removed. For example amplifiers will generate a few microvolts of internal noise which limits the resolution of the signal to this level. The

amount of noise added to the signal depends on the bandwidth of the system and the temperature. The noise power in a system is determined by:

$$N = kTB \tag{25.1}$$

where N is the noise power (W), k is Boltzman's constant (1.38 x 10^{-23} J K^{1}), T is the noise temperature of the antenna (K) and B is the band width of the system (Hz).

Bandwidth can refer to two main concepts. In computer networks, bandwidth is often used as a synonym for data transfer rate - the amount of data that can be carried from one point to another in a given time period; however in communication systems, bandwidth refers to the range of frequencies that a signal uses on a given transmission medium. In this case, bandwidth is expressed in terms of the difference between the highest-frequency signal and the lowest-frequency signal sent along the communication channel.

Systems with narrow bandwidth will be less noisy than those with excessively large bandwidths. One of the most effective methods of reducing bandwidth in a data acquisition system is to introduce appropriate filtering systems. Filters are usually very simple circuits that limit the range of frequencies that can pass onto the next part of the system. For example the tuner of a radio is actually a filter that limits the incoming signals from all the available stations so that only one station's signal can get to the rest of the radio circuitry.

For most data acquisition applications a low-pass filter is used to reduce noise. This allows lower frequency components through but removes the higher frequencies. The cut-off frequency must be compatible with the frequencies present in the actual signal and the sampling rate used for the analogue to digital conversion.

The second method of reducing internal noise is to cool the circuitry. For example, many radio telescopes and satellite dishes, like the one shown in Figure 25.1, use a cryogenically cooled feed system in order to reduce the internal noise of the system and increase its sensitivity to very low level signals from space (Electronics News 2004). Chapter 8 provides an introductory section on aperture antennae, like the dish antenna shown in Figure 25.1.

External noise is also added to a data system because the signal leads act as antennae picking up environmental electromagnetic activity. Most of this injected noise is common to both signal wires; therefore using a differential amplifier will remove most of this common mode voltage. Differences between the signal wires (for example if they are separated rather than twisted together) will lead to residual voltages being added to the signal, increasing noise. It is important when setting up automatic data acquisition systems to keep signal wires as short as possible and as far away from electrical machinery as possible.

Figure 25.1: Typical satellite antenna.

Differential amplifiers measure the difference in voltage between two wires. By only reacting to differences on the input wires much of the injected noise can usually by eliminated from the system. Usually there is a third connector which allows these signals to be referenced to ground. The two wires go into separate high-impedance amplifiers which monitor the voltage between the input and ground. The outputs of the two amplifiers are then subtracted to give the difference between the two inputs, meaning that any voltage which is common to both wires is removed.

The ability of the amplifier to obtain the difference between two inputs whilst rejecting the common signal to both wires is defined by the common mode rejection ratio and the common mode range. A common problem when using differential amplifiers is neglecting the connection to ground. Unless some connection is made between the amplifier and ground the reference voltages are undefined quantities and may lead to some very unusual output from the amplifier.

25.5.2 Amplification

Amplification is used to magnify (or occasionally to reduce) an input signal. In times past, triodes (a type of valve) and transistors were used to provide amplification; however most instruments use operational amplifiers (or op-amps) to boost the outputs from transducers.

An ideal Operational Amplifier is a three-terminal device which consists of two high impedance inputs, one called the Inverting Input, marked on circuit diagrams with a negative sign, and the other one called the Non-inverting Input, marked with a positive sign (Smith 1976). The third terminal represents the amplifier output port which can both sink and source either a voltage or a current. In a linear operational

amplifier, the output signal is the amplification factor, known as the amplifier's gain (A), multiplied by the value of the input signal. The sign of this gain factor depends on whether the input voltage is fed into the inverting or non-inverting input (Smith 1976). The gain of operational amplifiers is controlled by feedback resisters placed in the circuit around the amplifier (Smith 1976). The gain of an inverting amplifier (Figure 25.2) is:

$$A = -\frac{R_f}{R_1} \tag{25.2}$$

The gain of a non-inverting amplifier (Figure 25.3) is:

$$A = \frac{R_1 + R_f}{R_1} \tag{25.3}$$

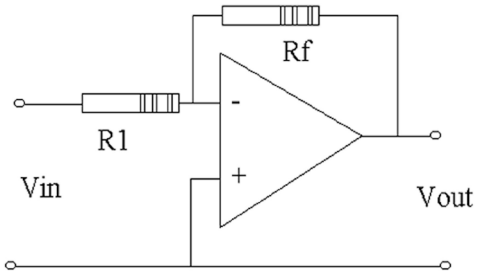

Figure 25.2: An inverting amplifier configuration.

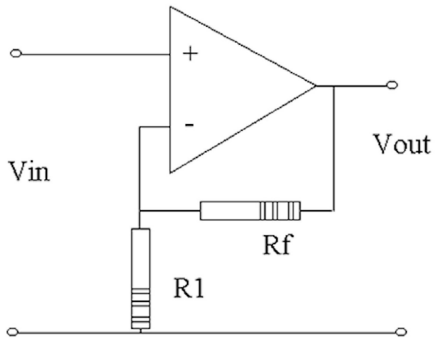

Figure 25.3: A non-inverting amplifier configuration.

Inversion simply means that when the input voltage goes above the zero voltage point (positive) the output goes below the zero voltage point (negative) and vice versa. A nice feature of an inverting amplifier configuration is that it allows several inputs from different sources to be added together in one device. There are some other useful features about inversion, which for the moment are beyond the scope of this book.

25.5.3 Offset Adjustment

As mentioned earlier, the industry standard output from a transducer ranges between 4 mA and 20 mA, where 4 mA represents the zero value of the measurement being made. Having at least 4 mA running through the connection from the transducer identifies when the device is working properly; however it confounds the actual measurement process. The easiest way to remove this confounding influence is to add a small negative DC voltage to the input signal to shift the signal down so that the output reads zero when the input from the transducer is at 4 mA. This can be done using the adding feature of the inverting amplifier configuration mentioned earlier (Figure 25.4).

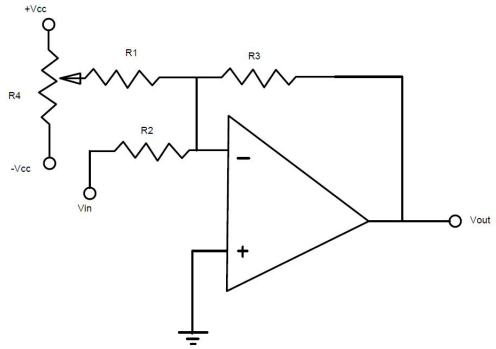

Figure 25.4: An offset adjusting inverting amplifier.

The output from the amplifier circuit in Figure 25.4 is:

$$V_{out} = -\frac{R_3}{R_2}V_{in} - \frac{R_3}{R_1}V_{DC} \tag{25.4}$$

Where V_{DC} is provided by an adjustable voltage divider R_4. The circuit is set up and adjusted while the transducer is reading a zero input (i.e. 4 mA).

25.6 Digital Data Acquisition

Most data analysis, particularly for very large quantities of data, involves computer systems. By their very nature, computers cope with numbers rather better than with constantly changing voltages or currents. Therefore an integral component in most data acquisition systems is a circuit that converts an incoming voltage into a number. This process begins with a sample and hold system that feeds a sampled voltage into circuits called analogue-to-digital converters (A/D converter) (Vandoren 1982). It is common to have several transducers, which are measuring several parameters, feeding into a single data acquisition system. Therefore multiplexing is used to sample across several input channels is used to sequentially acquire data from each transducer in turn (Vandoren 1982).

25.6.1 Sample and Hold Circuits

As the name indicates, a sample and hold circuit is a circuit, which samples an input signal and holds onto its last sampled value until the input is sampled again. Sample and hold circuits are commonly used in analogue to digital converts, communication circuits, etc. A typical sample and hold circuit stores charge in a capacitor (Figure 25.5). It uses electronic switching arrangements, commonly provided by a field effect transistor (FET), to connect or disconnect the capacitor from the input signal at regular time intervals. To sample the input signal the switch connects the capacitor to the input signal, via a buffer amplifier. The buffer amplifier charges or discharges the capacitor so that the voltage across the capacitor is proportional to the input voltage. In hold mode the switch disconnects the capacitor from the buffer. The capacitor is invariably discharged by its own leakage currents and useful load currents, but the loss of voltage (*voltage drop*) within a specified hold time remains within an acceptable error margin. The resulting output from the sample and hold circuit has a staircase appearance that approximates the analogue input (Figure 25.6). The staircase approximation of the input signal becomes a better approximation to the real signal when the sampling rate is high.

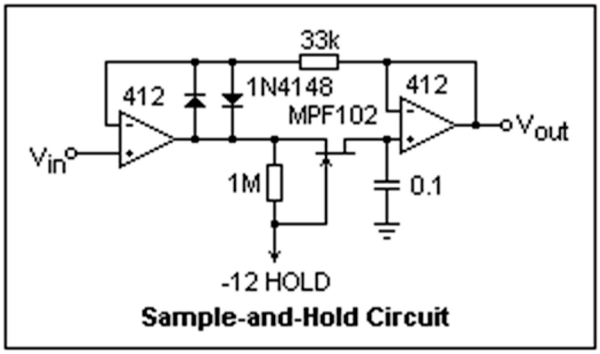

Figure 25.5: An example of a sample and hold circuit.

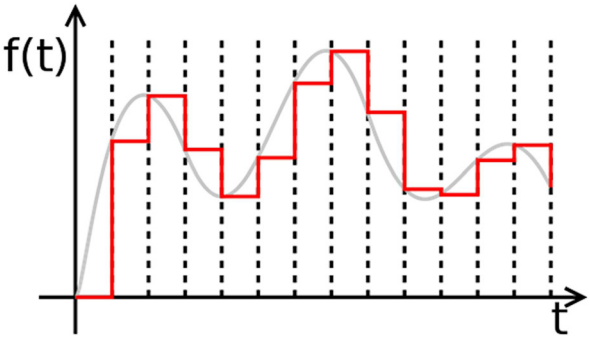

Figure 25.6: Typical output from a sample and hold circuit – the lighter coloured input signal is approximated by the darker coloured staircase wave.

25.6.2 Aliasing

Aliasing refers to an effect that causes different continuous signals to become indistinguishable (or aliases of one another) when they are sampled. For example, Figure 25.7 shows a continuous sinusoidal signal that has been sampled at regular time intervals. However, Figure 25.8 shows another sinusoidal wave that passes through each sample point from the first signal. The two waves are "aliases" of one another. Aliasing can be avoided by ensuring that the sampling frequency is greater than twice the frequency of the highest frequency signal in the original data. This is referred to as the Nyquist sampling rate (Nyquist 2002).

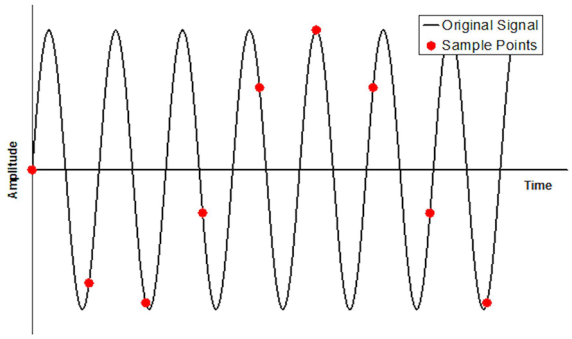

Figure 25.7: Sampled sinusoidal wave.

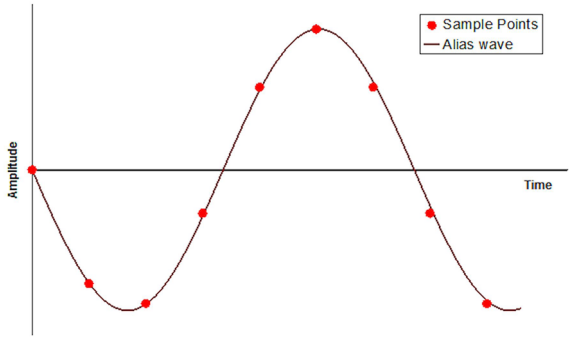

Figure 25.8: Another sinusoidal wave that passes through the same data sample points.

25.6.3 Multiplexing

Multiplexing is sending multiple signals or streams of information on a carrier at the same time in the form of a single, complex signal and then recovering the separate signals at the receiving end (Taub and Schilling 1971). For data acquisition from multiple input devices, multiplexing can be achieved by using the equivalent of a multi-way switch that pols each input one after the other in sequence. Technically this is referred to as time-division multiplexing because each input is allocated a set amount of time to communicate with the remainder of the system.

25.6.4 Analogue-to-Digital Conversion

For digital data acquisition that directly interfaces with a computer, such as can be found in many laboratories, Analogue to digital conversion is typically handled with a plug-in board or card. They are commonly referred to as DAQ-boards or DAQ-cards. In a stand alone data logging system, these circuits are hard-wired into the system itself.

An analogue to digital converter (Figure 25.9) works by comparing digital numbers with the sampled input signal. It actually uses a digital to analogue converter (D/A) to help in this process. The D/A converter is another clever application of a summing inverting amplifier (Figure 25.10) that can build an equivalent voltage from a stored binary number. The input from the D/A converter is fed from the output of the A/D converter. The output from the D/A converter is compared with the input signal. If the output from the D/A converter is too low, the comparator boosts the A/D counter so it adopts a higher digital number. If the output from the D/A converter is too high, the comparator reduces the A/D counter so it adopts a lower digital number. When the digital number is as close as possible to the input signal's value, the digital number is transferred along a bus system to some storage device or computer.

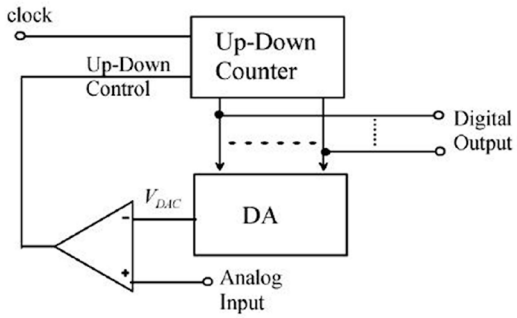

Figure 25.9: Analogue to digital converter diagram.

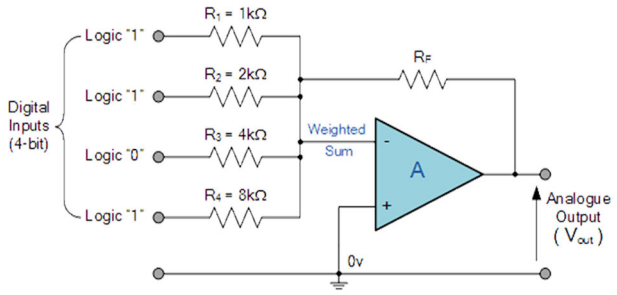

Figure 25.10: Example of a 4-bit digital to Analogue converter.

The vast majority of DAQ boards and cards have either 12-bit or 16-bit resolution. This translates to being able to distinguish either 4096 or 65536 individual units of measure respectively. Ultimately this ability to subdivide the full range of the transducer's output into small subdivisions determines the resolution of the final data. The number of divisions that can be distinguished is:

$$R = 2^N \tag{25.5}$$

Where R is the number of divisions and N is the number of binary digits that can be produced by the A/D converter.

Consider the case of a thermocouple that has a full scale capability of 0 to 1000 degrees. If a 12-bit A/D converter is used, then the 12-bit A/D converter will split the measurement range into 4096 steps with each step being (1000 degrees)/4096 or about ¼ of a degree. That will be the finest resolution of the temperature available from this system.

25.7 Software

There are plenty of software products available for data analysis. Many of these are system-specific. By far, the most common solution used by engineers for PC-based DAQ systems are the graphical DAQ software languages. These are designed to reduce the programming time and minimize the expertise required.

Popular examples of this type of DAQ software are: LabVIEW, Agilent VEE (previously known as HP VEE), DasyLab, and MatLab. Many engineers program the software themselves. Others will hire system analysts or programmers to do the programming for them.

Probably one of the most useful software tools for analyzing data is a simple spreadsheet. In conjunction with proper geo-referencing using latitude and longitude or some other map grid system, data that has been summarised using a spreadsheet may also be exported into a Geographic Information System (GIS) for further spatial analysis.

Hopefully it is clear from this discussion that data acquisition can be an expensive process in terms of both time and equipment. Therefore every effort should be made to protect and preserve both the system and the data. One of the biggest problems with long term field based data acquisition systems is lightning.

25.8 Lightning Protection

One of the most destructive environmental phenomena is lightning. Lightning occurs as a result of unstable upper atmospheric conditions. The first stage of a lightning strike is a series of stepped downward leaders moving from the clouds toward the ground. These leaders are invisible to the naked eye. Prominent features such as buildings and trees develop high positive charges which emit upward moving streamers competing with each other for connection with the downward leaders. When connection occurs, a path to ground is formed for the lightning current. This return stroke is the lightning flash that is visible to the eye, as seen in Figure 25.11.

Figure 25.11: Lightning over Sydney harbour.

During lightning storms, huge voltage differences develop between the air and the earth. Huge voltage differences can also build up in the ground itself. It is possible to receive a severe or even fatal shock because of these voltage differences in the earth, even if the victim is some distance from where lightning struck the ground. There have been many instances where cattle have been killed during lightning storms because the voltage difference between their front and hind feet is enough to cause lethal electrical currents to flow through their bodies.

Voltage differences in the ground cause electrical currents to flow through the soil. When these currents are intercepted by something which is a better conductor than the soil, they will flow through the object rather than the soil. This causes current surges through telephone wires and sensor cables. Longer cables tend to capture ground currents from distant lightning strikes better than shorter cables and can therefore cause considerable damage to a data acquisition system. The same can be said about people who are holding onto cables during lightning storms.

The problem with lightning strikes is voltage differences between one part of a system and another. This voltage difference gives rise to unwanted current flowing through the system. These currents cause damage to equipment and place personnel in danger.

By knowing the nature of lightning it is possible to develop a strategy to redirect unwanted currents away from vital parts of the system.

The first strategy is to capture the lightning strike. Rather that trying to eliminate the strike, it is better to adopt a more subtle approach and provide a predictable path that diverts it away from the more vulnerable parts of the system. A structure may be protected by erecting a lightning rod adjacent to it. A lightning rod will provide a cone of protection, as shown in Figure 25.12, having a base radius of approximately twice the height of the rod itself.

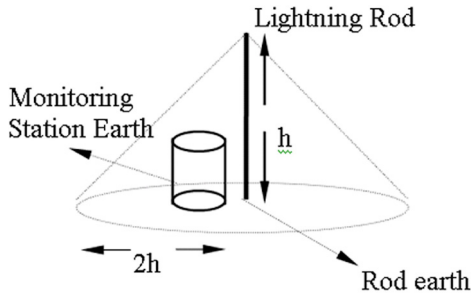

Figure 25.12: Cone of protection provided by lightning rod.

A lightning rod in combination with a good earthing system, like that shown in Figure 25.13, will intercept the strike and safely conduct the energy to earth, away from sensitive parts of the system.

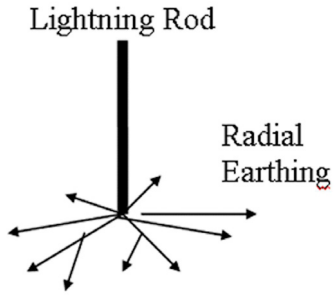

Figure 25.13: Lightning rod with multiple earth connections to provide good dissipation of energy.

The first strategy is to protect people. Personnel protection is a two fold process:

1. Holding a common voltage - The objective of this approach to lightning protection is to hold all parts of the system at the same voltage until the energy from the lightning strike has time to dissipate. In remote areas this can be accomplished by:

– Installing multiple earth spikes on the system. This is even more effective if the earth spikes are arranges in a loop around any structures that people may touch, as shown in Figure 25.14. This will effectively hold the structure and a sizeable volume of soil around it at the same voltage, reducing the risk of shock.
– Electrically connecting structures together using lengths of electrical cable will ensure that the entire structure remains at the same electrical voltage. This will stop currents flowing from one place to another and it will reduce the risk of electrical shock.

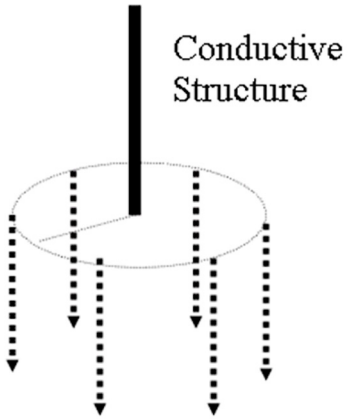

Figure 25.14: Loop earthing system designed to protect personnel who are touching conductive structures.

2. Eliminate earth currents - Because the soil itself can sustain sizeable voltage differences between one location and another, it is possible that a current may be set up in a long cable which has been earthed at both ends. It is better to totally isolate one end of the cable and solidly earth the other to a common earth point.

The objective of isolation is to provide an electrical break between two systems, yet still allow signal transfer to take place across this break. Isolation is only possible when both sides of the isolation point have independent power supplies. In an instrumentation system it is impossible to isolate between the logger and the probes, because the probes take their power supply from the logger.

The only part of the system where this technique could be used effectively would be at the interface between the data transmission system and the data logging system. One technique which could provide good isolation is to use optical coupling between the output of the data logger and the telephone line.

Normal monolithic opt-coupling devices are not effective. Experience shows that for large voltage surges these devices self destruct. One option could be to install short lengths of optical fibre to provide isolation. Another option is to use radio links or mobile telephones to link the data logger to a central computer system.

25.8.1 Some Notes on Earthing Systems

The best way to protect a circuit against lightning strike is to ensure there is a direct path to earth other than through a person or a vital circuit. This is normally achieved by enclosing the circuit in a metal container and connecting the container directly to the earth via a copper strap.

One of the major problems with earthing is that soil is not always a good conductor. Soil resistivity varies greatly from one location to another. For example, saturated soils near rivers may have a resistivity of less than 1.5 ohm metres. In the other extreme, dry sand can have resistivity values as high as 10,000 ohm metres. Soil type profoundly affects the quality of any earthing system. Table 25.1 shows the electrical resistivity of several common soil types.

Table 25.1: Resistivity values for several types of soil and water (Source: AS/NZS 1768:2007 2007).

Type of Soil or Water	Typical Resistivity (Ohm metres)	Usual Limits (Ohm metres)
Sea Water	2	0.1 to 10
Clay	40	8 to 70
Ground well and spring water	50	10 to 150
Clay and Sand mixture	100	4 to 300
Shale, slate, sandstone etc.	120	10 to 1,000
Peat, loam and mud	150	5 to 250
Lake and creek water	250	100 to 400
Sand	2,000	200 to 3,000
Moraine gravel	3,000	40 to 10,000
Ridge gravel	15,000	3,000 to 30,000
Solid granite	25,000	10,000 to 50,000
Ice	100,000	10,000 to 100,000

Soil moisture content is also important. Soils normally contain some salt. When water enters the soil profile, salt is dissolved to form an electrolyte (a solution containing charged particles). These charged particles can drastically reduce the soil's resistivity, as shown in Table 25.2. Table 25.3 demonstrates the influence temperature has over soil resistivity.

Table 25.2: Variation of soil resistivity with moisture content (Source: AS/NZS 1768:2007 2007).

Moisture Content (% of weight)	Typical soil resistivity of clay mixed with sand (Ohm metres)	Typical soil resistivity of sand (Ohm metres)
0	10,000,000	----
2.5	1,500	3,000,000
5	430	50,000
10	185	2,100
15	105	630
20	63	290
30	42	----

Table 25.3: Variation of resistivity with temperature in a mixture of sand and clay with a moisture content of 15% by weight (Source: AS/NZS 1768:2007 2007)

Temperature (°C)	Typical value of soil resistivity (Ohm metres)
20	72
10	99
0 (Water)	138
0 (Ice)	300
-5	790
-15	3,300

The Lightning Protection Standard (2007) specifies that the maximum earth resistance for an earthing system for lightning protection purposes should be 10 ohms in dry soil. Earth resistance can be measured using a special type of meter called a mega. Where the desired resistance can not be obtained by installing one earth rod, it is possible

to reduce the overall resistance by installing additional earthing rods. The overall resistance will be higher than would be expected from simple resister theory because of interference from one rod to the next within the soil. To minimise interference the distance between electrodes should be at least twice the length of the rod in the ground, as shown in Figure 25.15.

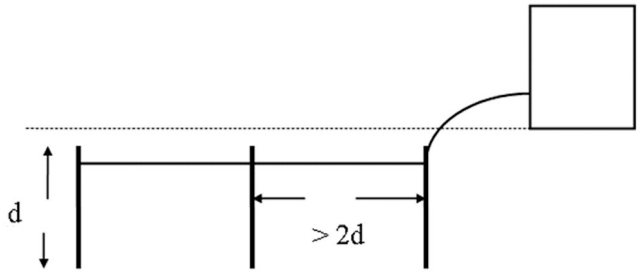

Figure 25.15: Installation of multiple earth stakes at a data acquisition station.

To protect equipment from damage due to lightning strikes and other electrical surges it is essential to use a transient barrier. A transient barrier is designed to prevent very high voltage pulses from passing through to sensitive electronic equipment from external wires and cabling. When the transient barrier is operating normally, signals pass through the barrier without change. When a high voltage surge, which is greater than the transient barrier's rating, arrives on the line, the barrier will conduct the surge currents in the line to ground.

The protection level of the barrier specifies the method used by the transient barrier to do this. A protection level 3 is the recommended rating for data logging applications. The voltage at which the transient barrier begins to conduct to ground must also be specified (Cody 1993).

Once the data has been acquired and stored by the acquisition system it must be made available to the landscape manager for analysis. Often this involves connecting a portable computer to the system and downloading the data from the logger to the computer. Many large scale systems such as the national weather monitoring network cover far too large an area to do this effectively. Therefore they use data communication systems. Data communication will be discussed in the next chapter.

References

AS/NZS 1768:2007. 2007. AS/NZS 1768:2007 Lightning

Brain, M. 1998-2004. *Marshall Brain's How Stuff Works*. February, 2004. http://www.howstuffworks.com/

Cody, S. 1993. *Transient protection for data loggers: Technical bulletin*. Mindata
Electronics News. 2004. Australian telescope designs with US EDA tools. *Electronics News*. January: 6.
Frey, R. and Williams, D. 1994, *PC Instrumentation for the 90s*, 4th edn, Perth: Boston Technical Books Pty Ltd.
Nyquist, H. 2002. Certain topics in telegraph transmission theory. *Proceedings of the IEEE*. 90(2): 280-305.
Smith, R. J. 1976, *Circuits, Divices and Systems*, 3rd edn, New York: Wiley International.
Taub, H. and Schilling, D. L. 1971, *Principles of Communication Systems*, Tokyo: McGraw-Hill Kogahusha.
Vandoren, A. 1982, *Data Acquisition Systems*, Reston, Virginia: Reston Publishing.

26 Radio Frequency and Microwave Communication Systems

Information and communication have always mattered in agriculture (McNamara, *et al.* 2012). Humanity still faces a challenging future and filling the stomachs of the growing population is only one reason agriculture is critical to global stability and development (McNamara, *et al.* 2012). It is also critical because one of the most effective ways of reducing poverty is to invest in and make improvements in the agricultural sector (McNamara, *et al.* 2012). Given the challenges, the arrival of information communication technology (ICT) is well timed (McNamara, *et al.* 2012). Smart agricultural systems make use of every available technology to improve production and increase efficiency. This includes adopting better communication systems across the industry. Historically, communication systems have been readily adopted by agricultural and rural communities. Australia's Royal Flying Doctor Service (RFDS), which was conceived in 1912 by the Rev. John Flynn, became practical when an Adelaide (Australia) based electrical engineer, A.H. Traeger, developed a low-powered, portable, pedal-driven, Morse radio transmitter-receiver with a range of about 500 km (Anonymous 2014). This communication system made regular medical consultations and transport of doctors and patients in remote areas of Australia possible.

The same underlying wireless technology had other applications as well. In 1946, Ms. Adelaide Miethke instigated the idea for the School of the Air when she noticed how children from remote areas in Australia were all taught to use the Royal Flying Doctor radio service. She saw that there were other ways this network could be used and in 1948, the Alice Springs RFDS base was used to broadcast the first school lessons to children in remote places of central Australia. Just a few years later, the School of the Air (SOA) was officially established. Wireless technology was transforming agricultural communities.

More recently, Hornbaker et al (2004) reported on a system that increases the operational efficiency of multi-vehicle agricultural operations, such as harvest and planting. The system incorporates hardware, software and wireless connectivity to communicate with vehicle operators about the status and position of other vehicles and their grain bin fill levels and grain attributes. The system provides assistance to the operator to optimize the movement of harvesters, grain wagons and road transport so that logistical bottlenecks and time the harvesters are waiting to be unloaded in the field are minimized.

Communication technology and in particular, wireless technology are almost ubiquitous. Although examples like broadcast radio, television and telephones have been in common use for decades, modern communication systems are becoming more pervasive and much less to do with voice communication and much more to do with data communication and control. Radiofrequency and microwave fields

have been used for communication systems for a very long time. These waves can be channelled through cables, waveguides and open space to carry messages to and from transceivers near and far. This chapter will outline the key principles for using radiofrequency and microwaves to communicate.

26.1 Principles of RF and Microwave Communication

Radiofrequency and microwave communication systems use wave lengths that vary from a few centimetres to 1500 metres long. Each system transmits its signal on its own wavelength and tuning circuits are used to filter out all but one broadcast station from the incoming signals.

There are four main frequency bands that are used for radio broadcasting - short wave, medium wave, long wave and VHF (very high frequency). Television broadcasts use a higher range of frequencies than radio, which typically have wavelengths of about 500 mm. This is the UHF (ultra-high frequency) band. Data networking systems operate at microwave frequencies such as 2.4 GHz. One of the earliest applications of radiofrequency communication was wireless (or radio) transmission.

26.2 Principles of Wireless Communication

Wireless communication, as the name suggests, involves communicating a message without the use of connecting wires. To achieve this requires: the generation of radio waves (RF) using a carrier signal generator (oscillator); one or more frequency multiplication stages to shift the transmission frequency to a suitable range for broadcast; a modulator that encodes a message onto the carrier signal; a power amplifier to boost the final signal ready for transmission; a filter with matching network to remove unwanted sidebands and noise from the transmitted signal; a short transmission line (or wave guide) to connect to an antenna; and finally the antenna itself that transfers the electromagnetic waves into open space as efficiently as possible (Taub and Schilling 1971, Smith 1976).

A typical radio receiver has: an antenna system that receives the RF energy from open space; a short section of transmission line (or waveguide) to guide the incoming signal to the receiver circuitry; a filter that tunes to the desired carrier wave frequency; an RF amplifier that amplifies the energy of the incoming signal so that it is raised above the noise generated by the radio itself (Note: too much RF amplification can result in “spurs” or spurious mixer products, sometimes called cross-modulation or inter-modulation); one or more mixing stages in which the incoming RF signal is mixed with a second, internally generated RF frequency to produce a lower intermediate frequency (IF); one or more IF amplifiers that boost the signal; a detector, which extracts the modulated information from the IF signal, is used to extract the

audio frequencies (AF) from the original carrier; and finally, an audio amplifier that increases the energy of the extracted data (Taub and Schilling 1971, Smith 1976). The type of detector circuitry depends on the type of modulation used to encode the data onto the carrier wave.

26.3 Modulation

There are three main features about electro-magnetic radiation, which can be altered to carry information (Smith 1976):

1. The intensity (or Amplitude) of the radiation
2. The colour (or Frequency) of the radiation.
3. The Presence and absence of the radiation (Pulses).

If the amplitude, or strength, of the signal is changed in a way corresponding to the information being sent amplitude modulation (or AM) is created. AM transmitters vary the signal level smoothly in direct proportion to the data being transmitting. Positive peaks of the signal produce maximum radio energy, and negative peaks of the signal produce minimum energy.

The main disadvantage of AM is that most natural and man-made noise is actually modulated onto the carrier like AM, and AM receivers have no means of rejecting that noise. Also, weak signals are quieter than strong ones, which require the receiver to have circuits to compensate for the signal level differences (Radio Design Group 2001). Amplitude modulation can be described by (Taub and Schilling 1971):

$$E(t) = A\left[1 + m(t)\right]Cos(\omega t) \tag{26.1}$$

Where E is the electric field, A is the applied carrier, m(t) is some time varying message signal, w is the angular velocity of the carrier wave, and t is time. The maximum amplitude of m(t) should be less than 1.0, otherwise the electric field will be over modulated causing cross over distortion.

In an attempt to overcome noise problems, Edwin Armstrong invented a system that would overcome the difficulties of amplitude noise (Taub and Schilling 1971). Instead of modulating the strength (or amplitude) of the transmitted carrier, he modulated its frequency. Though many engineers at that time said that frequency modulation (or FM) was not practical, Armstrong proved them wrong. Today FM is the mainstay of the broadcast radio services (Radio Design Group 2001). It is also popular for short haul data transmission and is commonly used in radio microphones.

In a frequency modulated system, the frequency of the carrier is varied according to the modulating signal. For example, positive peaks would produce a higher

frequency, while negative peaks would produce a lower frequency. At the receiving end, a limiting circuit removes all amplitude variations from the signal, thus eliminating much of the noise, and a discriminator circuit converts the frequency variations back to the original audio or data signal. Since the recovered data is dependent only on the frequency, and not the strength, no compensation for different signal levels is required, as is the case with AM receivers.

Frequency modulation can be described by (Taub and Schilling 1971):

$$E(t) = A \cdot Cos\left[\omega t + k \cdot m(t)\right] \tag{26.2}$$

Where E is the electric field, A is the applied carrier, k is modulation factor (a constant), m(t) is some time varying message signal, w is the angular velocity of the carrier wave, and t is time. The deviation of the instantaneous frequency from the unmodulated carrier frequency is:

$$\Delta f = \frac{k}{2\pi} m(t) \tag{26.3}$$

Many FM broadcast stations now transmit sub-carriers on their signals. Sub-carriers are signals that are modulated on the carrier, just like the normal data signals, except that they are too high in frequency to be heard. Normal audio signals range in frequency from 20 to 20,000 Hz. Most sub-carriers start at about 56,000 Hertz (56 kHz). These sub-carriers are themselves modulated, sometimes with audio signals, such as background music, but more often with other forms of data (Radio Design Group 2001). Some of the information that is carried on these sub-carrier data services include: stock quotes, weather reports, news, sports, paging signals and differential GPS error corrections.

Various forms of pulse modulation (turning the carrier wave on and off) have been developed. Pulse amplitude modulation used the amplitude of regularly generated pulses to carry the message (Taub and Schilling 1971). This is somewhat analogous to amplitude modulation. Pulse width modulation uses pulses that begin at regular time intervals; however the duration of the pulses depends on the amplitude of the message signal. In both these cases, the message signal is analogue, implying that it has a variable value at any instant in time.

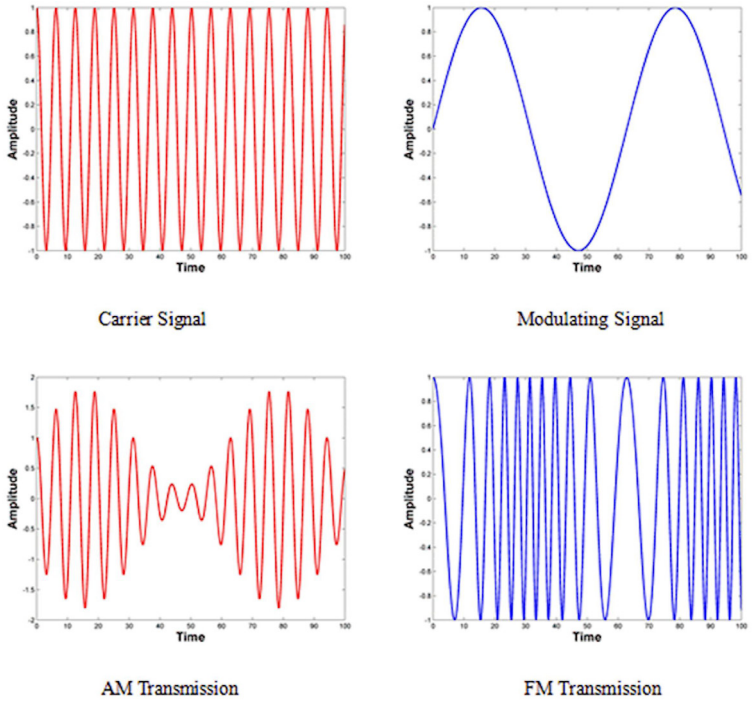

Figure 26.1: AM and FM Modulation.

26.4 Simplex, Half-duplex and Duplex Communication Systems

Simplex communication is permanent unidirectional communication (Taub and Schilling 1971, Smith 1976). Broadcast radio and television would be classified as simplex systems. Some of the very first serial connections between computers were also simplex connections. Simplex links are built so that the transmitter sends a signal and the receiving device transforms the received signal into information. No traffic is possible in the other direction across the same connection. Many environmental data gathering systems, such as automatic weather stations and water gauging systems use simplex data transfer from the field site to some central data hub. In these cases, two way communications is seldom necessary so the system is designed to be as simple as possible.

A half-duplex link can communicate in only one direction at a time, but it supports two way communications (Taub and Schilling 1971). Walkie-talkies and citizen's band (CB) radios are common half-duplex communication devices in that the same frequency is used for both transmission and reception; therefore only communication can only take place while the radio channel is not in use by someone or something

else. Half-duplex radio has been used for communication in rural and remote areas for a very long time.

Full duplex communication is two-way communication, achieved over a physical link that has the ability to communicate in both directions simultaneously (Taub and Schilling 1971). With most electrical, optic fibre, two-way radio and satellite links, this can be achieved by using separate carrier wave frequencies for transmission and reception, to avoid interference during two way communication. In some agricultural systems this allows data to be transferred from the field to a central point and control signals to be sent from the central point to the field. For example, full-duplex systems could be used to manage an automatic irrigation system.

26.5 Digital Communication

As was pointed out in the previous chapter, data is commonly converted to digital form for processing in computers. Communication systems have also become digital. Frequency-shift keying (FSK) is one way of facilitating digital communication (Taub and Schilling 1971). FSK is a special form of frequency modulation in which digital information is transmitted through discrete frequency changes of a carrier wave. Binary frequency shift keying (BFSK) uses a pair of discrete frequencies to transmit binary information. The resulting carrier wave has the form (Taub and Schilling 1971):

$$E(t) = A \cdot \cos\left[(\omega \pm \Omega)t\right] \tag{26.4}$$

Where Ω is a constant.

BFSK transfers data as a serial data packet, usually with: a leading address (to direct the data to its final destination over a network); the main data (encoded as binary numbers); and following bits that provide error checking services.

Unlike pulse modulation which allows for the absence of the carrier, BFSK provides a continuous carrier signal, irrespective of whether a 1 or a 0 is being transmitted. This provides a rudimentary link error check, somewhat like the 4 mA current used for data acquisition that was spoken about in the previous chapter.

26.6 Transmission Channels

Two options exist for transmitting data or information through a communication system: it can be via a physical channel such as a transmission line or wave guide; or it can be through free space. Both are commonly used in agricultural communication systems.

26.6.1 Transmission Lines

Common examples of transmission lines used for data communication are the twisted pair wires and coaxial cables.

An unshielded twisted-pair (UTP) cable consists of two braided copper wires with insulation around each individual wire. Twisted-pair cabling must follow exact specifications about how many twists or braids are permitted per meter of cable. Groups of unshielded twisted-pair wires are often placed within a protective jacket to form a cable. The wiring used for many short haul telephone systems and computer networks use unshielded twisted-pairs. Unshielded twisted-pair technology for data communications is growing rapidly and most data networks can now utilise unshielded twisted-pair wiring.

Shielded twisted-pair cable differs from UTP in that it has a much higher quality protective jacket with a greater insulation factor. Thus shielded twisted-pair has a longer signal transmission range. It is also less prone to electrical interference from outside sources. However, the majority of twisted-pair cabling is unshielded twisted-pair. Twisted-pair cabling is usually low in cost and easy to connect.

Unfortunately twisted-pair cabling is prone to electrical noise and interference. It generally has a low data transmission rate and can not transmit data very far without occasionally boosting the signal strength.

Coaxial cables, as shown in Figure 26.2, are a special case of the twisted pair where the return conductor is wrapped around the main conductor to provide additional mechanical protection and electrical shielding to the cable. Coaxial cable is capable of carrying network data at very high rates.

Coaxial cable has one central wire, which is surrounded by an insulating material. A stranded shield is wound over this insulating material to acts as the secondary conductor for the return path. All of this is protected by an outside protective jacket. Coaxial cable comes in different varieties and thicknesses. It also comes in different impedances. Impedance determines the amount of resistance offered to electrical impulses transmitted through the cable and is usually measured in ohms.

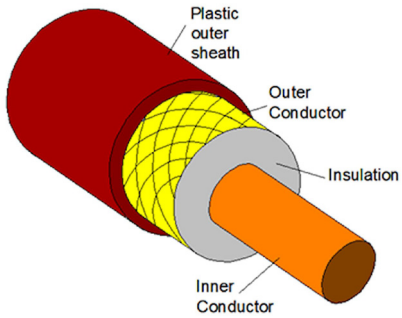

Figure 26.2: Diagram illustrating the arrangement of Coaxial Cable.

A uniform transmission line must be visualised as a "*distributed circuit*", as shown in Figure 26.3. A distributed circuit can be described as a cascade of identical cells of infinitesimal length *dz*. The conductors used in a transmission line possess a certain series inductance and resistance. In addition, there is a shunt capacitance between the conductors and even a shunt conductance if the medium insulating the wires is not a perfect insulator.

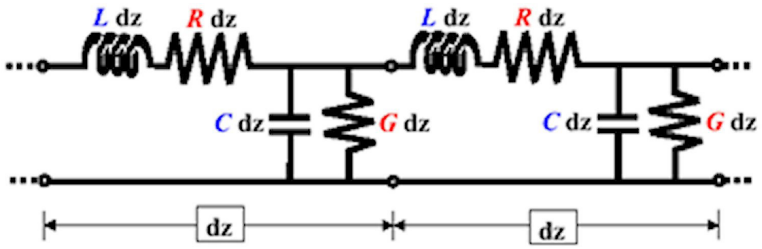

Figure 26.3: Distributed impedance in a transmission line (Source: Amanogawa 2001).

26.6.2 Loss-Less Transmission Line

In many cases, it is possible to neglect the resistive effects in the transmission line.

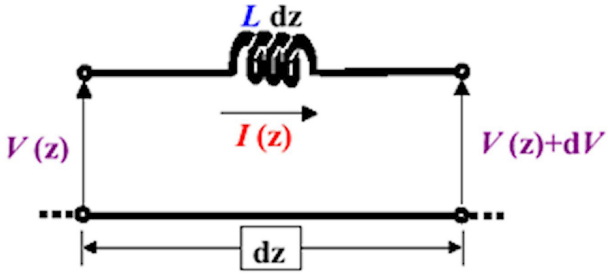

Figure 26.4: Inductive element (Source: Amanogawa 2001).

From this analysis it is clear that:

$$V(z) + dV - V(z) = -j\omega L \cdot dz \cdot I(z) \tag{26.5}$$

Therefore:

$$\frac{dV}{dz} = -j\omega L \cdot I \tag{26.6}$$

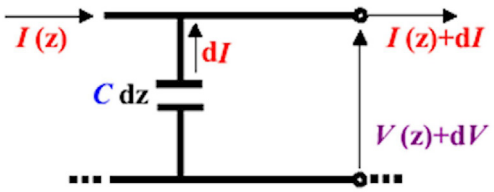

Figure 26.5: Shunt capacitance (Source: Amanogawa 2001).

Now considering the shunt element:

$$dI = -j\omega C \cdot dz \cdot \left(V(z) + dV\right) = -j\omega C \cdot dz \cdot V(z) - j\omega C \cdot dz \cdot dV \tag{26.7}$$

Now $\lim_{dz \to 0} dz \cdot dV = 0$; therefore

$$\frac{dI(z)}{dz} = -j\omega C \cdot V(z) \tag{26.8}$$

Taking the derivative of equations (26.6) and (26.8) with respect to z yields:

$$\frac{d^2V(z)}{dz^2} = -j\omega L \frac{dI(z)}{dz} = -\omega^2 LCV(z) \tag{26.9}$$

$$\frac{d^2I(z)}{dz^2} = -j\omega C \frac{dV(z)}{dz} = -\omega^2 CLI(z) \tag{26.10}$$

These are wave equations, the solution of which is:

$$V(z) = V_1 e^{-j\omega\sqrt{LC}z} + V_2 e^{j\omega\sqrt{LC}z} \tag{26.11}$$

In this case the general solution represents a wave propagating in both the +z and –z direction with a wave number of $k = \omega\sqrt{LC}$ and a velocity $c = \frac{1}{\sqrt{LC}}$.

Differentiating voltage with respect to z yields:

$$\frac{dV}{dz} = -j\omega\sqrt{LC}\left(V_1 e^{-j\omega\sqrt{LC}z} + V_2 e^{j\omega\sqrt{LC}z}\right) = -j\omega LI \tag{26.12}$$

Thus:

$$I = \sqrt{\frac{C}{L}}\left(V_1 e^{-j\omega\sqrt{LC}z} + V_2 e^{j\omega\sqrt{LC}z}\right) = \sqrt{\frac{C}{L}}V \tag{26.13}$$

Applying Ohm's law, the *intrinsic impedance* of the transmission line is defined as:

$$Z_o = \sqrt{\frac{L}{C}} \tag{26.14}$$

26.6.3 Lossy Transmission Line

The series impedance determines the variation of the voltage from input to output of the cell, according to the sub- circuit shown in Figure 26.6.

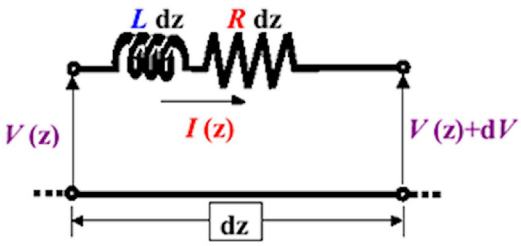

Figure 26.6: Serial elements (Source: Amanogawa 2001).

The current flowing through the shunt admittance determines the input- output variation of the current, according to the sub- circuit shown in Figure 26.7.

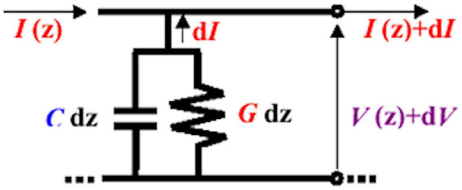

Figure 26.7: Shunt elements (Source: Amanogawa 2001).

In this case:

$$Zo = \sqrt{\frac{j\omega L + R}{j\omega C + G}} \tag{26.15}$$

and

$$V = V_1 e^{-\frac{1}{2}\left(R\sqrt{\frac{C}{L}}+G\sqrt{\frac{L}{C}}\right)z} e^{-j\omega\sqrt{LC}z} + V_2 e^{\frac{1}{2}\left(R\sqrt{\frac{C}{L}}+G\sqrt{\frac{L}{C}}\right)z} e^{j\omega\sqrt{LC}z} \tag{26.16}$$

Therefore the voltage will be attenuated with distance along the line. At high frequencies the unit resistance associated with the contraction of the current carrying cross-section becomes significant and the voltage wave traveling along the transmission line will be significantly attenuated. Therefore a transmission line has an effective upper limit to its frequency range. At microwave frequencies, a transmission line may only be used for a very short distance. A different system of transmission is needed to propagate radiofrequency and microwaves further than a few metres.

26.6.4 Optic Fibre

Although it is not so commonly used in agriculture, optic fibre, shown in Figure 26.8, is a special case of a wave guide for wavelengths near to and in the visible range of the electromagnetic spectrum. As depicted in Figure 26.10, when light passes from a material with a high refractive index, such as glass or plastic, into a material with a low refractive index, such as air, the light ray is bent back toward the interface surface. Thus there must be a stage at which the light ray travels along the surface of the glass. This is called the critical angle. If the angle at which the light ray strikes the surface is greater than the critical angle all the light will be reflected back into the glass. This is called total internal reflection.

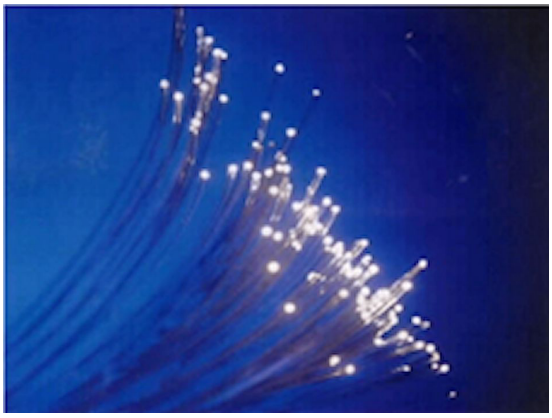

Figure 26.8: Optic Fibres.

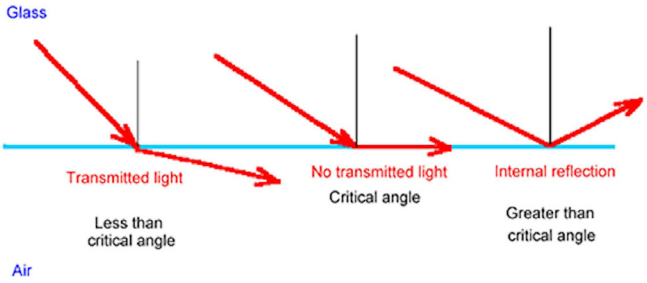

Figure 26.10: Principle of total internal reflection.

In an optic fibre, light is shone into the end of the fibre; thus all the light strikes the internal surfaces of the fibre at an angle that is greater than the critical angle. Therefore the light stays inside the fibre rather than escaping out into the air. Therefore the optic fibre can be used to guide the light, just like the metallic wave-guides used for microwaves. Optical fibres come in two types: Single-mode fibres; or Multi-mode fibres.

Single-mode fibres have a small core (about 9 microns in diameter) and transmit infrared laser light (wavelength = 1,300 to 1,550 nanometers). Multi-mode fibers have a larger core (about 62.5 microns in diameter) and transmit infrared light (wavelength = 850 to 1,300 nm) from light-emitting diodes (LEDs). Some fibres have a very large core (about 1 mm diameter) and transmit visible red light (wavelength = 650 nm) from LEDs.

Optic fibre relay systems consist of a transmitter, for producing and encoding the light signals, the optical fibre itself, an optical regenerator, to boost the light signal and an optical receiver that receives and decodes the light signals.

The transmitter is close to the optical fibre and uses a lens to focus the light into the fiber. Lasers or LEDs are commonly used as transmitters. Lasers have more power than LEDs, but vary more with changes in temperature and are more expensive. The most common wavelengths of light signals are 850 nm, 1,300 nm, and 1,550 nm (infrared, non-visible portions of the spectrum).

An optical regenerator consists of optical fibers with a special coating that has been doped with a small amount of specially chosen impurity. The doped portion is pumped with a laser. When a degraded light signal comes into the doped coating, the energy from the laser allows the doped molecules to emit a new, stronger light signal with the same characteristics as the incoming weak light signal. Basically, the regenerator is a laser amplifier for the incoming signal. The receiver uses a photocell or photodiode to detect the light and convert this into an electrical signal.

Optic fibres can be composed of either glass or plastic. The plastic optic fibre cable is easier to install but it has a much shorter transmission distance than glass optic fibre cable. Optic fibre cable is capable of very high-speed data transfer. Since it does not carry electrical impulses; therefore it is less affected by electrical noise or interference. Optic fibre lines can not be tapped into very easily, making it an excellent choice for security reasons.

Optic fibre cable requires considerable skill and specialized equipment to install. Generally the price of fibre-optic cable can be quite high. The same can also be said for metallic wave guides. In many cases data must be transmitted over substantial distances. In these cases a radio link can be used.

26.7 Wireless Radio Channels

Wireless channels that use antennae and electromagnetic waves to transfer messages through free space are commonly used. An antenna projects the electromagnetic waves in a particular directs, depending on its radiation pattern. As outlined in Chapter 8, an important measure of an antenna's performance is its gain. When considering a wireless radio link as part of a communication system, the gain of the transmitting and receiving antennae play a vital role in determining the distance over which the system can operate. This distance is determined by the Friis Transmission Equation:

$$P_r = \frac{P_t G_t G_r \lambda^2 \tau}{4\pi R^2} e^{-2\alpha R} \tag{26.17}$$

Where P_r is the received power (W), P_t is the transmitted power (W), G_t is the gain of the transmitting antenna, G_r is the gain of the receiving antenna, λ is the wavelenght of the carrier wave (m), τ is the matching coefficient from the receiving antenna to the rest of the receiving circuitry, α is the attenuation coefficient of the medium though

which the electromagnetic wave passes, and R is the range between the transmitter and the receiver (m).

The attenuation coefficient (α) is defined in equation (4.11) in Chapter 4. The matching coefficent for the antenna is (Bhattacharyya, *et al.* 2011):

$$\tau = \frac{4R_a R_c}{\left|Z_a + Z_c\right|^2} \tag{26.18}$$

Where R_a and R_c are the respective resistances of the antenna and the receiver circuitry (W), and Z_a and Z_c are the respective impedences of the antenna and the receiver circuitry. The matching coefficent (τ) ranges between 0.0 and 1.0, with and ideal match being achieved when $\tau = 1.0$.

Because wireless systems must contend with noise, it is important to ensure that the received signal is stronger than the background noise. The power associated with noise was defined in the previous chapter in equation (25.1). A useful measure of performacne is to ensure that the signal to noise ratio is well above 1.0. For a free space wireless link the signal to noise ratio is:

$$S = \frac{P_r}{P_n} = \frac{P_t G_t G_r \lambda^2 \tau}{4\pi k T B R^2} e^{-2\alpha R} \tag{26.19}$$

Where S is the desired signal to noise ratio for the wireless link.

Therefore longer wavelengths (i.e. lower frequencies) provide better signal to noise ratios for wireless links. Other factors such as terrain, obstructions, and the ability for the electromagnetic wave to be guided around the curvature of the earth also influence the effective range of a wireless link. For most agricultural activities these links are over moderately short distances and these other influences are not so critical.

Automatic data acquisition and wireless data transfer systems are becoming important for modern agriculture. One way of enhancing both the acquisition of useful data and the transmission of this data over longer distances is to use networks where the nodes of the network act as sensors in their own right and as boosters for signals from more distant sensors in the network. These wireless sensor networks are being developed for agricultural applications and will be discussed in the next chapter.

References

Amanogawa. 2001. Transmission Line Equations.

Anonymous. 2014. Flying Doctor Service. *Encyclopedia Britannica*.

Bhattacharyya, R., Floerkemeier, C., Sarma, S. and Deavours, D. 2011. RFID tag antenna based temperature sensing in the frequency domain. *Proc. RFID (RFID), 2011 IEEE International Conference on*. 70-77.

Hornbaker, R., Hansen, A., Kindratenko, V., Pointer, D. and Apgar, A. 2004. Improving Agricultural Operational Efficiency with Wireless Communication. *ICPA04 Conference*.

McNamara, K., Belden, C., Kelly, T., Pehu, E. and Donovan, K. 2012, *ICT in Agriculture Sourcebook*.

Radio Design Group. 2001. How It Works: Radios. 2004 (February):

Smith, R. J. 1976, *Circuits, Divices and Systems*, 3rd edn, New York: Wiley International.

Taub, H. and Schilling, D. L. 1971, *Principles of Communication Systems*, Tokyo: McGraw-Hill Kogahusha.

27 Wireless Ad Hoc Sensor Networks

Wireless data communication for agricultural purposes relies on: one or more sensors of environmental data (temperature, humidity etc.); a signal conditioner; an analogue to digital converter; a microprocessor with an external memory chip; and a radio module for wireless communication between other sensor nodes and/or a base station (Popescu 2007).

One of the first wireless networks for agriculture was built for the Dutch Lofar Agro research project (Visser 2005). It consisted of 150 sensor boards (based on the Mica2 Crossbow wireless sensor platform) deployed in a field for gathering temperature and humidity data (Popescu 2007). The data received by the sensors was handled by a microprocessor implementing the TinyOS operating system, and transmitted via radio in the 868/916 MHz band to a field-gateway and from there via Wi-Fi to a personal computer for data logging (Popescu 2007). Since then there has been considerable interest in using ad hoc wireless networks for automatic data acquisition in agricultural enterprises.

Australia's Commonwealth Scientific and Industrial Research Organisation (CSIRO) have developed a series of devices for agricultural wireless network systems. These devices incorporate: a Nordic radio with a range of over 1 km that operates on the 433- MHz or 915-MHz band; an integrated solar battery charging circuit; and an extensive range of sensors (Wark, *et al*. 2007). Their system also incorporates a real-time clock chip to reduce microcontroller overheads. Their system was also based on the TinyOS operating system (Wark, *et al*. 2007).

In precision agriculture, various parameters including soil moisture and soil temperature vary dramatically. Off-the-shelf irrigation controllers are not effective in managing water applications under these circumstances; however an irrigation management system based on wireless sensor networks can better respond to high resolution water application requirements (Mafuta, *et al*. 2013).

27.1 Network Configurations

Early computer networks could be divided according to their underlying topology. They loosely divided into: a star connected system; a bus connected system; or a ring connected system. The star connection is the oldest topology for networked systems (Parker 2000). The star arrangement uses point to point links from peripheral network nodes to a central machine (Parker 2000). In the bus configuration, the network nodes are connected onto a long bus as a series of tee junctions (Parker 2000). The ring system, as the name suggests, has a central ring bus onto which the nodes connect (Parker 2000).

There are no wired infrastructures or cellular networks in ad hoc wireless networks (Li 2003). Different configurations are possible; however many systems

use wireless nodes with omni-directional antennae. Any transmission from a node can be received by any node within its vicinity. It is also possible to use directional antennas to directly link fixed nodes (Li 2003). Each mobile node has a transmission range. If the signal from one node can not be directly received from a second node, the data message must be communicated through multi-hop wireless links by using intermediate nodes to relay the message (Li 2003). Consequently, each node in the wireless network also acts as a router, forwarding data packets for other nodes (Li 2003).

Wireless ad hoc network have their own special characteristics and some unavoidable limitations compared with wired networks. Wireless nodes are often powered by batteries and have limited available storage memory (Li 2003). Data transmission from a wireless node can be received by several neighbouring nodes. This can cause interferences (Li 2003). Unlike traditional static communication devices, the wireless nodes are often moving during the communication process (Li 2003).

Several data routing options can be used in ad hoc networks. Most routing systems require pre-knowledge of the destination node's physical location. Compass Routing forwards data via other nodes such that the angles among the neighbouring nodes to the destination node are the smallest possible (Li 2003). Greedy Routing transfers data based on the shortest possible overall transfer distance rather than calculated transfer angles (Li 2003).

Many ad hoc networks in agricultural systems have limited power resources; therefore consideration needs to be given to minimising the power needed to transfer data. This can be achieved in several ways. Firstly, the data should be as information dense as possible. This usually requires some pre-processing of the data before transmission. For example, calculation and transmission of means and standard deviations, rather than transmitting raw data reduces the size of data being transmitted. Secondly, when a wireless network has a sufficient density of nodes, only a small number of them need to turn on at any given time to forward data traffic (Chen, *et al.* 2002).

27.2 Open Source Platforms

Several commercial wireless systems have been developed; however for small scale experimental systems, a number of open source platforms have are available. Two options include the Arduino and the Raspberry Pi.

27.2.1 Raspberry Pi

The Raspberry Pi is a credit-card sized computer that plugs into a TV (or monitor) and a keyboard. It is a capable little computer which can be used in electronics projects, and for many of the things that a desktop PC does, like working with spreadsheets, word-processing and games. It can also play high-definition video (Anonymous 2014b). The Raspberry Pi can support a complete operating system such as Linux and can be programed in languages like Scratch and Python (Anonymous 2014b).

The Raspberry Pi platform also supports various add-ons, including wireless adaptors that support wireless connectivity.

27.2.2 Arduino

Arduino is a tool for making computers that can sense and control other devices. It is an open-source physical computing platform based on a simple microcontroller board, and a development environment for writing software for the board. Arduino can be used to develop interactive objects, taking inputs from a variety of switches or sensors, and controlling a variety of lights, motors, and other physical outputs (Anonymous 2014a). The Arduino platform supports plug in devices called shields, including the Xbee, Wireless SD and Cellular mobile devices.

The Xbee shield allows an Arduino board to communicate wirelessly using Zigbee (Anonymous 2014a). The module can communicate up to 100 feet indoors or 300 feet outdoors (with line-of-sight). It can be used as a serial/USB replacement or it can put into a command mode and configured for a variety of broadcast and mesh networking options (Anonymous 2014a).

The Wireless SD shield allows an Arduino board to communicate wirelessly using a wireless module. It is based on the Xbee module, but can use any module with the same footprint. The module can communicate up to 100 feet indoors or 300 feet outdoors (with line-of-sight) (Anonymous 2014a).

The Cellular Shield allows the Arduino to access a mobile telephone network, providing simple messaging systems (SMS), *Global System for Mobile* Communications/ *General Packet Radio Service* (GSM/GPRS), and *Transmission Control Protocol/Internet Protocol* (TCP/IP) functionalities (Anonymous 2014a). The cellular module requires a SIM card (pre-paid or straight from an existing mobile phone) and an antenna. Data can be sent using "Serial.print" (Anonymous 2014a).

27.3 Mobile Telephone Networks

The *Universal Mobile Telecommunications System* (UMTS) is a third generation mobile cellular system for networks based on the GSM standard. UMTS uses wideband

code division multiple access (W-CDMA) radio to offer a broad range of data and communications services. The technology described in UMTS is sometimes also referred to as Freedom of Mobile Multimedia Access (FOMA) or 3GSM. If sufficient coverage is available, using the mobile telephone network as part of an ad hoc wireless sensor network provides greater range than can be achieved using low power wireless links alone.

As an example, a sensor system for testing wood condition contained three sensors: one audio sensor; one temperature and humidity sensor; and a temperature and pressure sensor. All these sensors were integrated into Arduino Mega 2560 and 1280 boards. A programme was written to collect readings from the sensors on an hourly basis and sends them to a remote place as an SMS text message using a mobile module with the Arduino board (Turnbul, *et al*. 2012).

27.4 Power Supply

Most ad hoc networks used in agricultural systems operate from batteries. The capacity of these batteries depends on the number of sensors attached to the node, the sampling frequency, and the amount of data being transferred. Because networks can be costly and data has real financial value, power reliability becomes critical. This implies that battery power needs to continually topped-up whenever possible. Part of the data stream should also include battery status so that power supply issues can be identified early. Usually photovoltaic cells are used to charge the batteries during daylight hours.

27.4.1 Available Solar Energy

Photo-voltaic solar collectors convert sunlight into direct current electricity. The use of solar energy has many advantages. In the field, it is a clean, quiet and reliable energy source. About seven million households around the world use solar hot water systems. In remote areas, without a connection to a public energy grid, solar energy is used for heating water and generating electricity.

The average solar power density falling onto the upper atmosphere, otherwise known as the solar constant, is 1353 ± 20 W m^{-2} (Howell, *et al*. 1982). Depending on the wavelength, much of this radiant power penetrates the atmosphere (Drury 1998). Analysing a sun-ray (Howell, *et al*. 1982), based on the geometry displayed in Figure 27.1, reveals that the solar power incident on a horizontal plane at the earth's surface on a clear day is:

$$I_r = \frac{1353}{r^2}\tau_s^{\sqrt{1-\frac{R_e\cos^2(\alpha)}{R_e+A}}^{\frac{1}{}}}\left[\sin(\xi)\sin(\psi)+\cos(\xi)\cos(\psi)\cos(\zeta t)\right] \tag{27.1}$$

Where Ir is the incident radiation power at the earth's surface (W m^{-2}), r is the distance from the sun to the earth (m), τ_s is the transmission coefficient of the earth's atmosphere, R_e is the earth's mean radius (m), A is the mean thickness of the atmosphere (m), a is the solar altitude (Radians), ξ is the Geographic latitude (Radians), ψ is the Solar declination (Radians); ζ is the Angular velocity of the earth's rotation (Radians s^{-1}), and t is time (s).

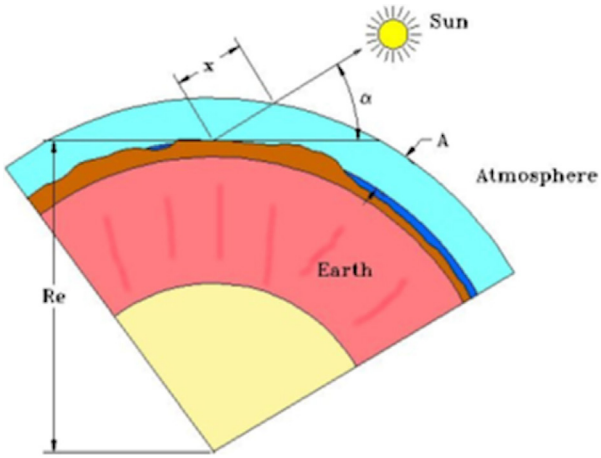

Figure 27.1: Geometry of a solar ray pathway through the Earth's atmosphere.

Blewitt (1973) and Howell, *et al.* (1982) show that the solar altitude (a) may be determined using:

$$\alpha = \sin^{-1}\left[\sin(\xi)\sin(\psi) + \cos(\xi)\cos(\psi)\cos(\zeta t)\right] \tag{27.2}$$

Atmospheric transmittance (t_s) is about 0.7 for a clear day (McMullan, *et al.* 1978, Studman 1990, Sturman and Tapper 1996) and much less on cloudy days.

Spencer (1971) has developed a set of equations to describe some of the important parameters for calculating solar power unavailability. The distance from the earth to the sun, in astronomic units, can be calculated using:

$$\frac{1}{r^2} = \begin{Bmatrix} 1.000110 + 0.034221\cos(\theta) - 0.001280\sin(\theta) \\ -0.000719\cos(2\theta) - 0.000077\sin(2\theta) \end{Bmatrix} \tag{27.3}$$

Solar declination can be calculated accurately using:

$$\psi = \left\{ \begin{array}{l} 0.006918 - 0.399912\cos(\theta) + 0.070257\sin(\theta) - 0.006758\cos(2\theta) \\ +0.000907\sin(2\theta) - 0.002697\cos(3\theta) + 0.00148\sin(3\theta) \end{array} \right\} \tag{27.4}$$

where $\theta = \frac{2\pi(n-1)}{365}$ is the "orbit angle" of the earth about the sun for the nth day of the year.

Ideally, the solar absorber should track the sun in such a way that its surface is always perpendicular to the sun's rays. In practice, this is expensive to implement. Consequently, fixed non-tracking absorbers are commonly used in solar heating systems. More consistent year-round performance can be achieved when a fixed solar absorber is tilted toward the equator in such a way that it is in a plane parallel to the earth's axis. This implies that the tilt angle of the absorber should be equal to the local geographic latitude of the system. The basic arrangement of a tilted absorber is shown in Figure 27.2.

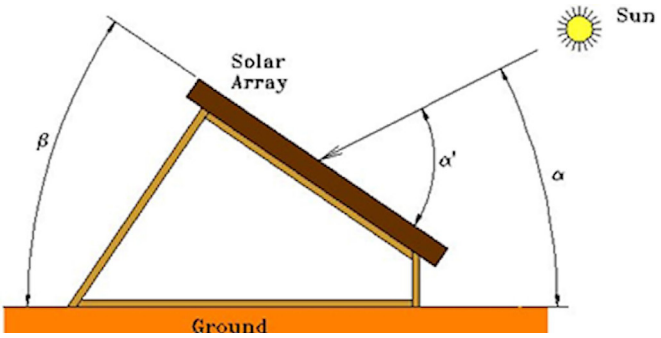

Figure 27.2: Geometry of a tilted solar absorber.

When this is done, equation (27.1) becomes:

$$I_r = \frac{1353}{r^2}\tau_s^{\sqrt{1-\frac{R_e\cos^2(\alpha)}{R_e+A}}}\left[\sin(\xi-\beta)\sin(\psi) + \cos(\xi-\beta)\cos(\psi)\cos(\zeta t)\right] \tag{27.5}$$

Because $\xi = \beta$, equation (27.5) reduces to:

$$I_r = \frac{1353}{r^2}\tau_s^{\sqrt{1-\frac{R_e\cos^2(\alpha)}{R_e+A}}}\left[\cos(\psi)\cos(\zeta t)\right] \tag{27.6}$$

Figure 27.3 shows the effect of using a tilted collector on year-long solar power absorption.

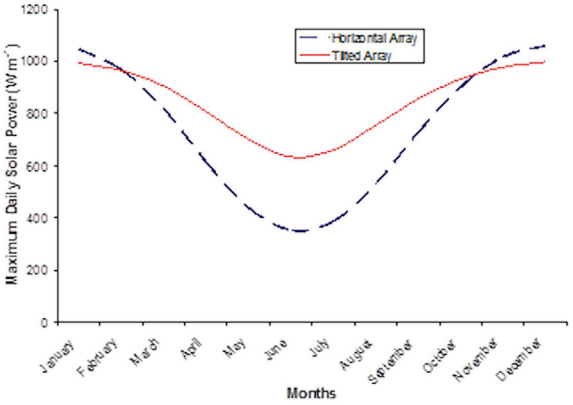

Figure 27.3: Effect of tilting the absorbing surface on solar performance throughout the year at 36o South latitude.

In addition to this ray intensity there is also a diffuse component of solar radiation due to atmospheric scattering. The US Department of Energy (1999) suggests that the diffuse component of solar radiation can be approximated by:

$$I_{diff} = \frac{676.5}{r^2}\left(1-\tau_s^{\frac{1}{\sqrt{1-\frac{R_E^2\cos^2(\alpha)}{R_E+A}}}}\right)\left[\sin(\xi)\sin(\psi)+\cos(\xi)\cos(\psi)\cos(\zeta t)\right] \tag{27.7}$$

Therefore the total solar radiation intensity can be defined by:

$$I = I_r + I_{diff} \tag{27.8}$$

Power supply is an ongoing issue for data acquisition. Various methods of harvesting energy from stray RF have been developed (Aguilar 2012). One of the earliest examples of this strategy was the RF-ID system where the ID chip harvests its energy needs from the RF reader during a scanning process. The next chapter will explore RF-ID systems.

References

Aguilar, A. 2012. RF Energy Harvesting. Unpublished thesis. University of Cincinnati,

Anonymous. 2014a. *Arduino*. http://arduino.cc/

Anonymous. 2014b. *Raspberry Pi*. http://www.raspberrypi.org/

Blewitt, M. 1973, *Celestial Navigation for Yachtsmen*, 5th edn, London: Edward Stanford.

Chen, B., Jamieson, K., Balakrishnan, H. and Morris, R. 2002. Span: An Energy-Efficient Coordination Algorithm for Topology Maintenance in Ad Hoc Wireless Networks. *Wireless Networks*. 8(5): 481-494.

Drury, S. A. 1998, *Images of the Earth: A guide to Remote Sensing*, 2nd edn, Oxford University Press.

Howell, J. R., Bannerot, R. B. and Vliet, G. C. 1982, *Solar - Thermal Energy Systems, Analysis and Design*, New York: McGraw-Hill.

Li, X.-Y. 2003. Topology control in wireless ad hoc networks. *Mobile Ad Hoc Networking*. 175-204.

Mafuta, M., Zennaro, M., Bagula, A., Ault, G., Gombachika, H. and Chadza, T. 2013. Successful Deployment of a Wireless Sensor Network for Precision Agriculture in Malawi. *International Journal of Distributed Sensor Networks*. 2013: 1-13.

McMullan, J. T., Morgan, R. and Murray, R. B. 1978, *Energy Resources*, London: Edward Arnold.

Parker, C. 2000, *Understanding Computers: Today and Tomorrow*, Fort Worth: The Dryden Press.

Popescu, V. 2007. Wireless Data Communication in Agricultural Engineering. Trends and Practical Experiments. *Proc. Research People and Actual Tasks on Multidisciplinary Sciences*. Lozenec, Bulgaria

Spencer, J. W. 1971. Fourier series representation of position of the sun. *Search*. 2(5): 172.

Studman, C. 1990, *Agricultural and Horticultural Engineering*, Wellington: Butterworth's Agricultural Books.

Sturman, A. P. and Tapper, N. J. 1996, *The Weather and Climate of Australia and New Zealand*, Oxford University Press.

Turnbul, C., Brodie, G., Thanigasalam, D. b., Farrell, P., Kealy, A., French, J. and Ahmed, B. 2012. *Final Project Report - Investigate control of in-situ termite and decay protection and control using microwave technologies*. University of Melbourne

US Department of Energy. 1999. *WIMOVAC Macroclimate Module*. March, 2004. http://face.das.bnl.gov/Modelling/newpage9.htm

Visser, O. W. 2005. Localisation in Large-Scale Outdoor Wireless Sensor Networks. Unpublished thesis. Delft University of Technology, Faculty of Electrical Engineering, Mathematics, and Computer Science

Wark, T., Corke, P., Sikka, P., Klingbeil, L., Ying, G., Crossman, C., Valencia, P., Swain, D. and Bishop-Hurley, G. 2007. Transforming Agriculture through Pervasive Wireless Sensor Networks. *Pervasive Computing, IEEE*. 6(2): 50-57.

28 RFID Systems

Although bar codes and bar code readers have been used for some time to provide quick computer based identification, the technology needed to support these systems is older and in many cases limiting. Radio frequency identification (RFID) tags are intelligent devices that can be attached to or implanted in almost anything and are being used to track products through the supply chain. RFID tags are an improvement over bar codes because the tags have read and write capabilities. Data stored on RFID tags can be changed, updated and locked (Bonsor and Fenlon 2014). RFID was originally developed for short-range product identification, typically covering the 2 mm - 2 m read range (Ruiz-Garcia 2011).

In agriculture RFID tags have been used for some time to track beef cattle from birth to consumption (Ruiz-Garcia 2011). In recent years RFID tracking applications have expanded to include most manufactured products, with many manufacturers using the tags to track the location of each product they make from the time it is made until point of sale (Wang, *et al.* 2007). Other similar applications of RFID tags include tracking of: vehicles; airline passengers; Alzheimer's patients; and pets (Bonsor and Fenlon 2014). RFID technology has been widely accepted for a well-structured traceability system.

These devices have also been used to monitor animal behaviour in mid-size outdoor pens, such as in a feed-lot; however, newer RFID hardware that is fitted with various sensors have extend the range of application (Ruiz-Garcia 2011). There are commercial active and semi-passive tags that can collect temperature, humidity, vibration, light, pH and concentration of various gases, such as acetaldehyde or ethylene (Ruiz-Garcia 2011).

RFID tags have also been added to transportation devices like highway toll pass-cards and public transport key-cards (Bonsor and Fenlon 2014). Because of their ability to store data so efficiently, RFID tags can tabulate the cost of tolls and fares and deduct the cost electronically from the amount of money that the user places on the card (Bonsor and Fenlon 2014).

28.1 Active, Semi-passive and Passive RFID Tags

RFID tags can be categorised as active, semi-passive and passive. Active and semi-passive RFID tags use internal batteries to power their circuits. An active tag also uses its battery to broadcast data to a reader, whereas a semi-passive tag relies on the reader to supply its power for broadcasting (Bonsor and Fenlon 2014). Active and semi-passive tags usually broadcast in the frequency range between 850 to 950 MHz; however the exact frequency is variable and can be chosen to avoid interference with other electronic devices including other RFID tags and readers.

Passive RFID tags rely entirely on the reader for power. These tags are read from up to 6 meters away (Bonsor and Fenlon 2014). Passive tags have lower production costs than active or semi-passive tags and are often manufactured to be disposable.

Another way of categorising RFID tags depends on how data is stored on the tag. These are defined as: read-write, read-only and WORM (write once, read many) (Bonsor and Fenlon 2014). As the names imply, read-write tags can be used almost like a USB thumb drive with data being added to or overwritten at any time. Read-only tags cannot be changed from their originally installed data. WORM tags can have additional data (like another serial number) added once, but they cannot be overwritten (Bonsor and Fenlon 2014).

28.2 Animal Tracking Systems

Agricultural systems have been using RFID for many years to track the movement of livestock. Australia pioneered the implementation of a mandatory RFID identification system, developing its own individual whole-of-life traceability program for livestock called the National Livestock Identification Scheme (NLIS) (Ruiz-Garcia 2011). The NLIS requires all calves to have RFID devices fitted, often as an ear tag or rumen bolus/ear tag combinations, before leaving the property on which they were born (Ruiz-Garcia 2011). Animals are registered into a national data base, and their identity and movements are recorded by readers at sale yards, abattoirs, or on farms (Peck 2003). The data base can store information about: diseases and chemical residue status; market eligibility; lost, stolen or mortgaged cattle; and commercial value (Peck 2003). The United States Department of Agriculture (USDA) established the National Animal Identification System (NAIS) in 2005 as a voluntary program (Ruiz-Garcia 2011). It provides registration and tracking of Camelids (llamas and alpacas), cattle, bison, Cervids (deer and elk), Equines, Goats, Poultry, Sheep and Swine (Ruiz-Garcia 2011). Other countries, including: Argentina, Brazil, Canada, Japan, Mexico, the United Kingdom, New Zealand, and several European Union countries have also implemented national RFID based herd registries (Peck 2003).

Other animals such as domestic pets have also been injected with RFID chips to allow quick identification of ownership for stray animals. There are however some concerns about the use of these chips: research from as far back as 1996 shows that these implants can cause cancerous tumours in lab rats and mice (Lowan 2007). Specifically, the implants caused sarcomas, which affect body tissue. No studies have proven yet that cancer can form in animals other than lab rats and mice, and it's still too early to tell what effects the chips can have on humans. No negative health effects have been linked to the radio waves emanating from RFID chips. Despite this evidence, or lack thereof, other disadvantages of human chipping may outweigh its advantages.

28.3 Environmental Sensor Applications

RFID has great potential for very low cost environmental sensing. The sensor can be integrated either in the chip or simply as an antenna on an RFID tag that directly responds to the environmental parameter of interest.

Antenna-based sensory RFID tags utilise the influence of the physical or chemical parameters of interest over the matching coefficient of the tag antenna (Gao 2013). Recalling the Friis Transmission Equation, which was Equation (26.57) from chapter 26, the coupling between the RFID reader and the tag antenna, will depend on the matching coefficient (τ) between the antenna and the remainder of the tag's circuitry (or structure). If the tag antenna is designed to change this coefficient in proportion to the environmental parameter of interest, then the tag antenna can be used to as a sensor (Bhattacharyya, *et al.* 2011, Gao 2013).

For example, an antenna can be printed onto a very thin substrate. If this substrate directly responds to moisture, the matching coefficient the antenna to the substrate changes as a function of moisture; therefore the response of the antenna tag to the RFID reader's electromagnetic fields will change as the substrate's moisture status changes. This passive antenna system (i.e. the RFID tag) is simple, can be mass produced at extremely low cost, needs no power supply and can provide accurate moisture data as the RFID reader passes nearby.

The trade off in this type of data acquisition is that measurements are only made when the RFID reader passes over the passive antenna tag. The advantage of this kind of system is that the sensors cost a few cents each and can be regarded as expendable after the sensing project has been completed. An interesting application of this type of system may be for high resolution monitoring of soil moisture for irrigation scheduling. Thousands of passive RFID antennae, printed on a biodegradable moisture sensitive substrate, such as paper, could be deployed across a paddock and regularly read by a passing RFID reader to determine site specific soil moisture deficit. This data could be used to provide high resolution irrigation application. Once the irrigation season was finished, these sensors could effectively be "ploughed in" during preparations for the next crop and new passive sensors deployed.

A slightly more sophisticated, and expensive, approach to RFID data acquisition is to use a microchip system that incorporates: an RF power harvesting system; some kind of ultra low power sensor circuitry; a small amount of processing power to summarise the data; some rewritable memory; and a high efficiency capacitor that acts as a very fast charging, rechargeable power supply (Sample, *et al.* 2007). As the RFID reader passes over these sensors they harvest electrical energy from the reader's electromagnetic fields and store this energy as electrical charge on the high efficiency capacitor. Over time, as the charge on the capacitor is depleted, the sensor circuitry captures and condenses data about the environmental parameter of interest and stores this summarised data as the equivalent of an ID code in the rewritable memory. Upon the next pass of the RFID reader, this summarised data is transferred to the

reader for further processing and the capacitor is recharged for the next sequence of data acquisition. This strategy utilises near field communication systems.

28.4 Near Field Communication

Near Field Communication (NFC) allows wireless data exchange at very close range. More precisely, NFC is a set of technical specifications and standards for transferring information between two objects via the inductive coupling of radio frequency fields at 13.56 MHz (McHugh and Yarmey 2014). NFC was developed from radio-frequency identification (RFID) standards. The primary distinction between NFC and other RFID technologies, however, is its operating range: typically within 3 to 5 cm (McHugh and Yarmey 2014).

Among many potential applications, Near Field Communication (NFC) technology has been developed for credit cards. Some credit cards have NFC chips embedded in them and can be tapped against NFC payment terminals instead of being swiped through a magnetic reader. Near Field Communication devices can also read passive RFID tags and extract the information stored in their memory (Bonsor and Fenlon 2014), as described above.

Like RFID systems, the NFC implant chips can be either active or passive. In passive communication, only one device (the initiator) actively generates a radio frequency field, to which the other object (the target) responds by modulating the initiator's field (McHugh and Yarmey 2014). A passive target is energised by the magnetic field generated by the initiator (McHugh and Yarmey 2014).

In both active and passive modes, NFC data exchange is based on a half-duplex system, where one device must receive while the other is transmitting. Data exchange can be at a rate of 106, 212, or 424 kbps; 848 kbps is available in some NFC-enabled devices but is not yet standardized (McHugh and Yarmey 2014). As a result, NFC is significantly slower than other wireless communication technologies such as Bluetooth and Wi-Fi, and most applications of NFC involve transfer of very small amounts of data (McHugh and Yarmey 2014), usually is a summarised form.

References

Bhattacharyya, R., Floerkemeier, C., Sarma, S. and Deavours, D. 2011. RFID tag antenna based temperature sensing in the frequency domain. *Proc. RFID (RFID), 2011 IEEE International Conference on*. 70-77.

Bonsor, K. and Fenlon, W. 2014. *How RFID Works*. 27th August, 2014, http://electronics.howstuffworks.com/

Gao, J. 2013. Antenna-Based Passive UHF RFID Sensor Tags. Unpublished thesis. Mid Sweden University, Department of Electronics Design

Lowan, T. 2007. Chip Implants Linked to Animal Tumors. *The Washington Post*.

McHugh, S. and Yarmey, K. 2014. Near Field Communication: Recent Developments and Library Implications. *Synthesis Lectures on Emerging Trends in Librarianship*. 1(1): 1-93.

Peck, C. 2003. Around The ID World. *BEEF*. 40(4): 52-54.

Ruiz-Garcia, L. 2011. THE ROLE OF RFID IN AGRICULTURE. *Journal of Current Issues in Media & Telecommunications*. 3(1): 25-41.

Sample, A. P., Yeager, D. J., Powledge, P. S. and Smith, J. R. 2007. Design of a Passively-Powered, Programmable Sensing Platform for UHF RFID Systems. *Proc. RFID, 2007. IEEE International Conference on*. 149-156.

Wang, L.-C., Lin, Y.-C. and Lin, P. H. 2007. Dynamic mobile RFID-based supply chain control and management system in construction. *Advanced Engineering Informatics*. 21(4): 377-390.

29 Conclusions

As pointed out in chapter 2, Thomas Malthus (1798) forecast that humanity was destined for starvation and dire poverty because of the disparity between population growth and food production growth. His worst predictions have not been realised because of the development and wide spread adoption of innovation in modern agricultural practices. Historical evidence also suggests that agriculture is the key to modern economic development. Gollin, *et al.* (2002) show that once agriculture switches from traditional to modern technology, labour is released to the industrial and technology sectors and the economy grows at higher rates.

One of the interesting feedback mechanisms involved in this labour release is that the subsequent technology development in the economy supports greater agricultural production. Chapter 2 outlined a brief review of technology adoption in the agricultural sector over the past several centuries. In more modern times, newer technologies, including the Information Communication Technologies (ICT) of computers, the internet, RFID and automatic data acquisition have allowed agricultural production to once again focus on individual plants and animals in a large production system. This has been generically called Precision farming or High resolution farming.

Radiofrequency and microwave systems provide an array of services for ICT, including telecommunication and networking services. Electromagnetic radiation may provide three important services: it can transfer energy (such as in the case of RF and microwave heating); it can transfer information (such as in the case of wireless transmission); and it can acquire information about the materials it passes through (as in the case of dielectric material characterisation and microwave and radar detection). These three services can readily be applied to agricultural production systems.

29.1 Heating Applications

Radiofrequency and microwave drying is a rapid drying technique that can be applied to specific foods, particularly high value products such as fruits and vegetables (Zhang, *et al.* 2006). The advantages of these systems include: shorter drying time, improved product quality, and flexibility in producing a wide variety of dried products (Zhang, *et al.* 2006); however current applications are limited to small categories of fruits and vegetables due to high start-up costs and relatively complicated technology as compared to conventional convection drying (Zhang, *et al.* 2006).

Dried timber, nuts and fruits can also be treated with RF and microwave fields to disinfest them of insect and other pests. Nelson (1996) has shown that microwaves can kill insects in grain; however one of the challenges for microwave insect control is to differentially heat the insects in preference to the grain that surrounds them. Nelson (1996) shows that differential heating depends on microwave frequency. It appears

that using a 2.45 GHz microwave system, which is the frequency used in domestic microwave ovens, heats the bulk grain material, which then transfers heat to the insects; however lower frequencies heat the insects without raising the temperature of the surrounding material beyond 50 °C (Nelson 1996).

It is also possible to kill weeds and their seeds in the soil using microwave heating. Davis *et al.* (Davis, *et al.* 1971, Davis 1973) were among the first to study the lethal effect of microwave heating on seeds. They treated seeds, with and without any soil, in a microwave oven and showed that seed damage was mostly influenced by a combination of seed moisture content and the energy absorbed per seed. Bigu-Del-Blanco, *et al.* (1977) exposed 48 hour old seedlings of *Zea mays* (var. Golden Bantam) to 9 GHz radiation for 22 to 24 hours. The power density levels were between 10 and 30 mW cm^{-2} at the point of exposure. Temperature increases of only 4 °C, when compared with control seedlings, were measured in the microwave treated specimens. The authors concluded that the long exposure to microwave radiation, even at very low power densities, was sufficient to dehydrate the seedlings and inhibit their development. On the other hand, recent studies on fleabane (*Conyza bonariensis*) and paddy melon (*Cucumis myriocarpus*) (Brodie, *et al.* 2012a, b) have revealed that a very short (less than 5 second) pulse of microwave energy, focused onto the plant stem, was sufficient to kill these plants. Microwave radiation is not affected by wind, which extends the application periods compared with conventional herbicide spraying. Energy can also be focused onto individual plants without affecting adjacent plants (Brodie, *et al.* 2012b). This would be very useful for in-crop or spot weed control activities. Microwave energy can also kill the roots and seeds that are buried to a depth of several centimetres in the soil (Diprose, *et al.* 1984, Brodie, *et al.* 2007).

Dong *et al.* (2005) discovered that organic matter degradability of wheat straw in the rumen of yaks was increased by around 20% after 4 min of treatment in a 750 W, 2.54 GHz, microwave oven. Sadeghi and Shawrang (2006a) showed that microwave treatment of canola meal increased *in vitro* dry matter disappearance, including substances that were deemed to be ruminally undegradable. Sadeghi and Shawrang (2006b) also showed that microwave treatment reduced the rumen degradable starch fraction of corn grain and decreased crude protein degradation of soya-bean meal (Sadeghi, *et al.* 2005) compared with untreated samples. When 25 kg bags of lucerne fodder were treated in an experimental 6 kW, 2.45 GHz, microwave heating chamber (Harris, *et al.* 2011) were subjected to a similar *in vitro* pepsin-cellulase digestion study, dry matter disappearance significantly increased compared to the untreated samples; however there was no significant difference attributable to the duration of microwave treatment. Feeding 12-14 month old Merino sheep on a "maintenance ration" of microwave treated Lucerne resulted in a significant increase in body weight instead of the relatively constant body weight that would be expected from a maintenance ration. By the end of the 5 week feeding trial the control group was only 0.4 % heavier than when they started, which would be expected from a maintenance ration. However the group being fed the microwave treated lucerne gained 7 % of

their initial body weight in the second week of the trial and maintained this body weight until the end of the trial. Their finishing weight after 5 weeks was 8.1 % higher than their starting weight (Brodie, *et al.* 2010).

During microwave assisted extraction, plant materials such as wood, seeds and leaves are suspended in solvents and the mixture is exposed to microwave heating instead of conventional heating. Enhanced rates of plant oil extraction have been observed for a range of plant materials (Chen and Spiro 1994, Saoud, *et al.* 2006). Chemat et al. (2005) found that microwave assisted extraction led to more rapid extraction; increased yields; and a more chemically complex extract, which was thought to be a better representation of the true composition of the available oils in caraway seed.

29.2 Sensor Applications

When microwaves are transmitted through an air dry organic material, such as wood or grain, the wave will be partially reflected, attenuated and delayed compared to a wave traveling through free space (Lundgren 2005, Brodie 2008). Wave attenuation; reflections from the surface; and internal scattering from embedded objects or cavities causes a "shadow" on the opposite side of the material from the microwave source. An x-ray image is a good example of the information that can be derived from wave attenuation and phase delay measurement. The transparency of the material to electromagnetic waves is linked to the complex dielectric properties of the material under study (James 1975, Torgovnikov 1993, Olmi, *et al.* 2000).

Microwaves can also be used in active sensors. Active sensors are generally divided into two distinct categories: imaging and non-imaging. The most common form of active imaging sensor is RADAR. Non-imaging sensors include altimeters and scatterometers. Radar altimeters transmit short microwave pulses and measure the round trip time to targets to determine their distance from the sensor (Canadian Centre for Remote Sensing 2003). Scatterometers are used to make precise quantitative measurements of the amount of energy reflected from targets. The amount of reflected energy is dependent on the surface properties (roughness) and the angle at which the energy strikes the target (Canadian Centre for Remote Sensing 2003).

In the case of terrain imaging radar, the radar beam is projected at right angles to the motion of the aircraft or satellite platform at an oblique angle to the terrain and reflects back to the source. This is similar to the flash of a camera. The antenna receives a portion of the reflected energy (or backscatter) from various objects within the illuminated beam (Sabins 1987, Drury 1998, Canadian Centre for Remote Sensing 2003). By measuring the time delay between the transmission of a pulse and the reception of the echo from different targets, their distance from the radar and thus their location in the resulting image can be determined (Sabins 1987, Drury 1998, Canadian Centre for Remote Sensing 2003).

Ground penetrating radar (GPR) has been used for over twenty years at chemical and

nuclear waste disposal sites as a non-invasive technique for site characterization. Standard GPR surveys are conducted from the surface of the ground providing geotechnical information from the surface to depths of 2 to 15 m, depending on GPR's operating frequency and soil conductivity. Commercially available GPR systems operate over the frequency range from 50 MHz to 1,000 MHz.

29.3 Communication Systems

Modern agricultural production systems rely as much on good dissemination of information as they do on physical systems that directly contribute to production. Communication has always mattered in agriculture. Updated information allows farmers to: keep up to date with markets; maintain contact with family, colleagues and workers; automate many aspects of their production systems; and provide important knowledge about new production systems. The arrival of information communication technology (ICT) is well timed (McNamara, *et al*. 2012). The benefits of the green revolution greatly improved agricultural productivity; however, there is a demonstrable need for a new revolution that will contribute to "smart" agriculture that can increase production (McNamara, *et al*. 2012) and potentially ward off Malthus' predicted catastrophe (Malthus 1798). Available technology has allowed access to unprecedented amounts of agricultural and scientific data and mobile telephony, wireless data transmission, and the Internet have found a foothold, even in poor small farms (McNamara, *et al*. 2012).

29.4 Conclusion

Microwave and radiofrequency energy has many potential applications in agricultural industries. This book has discussed a few of these, but there are many more that have not been included. The purpose of this book was to encourage practitioners within the microwave engineering and agricultural industries to explore the many possibilities of applying radio frequency and microwave energy to address many problems and opportunities within primary industries.

References

Bigu-Del-Blanco, J., Bristow, J. M. and Romero-Sierra, C. 1977. Effects of low-level microwave radiation on germination and growth rate in corn seeds. *Proceedings of the IEEE*. 65(7): 1086-1088.

Brodie, G., Hamilton, S. and Woodworth, J. 2007. An assessment of microwave soil pasteurization for killing seeds and weeds. *Plant Protection Quarterly*. 22(4): 143-149.

Brodie, G., Rath, C., Devanny, M., Reeve, J., Lancaster, C., Harris, G., Chaplin, S. and Laird, C. 2010. Effect of microwave treatment on lucerne fodder. *Animal Production Science*. 50(2): 124–129.

Brodie, G., Ryan, C. and Lancaster, C. 2012a. The effect of microwave radiation on Paddy Melon (Cucumis myriocarpus). *International Journal of Agronomy*. 2012: 1-10.

Brodie, G., Ryan, C. and Lancaster, C. 2012b. Microwave technologies as part of an integrated weed management strategy: A Review. *International Journal of Agronomy*. 2012: 1-14.

Brodie, G. I. 2008, *Innovative wood drying: Applying microwave and solar technologies to wood drying*, Saarbruecken, Germany: VDM Verlag.

Canadian Centre for Remote Sensing. 2003. *Fundamentals of Remote Sensing*. February 6, 2004. http://www.ccrs.nrcan.gc.ca/ccrs/learn/tutorials/fundam/fundam_e.html

Chemat, S., Aït-Amar, H., Lagha, A. and Esveld, D. C. 2005. Microwave-assisted extraction kinetics of terpenes from caraway seeds. *Chemical Engineering and Processing*. 44(12): 1320-1326.

Chen, S. S. and Spiro, M. 1994. Study of microwave extraction of essential oil constituents from plant materials. *Journal of Microwave Power and Electromagnetic Energy*. 29(4): 231-241.

Davis, F. S., Wayland, J. R. and Merkle, M. G. 1971. Ultrahigh-Frequency Electromagnetic Fields for Weed Control: Phytotoxicity and Selectivity. *Science*. 173(3996): 535-537.

Davis, F. S., Wayland, J. R. and Merkle, M. G. 1973. Phytotoxicity of a UHF Electromagnetic Field. *Nature*. 241(5387): 291-292.

Diprose, M. F., Benson, F. A. and Willis, A. J. 1984. The Effect of Externally Applied Electrostatic Fields, Microwave Radiation and Electric Currents on Plants and Other Organisms, with Special Reference to Weed Control. *Botanical Review*. 50(2): 171-223.

Dong, S., Long, R., Zhang, D., Hu, Z. and Pu, X. 2005. Effect of microwave treatment on chemical composition and in sacco digestibility of wheat straw in yak cow *Asian-Australasian Journal of Animal Sciences*. 18(1): 27-31.

Drury, S. A. 1998, *Images of the Earth: A guide to Remote Sensing*, 2nd edn, Oxford University Press.

Gollin, D., Parente, S. and Rogerson, R. 2002. The role of agriculture in development. *American Economic Review*. 92(2): 160-164.

Harris, G. A., Brodie, G. I., Ozarska, B. and Taube, A. 2011. Design of a Microwave Chamber for the Purpose of Drying of Wood Components for Furniture. *Transactions of the American Society of Agricultural and Biological Engineers*. 54(1): 363-368.

James, W. L. 1975. *Dielectric properties of wood and hardboard: Variation with temperature, frequency, moisture content, and grain orientation*. U.S. Department of Agriculture

Lundgren, N. 2005. Modelling Microwave Measurements in Wood. Unpublished thesis. Luleå University of Technology, Department of Skellefteå Campus, Division of Wood Science and Technology

Malthus, T. 1798, *An Essay on the Principle of Population*, London: J. Johnson, in St. Paul's Church-Yard.

McNamara, K., Belden, C., Kelly, T., Pehu, E. and Donovan, K. 2012, *ICT in Agriculture Sourcebook*.

Nelson, S. O. 1996. Review and assessment of radio-frequency and microwave energy for stored-grain insect control. *Transactions of the ASAE*. 39(4): 1475-1484.

Olmi, R., Bini, M., Ignesti, A. and Riminesi, C. 2000. Dielectric properties of wood from 2 to 3 GHz. *Journal of Microwave Power and Electromagnetic Energy*. 35(3): 135-143.

Sabins, F. F. 1987, *Remote Sensing, Principles and Interpretation*, New York: W. H. Freeman and Co.

Sadeghi, A. A., Nikkhaha, A. and Shawrang, P. 2005. Effects of microwave irradiation on ruminal degradation and in vitro digestibility of soya-bean meal. *Animal Science*. 80(3): 369-375.

Sadeghi, A. A. and Shawrang, P. 2006a. Effects of microwave irradiation on ruminal degradability and in vitro digestibility of canola meal. *Animal Feed Science and Technology*. 127(1-2): 45-54.

Sadeghi, A. A. and Shawrang, P. 2006b. Effects of microwave irradiation on ruminal protein and starch degradation of corn grain. *Animal Feed Science and Technology*. 127(1-2): 113-123.

Saoud, A. A., Yunus, R. M. and Aziz, R. A. 2006. Yield study for extracted tea leaves essential oil using microwave-assisted process. *American Journal of Chemical Engineering*. 6(1): 22-27.

Torgovnikov, G. I. 1993, *Dielectric Properties of Wood and Wood-Based Materials*, Springer Series in Wood Science, Berlin: Springer-Verlag.

Zhang, M., Tang, J., Mujumdar, A. S. and Wang, S. 2006. Trends in microwave-related drying of fruits and vegetables. *Trends in Food Science & Technology*. 17(10): 524-534.